Genetic Engineering of Antibody Fragments for the detection of Illicit Drugs

A thesis submitted for the degree of Ph.D.

By

Sue Townsend B.Sc .(Hons)

March, 2009.

Based on research carried out at

School of Biotechnology,

Dublin City University,

Dublin 9,

Ireland.

Under the supervision of Professor Richard O'Kennedy.

This thesis is dedicated to my parents, Robert and Helen, for their endless love and support throughout the years

Declaration

I hereby certify that this material, which I now submit for assessment on the programme of study leading to the award of Doctor of Philosophy, is entirely my own work and has not been taken from the work of others, save and to the extent that such work is cited and acknowledged within the text.

Signed: _____

Date: _____

Acknowledgements

There are so many people I would like to mention, almost too many to fit in!
My colleagues in the ABG lab are many; Barry B, Barry Mc, Om, Carol, Viji, Sushrut, Paul C, Edwina, Ger, Carolyn, Catherine H, Meg and Valerie. In such a large group there are always people that you are drawn to most and it is in these that I have made friends for life, thank you with all my heart Niamh, Katherine, Caroline, Weili, Conor, Dorota, Jenny and Elaine. You are all amazing, I could not have asked for better. Marie, although you have since left the ROK lab, you were there for me at every tear and for every triumph during the hardest years of my PhD. I expect we will remain fast friends for life. Some day we will have to explain our 'pacs' to our children!!
Jonny, although I think you scared me when I first met you, I want to thank you for all your advice, for your constant support and your friendship throughout my PhD. You challenged me, inspired me and reminded me that my hard work would pay off in the end. It did, thank you. Your advice almost always came with a few glasses of wine or a dinner in town, sometimes that element was as important as the science. You will always be someone I can turn to and I hope to be the same for you.
Steve and Paul, you were always available to bounce my (often ridiculous) notions off – thanks for steering me straight and for the Friday morning interrogations.
Of course I can not leave out some of my closest friends, the people who cheered me up when I was feeling down, made me laugh, listened while I moaned about my workload or the fact that nothing was working, understood the pressure I felt and most of all still talk to me now that its all over. Jenny and Eva thank you for indulging my love of Christmas fancy dress. Caroline, thanks for all the dvd nights. Katie, I never knew how you managed to understand EXACTLY how I felt all the time, thanks for keeping me focused and reminding me that it would all end some day. Cara and Sarah my absentee best friends, thank you, you are both amazing. Aoife S, Aoife R, Vinny and Dermot, thank you for your amazing friendship over the past 10 years.

Helen and Robert, my parents, I can not possibly put down in words how much I owe you both. You instilled drive, passion, determination, humour and self awareness in me, all of these things I relied on over the course of my PhD. I hope that I have made you proud. Thank you also to my brothers Alan, Robbie and Derry. Michael you came to the rescue when my laptop died and on countless other times.

Andrew I met you as I was finishing my PhD but unfortunately for you, right before I started writing my thesis. You are such an amazing strong person and it was you who kept me from going insane for the long three months of solitary writing. Not to mention the printer, paper and ink!!

Finally, to my supervisor Prof. Richard O'Kennedy, although we have argued and fought over science over the past 5 years you have always been someone I can turn to for help, reassurance and advice even if you had million other things on your mind. You inspired me to be the best that I can be. We have worked together on the Olympiad and been through some tough jury sessions in china, argentina and canada – but we survived and always brought back the same number of students that we left with. I now regard you not only as an advisor, but as a friend.

Thank you.

Table of contents

Chapter 2: Materials and Methods

Abbreviations

Ab	Antibody
Abs	Absorbance
Ag	Antigen
AP	Alkaline phosphatase
BIA	Biomolecular interaction analysis
bp	Base pairs
BSA	Bovine serum albumin
Cam	Chloramphenicol
cDNA	Complementary DNA
CE	Capillary electrophoresis
cfu	Colony forming units
CDR	Complementary determining region
CH_1	Constant heavy chain 1
CH_2	Constant heavy chain 2
CH_3	Constant heavy chain 3
CL	Constant light chain
CM	Carboxymethylated
conc (c)	Concentration
DNA	Deoxyribonucleic acid
dNTP	Deoxynucleotidyl triphosphates
E.coli	*Escherichia coli*
EDC	N-ethyl-N'-(dimethylamiopropyl) carbodiimide
EDTA	Ethylenediaminetetra-acetic acid
ELISA	Enzyme-linked immunosorbent assay
EMIT	Enzyme-multiplied immunoassay techniques
Fab	Antibody binding fragment
Fc	Constant region of an antibody molecule

FPIA	Fluorescence polarization immunoassay
Fv	Variable binding region of an antibody
GC/MS	Gas chromatography coupled with mass spectroscopy
HBS	Hepes buffered saline
HRP	Horse radish peroxidase
HPLC	High performance liquid chromatography
IgG	Immunoglobulin class G
IMAC	Immobilised metal affinity chromatography
Kan	Kanamycin
Log	Logarithmic
LLE	Liquid-liquid extraction
MDMA	3,4-methylenedioxymethamphetamine
mRNA	Messenger RNA
MW	Molecular weight
M3G	Morphine-3-glucuronide
NIDA	National institute of drugs of abuse
NHS	N-hydroxysuccinimide
OD	Optical density
PAGE	Polyacrylamide gel electrophoresis
PBS	Phosphate buffer saline
PBST	Phosphate buffer saline tween
PEG	Polyethylene glycol
pH	Log of the hydrogen ion concentration
RIA	Radioimmunoassay
RI	Refractive index
RT	Room temperature
RU	Response units
SAMSHA	Substance abuse and mental health service administration
scFv	Single chain Fv antibody derivative

SDS	Sodium dodecyl sulphate
SOE	Splice by overlap extension
SPR	Surface plasmon resonance
THC	Tetrahydrocanabinol
TLC	Thin layer liquid chromatography
Tet	Tetracycline
TMB	Tetramethylbenzidine dihydrochloride
V_H	Variable region of heavy chain
V_L	Variable region of light chain

Units

µg	microgram
kDa	(kilo) Daltons
µl	microlitre
µM	micromoles
^oC	degrees Celcius
cm	centimetres
g	grams
h	hours
kg	kilogram
l	litre
m	metre
M	molarity
mg	milligram
min	minute
ml	millilitre
mm	millimetres
nM	nanomolar

mol	moles
pg	picograms
rpm	revolutions per minute
RU	response units
sec, s	seconds
v/v	volume per unit volume
w/v	weight per unit volume

Publications

1. **S. Townsend**, W.J.J. Finlay, S. Hearty, R. O'Kennedy. (2006). "Optimising recombinant antibody function in SPR immunosensing of illicit drugs. The influence of antibody structural format and chip surface chemistry on assay sensitivity", Biosensors and Bioelectronics; **22**(2), 268-74

2. **S. Townsend**, L. Fanning, R. O'Kennedy. (2008). "Salivary analysis of drugs-potential and difficulties", Analytical Letters; **41**(6), 925-948.

3. R. O'Kennedy, W.J.J Finlay, S. Hearty, P. Leonard, J. Brennan, S. Stapleton, **S. Townsend,** A.D. Sheehan, A. Baxter and C. Jones. (2009). Chapter contribution to "Sensors for Chemical and Biological Applications"; Chapter 7: Applications of Sensors for Food and Environmetnal Analysis. CRC press.

4. R O'Kennedy, **S. Townsend,** P. Leonard, S. Hearty, B. Byrne and G. Donahoe Chapter contribution to "Rapid Methods"; Chapter title: Speedy, Small, Sensitive and Specific-reality of myth for future analytical methods; (2009 in press).

5. **S. Townsend** and R O'Kennedy. Development of novel recombinant antibodies and associated assays for the detection of tetrahydrocannabinol. Manuscript in preparation. (awaiting IP approval).

6. **S. Townsend** and R O'Kennedy. Novel recombinant antibodies and their incorporation into a multi analyte chip array demonstrating simultaneous measurement of drugs of abuse. Manuscript in preparation (awaiting IP approval).

Posters

1. **S. Townsend,** S. Spillman and R. O'Kennedy. "Novel platform for enhanced multi-abuse analyte detection of drugs of specifically designed for 'in-field' use" Europtrode IX, Dublin, Ireland, April 2008.

2. R. O'Kennedy, S. Hearty, P. Leonard, B. Byrne, A.D. Sheehan, C. Viguier, N. Gilmartin, E. Tully, S. Stapleton, **S. Townsend**, C. Hayes, B. McDonnell, G. Donohoe, M. Ryan, E. Darcy, and J. Fitzgerald. Antibody engineering. US-Ireland R&D Partnership Sensors Workshop, Dublin, February 2007.

3. **S. Townsend,** W. Finlay, S. Hearty, P. Leonard, and R. O'Kennedy. The influence of antibody structural format on the sensitivity of ELISA and SPR assays for illicit drugs. Cambridge Healthcare Institutes Third Annual Monoclonal Antibodies Conference, Protein Engineering Summit, Boston M.A., USA, April 2006.

4. S. Stapleton, L. Dunne, A. Darmanin Sheehan, W.J.J. Finlay, **S. Townsend**, R O'Kennedy and B. MacCraith. The use of recombinant antibodies for the detection of food contaminants. BDI/SFI Openday, Dublin City University, Dublin, May 2005.

Abstract

The monitoring of illicit drugs is now of major importance. Key areas of analysis include the detection of illicit use by drivers, workplace testing, forensic investigations and general monitoring to detect or reduce abuse. Thus, the development of a highly sensitive and reliable array-based assay for saliva, an assay-friendly matrix for detection of illicit drugs, would be of major benefit. This thesis describes the production and affinity maturation of antibodies for the detection of illicit drugs and their application in ELISA, Biacore surface plasmon resonance -based biosensor assays and, finally, in a multidrug-based assay.

The first phase of this work focused on the development of a repertoire of antibody fragments against various illicit drugs including morphine-3-glucuronide (M3G), amphetamine and tetrahydrocannabinol (THC). Antibody libraries were generated from murine, avian and leporine immune systems. A number of antibody fragments were produced, purified and characterised by SDS-PAGE, Western blotting and ELISA.

A pre-characterised, murine anti-M3G, whole IgG structure was used for conversion to scFv and Fab antibody fragments. This permitted SPR-based comparative studies regarding the validity of using either scFv or Fab fragments in current high throughput screening strategies. The Fab fragment revealed an apparent off rate 40-fold higher than that of the scFv, that did not translate to higher affinity for the target in question. A murine anti-amphetamine Fab fragment demonstrated a 3-fold higher affinity than that of the parent IgG clone.

Diverse leporine immune libraries were utilised in the development of novel recombinant Fab and scFv fragments against amphetamine and THC. Subsequently the antibodies were solubly expressed in *Escherichia coli*, and fully characterised with respect to their binding capabilities on ELISA and Biacore-based analytical platforms.

The next phase of the work involved the *in-vitro* affinity maturation of the anti-M3G Fab and anti-THC scFv fragments. The wild-type antibodies were used as templates for

construction of mutant recombinant antibody libraries. Initial mutagenesis strategies exploited error prone-PCR, DNA shuffling, light-chain shuffling and various methods of site-directed mutagenesis to generate improved affinity antibody fragments. Kunkle-style, site-directed mutagenesis, proved to be the most successful method for the generation of an anti-M3G Fab mutated library. The highest affinity anti-THC clones, characterised by ELISA, were carried forward for light-chain shuffling and subjected to specifically-tailored affinity selection conditions. Comparative gene and amino-acid sequence analyses were carried out on the wild-type and selected mutants and confirmed the presence of mutations in the selected CDR's.

The final phase of this research involved the incorporation of the antibodies onto multi-analyte assay formats. Optimisations were carried out with respect to immobilisation strategies, surface chemistries, recombinant antibody fragment selection, use of drug-protein conjugates and detection strategies.

Chapter 1

1.0 Introduction

1.1 Drugs of abuse

1.1.1 Opioids

Heroin is the most commonly abused opiate, due to its highly addictive nature and availability. Heroin can be administered orally, intravenously, intranasally or by inhaling vapours of the heated powder. Heroin is rapidily metabolized to 6-monacetylmorphine (6-MAM). This is the only metabolite specifically associated with heroin abuse. 6-MAM is then hydrolysed to morphine, which is rapidly converted to morphine-3-glucuronide (M3G) and to a lesser extent, morphine-6-glucuronide (M6G), via glucuronidation, as shown in figure 1.1.1.1. M3G and M6G detected in urine account for 55 % and 10 %, respectively, of the administered dose (Zheng *et al.,* 1998).

Morphine is a highly potent opiate analgesic drug and it is the primary active ingredient is opium. The content of morphine in raw opium ranges from 2-25% of its total weight. Commercial or medicinal opium is standardized to contain 10% morphine. Although codeine is naturally present in opium (at levels as low as 0.3%) a large portion of morphine is used in the manufacture of codeine and other compounds used in prescription pain relief medicines. Morphine abuse has escalated in recent years and a significant portion of the morphine refined from opium is used in the manufacture of semi-synthetic derivatives including, heroin, and dihydrocodeine. Slang terms or street names for morphine, used among addicts include, “dreamer”, “miss emma” and “morf”.

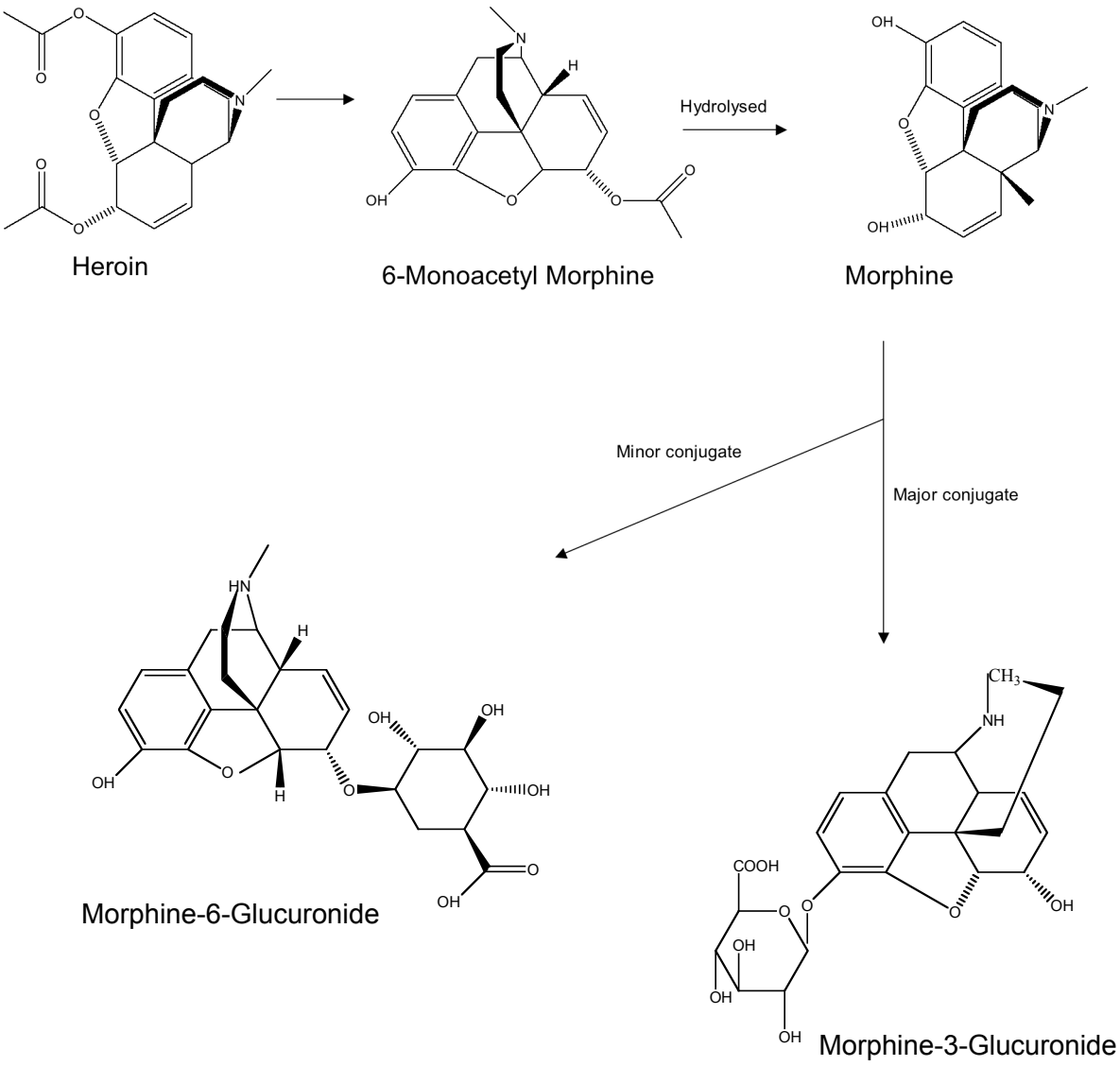

Figure 1.1.1.1 Metabolic pathway of heroin and morphine.

1.1.2 Amphetamine

Amphetamines and other related compounds are a group of drugs which act by increasing the concentrations of serotonin and dopamine in the brain (Puder *et al.,* 1988). Amphetamines were initially introduced as a treatment for obesity under various market brand names. The prescription drugs used for treatment of attention deficit disorder (ADD) and attention deficit hyperactivity disorder (ADHD) are also members of the amphetamine drug group. However, they are now a commonly misused drug among young people. Amphetamines are a Class B drug in the United Kingdom although methamphetamine has been upgraded to a Class A drug under the misuse of drugs act, 1971. Slang terms or street names used among abusers includes, "meth", "ice", "crystal" and "glass".

Amphetamines are available in d- and l- isomeric forms and also in the racemic mixture form (Cone *et al.,* 1993). Amphetamines can be administered orally and intravenously. The most commonly abused form is 3,4-methylenedioxymethamphetamine (MDMA), also known as ecstasy, as shown in figure 1.1.2.1.

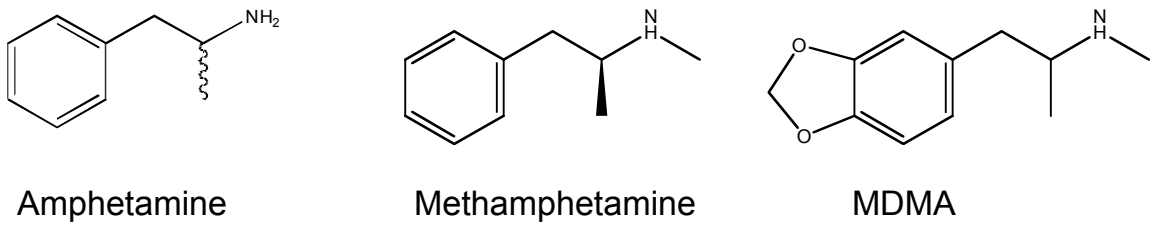

Figure 1.1.2.1 Structures of amphetamine, methamethamine and the most commonly abused synthetic derivative, MDMA (ecstasy).

It is important to consider that derivatives of the drug are widely used in medicinal allergy and cold formulations when developing a detection system for amphetamine abuse (Cone *et al.,* 1993). Compounds such as ephedrine and phenylpropanolamine are amphetmaine derivatives used in non-prescription cold medication. They demonstrate very high structural similarity with the illicit compounds (figure 1.1.2.2).

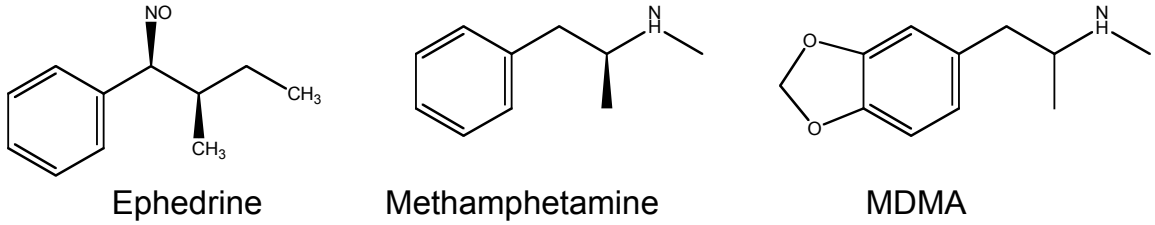

Figure 1.1.2.2 Structure of "over the counter" cold medication, ephedrine, and the commonly abused drugs, methamphetamine and MDMA. (Braithwaite *et al.,* 1995)

Amphetamine is largely unaffected during metabolism with more than 60% being excreted unchanged. However, amphetamine is metabolised to some extent (> 35%) via deamination, oxidation and hydroxylation. Deamination produces phenyl acetone, which is then oxidized to benzoic acid followed by excretion in urine in hippuric acid and glucuronide-conjugated forms. Amphetamine is also oxidized to p-hydroxyamphetamine by the hydroxylation of the phenolic ring (figure 1.1.2.3).
Saliva is a more suitable matrix for the detection due to the influence of urinary pH on the levels of amphetamines measured in urine. The reason for this is that salivary pH remains constant, even under conditions used to induce pH changes in urinary conditions, such as ingestion of sodium bicarbonate (Wan *et al.,* 1978).

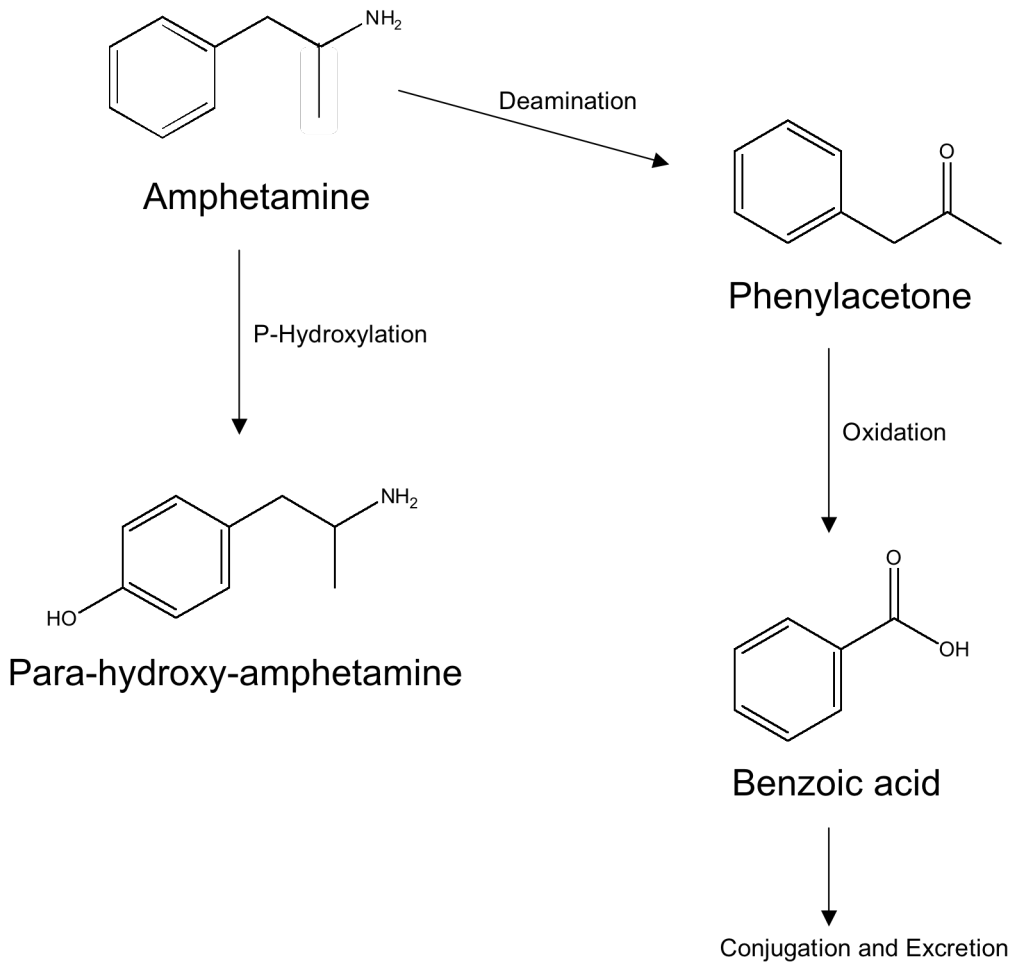

Figure 1.1.2.3 Schematic representation of the metabolic pathway of amphetamine (adapted from Karch, 1998). Amphetamine is metabolised via deamination, oxidation and hydroxylation and finally excreted in urine as hippuric acid and glucuronide conjugates.

1.1.3 Tetrahydrocannabinol

Cannabis is a genus of flowering plants. It is a dioecious plant with both male and female plants producing good quality hemp for use in the textile industry. The female plants produce the highest quality canabinnoids. Canabinoids make up the primary psychoactive compounds of the plant with tetrahydrocannabinol (THC), as shown in figure 1.1.3.1, being the primary psychoactive substance in the plant. It it thought that THC plays a similar role in plant life to caffeine or nicotine in that it may act as a form of protection against herbivores. Medicinal use of THC in the treatment of migraine and pain management has been reported (Campbell *et al.,* 2001).

In its pure, cold form, THC, is a glassy solid and is completely insoluble in water. THC demonstrates good solubility in most organic solvents such as ethanol and butane. Its insolubility is an important factor in this work as it renders it difficult for use in immunoassay development. In the human body, THC is metabolised to 11-hydroxy-delta-9-THC (11-OH-THC). This metabolite remains psychoactive until it is further oxidised to 11-nor-9-carboxy-delta-9-THC (THC-COOH). Over 50% of THC's are excreted in faeces while THC-COOH excreted in the urine acounts for ~ 20% of total THC.

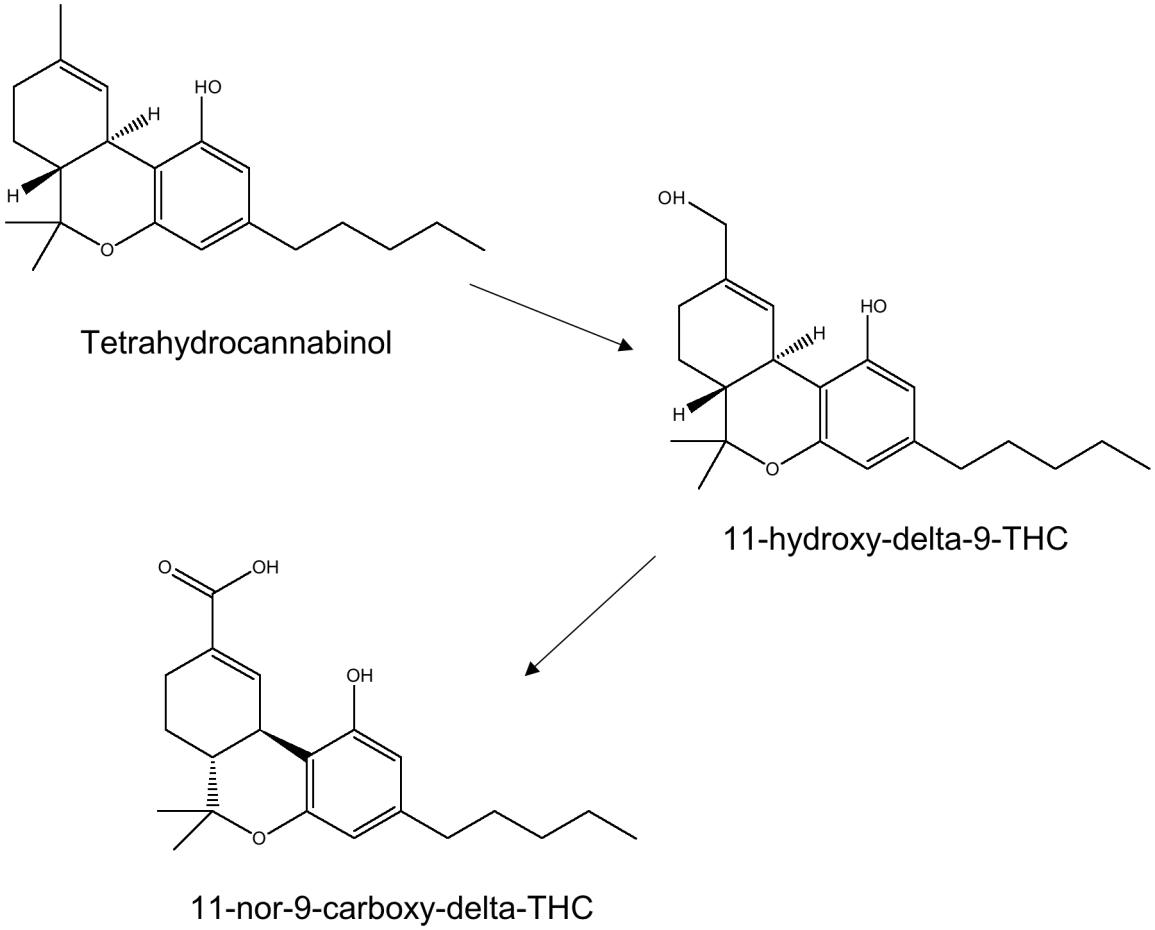

Figure 1.1.3.1 Structure of tetrahydrocanabinnol, the primary phsycoactive constituent in cannabis, and its metabolism in the human body to the inactive form 11-nor-9-carboxy-delta-THC.

1.2 Levels of detection and cutoffs

Current international guidelines recognized by the Substance Abuse and Mental Health service Administration (SAMSHA) and the National Institute of Drugs of Abuse (NIDA) are available only for matrices such as plasma and urine. Internationally recognized screening (RIA) and confirmation (GC-MS) cut-off levels for detection in saliva were updated in 2005 by the division of workplace programs and outlined on **www.workplace.samsha.gov** and in table 1.2.1 below. An extensive list of cut-off levels for drugs of abuse in saliva samples was presented in Clarke *et al.* (2005). The relevant figures are listed in table 1.2.2.

Table 1.2.1 Cut-off concentrations of drugs of abuse in urine

Drug	Screening cut-off (ng/ml)	Confirmation cut-off (ng/ml)
Amphetamine	1000	500
THC	50	15
Morpine	300	300

Table 1.2.2 Cut-off concentrations of target analytes in saliva applied to the OraSure Technologies Inc. Intercept® EIA kit. (adapted from Clarke *et al.*, 2005)

Test Group	Cut-off (ng/ml)	Calibrator compound
Amphetamine specific	100	d-Amphetamine
Cannabinoids	1	THC
Opiates	10	Morphine

1.3 Methods of drug detection

Methods for the detection of drugs of abuse in clinical samples include thin-layer chromatography (TLC), gas chromatography coupled with mass spectroscopy (GC-MS), (Ewald *et al.,* 2007), high performance liquid chromatography (HPLC) and capillary electrophoresis (CE) (Lurie *et al.,* 1998), raman spectroscopy (Eliasson *et al.,* 2008). GC-MS is the primary test for the confirmation of the presence of drugs of abuse in biological samples. However, this method would typically be performed on samples that had been previously screened using more rapid methods, such as immunoassay. Recent studies reporting on head-space solid phase micro-extraction, illustrate complementary techniques and are suggested for use alongside some of the more traditional methods outlined above (Fucci *et al.,* 2003).

Immunoassays require less preparative steps. They are highly characterised with very specific antibodies available. The initial set-up costs of a traditional analytical laboratory are quite large and it can take a significant amount of time per sample analysis. Various expensive instruments are required for a functioning analytical laboratory, for example, use of liquid–liquid extraction (LLE) and solid phase extraction (SPE) combined with HPLC / GC / CE (Zhang *et al.,* 2008), while a single immunoassay is capable of analysing multiple samples simultaneously without the need for large instrumental costs. Each of these elements impacts on the cost effectiveness and speed of using an immunoassay as an initial screening system prior to further analysis in an analytical laboratory (Zhang *et al.,* 2008; Braithwaite *et al.,* 1995) The extensive preparation of the samples required in order to run chromatographic tests is well documented (Xu *et al.,* 2007). Modified solvent extraction and solid phase extraction techniques are also used and commercial kits are available. The chromatographic methods, which are most commonly used for drugs of abuse are concisely reviewed by Braithwaite *et al.* (1995).

The main types of immunoassay used for detection include enzyme-linked immunosorbant assay (ELISA), enzyme-multiplied immunoassay techniques (EMIT), fluorescence polarisation immunoassays (FPIA) and up-converting phosphor technology. These immunoassays are regarded as the initial qualitative testing method, with chromatographic techniques mentioned previously providing quantitative confirmatory results. However, several research groups are moving away from this ideology due to the advent of antibody-based microarrays. The increase and widespread abuse of multiple drugs has hastened the need for an easy and fast technique with the ability to detect a wide range of drugs from low sample volumes. There are a number of factors to be considered in order to improve on existing techniques. The development of rapid "on the spot" testing for drugs of abuse makes the move from conventional analytical techniques to easy-to-use biosensors absolutely essential. New detection methods must be user-friendly so as to allow the test to be carried out by non-lab-trained personnel such as law enforcement officials and counselors.

1.3.1 Immunoassays

The basis of all enzyme immunoassays is the binding of an antibody to its cognate antigen. The interaction is detected using an antibody-coupled enzyme which converts a colourless substrate to a coloured or luminescent product. Two broad classifications of immunoassay are competitive and non-competitive. A schematic of a competitive assay is shown in Figure 1.3.1.2. One of the most common rapid assay formats currently available are the dip-stick or test strip immunoassays. These involve antibodies being coated on surfaces such as nitrocellulose strips. Test strip assays often employ a competitive immunoassay format and lateral flow. The format is shown in figure 1.3.1.1. An example is the One-Step Rapid Opiates Test, (Craig Medical, USA), for detection of opiates in urine. Further examples of this type of immunoassay are outlined later in the text.

Ogert *et al.* (1992) developed what they describe as a fast, reliable, inexpensive system, which requires little user input for the detection of cocaine in urine. The system consists of antibodies specific for benzoyleconine, the primary metabolite of cocaine, immobilized on the surface of a continuous flow immunosensor. The basis for detection is bound labelled antigen competing with free unlabelled drug in the sample. Upon testing the assay appeared to have very high specificity with cross reactivity tests resulting in fluorescence intensities close to zero even at microgram concentrations of various other drugs. While this system is not technologically much more advanced than that of a simple competitive immunoassay such as ELISA, the novel element lies in its portability and ease of use. This is a good example of an ideal system that if applied to saliva testing, would meet all requirements for a totally non-invasive, rapid and easy to use system. A simplified schematic is outlined in figure 1.3.1.1.

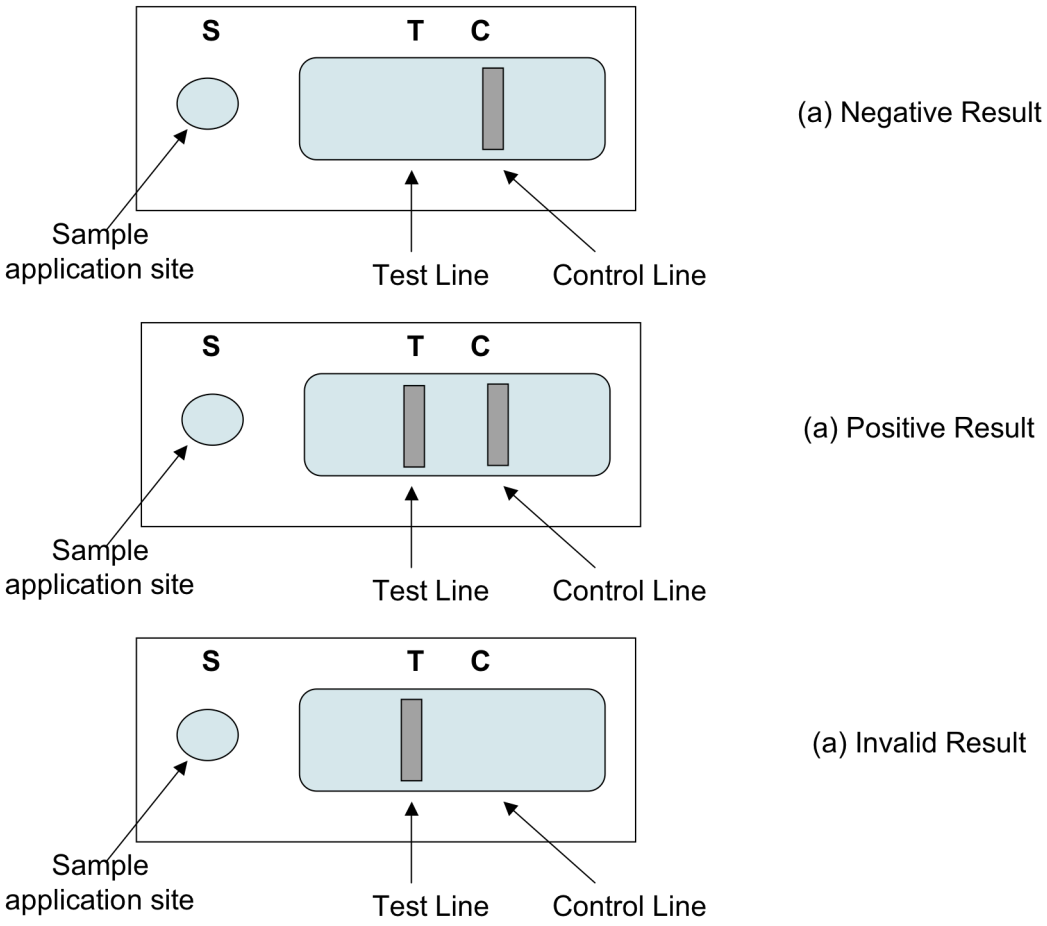

Figure 1.3.1.1 Diagrammatic example of lateral flow immunoassay for the detection of drugs in a sample. An example of this type of assay is the Smartclip-rapid test for drugs of abuse, from Envitec. The development of the two lines, a test line and a control line, indicates a negative test for the targeted drug (i). The development of the control line and absence of the test line indicates a positive result (ii). The absence of a control line in the window indicates an invalid result regardless of the test line result (iii).

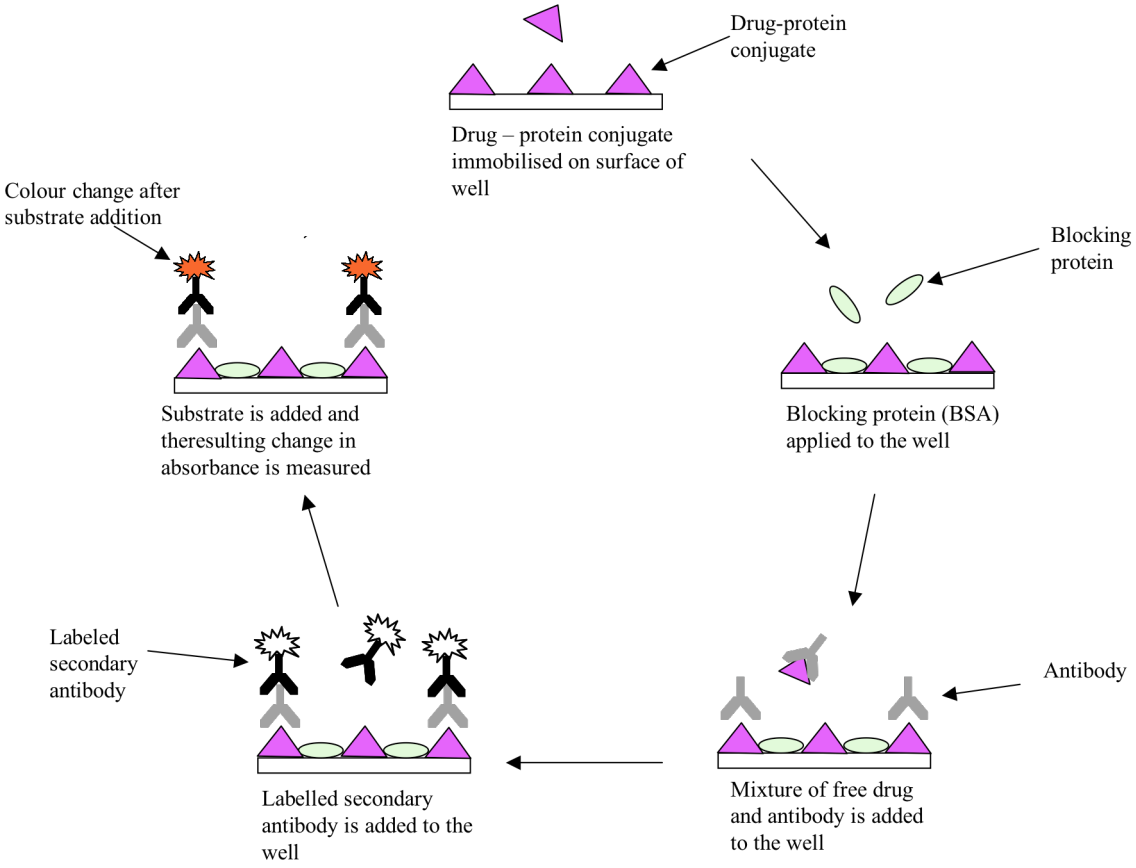

Figure 1.3.1.2 Schematic of a competitive ELISA. Antigen is immobilised on the surface of the wells. A mixture of sample containing free antigen and a known constant concentration of antibody is applied to the blocked wells. Competition occurs between the immobilized antigen and the free antigen for binding to the antibody. A labeled secondary antibody, which recognizes the bound antibody, is added. Substrate is added to each well and the resulting change in absorbance is measured. Based on an initial antibody titration curve the intensity of the response from the competitive ELISA is inversely proportional to the concentration of antigen in a test solution.

1.3.1.1 Enzyme-Multiplied Immunoassay Technique

Enzyme-multiplied immunoassay technique (EMIT) is a homogenous competitive assay. The drug antigen is labelled with an enzyme and mixed with a solution of sample antigen and antibodies. Competitive binding takes place and the binding of the antibody, to the drug attached to the enzyme, sterically hinders the active site of the enzyme thereby preventing enzyme activity. When unlabelled free antigen is added, it competes with the labelled antigen for binding to the antibody. The greater the level of antigen added, the greater the level of unbound enzyme-labelled antigen, resulting in greater enzymatic activity. Behring Diagnostics Inc. supply a number of EMIT kits for the detection of cannabinoids, opiates, cocaine and amphetamine. The EMIT kits efficiency in drug detection was reported by Lu and Taylor (2005).

1.3.1.2 Biosensors

A biosensor is an analytical device that incorporates a biological recognition component (DNA, enzymes, micro-organism or antibodies) and a transducer element (electrochemical, optical, acoustic or thermal), which together allow analysis to relate the concentration or properties of the analyte to a measurable electronic signal. A biosensor has the potential to be a rapid, sensitive, highly specific, quantitative system that needs minimum sample preparation and can be used by relatively unskilled personnel. As illicit drug abuse continues to rise worldwide there is a need for a detection system with these characteristics.

Biosensors are comprised of three elements:

1. A sensitive biological element specific for a particular analyte e.g. a cell receptor, antibody or enzyme.
2. A transducer, which makes use of some change that occurs during the reaction; e.g. electrochemical, piezoelectric or optical.
3. The output or signal is proportional to the concentration of analyte detected.

Examples of the technology are surface plasmon resonance (SPR) - based biosensors such as the Biacore series. They have considerable advantages over other technologies, including the following:

- there are no labeling requirements - this involves less preparatory work and eliminates steric and other problems sometimes encountered when labeling antibodies or antigens.
- the reactions are monitored in 'real-time', thereby providing rapid, quantitative data.
- the stability of the sensor surface can be monitored.
- the systems are fully automated and can handle large amounts of samples.
- the assays developed require little or no sample preparatory steps. Reports include assay development in cell culture supernatant, urine and saliva (Fanning, unpublished data, Dillon *et al.,* 2003 and Brennan *et al.,* 2003).
- the multi-channel analysis feature means that interactions can be monitored over different immobilized-ligand sensor surfaces and provide direct comparison between cross-reactive substances.
- The amounts of materials required for immobilisation of ligands are minimal.

Biosensor technology has not been exploited to its full potential with regard to illicit drug testing to date. There are a number of examples of their use in related areas that demonstrate promise for the technology. This includes detection of animal growth hormones in urine (Elliot *et al.,* 1998), optimising antibody structural format for use in illicit drug testing (Townsend *et al.,* 2006) and the use of electrochemical immunosensors for detection of hormones in livestock (Lu *et al.,* 2007).

Biacore and its application in recombinant antibody characterisation is detailed in full in chapter three.

1.4 Matrices used for the detection of drugs

Traditionally, drug detection has focused on matrices such as blood and urine but recent advances in sensitivity have permitted the use of matrices, such as, sweat and saliva. (Hofman *et al.,* 2001). Intra-nasally administered or ingested drugs have a large impact on contamination of the sample. It is important to account for these contaminants in order to reduce the occurrence of false positives. However, it is now generally accepted that there is high correlation between salivary and plasma drug concentration once the drug was eliminated from the buccal cavity (Huestis *et al.,* 2004). Many advantages of measuring drugs in saliva are based on the non-invasiveness of the procedure. For this reason the collection of whole / mixed saliva is the practical option, suggesting that any assay being developed should take this into consideration. Practical considerations and usefulness of a number of matrices are outlined in Tables 1.4.1 and 1.4.2.

Table 1.4.1 Matrices used for the detection of drugs of abuse

Matrix	Collection Procedure	Sample Preparation	Time Period & concentration detected	Correlation to Current Intoxication levels	Possible Problems
Sweat	• Non - Invasive	• Minimal	• Dependent on metabolism of drug –indicates recent drug use • Low concentrations	• Correlation can be made to an extent	• Small sample volume
Hair	• Non - Invasive	• Yes, extensive	• Cannot be correlated to plasma levels • Indicates prior use over previous weeks • Higher Concentrations	• Correlation cannot be made	• Interference by external chemicals such as hair dyes
Blood	• Invasive • Requires healthcare professional • Exposes professional to health risk	• Yes, extensive	• Dependant on metabolism of drug – indicates recent use. • Low concentration.	• Correlation can be made	• Small sample volume
Urine	• Invasion of privacy • Requires additional staff to monitor procedure	• Yes, significant	• Cannot be correlated to plasma levels • Indicates prior use over last few days and subsequent metabolism • Higher concentration build up.	• Correlation can be made	• pH can be altered and concentrations of drugs/metabolit as affected
Saliva	• Non – Invasive	• Minimal	• Dependant on metabolism of drug – indicates recent use • Can be correlated to plasma levels • Low concentrations	• Correlation can be made	• Small sample volume • Buccal and oral contamination.

Table 1.4.2 Metabolism and characteristics of selected drugs in saliva.

Drug	Form of drug found in saliva	Comment
Cocaine	Cocaine, Benzoylecgonine (BEC)	Cocaine appears initially followed by lower quantities of BEC. Significant correlation between mood effects and cocaine concentration in saliva and plasma is reported (Kato *et al.,* 1993)
THC (Tetrahydrocannabinol)	THC	Found mainly as a contaminant and not passed from plasma to saliva. (Gross *et al.,* 1995)
Amphetamines	Parent drug	S/P >1.0. Saliva is the preferable matrix as concentrations measured in urine are too highly dependant on urinary pH. (Wan *et al.,* 1978)
Heroin	Morphine	Rapid metabolism of heroin to morphine with a longer elimination half-life. (Braithwaite *et al.,* 1995)

1.5 Commercially available tests

There are a number of commercially available tests for detection of the presence of illicit drugs in oral fluid. Many of these tests target opiates in particular. These include, Cozart® Rapiscan oral fluid drug test systems for opiates and cocaine, Toxiquick® from Biomar Systems GmbH, On-site Oraline® IV s.a.t, Drugwipe® by Securetec, ORALscreen™ from Avitar Inc., Intercept™ by Labone (Orasure technologies), Salivascreen 5™ from Kabat Enterprises and the Smartclip from Envitec. This section describes a number of these devices in detail and a summary is provided in Table 1.5.2.

The ability to detect recent drug use is invaluable in the area of criminal investigation and drug withdrawal clinics. It was shown that subjects under investigation often under report recent drug use (Wish *et al.,* 1997; Yacoubian *et al.,* 2000). Urinalyses was the accepted standard for drug testing in the past. With the innovation of Intercept oral s pecimen collection device (IOSCD®) a number of field studies have compared the two matrices, saliva and urine, (Moore *et al.,* 2001; Niedbala *et al.,* 2001b; Yacoubian *et al.,* 2001; Yacoubian *et al.,* 2002). A summary of agreement between analysis in urine and oral fluid, using IOSCD® (Yacoubian *et al.*, 2002), is shown in Table 1.6.1. It is essential to note here that the urinanalysis testing was carried out via EMIT while the oral fluid analysis was carried out via ELISA and therefore cannot be regarded as an infallible comparison.

Table 1.5.1 Agreement between urinalyses and oral fluid determination (%) using Intercept oral specimen collection device IOSCD®

Drug Tested	**Percentage agreement (%)**
Methadone	96
Cocaine	93
Opiates	96
Marijuana	89
Benzodiazepines	100

Yacoubian also reports that both the urinalyses and IOSCD® cost $10 per sample. However, the IOSCD was favoured by subjects and staff due to its small size, ease of use and minimal personal invasiveness.

One study reported by Kacinko *et al.* (2004), compared the sensitivity, specificity and efficiency of the Cozart® Rapiscan oral fluid drug test (Opiates CRS) to a microplate EIA oral fluid kit and to gas chromatography / mass spectrometry (GC/MS). The opiate CRS device is preset with a positive cut-off level of 30ng/ml. Three opiate ELISA cut-offs were used: 2.5, 30 (UK cut-off) and 40 ng/ml (SAMHSA proposed cut-off). Four opiate GC/MS cut-offs were used: 2.5, 15 (UK confirmation cut-off), 30 and 40 ng/ml. At current UK cut-off levels of 30 ng/ml and SAMHSA proposed levels of 40 ng/ml, sensitivity, specificity and efficiency were comparable. In cases where the higher cut-off was implemented there were a lower number of false negatives demonstrated. Performance characteristics of the opiate CRS were >96% and >91% when compared to the ELISA and GC/MS, respectively. (Cut-off levels were obtained from www.samhsa.gov).

A similar study was carried out while testing for cocaine. Biermann *et al.* (2004) reported on an immunological quantitative test device, toxiquick®. A 1-2ml oral fluid sample was taken, the test strip was submerged in the sample for approximately 10 seconds, read and recorded. Blood samples were taken in parallel and the serum results were analysed by GC-MS for comparison. False positives were < 10% for all drugs, including, amphetamines, methamphetamines, cocaine, opiates and methadone with the exception of cannabinoids which resulted in 20% false negatives. The authors conclude that positive results should be confirmed by serum analysis. This review has highlighted the major advantages of oral fluid testing including the ease of use and speed of analysis. However, with regard to this particular device, the police found that it was often difficult to read the result without getting a second and third opinion.

It is clear that the research into on-site OF testing is making positive progress over the past number of years. Very high false negatives (30% in some cases) were recorded when OF testing was compared to GC-MS for THC detection in earlier studies (Kintz, *et al.,* 1999; Samyn *et al.,* 2000). In 2006 the oraline® demonstrated very low numbers

of false negatives (<10%). Sensitivity and specificity of 69.2% and 91.6%, respectively, were shown when compared to GC-MS (Crimele *et al.,* 2006).

In a study carried out by Cone *et al.* (2002) oral fluid specimens were analysed by the Intercept MICRO-PLATE Enzyme immunoassay (EIA) (Orasure technologies, Bethlehem, PA). Relevant controls were provided including an interesting valid specimen control. This contained human antibody as a confirmatory control to demonstrate that the sample was of human origin. Oral fluid sample were analysed for IgG content and each specimen response was compared to the IgG calibrator value. Any specimen with an IgG concentration equal to or greater than the calibrator was deemed valid. The definition of a valid specimen is one that is human-derived and has an adequate volume for testing (Connell *et al.,* 1993). However, once the "presumptive positive" oral fluid specimens were identified, all samples were confirmed and quantified by GC-MS-MS.

The introduction of multi-analyte chip platforms into the drug detection arena is very exciting. There are a number of commercial kits that use this technology. Randox® have developed a biochip array technology system called evidence investigator™. The device enables simultaneous measurement of analytes using a single drop of sample on the biochip. This drugs of abuse array permits detection of 10 different substances including amphetamines, methamphetamines, cocaine, barbiturates, cannabinoids, benzodiazepines and opiates. Another company at the top of this field is the Cozart® group who in 2006, together with Philips Corporate Technologies, announced their intention to develop a new biosensor platform consisting of a microfluidic cartridge with an integrated magnetic biochip. The focus of their product development is the decrease of sample volume, testing time and size of the actual device. A number of other commercially available tests are compared and contrasted in Table 1.5.2.

Well - developed and defined immunoassay strategies, such as those mentioned previously, have paved the way for the development of recombinant antibody-based microarrays for drugs of abuse. Microarrays have already been exploited very successfully in the fields of both proteomics and genomics and are a potential lead-technology in point-of-care diagnostics. Antibody-arrays could be spotted onto plastic chips and used for multiple illicit drug detections. Careful selection/engineering of large antibody arrays would ensure high sensitivity and specificity and would eliminate false positives. The availability of a vast array of antibodies to interrogate any given sample would also provide a far greater chance of detecting 'newly developed' designer drugs of abuse. Integration of this approach with enhanced fluorescence signal amplification could provide significant improvements in sensitivity that may become of increased significance for the detection of new drugs having significant effects at very low concentrations. This array approach is particularly advantageous, as it offers high sensitivity, large sample throughput and low cost and is thus ideal for large screening programmes.

Table 1.5.2 Examples of commercially available drug testing kits

Company	Test name	Drugs tested and available cutoff (ng/ml)	Application	Comments	Reference
Cozart	Cozart DDS (Drug detection system)	Cocaine, 30; opiates, 30; methamphetamine, 50; and amphetamine, 50.	Roadside; workplace; criminal justice drug testing; Drug rehabilitation centres.	Assay time: Class A - 90 sec. Others - 5 min Principle: Lateralflow	www.cozartgroup .com
BMC™	Oratect plus	Cocaine, 20; opiates, 10; amphetamine, 25; methamphetamine, 25; and THC, 40.	Roadside;workplace; criminal justice drug testing; Drug rehabilitation centres.	Assay time: 7 min Principle: Lateral flow	www.Salivadrug .com
Avitar inc.	Oralscreen Drugometer	Marijuana, 500; cocaine, methaphetamine and opiates detected	Roadside; workplace; criminal justice drug testing; Drug rehabilitation centres	Assay time: 10 min Principle: Lateral flow	www.avitar.com
Orasure technologies Inc.	Intercept®	Cocaine, 5; opiates, 10; amphetamine, 40; methamphetamine, PCP, 1; Marajuana, 1 and MDMA detected	Only where an on-site result is not required.	Assay time: Days Principle: Microplate EIA (enzyme immunosassy)	www.4intercept .com
Varian Inc.	Onsite oralab	Cocaine, 20; opiates, 40; amphetamine, 50; methamphetamine, 50; PCP, THC, 100; and MDMA detected	Workplace; criminal justice drug testing; drug rehabilitation centres.	Assay time: 15 min Principle: Lateral flow	www.varianinc .com
Varian Inc.	Ontrack oratube	Cocaine, opiates, amphetamine, methamphetamine, PCP, and THC detected	Only where an 'on-site' result is not required.	Assay time: Days Principle: GC/MS	www.varianinc .com

1.6 Introduction to the immune system

The immune system consists of two major defence systems. Innate and acquired immunity. However, in reality these systems are closely integrated.

1.6.1 Innate immunity

The first of these systems is the innate immune response, innate immunity is present before any exposure to an antigen and is the bodies primary defence line against pathogens. It is largely non-specific but very fast acting in its response and is characterised by two separate elements.

I. Physical barriers such as skin, mucous membranes, secretions such as stomach acid, tears and sweat.
II. The internal chemical and cellular mechanisms, such as phagocytosis, antimicrobial proteins, inflammatory response and natural killer cells.

If the first barrier of physical defense is compromised the second component of the innate immune system takes over.

Phagocytosis: Phagocytosis involves the ingestion of invading micro-organisms by white blood cells known as phagocytes. There are 4 types of phagocytic cells, neutrophils, monocytes (macrophage), eosinophils and dendritic cells. Once engulfed by macrophage, microbes are destroyed in vacuole - lysosome fusion via lysosomal enzymes and other toxic compounds (this process is similar in other phagocytes).

Inflammatory response: Upon invasion, chemicals are released which signal increased blood flow, dilation and vascular permeability in the effected area. The resulting increased permeability allows for enhanced delivery of antimicrobial proteins and clotting elements. Increasing blood flow to the injured area also permits faster delivery of neutrophils and monocytes. One of the most active signalling chemicals is histamine which is released from mast cells.

Antimicrobial proteins: Antimicrobial proteins include the serum proteins that make up the complement system. Substances on the surface of microbes trigger the complement system leading to lysis of invading cells and inflammation.

Natural killer cells: Natural killer cells seek out cells that fail to display the major histocompatability complex (MHC) class I molecules and release apoptosis inducing chemicals.

The innate immune system is not described in detail as it is the exploitation of the acquired immune system which is the focus of this research.

1.6.2 Acquired Immunity

The major differentiaton between the innate and the acquired immune response is the specificity of the latter. The acquired response can be sub-divided into two categories:

I. Humoral response (mainly antibody production)
II. Cell-mediated response (mainly T lymphocytes)

The body is populated by two major types of lymphocytes; B lymphocytes and T lymphocytes (helper T cells and cytotoxic T cells). The combined effort of these two lymphocytes with input from antigen presenting cells (APC's) results in the secretion of soluble antibody into the blood stream. The humoral or antibody response involves the combination of both B-cell and Helper T-cell activation resulting in the production and secretion of soluble immunoglobulins into the blood stream. The cell-mediated response requires the activation of cytotoxic T-cells, which cause immediate cell death via apoptosis. The action of each of the T helper cell, T cytotoxic cell and B cell and how their co-operation is essential in the immune response is outlined in figure 1.6.2.1.

Cytotoxic T-cells directly kill cells that are infected with a virus or some other intracellular organism, preventing the spread of the microorganism before it has time to proliferate. Helper T-cells are crucial for stimulating responses to extracellular invaders such as, parasites or mycoplasma. They function by secreting cytokines which in turn

stimulate the action of macrophage and antibody-producing B cells. The T-cell response depends on the direct contact between the target cell and the surface bound TCR (T-cell receptor). Unlike the B-cell antigen receptors the TCR are not secreted.
The T-cells only activate when foreign antigen peptides are displayed in association with an MHC molecule. The MHC molecule is critical in the immune response and as such T-cell responses are said to be MHC restricted. The MHC molecules can be subdivided into two categories; MHC class I and MHC class II.

MHC class I: Collect peptides derived from proteins synthesised in the cytosol and display fragments of these proteins on the cell surface awaiting contact with the Cytotoxic T-cell. MHC class I have the ability to bind self-peptides acting as a monitor for the immune system.
MHC class II: Bind peptides derived from proteins in intracellular membrane bound vesicles and display peptides from pathogens living in marcophage vesicles or internalised by phagocytic cells.

1.6.2.1 Antigen presentation by MHC class II molecules

MHC class II molecules are primed for action once they are synthesised. Upon synthesis in the lumen of the endoplasmic reticulum they are transported together with an additional invariant chain to the endosome containing the antigen of interest. After antigen collection from the endosome the MHC molecule carries it to the surface of the cell where the peptide can be recognised by the $CD4^+$ T-cells. This is the primary differentiation between the $CD4^+$ and $CD8^+$ T-cells. Instead of directly killing the cell via apoptosis, the $CD4^+$ T-cells trigger a signalling cascade resulting in the release of numerous cytokines.

The $CD4^+$ helpher cells are further subdivided, depending on the origin of the antigen presenting cell, into T_H1 and T_H2. (The T_H1 pathway is primarily responsible for the

cell mediated immunity and not the humoral response and is therefore not as important in this discussion).

T_H2: is essential for the humoral immune response and secretes a number of cytokines inlucding IL-4, IL-5, IL-10 and IL-13. These cytokines are key to class switching in B-cells, for IgE production, positive feedback devices promoting more T_H cells to enter the T_H2 pathway and activation of eosinophils.

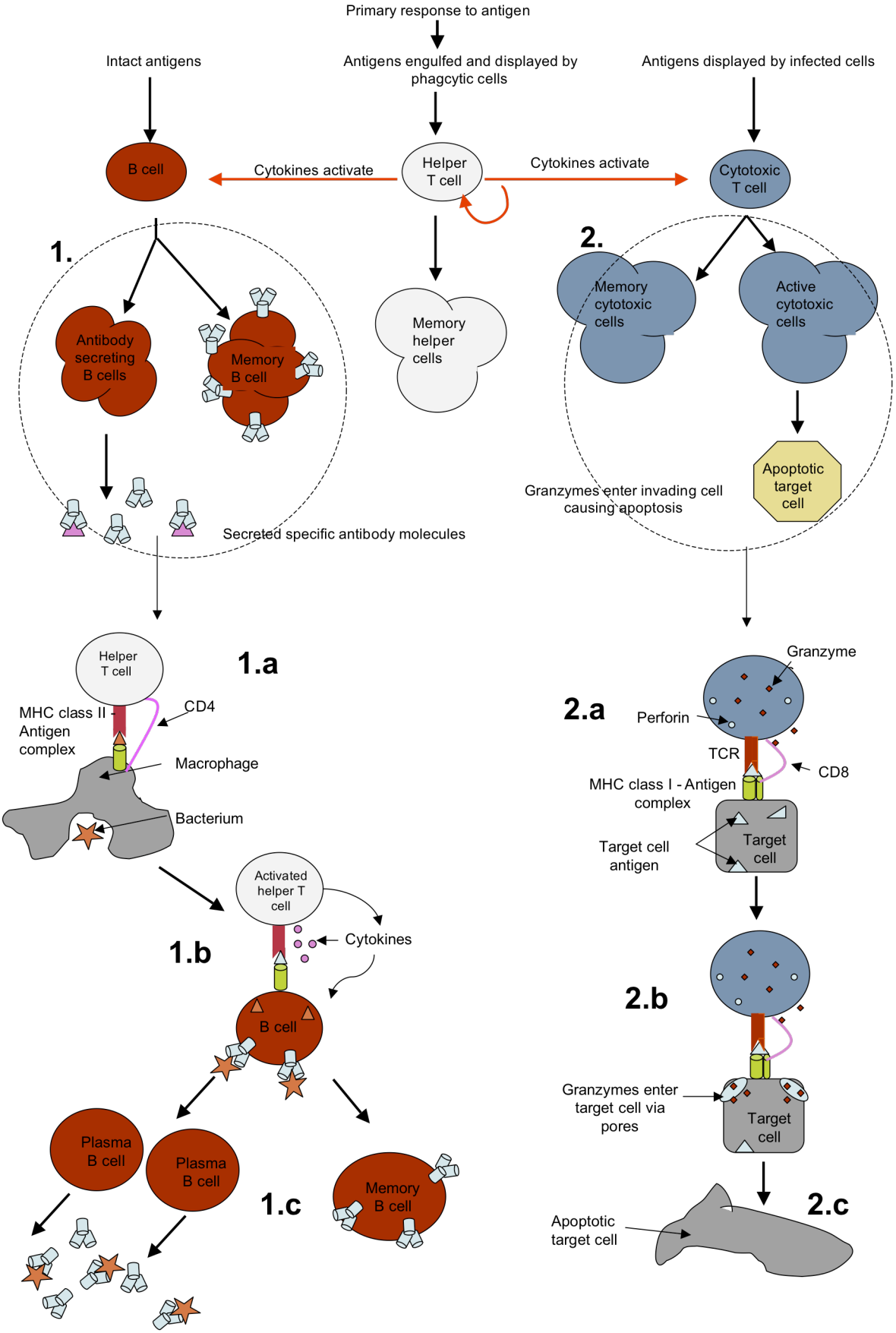
Primary response to antigen
Intact antigens
Antigens engulfed and displayed by phagcytic cells
Antigens displayed by infected cells
B cell
Cytokines activate
Helper T cell
Cytokines activate
Cytotoxic T cell
1.
2.
Antibody secreting B cells
Memory B cell
Memory helper cells
Memory cytotoxic cells
Active cytotoxic cells
Apoptotic target cell
Granzymes enter invading cell causing apoptosis
Secreted specific antibody molecules
Helper T cell
1.a
MHC class II - Antigen complex
CD4
Macrophage
Bacterium
Activated helper T cell
1.b
Cytokines
B cell
Plasma B cell
Plasma B cell
1.c
Memory B cell
Granzyme
2.a
Perforin
TCR
CD8
MHC class I - Antigen complex
Target cell antigen
Target cell
2.b
Granzymes enter target cell via pores
Target cell
2.c
Apoptotic target cell

Figure 1.6.2.1 A schematic representing the overall acquired immune response is shown.

An overview of the acquired immune response is illustrated in 1. Upon activation, the helper T cells stimulate the hummoral response directly and indirectly, by contact with B cells and secreting cytokines, respectively. A more detailed illustration of the action of the B cell is presented in 1a – 1c and the action of the cytotoxic T cell in 2a – 2c.

(1a) The invading bacteria is engulfed and degraded by the macrophage thus displaying the foreign peptide antigen along with the MHC class II on the cell surface. (1b) Once activated, the helper T cells, which recognise this display, binds to the B-cell via specific receptors. The B-cell is now activated. (1c) The activated B-cell proliferates into both memory and antibody-secreting plasma B cells. The antibodies secreted are specific to the antigens of the original engulfed bacteria.

(2a) The active cytotoxic T-cell comes into contact with the MHC class I – antigen complex, leading to T-cell activation. (2b) Perforin molecules and proteolytic enzymes are released from the T-cell, the granzymes enter the target cell via the newly formed pores. (2c) Apoptosis is initiated and cell death occurs immediately.

1.7 Antibody structure

An antibody molecule is organised into three structural units. The two Fab units are responsible for antigen binding while the third unit, the Fc portion, is involved in complement triggering and cell receptor binding. The whole molecule is made up of 4 chains, two identical light chains which span each Fab portion and two identical heavy chains spanning the whole molecule.

There are five classes of immunoglobulin, IgG, IgM, IgA, IgD and IgE. IgM is the first class of antibody to be produced in the primary immune response.

- IgM's are pentamers therefore demonstrate high avidity for multimeric antigens which may mask their often low affinity.
- IgA exist as both monomers and dimmers. IgA are responsible for defending the externally exposed areas of the body and exist in abundance in saliva, sweat, tears, gastrointestinal tract and the nasal passage.
- IgD acts as the antigen receptor / cell surface receptor on B cells.
- IgE is responsible for initiating the inflammatory response and is present at only low levels in normal circulation.
- IgG is the most abundant class of antibody produced (Roitt *et al.,* 1994). In IgG, the Fab arm is linked to the Fc portion via a polypeptide chain called the hinge. The IgG subclasses are distinguishable in this hinge area. These subclasses are IgG1, IgG2, IgG3 and IgG4 in humans and IgG1, IgG2a, IgG2b and IgG3 in mice.

Commercial immunoassays for small haptens are mostly reliant on whole monoclonal or polyclonal antibodies rather than recombinant antibody fragments. Antibody fragments very often have lower affinity than there full size parental antibodies (Huston *et al.,* 1996). To combat this, specifically tailored panning strategies and *in-vitro* affinity

maturation of anti-hapten antibody fragments are employed (section 1.9.4, 1.9.5 and chapter 5). Recent advances in recombinant antibody technology have permitted the increased exploitation of scfv and Fab fragments over whole IgGs for commercial detection kits etc. (Chames *et al.,* 1998; Li *et al.,* 2000; Charlton *et al.,* 2001). These smaller molecules retain the specificity of the larger whole antibody molecule but can be engineered for superior performance and unique applications (Holliger and Hudson, 2005).

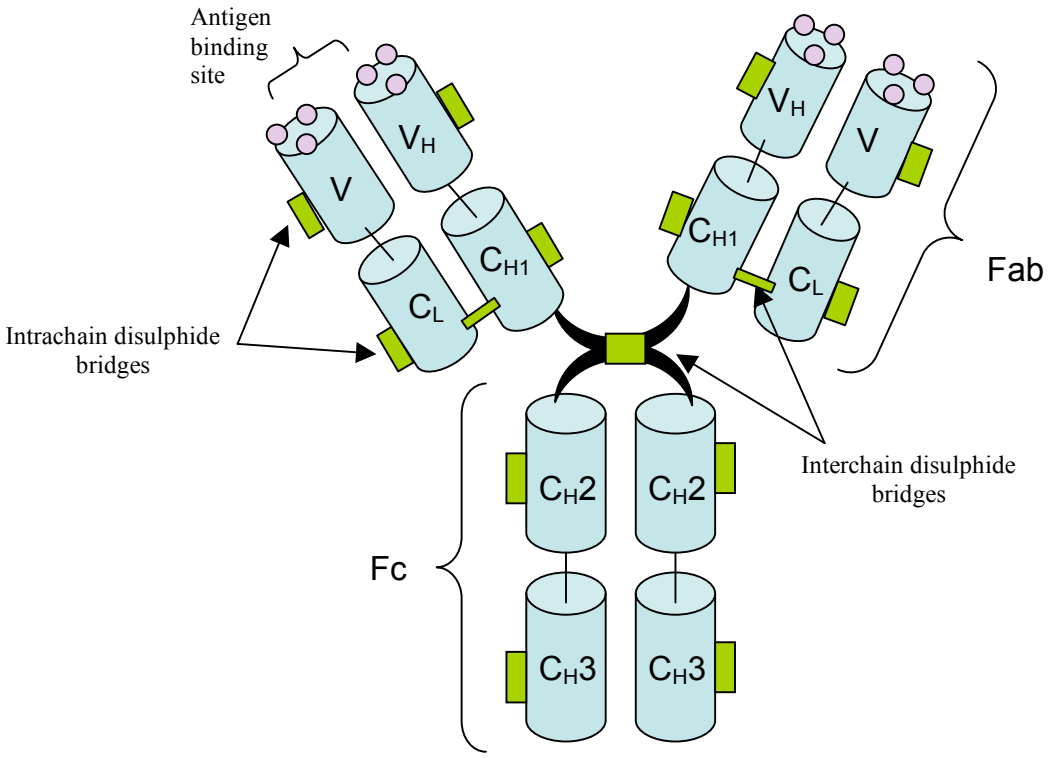

Figure 1.7.1 Structure of whole IgG molecule with domain nomenclature. Each heavy chain is folded into two domains in the Fab arms. The light chain forms two domains which only associate with the Fab arms. The heavy chains are composed of V_H, C_H1, C_H2 and C_H3 domains. The light chains are composed of V_L and C_L domains. All domains are paired except the C_H2 domain. Each domain has a molecular weight of roughly12,000 depending on the specific antibody. Each Fab is 50,000 and each whole IgG molecule is 150,000 daltons in weight.

1.8 Generation of antibody diversity.

The DNA encoding immunoglobulins is found in three unlinked gene groups

1. κ L-chain
2. λ L-chain
3. H-chain

Kappa and lambda chain genes are located on chromosome 2 and chromosome 22, respectively, and heavy chain genes are located as a gene family on chromosome 14. The κ L-chain group has one gene segment encoding the constant (C) κ regions. The λ L-chain group has 4 gene segments encoding the constant (C) λ regions. The H-chain variable region is encoded by V (variable), D (diversity) and J (joining) gene segments while the L-chain is encoded by just V (variable) and J (joining) gene segments. Regions of highly conserved amino acids are interrupted by three separate regions of highly variable segments known as the complementarity determining regions (CDR's) The CDR's interact forming the point of antigen contact of each antibody. VL and VH germline segments encode two CDR's each. The third CDR is made up by the recombination of the VJ (VDJ in the case of heavy chains) region, thus it is this CDR that is widely regarded as having the most variability (Alt *et al.*, 1987).

During B-cell development it randomly chooses from its H-chain gene group one V, one D and one J gene segment for translocation. It then selects from the λ or κ gene group one V and one J for gene translocation. This means the genes are brought into close contact with each other through a looping out process, mediated by lymphoid-specific recombinase enzyme complex (Roth and Craig, 1998). The first step involves bringing the D and J regions in contact, thus looping out the intervening DNA. The second recombination step involves bringing the V regions in contact with the DJ regions. This final recombination step determines the antibody specificity (figure

1.8.1). However, it is the constant regions which determine the isotype/class of the antibody produced.

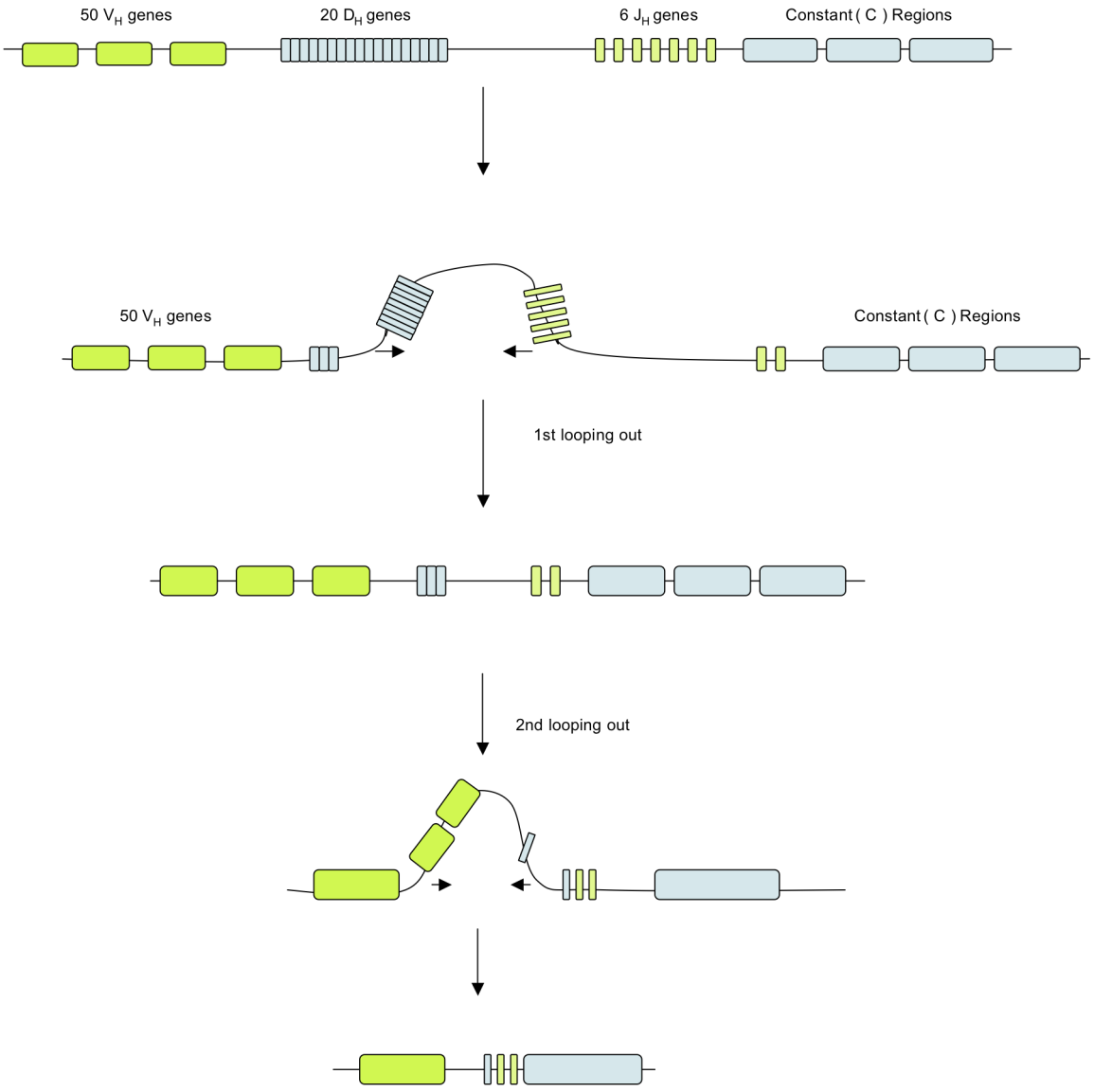

Figure 1.8.1 Schematic representation illustrating the recombinational arrangement of the DNA encoding V (variable), D (diversity) and J (joining) and C (constant) gene segments. The coding mechanism determines the antibodies specificity and the constant region chosen determines the isotype of the antibody produced.

1.8.1 Somatic hypermutation

Somatic hypermutation (SHM) introduces further diversity into the antibody sequence and occurs at a rate of 10^{-5} to 10^{-3} per base per generation over the lifespan of the B-cell (Li *et al*., 2004). These mutations are predominantly point mutations in the V(D)J unit of the antibody V genes that occur in mutation hotspots. It is as a result of this process that antibodies with increased affinities for the target antigen are produced (Benjamini *et al.,* 2000). The exact mechanism of SHM is not fully understood, however, recent experimental evidence supports the theory that activation-induced cystidine deaminase (AID) is key to the process (Poltoratsky et al. 2000) It is thought that deamination of cytosine to uracil in DNA by AID precedes the activity of UNG, a uricil DNA glycosylase, creating single base mutations in place of the uricil residues (Petersen-Mahrt *et al.,* 2002) The uracil bases are removed by the repair enzyme, uracil-DNA glycosylase. Error-prone DNA polymerases are then recruited to fill in the gap and create mutations. Such mutations, in the rapidly proliferating B-cells, result in the production of thousand's of B-cells possessing various specificities. The highest affinity antibody expressing B cell can then be selected and proliferated.

Further genetic rearrangement of antibody genes gives rise to the antibody class. Ultimately, this process allows the expression of an antibody with an antigen-specific binding site but with different C region genes. Thus giving rise to antibodies with a single antigenic specificity but with different effector functions.

Overall, antibody diversity is generated by means of both

- Antigen independent events
    - The availablitly of multiple germline genes
    - The random combination of V, D and J segments for the H-chain or V and J segments for the L-chain.
    - Pairing of different combinations of V_L and V_H chains occuring randomly.

- Antigenic dependant
    - At DNA level where somatic mutation can lead to higher affinity antigen recognition and binding.

Somatic affinity maturation processes play a major role in the design of *in-vitro* recombinant antibody affinity maturation strategies, this is outlined in greater detail in chapter five.

1.8.2 Antibody fragments: Single chain Fv and Fab fragments

To date, hybridoma technology involving immunizations is still the most widely used method of antibody generation (Persson *et al.,* 2008). However, since the first cloning of antibody repertoires in the last 20 years, (Huse *et al.,* 1989; Ward *et al.,* 1989) and the successful production of antibody fragments in bacteria, (Skerra and Pluckthun, 1988) phage display (see section 1.9) as a powerful tool in antibody generation has come forward (Hust and Dubel, 2004). Constant regions, as shown in figure 1.9.1, are fundamental to the biological effector function of the antibody, however, antibody manipulation for use in diagnostics and therapeutics can be achieved through fragmentation of the whole molecule. A whole antibody can be broken into several fragments. Recent advance in molecular engineering techniques have facilitated the production of antibody fragments via methods other than enzymatic or chemical cleavage. Recombinant antibody technology has permitted the production of antibodies from a variety of species such as mice (Dillion[B] *et al.,* 2003), rabbits (Li *et al.,* 2000), chickens (Andris-Widhopf *et al.,* 2000) llama, (Yau *et al.,* 2003) and sharks (Dooley *et al.,* 2003). A number of antibody fragments can be produced using recombinant antibody engineering, including Fab, scFv and Fv. The Fv fragment is the smallest fragment which comprises the complete antigen binding site, one V_L with 3 CDR's and one V_H with 3 CDR's. While Fab and Fc fragments can be cleaved off the whole molecule and remain relatively stable this is not the case with the smaller Fv region. This Fv fragment is not sufficiently stable for use in immunoassays etc. as it lacks the

stabilizing disulphide bond or serine glycine linker present in the Fab and scFv, respectively, (Glockshuber *et al.,* 1990). A linker is usually introduced between the V_H and V_L to produce a single-chain Fv (scFv). This results in improved folding and stability (Freund *et al.,* 1993). This linker can be incorporated in either of two orientations V_H - linker - V_L or V_L - linker - V_H. The linker can also vary in length, the longer linker (20 amino acids) giving a higher proportion of monomeric molecules while a shorter length linker (5 amino acids) favors dimeric scFv formation. The CDR is the smallest antibody capable of binding to an antigen, however, it is completely impractical for use in immunanalysis. Scfv's are the smallest useable antibody fragment as they contain the complete antigen-binding site (Brichta *et al.,* 2005). Antibody fragments (Figure 1.8.1.1) generally have lower avidity than the whole molecule, however, small molecules have improved pharmacokinetic properties due to their shorter retention times, more efficient target tissue penetration and clearance (Colcher *et al.,* 1998).

Figure 1.8.1.1 Monovalent antibody fragments capable of binding antigen. (a) CDR,

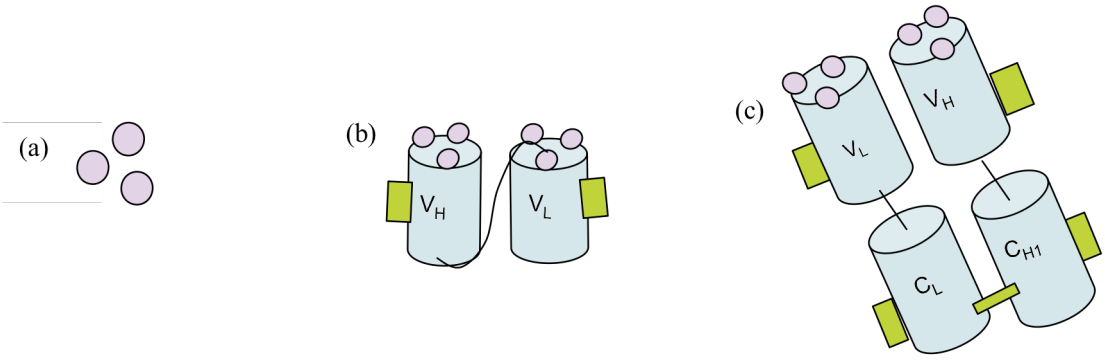

smallest fragment capable of antigen recognition, (b) scfv and (c) Fab.

In the research described in this thesis both scFv (b) and Fab (c) fragments are developed against a number of different target antigens since there is an ongoing debate

as to which structure is the more advantageous. The scFv library construction is simplified due to the single overlap extension PCR required. The smaller scFv fragment has the ability to multimerise which can enhance avidity for antigens. However, if later attempts are made to improve the affinity of the antibody, improvement may arise from changes in the multimerisation rather than improvements in the affinity of the antibody combining site. scFvs are expressed very efficiently in *E. coli*. However, the Fab construct is also a very stable, well characterised protein fragment. They do not generally multimerise which means that they can be converted to whole antibody format while maintaining or improving antigen affinity. Improvements in affinity via *in vitro* methods of the Fab construct generally results from improvements in antigen binding sites and are not simply due to multimerisation of the antibody fragment as is often the case with scFv's. The most significant disadvantage of working with Fabs is their general lower expression levels in *E. coli*.

1.9 Phage Display

Filamentous bacteriophage are a group of viruses that only infect bacteria and are not capable of human infection. They are made up of two components, consisting of genetic material and a protein coat. Phage contain a circular single-stranded DNA genome encased in a long protein capsid cylinder. Filamentous bacteriophage infect *E. coli* via pili formed as a result of the bacteria harboring the F` factor encoding proteins. It is, therefore, necessary to select for the bacteria harbouring this F` factor as it tends to separate from the cells rendering them insensitive to infection by the phage.

The Ff phage particle is approximately 6.5 nm in diameter and 930 nm in length (Barbas *et al.,* 2001). Each of the bacteriaphage genomes encodes 11 genes. pVIII, the major coat protein, makes up nearly the entirety of the capsid. The minor capsid proteins pIII and pVI which make up the infecting tip of the phage particle are present in several copies. The pIII is made up of three distinct domains each linked together via glycine rich regions. Figure 1.9.1 illustrates the display of the recombinant antibody fragment on the pIII. The first domain (N2) is required during the infection process for translocation of the DNA into the cytoplasm. The second domain (N2) is involved in binding to the F pilus of the bacteria. pVII and pIX cap the other end of the phage capsid, with all capsid proteins being integral cyctoplasmic membrane proteins prior to assembly (Simons *et al.,* 1981; Endemann and Model, 1995 ; Webster, 1996). Infection is reported to be a multistep process requiring interactions with the F conjugative pilus and the bacterial TolQ, R, and A cytoplasmic membrane proteins. These are bacterial proteins that appear necessary for maintaining the integrity of the bacterial outer membrane (Lazzaroni *et al.,* 1999). Assembly also requires three non-capsid phage-encoded proteins, pI, pIV and pXI. ATP and bacterial thioreductase are also necessary in the elongation process during assembly.

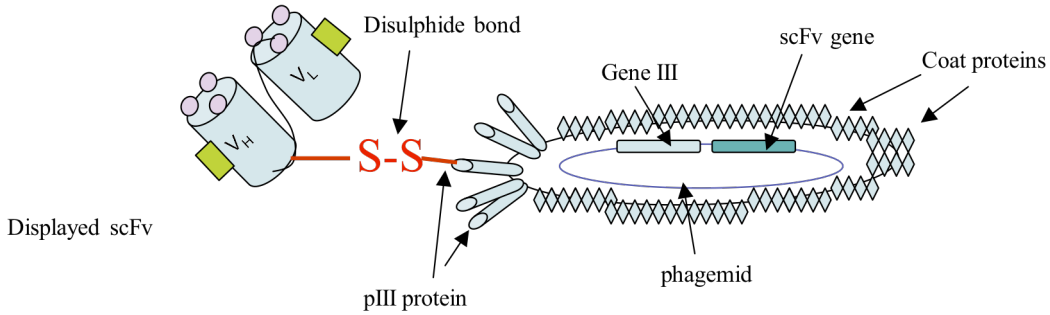

Figure 1.9.1 A schematic illustration of the disulphide bond between the pIII at the tip of the phage particle and the displayed recombinant antibody fragment

1.9.1 Infection

Infection begins with the binding of one end of the phage to the conjugative pilus. The pilis is recognized by the N2 amino terminal of gene III. Once this recognition has occurred the pilus retracts bringing the pIII end of the phage particle closer to the surface of the bacterium. The extent of this retraction or exactly how it works is not known (Lubkowski *et al.,* 1999). The chromosomal Tol Q, Tol R and Tol A genes are required to integrate the capsid protein into the bacterial cytoplasmic membrane and to translocate the DNA into the cytoplasm. Tol Q, R and A proteins are part of the Tol system which maintains outer membrane integrity in *E. coli.* Tol Q has three transmembrane helices in the cytoplasmic membrane. Tol R is present in the periplasm with its amino terminus embedded in the cytoplasmic membrane. Tol A has three domains with each domain joined by a glycine rich region. The amino terminal, domain 1, anchors Tol A in the cytoplasmic membrane. The central region, domain 2, basically consists of a long helical region connecting D1 and D3. The carboxyl terminal, domain 3, interacts with the outer membrane for activity (Click and Webster, 1997). The N1 domain of the pIII protein is thought to interact with D3 bringing the outer and inner membranes into closer proximity. The N2 domain then also interacts with D3 resulting

in the insertion of the pIII protein into the inner membrane. The phage genome can then by translocated into the bacterial cytoplasm host cell. (Karlsson *et al.,* 2003).

1.9.2 Replication and Assembly

Once the viral DNA is in the cytoplasm it is acted on by bacterial enzymes resulting in covalently closed, supercoiled, double stranded DNA called the parental replicative form (RF) DNA. Translated phage proteins are replicated via the 'rolling-circle' mode of replication. During assembly the viral DNA is extruded through the membrane and concomitantly enveloped by coat proteins (Weiss and Sidhu, 1997). The ends of the virion particle are capped with the four minor coat proteins - III, VI, VII and IX. The entire surface is coated with pVIII, it has been shown that both pVIII and pIII accommodate polypeptide fusion at their amino terminal. It is this physical linkage between phenotype and genotype that is exploited in phage display technology.

1.9.3 Phagemid vectors

In the past the DNA of interest was cloned directly into the whole phage genome. However, it is now possible to clone into a phagemid vector instead. A phagemid is a plasmid that contains a phage-derived origin of replication (major intergenic region) as well as its own plasmid origin of replication and it can be packaged in the phage coat. A phagemid can not produce infective phage particles alone. Phagemids are packaged as phage particles in the same fashion as phage DNA itself as long as they are propagated in cells which are superinfected with helper phage. Helper phage provide all the necessary phage-derived proteins and enzymes for phage replication. However, the helper phage posses a modified intergenic region, causing it to be replicated and packaged less efficiently than the wild type. This ensures that the genotype-phenotype are produced in the same single phage.

1.9.3.1 pComb3XSS vector used for anti-amphetamine Fab construction

The pComb3 phagemid vector series is a well-established system for phage display (Barbas *et al.,* 1991). The pComb3 vectors are designed to express antibodies and other proteins on the surface of phage and also to express these proteins in soluble form.

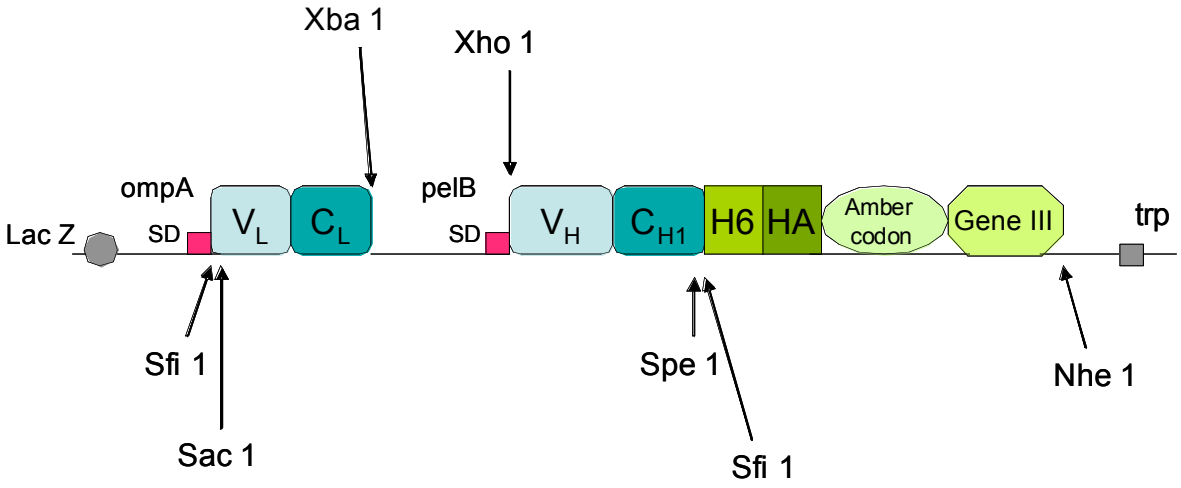

Figure 1.9.3.1.1 Map of the cloning regions of the pComb3X phagemid vector. The single lac Z promoter allows expression of the whole light and heavy chains. The presence of two Shine Dalgarno (SD) gives rise to separate polypeptide chains. A trp terminator provides transcription termination. The leader sequence ompA directs light chain to the periplasm while the pelB leader directs the heavy chain and coat protein III. The amber codon permits soluble expression of the protein in nonsuppressor strains of bacteria. The six-histidine tag allows for IMAC purification and the hemagglutinin tag permits detection of the protein via the use of an anti-HA secondary antibody during screening.

The pComb3X vector has a number of important aspects that make it suitable for Fab display in particular. This vector was an improved design based on the original phagemid vector pComb3.

- Instead of the original repeated *lacZ* promoter and *pelB* leader sequences it uses just one lac promoter followed by a combination of ompA and pelB. This directs expression of antibody light chain and heavy chain-pIII fusion proteins, respectively.
- pIII has a huge impact on the phage display system. It was discovered to be 406bp which, in its full-length form, causes immunity to superinfection by helperphage. Therefore a truncated pIII, aa203-406, fragment is used which serves as the fusion partner for the displayed proteins. Phage display vectors are classified according to the coat protein used and the number of coat protein genes present. PComb3X belongs to type 3 + 3. Varying numbers of wild-type pIII can be displayed on their surface due to the two types of pIII; wild-type, produced by the helper phage and the fusion protein produced by the phagemid. These two pIII's compete for incorporation during phage assembly (Barbas *et al.,* 1991).
- 6-Histidine (HIS) tag permits protein purification via IMAC.
- Hemagglutinin (HA) tag facilitates detection using the highly sensitive secondary antibody, anti-HA
- An amber condon has been inserted between the Sfi 1 restriction site and the 5' end of the gene III fragment allowing for soluble expression in non-supressor cells without removing the gene III. When phage are grown in *SupE,* suppressor strains of *E. coli,* the amber codon is read as a glutamine and the antibody fusion protein is displayed on the phage. In non-supressor strains of *E. coli* the same amber codon is read as a stop codon and soluble antibody is secreted.

Sfi 1 restriction sites, allow insertion of the gene of interest in the correct orientation and facilitates the design of large libraries with minimal steps.

1.9.3.2 pAK 100 and pAK 400

The pAK vector system (Krebber *et al.,* 1997) is designed to aid purification, detection, multimerisation and modification and can be used for both phage display and antibody expression. The pAK system was designed for scFv expression. A variety of vectors, pAK 100, 200, 300, 400, 500 and 600 are available for use with the Krebber system. The vectors used in this research were the pAK 100 and pAK 400.

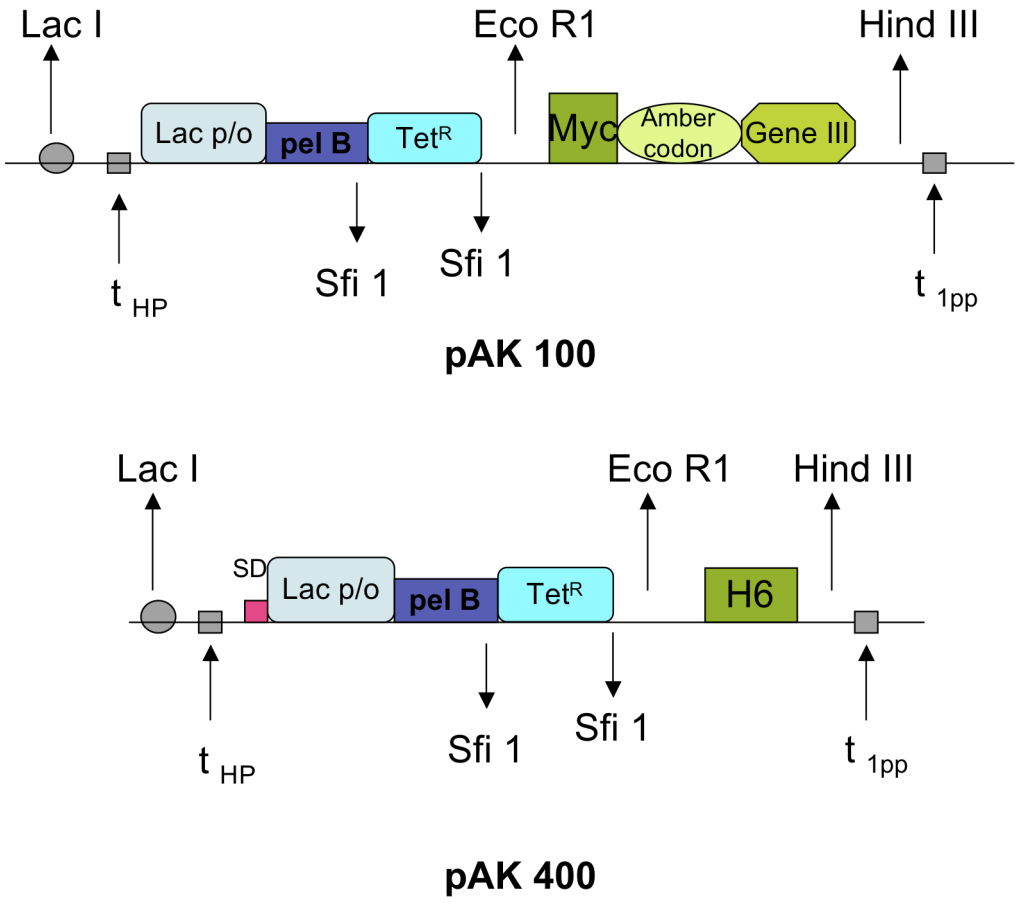

Figure 1.9.3.2.1 Map of the cloning regions of the pAK 100 and pAK 400 phagemid vectors.

There are a number of important design features of this phagemid vector series;

- Like the pComb series, it uses the very rare cutting restriction enzyme - *Sfi 1*. This restriction site is very rarely found in antibody genes.
- The tetracycline resistance cassette (Tet^R) present in all pAK vectors ensures identification of sufficiently cut vector. Uncut vector contamination is a common contamination of antibody libraries, with the loss if Tet resistance in efficiently cut vector, contamination is easily avoided.
- It contains the truncated version of gene III as was discussed previously in relation to the pComb3 vector series.
- The *lacI* repressor gene is encoded on the vector to ensure strain independent lac promoter repressor.
- The strong upstream terminator t_{HP} together with the inclusion of glucose eliminates any background expression.
- The synthetic Shine-Dalgarno sequence in combination with a pelB leader sequence permits only moderate levels of expression.
- Despite the pAK 100's ability to allow soluble expression (albeit low levels) pAK 400 has been designed for compatible high level expression via the stronger Shine-Dalgarno ($SDT7_g10$).
- pAK 400 permits IMAC purification via the 6-His tag.

1.9.4 Construction of a hapten-specific phage display library

A phage display antibody library consists of recombinant antibody fragments displayed on the surface of phage. Antibody genes are isolated from the spleen, bone marrow, hybridoma cell line, a naïve or synthetic source and fused to the phage genome (Hoogenboom *et al.,* 1998; Sheedy *et al.,* 2007). Naïve genetic material has no prior exposure to the antigen of interest while the immune library is generated from lymphocytes of an animal immunised with the antigen of interest (Marks *et al.,* 1991). The genetic material coding for the antibody (phagemid vector) is engineered so that the phage partical posesses both the individual genotype (gene) and phenotype (displayed protein) (Schmitz *et al.,* 2000). After construction, the library is exploited for isolation of hapten-specific antibody fragments a process known as "bio-panning" (see section 1.9.5). It has been reported that antibodies selected from naïve libraries have significantly lower affinities than those from immune libraries (Charlton *et al.,* 2001). The affinity is comparable to that of a primary immune response as the synthetic or naïve fragments have not undergone somatic hypermutation and other *in vivo* maturation steps. Li *et al.* (2000) reported anti-herbicide antibodies posessing sub-nanomolar affinities from a hapten-specific immune library. Such affinities are achieved through development of a suitably stringent and specifically tailored panning strategy. This is discussed in section 1.9.5 and also throughout all chapters in this thesis.

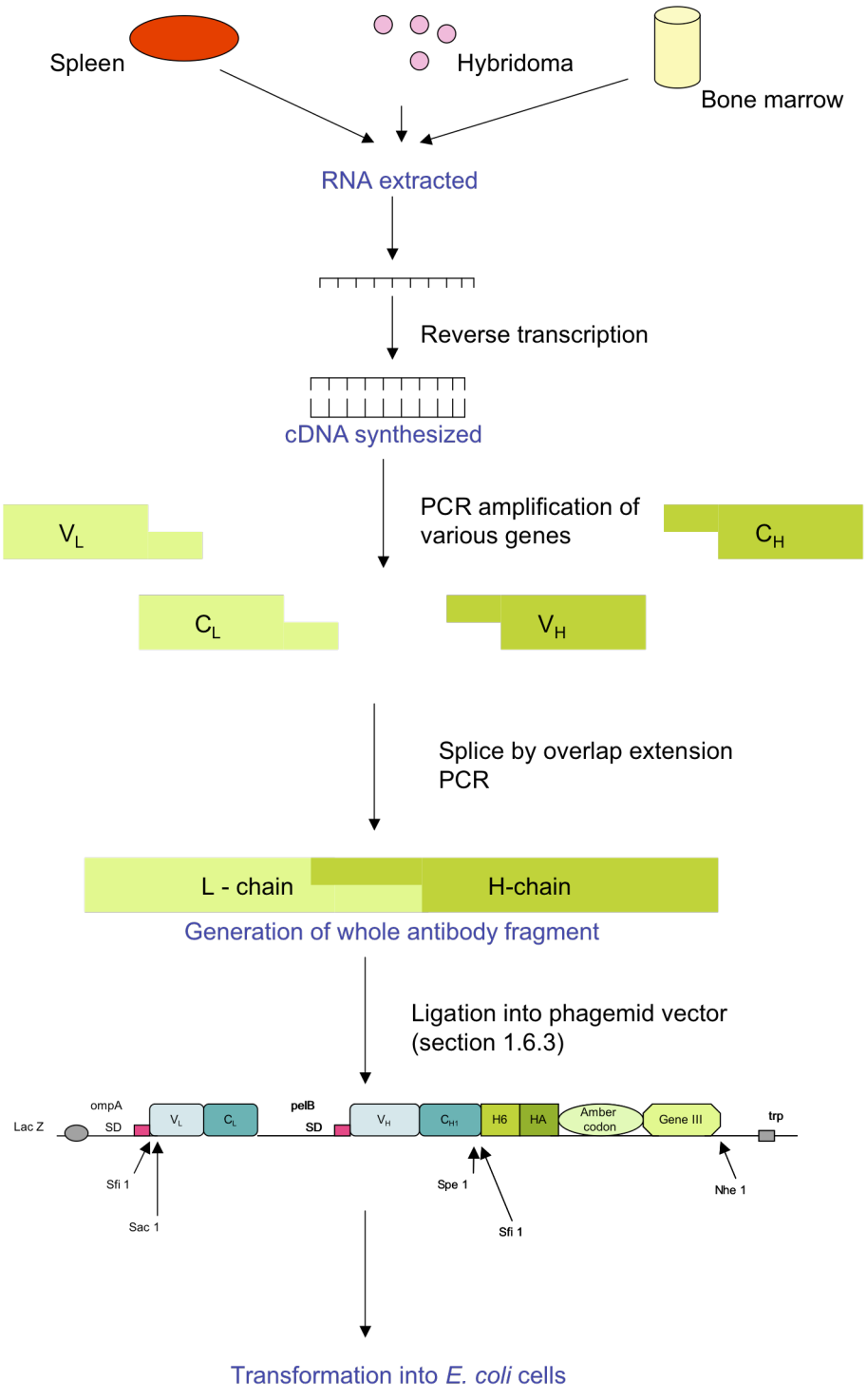

Figure 1.9.4.1 Schematic representation of a phage display library construction.

1.9.5 Phage-display for the selection of hapten-specific antibodies

The design of an appropriate panning strategy is essential for the isolation of any recombinant antibody fragment with optimal affinity and binding specificity for the target antigen. Phage selection through panning depletes the population of non-specific phage displaying clones while enriching the repertoire of clones harboring specific binding capabilities for the target antigen. The genetic material of the antibody is engineered so that it is included in the viral genome but also displayed on the surface of the phage particle (Schmitz *et al.,* 2000) A commonly used biopanning strategy is carried out on solid surface immobilized antigen, either on immunotubes (Krebber *et al.,* 1997) or microtitre wells (Barbas *et al.,* 2001). Methods other than solid phase panning include the use of streptavidin-coated magnetic beads for immunomagnetic separation of specific phage from non-specific phage pools (Santala and Saviranta, 2004).

Immune libraries are widely reported as the optimal source of anti-hapten antibodies where selection is carried out against the hapten-protein conjugate. Various modifications to the panning protocal are introduced to enchance the enrichment of positive clones:

- Decrease conjugate coating concentration from one round to the next round (Lu *et al.,* 2003).
- Increase washing times between successive rounds of panning (Lu *et al.,* 2003).
- Subtractive panning (the phage pool is preincubated with the carrier protein prior to incubation with the hapten-protein conjugate) (Chames *et al.,* 1998; Barbas *et al.,* 1993).
- Competition elution with free hapten (Chames *et al*., 1998).

After panning strategies have been optimized the next step in obtaining anti-hapten antibodies with high specificity is *in vitro* affinity maturation. Recombinant antibody engineering methods will be introduced and discussed in chapter 5.

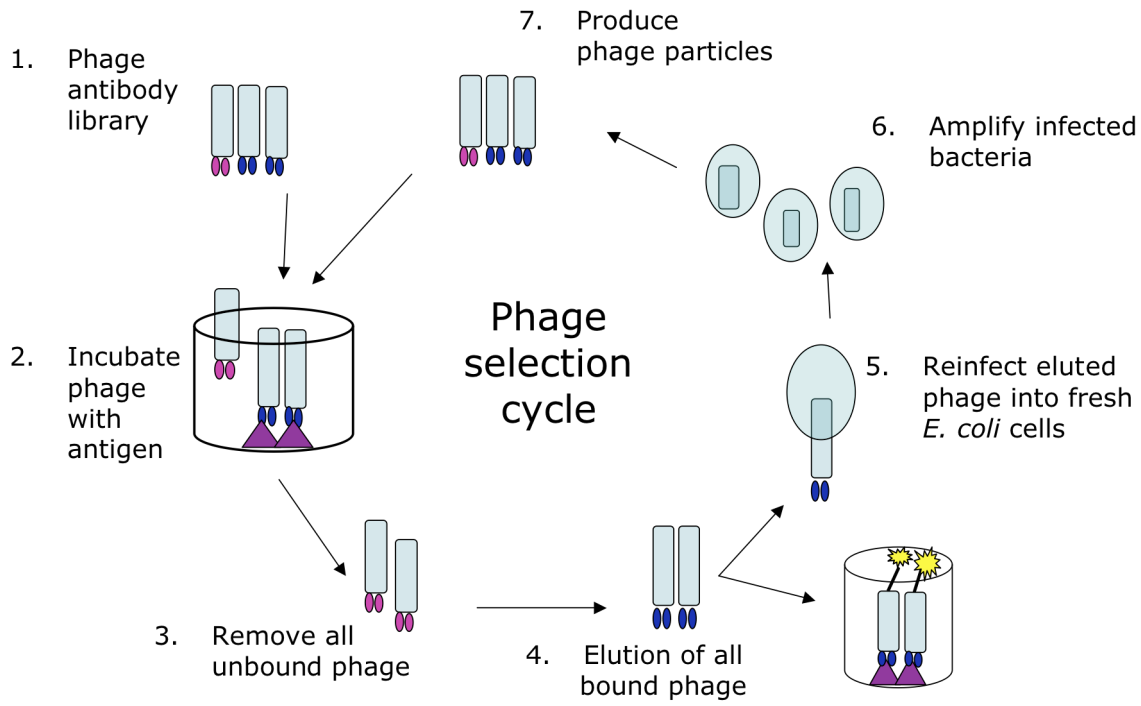

Figure 1.9.5.1 Schematic illustration of a typical phage selection process for the enrichment of antigen-specific phage clones. The phage library is incubated with the target antigen on a solid support surface. Phage that display antigenic-specific antibodies bind to the target surface while all non-specific antibody displaying phage are removed by washing. Elution of positive phage is achieved via various chemical additions. The positive phage are re-infected into *E.coli* for further rounds of selection and enrichment. Phage pools are analysed by polyclonal phage ELISA and individual clones are analysed by monoclonal phage ELISA.

1.10 Research aims

The main aim of the work presented in this thesis was the production of novel genetically – derived antibody fragments for the detection of the illicit drugs. The work describes the production characterisation of recombinant antibodies using phage display technologies against Morphine-3-glucoronide, amphetamine and tetrahydrocanabinnol. for immobilisation for future use on a low density microarray platform technology.

An anti-morphine-3-glucoronide Fab fragment was constructed using the previously reported anti-M3G scFv fragment as a template (Brennan *et al*, 2003). This Fab fragment was characterised and used in comparison studies with the scFv fragment in Biacore competitive and kinetic analysis studies (Chapter 3). This study revealed the importance of antibody fragment choice i.e. scFv or Fab and screening method for large libraries of potential clones. This study also facilitated a puplication in Biosensors and Bioelectronics.

Genetical material for an anti-amphetamine Fab fragment construction was sourced from a pre-existing anti-amphetamine IgG-secreting hybridoma (Fanning, 2001) in chapter 4. This Fab fragment was applied to the development of both ELISA and Biacore competitive studies. Comparison studies between the Fab and the parent monoclonal antibody illustrate a 3 fold improvement in affinity after conversion to Fab. An scFv library was constructed from the parent Fab DNA however no specific antibody was found, this is discussed in detail.

Several *in-vitro* affinity maturation strategies were examined in chapter 5. The study focused on improving the anti-M3G Fab fragment. Specific CDR's in the heavy and light chain were targeted. "Wild-type eliminating" and "mutated" phage display libraries were generated using a combination of the Kunkle style mutagenesis and the

commonly used oligonucleotide doping strategy NNK and NNS. An anti-M3G specific mutant was successfully selected and characturised. This work was exceptionally interesting given the current lack of progress on mutationally improving anti-hapten antibodies such as those described in this thesis.

Chapter 6 describes the construction of an anti-tetrahydrocannabinol scFv immune library. The genetic material was extracted from a leporine spleen which had been exposed to the drug-protein conjugate. Soluble scFv antibodies were isolated, espressed and purified from the library. A mutant phage display library was generated using a positive scFv-secreting clone as the heavy chain template and light chain shuffling was employed to optimise heavy – light chain pairing. Selected clones were compared through sequencing and affinity analysis. A multi analyte assay was set up on the biacore 3000 using the anti-M3G and anti-Amphetamine Fab fragments and also the anti-THC scFv fragment.

Chapter 7 provides a summary of research, conclusions and some proposed future work.

Chapter 2

2.0 Materials and Methods

2.1 General Formulations

2.1.1 Reagents

All reagents and antibodies were of analytical grade and purchased from Sigma-Aldrich Chemical Co. (Poole, Dorset, England), unless otherwise stated.

Reagents	**Supplier**
DNA Purification System Wizard Mini Prep Kit	Promega Corporation, 2800 Wood Hollow Rd., Madison, WI 53711-5399, USA.
Cy 5 reactive dye	Amersham Pharmacia Biotech AB, SE-751 84, Uppsala, Sweden.
Ni-NTA resin Sequencing services QIAquick®Nucleotide removal kit QIAprep® Spin M13 kit Buffer PN	QIAgen, QIAgen House, Fleming Way, Crawley, West Sussex, UK.
BamH1 enzyme T4 DNA ligase T7 DNA polymerase Taq polymerase	Biosciences, 13 Charlemont Tce., Crofton Rd., Dun Laoghaire, Co. Dublin.
Tryptone Agar Technical Yeast Extract	Oxoid, Basingstoke, Hampshire, RG24 8PW, UK.
Acetic acid / Hydrochloric acid	Riedel de-Haen AG, Wunstorfer, Strabe 40, D-30926, Hannover, Germany

Amphetamine – BSA	Fitzgerald Industries International Inc.
Tetrahydrocanabinnol – BTG	Concord, MA 01742-3049, USA
Tetrahydrocanabinnol – BSA	
PCR Oligonucleotides	MWG-Biotech Ltd., Milton Keynes
Milk Marvel	Chivers Ireland Ltd, Coolock Dublin 5

2.1.2 Equipment

Equipment	Supplier
3015 pH meter	Jenway Ltd., Gransmore Green, Felsted, Dunmow, Essex, UK.
Titertek Twin reader Plus	Medical Supply Company (MSC), Damastown, Mulhuddart, Dublin 15, Ireland.
Eppendorf	AGB Scientific ltd., Dublin Industrial Estate, Glasnevin, Dublin 9
Hermle Z233MK-2 (microcentrifuge)	Alpha Technologies Ltd., The Leinster Technology Centre, Blessington Industrial Estate, Blessington, Co. Wicklow, Ireland.
Beckman centrifuge (J2-21)	Beckman-Coulter Inc., 4300N Harbour Boulevard, Fullerton, CA 92834-3100, USA.
Biometra PCR machine	Anachem Ltd., Anachem House, Charles St., Luton, Bedfordshire, UK.
Hybaid PCR machine	BioRad, BioRad House, Maylands Ave., Hemel Hempstead, Hertfordshire, UK.
Grant waterbath (Y6)	Grant Instruments (Cambridge) Ltd., 29 Station Rd., Shepreth, Royston, Hertfordshire, UK.

Orbital incubator	Sanyo Gallenkamp plc, Monarch Way, Belton Park, Loughborough, Leicester, UK.
Tomy Autoclave (SS 325)	Mason Technology, Greenville Hall, 228 South Circular Rd., Dublin 8, Ireland.
UV-160A spectrophotometer	Shimadzu Corp., Albert-Hahn-Str. 6-10, 47269 Duisburg, Germany.
Safire^2 Platereader	Tecan Austria GmbH, Untersbergstrasse 1a, A-5082 Grodig / Salzburg, Austria.
Vivaspin Concentrator 5000 MWCO	Vivascience AG, Sartorius Group, 30625 Hannover, Germany.
Stuart platform shaker (STR 6)	Lennox, John F Kennedy Industrial Est., Naas Rd., Dublin 12, Ireland.
Image Master VSD gel documentation system	Amersham Pharmacia Biotech AB, SE-751 84, Uppsala, Sweden.
Nanodrop ND-1000	Lab tech International, East Sussex BN8 5NN, United Kingdom.
Nunc maxisorb 96-well plates	NUNC, Kamstrup DK, Roskilde, Denmark

2.1.3 Culture media formulations

All *E.coli* strains, containing specific phagemid vectors, were grown in their optimal media. All media formulations are included in the table below.

Culture Media	**Formulation**	
2x Tryptone Yeast extract (2x TY) medium	Tryptone	16g/l
	Yeast extract	10g/l
	NaCl	5g/l
Luria Broth medium	Tryptone	10g/l
	Yeast extract	5g/l
	NaCl	10g/l
Super Broth medium	MOPS	10g/l
	Yeast Extract	20g/l
	Tryptone	30g/l
Terrific Broth medium	Tryptone	12g/l
	Yeast extract	24g/l
	Glycerol	4ml/l
	KH_2PO_4	17mM
	K_2HPO_4	72mM

Super Optimal Catabolite (SOC) medium	Tryptone	20g/l
	Yeast extract	5g/l
	NaCl	0.5g/l
	KCl	2.5mM
	$MgCl_2$	20mM
	Glucose	20mM

2.1.4 Secondary antibodies

Antibody	**Enzyme - label**	**Source**
Anti – polyhistidine	Horseradish peroxidase	Mouse
Anti - flag	No label	Rabbit
Anti - Goat	Horseradish peroxidase / Alkaline phosphatase	Rabbit
Anti – rabbit	Horseradish peroxidase / Alkaline phosphatase	Goat
Anti - M13 bacteriaphage	Horseradish peroxidase	Mouse
Anti – human kappa light chain	Horseradish peroxidase	Goat
Anti – Haemaglutinain	Horseradish peroxidase	Mouse

2.1.5 Buffers

Buffer name	**Composition**
Phosphate buffered saline (PBS)	0.15M NaCl 2.5mM KCl 10mM Na_2HPO_4 18mM KH_2PO_4 pH 7.4
Tris-acetate/EDTA electrophoresis buffer (TAE)	40mM Tris-acetate 1mM EDTA pH 8.0
Tris-EDTA sucrose buffer (TES)	200mM Tris-HCl 0.5M Sucrose 0.5mM EDTA, pH 8.0
SCC buffer	200 mM Tris-HCl 100 mM MgCl2 500 mM NaCl 10 mM DTT

2.1.6 Bacterial Strains Used

Bactrerial Strain	**Genotype**
XL-1 Blue *E. coli*	*RecA endA1 gyrA96 thi-1 hsdR17 supE44 relA1 lac [F'proAB lacI^{q} ZΔM15 Tn10 (Tet^{r})]*
TG1 *E. coli*	*F′ traD36 lacI^{q} (lacZ)M15 proA^{+}B^{+}/supE (hsdM-mcrB)5 ($r_k^{-}m_k^{+}$McrB^{-}) thi (lac-proAB)*
TOP 10 F' *E. coli*	*F'{lacI^{q} Tn10(Tet^{R})} mcrA delta(mrr-hsdRMS-mcrBC) phi80lacZdeltaM15 deltalacX74 deoR recA1 araD139 delta(ara-leu)7697 galU galK rpsL (Str^{R}) endA1 nupG*
JM83 *E. coli*	λ⁻ ara (pro-lac) rpsL thi ϕ80 dlacZ ***M15***λ⁻
CJ236 *E. coli*	FΔ*(HindIII)::cat* (Tra^{+} Pil^{+} Cam^{R})/ *ung-1 relA1 dut-1 thi-1 spoT1 mcrA*

2.1.6.1 Maintenance of Bacterial Stocks

A working stock of bacteria was streaked on LB agar plates containing the appropriate antibiotic. A glycerol stock was prepare by growing an overnight culture from a single colony. This was stored in 15% (v/v) glycerol at -80^{o}C.

2.1.7 Antibodies

2.1.7.1 Anti-amphetamine monoclonal antibody

A monoclonal antibody, clone 4EP18E, directed against amphetamine, was obtained from Dr. Lorna Fanning, Dublin City University (Fanning, 2002).

2.1.7.2 Anti morphine – 3 – glucuronide (M3G) scFv

A recombinant scFv specific for M3G was obtained from Dr. Joanne Brennan, Dublin City University (Brennan *et al.,* 2003).

2.2 Hapten-Protein Conjugates

2.2.1 Production of M3G-OVA conjugates

Morphine-3-glucuronide was coupled to OVA (ovalbumin) using standard carbodiimide coupling chemistry. Briefly, a 1ml solution of 50 mg/ml of M3G (in 1ml of 20 mM HCl) was made up to a volume of 5ml with 0.2 M borate buffer, pH 9.0. NHS (N-hydroxysuccinimide) and EDC (N-ethyl-N-(dimethyl-aminopropyl) carbodiimide hydrochloride) were added to yield a final concentration of 0.1 M and 0.4 M, respectively. The solution was incubated to room temperature for 10 mins without agitation. OVA, prepared in 0.2 M borate buffer and at a molar ratio of 1:100 to M3G, was added dropwise to the activated solution with stirring. The solution was incubated at room temperature with gentle stirring for 2 hours and dialysed against 100 volumes of PBS (phosphate buffer saline, pH 7.4, 0.1M) overnight at 4^{o}C.

2.2.2 Conjugate concentration determination

Conjugate concentration was estimated using the nanodrop spectrophotometer.

2.2.3 Commercial conjugates

Amphetamine – BSA (bovine serum albumin) was obtained from Fitzgerald Industries International, MA, USA. The conjugation was achieved through the methylenedioxy group situated at the para-position of the phenyl ring.
Tetrahydrocanabinnol-BTG (bovine thyroglobulin) and Tetrahydrocanabinnol-BSA were obtained from Fitzgerald Industries International, MA, USA. THC-BTG was conjugated through the delta-9 position and THC-BSA was linked via the carboxyl carbon at the delta-9 position.

2.3 Immunisation for Recombinant Antibody Production

2.3.1 Immunisation schedule for the production of a recombinant library

Day 1
Mice were immunised by intraperitoneal injection and rabbits were immunised by sub-cutaneous injection with an emulsion (250µl) consisting of a 1mg/ml solution of peptide-protein conjugate mixed 1:1 with Freunds Complete Adjuvant.

Day 21

Mice, and rabbits were re-immunised intraperitoneally and sub-cutaneously, respectively, using an emulsion (250µl) consisting of a 1mg/ml solution of peptide-protein conjugate mixed 1:1 with Freund's incomplete adjuvant.

Day 28

Tail bleeds were taken from the mice, 5ml peripheral blood from the ear vein was taken from rabbits and 5 ml of peripheral blood from wing vein was taken from chickens to determine antibody titre against the respective antigens.

Day 52

The mice were boosted intraperitoneally, and rabbits and chickens are boosted sub-cutaneously, using an emulsion (250μl) consisting of a 1mg/ml solution of peptide-protein conjugate mixed 1:1 with Freund's incomplete adjuvant.

Day 59

Once the antibody titre was at sufficient levels (> 1/ 500,000) the animals were immunised intravenously (3-4 days prior to sacrifice) with the conjugate (250 µl at 1 mg/ml).

Antiserum recovery

After the 3-4 days, the animal was sacrificed and the blood and spleen recovered.

2.3.2 Preparation of serum for Estimation of Antibody Titre and specificity

For titre estimation the blood collected was allowed to clot at 4^{o}C overnight. It was then centrifuged at 13,000 rpm for 15 mins and supernatant removed for antibody titre determination by direct and competitive ELISA.

2.3.3 Direct Enzyme-linked immunosorbent assay (ELISA) for Antibody Titre.

Levels of antibody in serum from immunised animals were measured using ELISA. One series of wells were coated with 100µl of a 5µg/ml solution of drug protein conjugate (In the case of THC, THC-BSA was used) and incubated overnight at 4^{o}C. A second series of wells were coated with the protein (protein used as conjuagate) alone, and incubated overnight at 4^{o}C. The plates were washed three times with 0.1% (v/v) PBS/Tween and three times with PBS. The plates were then blocked with 200µl of 4% (w/v) Milk Marvel / PBS (M/PBS) for 1 hour at 37^{o}C. Serial dilutions of serum were carried out in 1% MPBST, from 1/200 – 1/1,638,400 and 100µl of each dilution was added to the wells and allowed to bind at 37^{o}C for 1 hour. The plates were washed again, three times with 0.1% (v/v) PBS/Tween and three times with PBS. 100 µl of commercial goat anti-rabbit IgG antibody, labelled with horseradish peroxidase at a dilution of 1 / 2,000 was added to the wells. The plates were washed again, three times with 0.1% (v/v) PBS/Tween and three times with PBS. Bound antibody was detected using o-phenylenediamine (o-PD), in 0.05M phosphate citrate buffer, pH the 5.0, and 0.4 mg/ml of urea hydrogen peroxidase) chromogenic substrate. Absorbances were read after 30 min at 450nm.

2.4 Methods for the development of a recombinant antibody library

2.4.1 RNA extraction and Complementary DNA synthesis.

Total RNA, was extracted from the anti-amphetamine antibody-secreting clone, 4EP18E, previously described by Fanning (2002), using Trizol reagent. It was then used for cDNA synthesis.

For the generation of an immunised recombinant antibody library; the spleen from an immunised rabbit was removed aseptically. The spleen was placed in an 'RNase-free' 50ml tube and weighed on an analytical balance. 2ml of Trizol reagent was added for every 100mg of spleen. The spleen was totally homogenized using a pre-autoclaved and baked head unit and the suspension transferred to an 85ml Oakridge 'RNase-free' tube. The suspension was left for 5 mins to ensure the complete dissociation of nucleoprotein complexes. Chloroform (0.2ml per ml of Trizol reagent) was added to the mixture and the tube was shaken vigorously for 15 secs and the resulting mixture was incubated at room temperature for 15 mins. After 15 mins, the mixture was centrifuged at 17500g for 20 min at 4^{o}C. The suspension separates into three distinct layers, with the top aqueous layer containing the RNA. This was transferred to a new 'RNase-free' Oakridge tube and the RNA was precipitated out of solution by addition of 0.5 ml Isopropanol per ml of Trizol used. The RNA suspension was left at room temperature for 5-10 min and centrifuged at 17,500g for 25 min. RNA forms a gel-like pellet on the side and the bottom of the tube. The supernatant was removed and the pellet was washed with 75% (v/v) ethanol (1ml of ethanol per ml of Trizol used) and vortexed. This was centrifuged at 17,500g for 10 min at 4^{o}C. The RNA pellet was allowed to airdry and then dissolved in molecular grade water. The RNA was dissolved via gentle shaking.

2.4.2 Complementary DNA Synthesis

Complementary DNA (cDNA) was synthesized by reverse transcription using the SuperScript Preamplification System for First Strand cDNA Synthesis (Life Technologies, Cat #18089-011).

Table 2.4.2.1 List of components and their concentrations for use in cDNA synthesis.

Component	**Concentration per reaction (50 µl)**
$MgCl_2$	5mM
10X Buffer	1X
dNTP mix	1mM
RNase ® ribonuclease inhibitor	1 U/µl
Oligo dT's	0.5 µg/µl
AMV RT	15 U
RNA	7 – 10 µg
Nuclease – free H_2O	Up to 20 µl

The cDNA synthesis mixture was incubated at room temperature for 10 minutes to allow annealing of the primers. The reaction was then incubated at 42^{o}C for 1 hour and DNA analysed by agarose gel electrophoresis (section 2.4.3).

2.4.3 Agarose gel electrophoresis

Agarose gel electrophoresis was used for DNA analysis. Briefly, agarose was dissolved in 1X TAE buffer at the required concentration (1 – 3% (w/v)) and boiled until the solution cleared. In the case of DNA to be used solely for analysis, 0.5 μg / ml of the intercalating dye, ethidium bromide (EtBr) was added to the gel. 1X SYBER Safe™ DNA gel stain in DMSO (Invitrogen Cat # S33102) was added for visualization, where the DNA was to be extracted and purified from the gel. Unlike ethidium bromide, SYBER Safe does not require exposure to UV light for visualization and, therefore, the DNA is not damaged by this light. However, EtBr was required for photographing gels for records as they were photographed using a UV image analyzer.

2.4.4 Construction of chimeric anti-amphetamine Fab from cDNA

Anti - amphetamine chimeric Fab was amplified from the prepared cDNA, using recommended PCR assembly methods (Andris-Widhopf *et al.,* 2000; Steinberger *et al.,* 2000; Barbas *et al.,* 2001). Human CH1, Cκ region was sourced from the pCOMB3X vector series, which contain standard Fab fragment inserts (Andris-Widhopf *et al.,* 2000). Fab constructs were synthesized with the mouse Vλ region in association with both Cκ regions.

2.4.4.1 The list of chimeric mouse/human Fab primers used in variable heavy and light chain amplifications are detailed below.

V_H5` Sense Primers

MHyVH1-F
5` GCT GCC CAA CCA GCC ATG GCC CTC GAG GTR MAG CTT CAG GAG TC 3`

MHyVH2 – F
5` GCT GCC CAA CCA GCC ATG GCC CTC GAG GTB CAG CTB CAG CAG TC 3`

MHyVH3 – F
5` GCT GCC CAA CCA GCC ATG GCC CTC GAG GTG CAG CTG AAG SAS TC 3`

MHyVH4 – F
5` GCT GCC CAA CCA GCC ATG GCC CTC GAG GTC CAR CTG CAA CAR TC 3`

MHyVH5 – F
5` GCT GCC CAA CCA GCC ATG GCC CTC GAG GTY CAG CTB CAG CAR TC 3`

MHyVH6– F

5` GCT GCC CAA CCA GCC ATG GCC CTC GAG GTY CAR CTG CAG CAG TC 3`

MHyVH7– F
5` GCT GCC CAA CCA GCC ATG GCC CTC GAG GTC CAC GTG AAG CAG TC 3`

MHyVH8– F
5` GCT GCC CAA CCA GCC ATG GCC CTC GAG GTG AAS STG GTG GAA TC 3`

MHyVH9– F
5` GCT GCC CAA CCA GCC ATG GCC CTC GAG GTG AWG YTG GTG GAG TC 3`

MHyVH10– F
5` GCT GCC CAA CCA GCC ATG GCC CTC GAG GTG CAG SKG GTG GAG TC 3`

MHyVH11– F
5` GCT GCC CAA CCA GCC ATG GCC CTC GAG GTG CAM CTG GTG GAG TC 3`

MHyVH12– F
5` GCT GCC CAA CCA GCC ATG GCC CTC GAG GTG AAG CTG ATG GAR TC 3`
MHyVH13– F

5` GCT GCC CAA CCA GCC ATG GCC CTC GAG GTG AAG CTG ATG GAR TC 3`

MHyVH14– F
5` GCT GCC CAA CCA GCC ATG GCC CTC GAG GTR AAG CTT CTC GAG TC 3`

MHyVH15– F
5` GCT GCC CAA CCA GCC ATG GCC CTC GAG GTG AAR STT GAG GAG TC 3`

MHyVH16– F
5` GCT GCC CAA CCA GCC ATG GCC CTC GAG GTT ACT CTR AAA GWG TST G 3`

MHyVH17– F
5` GCT GCC CAA CCA GCC ATG GCC CTC GAG GTC CAA CTV CAG CAR CC 3`

MHyVH18– F
5` GCT GCC CAA CCA GCC ATG GCC CTC GAG GTG AAC TTG GAA GTG TC 3`

MHyVH19– F
5` GCT GCC CAA CCA GCC ATG GCC CTC GAG GTG AAG GTC ATC GAG TC 3`

V_H3` Reverse Primers

MhyIgGCH1 – B1

5` CGA TGG GCC CTT GGT GGA GGC TGA GGA GAC GGT GAC CGT GGT 3`

MhyIgGCH1 – B2

5` CGA TGG GCC CTT GGT GGA GGC TGA GGA GAC TGT GAG AGT GGT 3`

MhyIgGCH1 – B3

5` CGA TGG GCC CTT GGT GGA GGC TGC AGA GAC AGT GAC CAG AGT 3`

MhyIgGCH1 – B4

5` CGA TGG GCC CTT GGT GGA GGC TGA GGA GAC GGT GAC TGA GGT 3`

V_K5` Sense Primers

MSCVK - 1

5` GGG CCC AGG CGG CCG AGC TCC AYA TCC AGC TGA CTC AGC C 3`

MSCVK – 2

5` GGG CCC AGG CGG CCG AGC TCC AYA TTG TTC TCW CCC AGT C 3`

MSCVK - 3

5` GGG CCC AGG CGG CCG AGC TCC AYA TTG TGM TMA CTC AGT C 3`

MSCVK - 4

5` GGG CCC AGG CGG CCG AGC TCC AYA TTG TGY TRA CAC AGT C 3`

MSCVK - 5

5` GGG CCC AGG CGG CCG AGC TCC AYA TTG TRA TGA CMC AGT C 3`

MSCVK - 6

5` GGG CCC AGG CGG CCG AGC TCC AYA TTM AGA TRA MCC AGT C 3`

MSCVK - 7

5` GGG CCC AGG CGG CCG AGC TCC AYA TTC AGA TGA YDC AGT C 3`

MSCVK - 8

5` GGG CCC AGG CGG CCG AGC TCC AYA TYC AGA TGA CAC AGA C 3`

MSCVK - 9

5` GGG CCC AGG CGG CCG AGC TCC AYA TTG TTC TCA WCC AGT C 3`

MSCVK – 10

5` GGG CCC AGG CGG CCG AGC TCC AYA TTG WGC TSA CCC AAT C 3`

MSCVK - 11

5` GGG CCC AGG CGG CCG AGC TCC AYA TTS TRA TGA CCC ART C 3`

MSCVK - 12

5` GGG CCC AGG CGG CCG AGC TCC AYA TTK TGA TGA CCC ARA C 3`

MSCVK - 13

5` GGG CCC AGG CGG CCG AGC TCC AYA TTG TGA TGA CBC AGK C 3`

MSCVK - 14

5` GGG CCC AGG CGG CCG AGC TCC AYA TTG TGA TAA CYC AGG A 3`

MSCVK - 15

5` GGG CCC AGG CGG CCG AGC TCC AYA TTG TGA TGA CCC AGW T 3`

MSCVK - 16

5` GGG CCC AGG CGG CCG AGC TCC AYA TTG TGA TGA CAC AAC C 3`

MSCVK - 17

5` GGG CCC AGG CGG CCG AGC TCC AYA TTT TGC TGA CTC AGT C 3`

V_K3` Reverse Primers

MHybJK12 – B

5`AGA TGG TGC AGC CAC AGT TCG TTT KAT TTC CAG YTT GGT CCC 3`

MHybJK4 – B

5`AGA TGG TGC AGC CAC AGT TCG TTT TAT TTC CAA CTT TGT CCC 3`

MHybJK5 – B

5`AGA TGG TGC AGC CAC AGT TCG TTT CAG CTC CAG CTT GGT CCC 3`

Table 2.4.4.1.1 PCR components for V region (heavy and light chain) amplification.

Component	Concentration per reaction	Volume (µl)
Sense primer mix (heavy / light chain)	0.06nM	1
Reverse primer mix (heavy / light chain)	0.06nM	1
10 X Buffer	1 X	5
$MgCl_2$	1.5 mM	3
dNTP`s	0.2 mM	1
cDNA	8 µg / reaction	x
Taq Polymerase	5 U / reaction	0.25
Molecular grade H_2O	Up to 50 µl	y

Table 2.4.4.1.2 PCR conditions for antibody V region amplifications

Temperature	Time (seconds)
94°C	120
94°C	15
56°C	30
72°C	90
Repeat step, 2 – 4, 30 times	
72°C	600
4 °C	--

2.4.4.2 Primers for the applification of human Cκ region and pelB leader sequence from a cloned human Fab fragment.

HKC – F sense
5` CGA ACT GTG GCT GCA CCA TCT GTC 3`

Lead – B reverse
5` GGC CAT GGC TGG TTG GGC AGC 3`

Human C_H1 primers

HIgGCH1 – F sense
5` GCC TCC ACC AAG GGC CCA TCG GTC 3`

dpseq reverse
5` AGA AGC GTA GTC CGG AAC GTC 3`

Table 2.4.4.2.1 PCR conditions for C region (heavy and light chain) amplification.

Component	Concentration per reaction	Volume (µl)
HKC – F / HIgGCH1 – F	0.05nM	1
Lead – B / dpseq	0.05nM	1
10 X Buffer	1 X	5
$MgCl_2$	1.5 mM	3
dNTP`s	0.2 mM	1
PComb3X plasmid	2 µg / reaction	x
Taq Polymerase	5 U / reaction	0.25
Molecular grade H_2O	Up to 50 µl	y

Table 2.4.4.2.2 PCR conditions for antibody C region amplifications.

Temperature	Time (seconds)
94°C	120
94°C	15
56°C	30
72°C	90
Repeat step, 2 – 4, 30 times	
72°C	600
4 °C	--

2.4.5 Purification of PCR reaction products

All PCR products were excised and purified following agarose gel electrophoresis. Purification was carried out using Eppendorf Perfectprep Gel clean - up kit. The correct bands were identified via the transilluminator, excised using a sterile scalpel, transferred to a sterile microcentrifuge tube and weighed. Three volumes of binding buffer were added to each gel slice, inverted 3 times to mix and incubated at 55^{o}C for 15 min or until the gel slice had been fully dissolved. One volume of isopropanol was added. The mixture was poured into a spin column and centrifuged for 2 min at 14,000 rpm at 4^{o}C. The flow through was discarded and the spin column was washed with 750 µl of wash buffer, the column was centrifuged for 2 min at 14,000 rpm. The flow through was discarded. The column was centrifuged once again to ensure all residual wash buffer has been removed before elution. The spin column was transferred to a sterile microcentrifuge tube and 30 µl 'nuclease – free' H_2O was added. The column was centrifuged for 1 min at 14,000 rpm to elute the DNA. Purified DNA was either used immediately in splice by overlap extension PCR or stored at -20 ^{o}C until required.

2.4.6 Splice by Overlap Extension PCR.

Variable and constant heavy and light chains were annealed and amplified using splice by overlap extension (SOE) to produce an 800bp light chain and an 800 bp heavy chain. The 3` end of the pelB sequence on each of the heavy and light chains serves as the overlap region in the final SOE PCR.

2.4.6.1 Mouse V_H and Human C_H1 SOE primers

LeadVH sense

5` GCT GCC CAA CCA GCC ATG GCC 3`

dpseq reverse

5` AGA AGC GTA GTC CGG AAC GTC 3`

Mouse V_L and Human C_K SOE primers

RSC – F sense

5` GAG GAG GAG GAG GAG GAG GCG GGG CCC AGG CGG CCG AGC TC 3`

Lead – B reverse

5` 5` GGC CAT GGC TGG TTG GGC AGC 3`

Table 2.4.6.1.1 PCR components for C region (heavy and light chain) amplification.

Component	Concentration per reaction	Volume (µl)
LeadVH / RSC – F	0.05nM	1
dpseq / Lead – B	0.05nM	1
10 X Buffer	1 X	5
$MgCl_2$	1.5 mM	3
dNTP's	0.2 mM	1
Purified PCR product ($V_{L,}C_K$ / $V_{H,}C_H1$)	100 ng of each / reaction	x
Taq Polymerase	5 U / reaction	0.25
Molecular grade H_2O	Up to 50 µl	y

Table 2.4.6.1.2 PCR conditions for antibody C region amplifications

Temperature	Time (seconds)
94°C	120
94°C	15
56°C	30
72°C	90
Repeat step, 2 – 4, 15 times	
72°C	600
4 °C	--

2.4.6.2 Chimeric Mouse/Human Fab primers used in the final overlap PCR to combine the chimeric light chain –pelB fragment and the Fd fragment.

RSC – F sense

5` GAG GAG GAG GAG GAG GAG GCG GGG CCC AGG CGG CCG AGC TC 3`

dp – EX reverse

5` GAG GAG GAG GAG GAG GAG AGA AGC GTA GTC CGG AAC GTC 3`

Table 2.4.6.2.1 PCR components for final Fab construct amplification.

Component	**Concentration per reaction**	**Volume (µl)**
RSC – F	0.05nM	1
dp –EX	0.05nM	1
10 X Buffer	1 X	5
$MgCl_2$	1.5 mM	3
dNTP's	0.2 mM	1
Fd and light chain	100 ng of each chain / reaction	x
Taq Polymerase	5 U / reaction	0.25
Molecular grade H_2O	Up to 50 µl	y

Table 2.4.6.2.2 PCR conditions for final Fab construct amplification

Temperature	Time (seconds)
94°C	120
94°C	15
56°C	30
72°C	90
Repeat step, 2 – 4, 15 times	
72°C	600
4 °C	--

2.4.7 Methods for the conversion of an anti-M3G scFv fragment to a chimeric Fab format.

Methods are as outlined in the previous sections 2.4.4 – 2.4.6 with the following changes in protocol.

2.4.7.1 Construction of the C_λ – associated Fab.

To facilitate the construction of the C_λ – associated Fab the reverse primer M-H-CL5 – B, was designed to amplify the mouse V_λ sequence and also to introduce a human C_λ sequence tail. The C_λ region along with the pelB leader sequence was amplified from the pComb3XSS vector using HLC-F and Lead-B. This V_λ PCR product was gel purified, as previously outlined, and combined with C_λ purified product to give the final λ light chain construct.

V_K3` Reverse Primer

M-H-CL5 –B

5` CGA GGG GGC AGC CTT GGG CTG ACC TAG GAC AGT CAG TTT GG 3`

Human Cκ region and pelB leader sequence primers

HLC – F sense

5` GGT CAG CCC AAG GCT GCC CCC 3`

Lead – B reverse

5` GGC CAT GGC TGG TTG GGC AGC 3`

2.4.8 Methods for the conversion of an anti-Amphetamine Fab to scFv format and construction of an anti-THC rabbit scFv.

2.4.8.1 Amplification of variable heavy and light chains from the anti – amphetamine Fab discussed in previous sections.

A standard primer mix compatible with the pAK vector system, as described by Krebber *et al.,* (1997), was used for the assembly of mouse scFv fragments.

2.4.8.1.1 Mouse scFv primers used in variable heavy and light chain amplification.

Variable light chain back primers

LB1 5′gccatggcggactacaaaGAYATCCAGCTGACTCAGCC3′

LB2 5′gccatggcggactacaaaGAYATTGTTCTCWCCCAGTC3′

LB3 5′gccatggcggactacaaaGAYATTGTGMTMACTCAGTC3′

LB4 5′gccatggcggactacaaaGAYATTGTGYTRACACAGTC3′

LB5 5′gccatggcggactacaaaGAYATTGTRATGACMCAGTC3′

LB6 5′gccatggcggactacaaaGAYATTMAGATRAMCCAGTC3′

LB7 5′gccatggcggactacaaaGAYATTCAGATGAYDCAGTC3′

LB8 5′gccatggcggactacaaaGAYATYCAGATGACACAGAC3′

LB9 5′gccatggcggactacaaaGAYATTGTTCTCAWCCAGTC3′

LB10 5′gccatggcggactacaaaGAYATTGWGCTSACCCAATC3′

LB11 5′gccatggcggactacaaaGAYATTSTRATGACCCARTC3′

LB12 5′gccatggcggactacaaaGAYRTTKTGATGACCCARAC3′

LB13 5′gccatggcggactacaaaGAYATTGTGATGACBCAGKC3′

LB14 5′gccatggcggactacaaaGAYATTGTGATAACYCAGGA3′

LB15 5′gccatggcggactacaaaGAYATTGTGATGACCCAGWT3′

LB16 5′gccatggcggactacaaaGAYATTGTGATGACACAACC3′

LB17 5′gccatggcggactacaaaGAYATTTTGCTGACTCAGTC3′

LBλ 5′gccatggcggactacaaaGATGCTGTTGTGACTCAGGAATC3′

Variable light chain forward primers

LF1 5′ggagccgccgccgcc(agaaccaccaccacc)$_2$ACGTTTGATTTCCAGCTTGG3′

LF2 5′ggagccgccgccgcc(agaaccaccaccacc)$_2$ACGTTTTATTTCCAGCTTGG3′

LF4 5′ggagccgccgccgcc(agaaccaccaccacc)$_2$ACGTTTTATTTCCAACTTTG3′

LF5 5′ggagccgccgccgcc(agaaccaccaccacc)$_2$ACGTTTCAGCTCCAGCTTGG3′

LFλ 5′ggagccgccgccgcc(agaaccaccaccacc)$_2$ACCTAGGACAGTCAGTTTGG3′

Variable heavy chain back primers

HB1 5′ggcggcggcggctccggtggtggtggatccGAKGTRMAGCTTCAGGAGTTC3′

HB2 5′ggcggcggcggctccggtggtggtggatccGAGGTBCAGCTBCAGCAGTC3′

HB3 5′ggcggcggcggctccggtggtggtggatccCAGGTGCAGCTGAAGSASTC3′

HB4 5′ggcggcggcggctccggtggtggtggatccGAGGTCCARCTGCAACARTC3′

HB5 5′ggcggcggcggctccggtggtggtggatccCAGGTYCAGCTBCAGCARTC3′

HB6 5′ggcggcggcggctccggtggtggtggatccCAGGTYCARCTGCAGCAGTC3′

HB7 5′ggcggcggcggctccggtggtggtggatccCAGGTCCACGTGAAGCAGTC3′

HB8 5′ggcggcggcggctccggtggtggtggatccGAGGTGAASSTGGTGGAATC3′

HB9 5′ggcggcggcggctccggtggtggtggatccGAVGTGAWGYTGGTGGAGTC3′

HB10 5′ggcggcggcggctccggtggtggtggatccGAGGTGCAGSKGGTGGAGTC3′

HB11 5′ggcggcggcggctccggtggtggtggatccGAKGTGCAMCTGGTGGAGTC3′

HB12 5′ggcggcggcggctccggtggtggtggatccGAGGTGAAGCTGATGGARTC3′

HB13 5′ggcggcggcggctccggtggtggtggatccGAGGTGCARCTTGTTGAGTC3′

HB14 5′ggcggcggcggctccggtggtggtggatccGARGTRAAGCTTCTCGAGTC3′

HB15 5′ggcggcggcggctccggtggtggtggatccGAAGTGAARSTTGAGGAGTC3′

HB16 5′ggcggcggcggctccggtggtggtggatccCAGGTTACTCTRAAAGWGTSTG3′

HB17 5′ggcggcggcggctccggtggtggtggatccCAGGTCCAACTVCAGCARCC3′

HB18 5′ggcggcggcggctccggtggtggtggatccGATGTGAACTTGGAAGTGTC3′

HB19 5′ggcggcggcggctccggtggtggtggatccGAGGTGAAGGTCATCGAGTC3′

Variable heavy chain forward primers

HF1 5′ggaattcggcccccgaggcCGAGGAAACGGTGACCGTGGT3′

HF2 5′ggaattcggcccccgaggcCGAGGAGACTGTGAGAGTGGT3′

HF3 5′ggaattcggcccccgaggcCGCAGAGACAGTGACCAGAGT3′

HF4 5′ggaattcggcccccgaggcCGAGGAGACGGTGACTGAGGT3′

2.4.8.2 Amplification of variable heavy and light chains from the rabbit cDNA

Anti-tetrahydrocannabinol scFv was amplified from the prepared cDNA, using recommended PCR assembly methods (Andris-Widhopf *et al.,* 2000; Barbas *et al.,* 2001).

2.4.8.2.1 The list of scFv primers used in variable heavy and light chain amplification are detailed below.

V_k5 Sense Primers

RSCVK1
5` GGG CCC AGG CGG CCG AGC TCG TGM TGA CCC AGA CTC CA 3`

RSCVK2
5` GGG CCC AGG CGG CCG AGC TCG ATM TGA CCC AGA CTC CA 3`

RSCVK3
5` GGG CCC AGG CGG CCG AGC TCG TGA TGA CCC AGA CTG AA 3`

V_k3 Reverse Primers, long linker

RKB9j1o-BL
5` GGA AGA TCT AGA GGA ACC ACC CCC ACC ACC GCC CGA GCC ACC GCC ACC AGA GGA TAG GAT CTC CAG CTC GGT CCC 3`

RKB9jo-BL
5` GGA AGA TCT AGA GGA ACC ACC CCC ACC ACC GCC CGA GCC ACC GCC ACC AGA GGA TAG GAT CTC CAG CTC GGT CCC 3`

RKB42jo-BL
5` GGA AGA TCT AGA GGA ACC ACC CCC ACC ACC GCC CGA GCC ACC GCC ACC AGA GGA TTT GAC SAC CAC CTC GGT CCC 3`

V_λ5 Sense Primers

RSCλ1

5` GGG CCC AGG CGG CCG AGC TCG TGC TGA CTC AGT CGC CCT 3`

V_λ3 Reverse Primer, long linker

RJλo-BL

5` GGA AGA TCT AGA GGA ACC ACC CCC ACC ACC GCC CGA GCC ACC GCC ACC AGA GGA GCC TGT GAC GGT CAG CTG GGT CCC 3`

V_H5 Sense primers

RSCVH1

5` GGT GGT TCC TCT AGA TCT TCC CAG TCG GTG GAG GAG TCC RGG 3`

RSCVH2

5` GGT GGT TCC TCT AGA TCT TCC CAG TCG GTG AAG GAG TCC GAG 3`

RSCVH3

5` GGT GGT TCC TCT AGA TCT TCC CAG TCG YTG GAG GAG TCC GGG 3`

RSCVH4

5` GGT GGT TCC TCT AGA TCT TCC CAG SAG CAG CTG RTG GAG TCC GG 3`

V_H3 Reverse primers

RSCG-B
5` CCT GGC CGG CCT GGC CAC TAG TGA CTG AYG GAG CCT TAG GTT GCC C 3`

Overlap Extension primers

RSC-F (sense)
5` GAG GAG GAG GAG GAG GAG GCG GGG CCC AGG CGG CCG AGC TC 3`

RSC-B (reverse)
5` GAG GAG GAG GAG GAG GAG CCT GGC CGG CCT GGC CAC TAG TG 3`

2.4.9 Recombinant Fab library construction

2.4.9.1 Preparation of pComb3XSS vector

A single colony of *XL - 1 Blue* (Stratagene, La Jolla, CA, USA) containing the required vector (pComb vector series, kindly provided by Prof. Carlos Barbas, (Scripps Research Institute) was isolated and grown overnight in 10ml LB media, plus 30 μg / ml tetracycline, at 37^{o}C and 220rpm. The plasmid was isolated and purified using the Wizard Plus SV Miniprep kit, according to the manufacturers instructions.

2.4.9.2 Restriction digest of Fab insert and pComb3XSS vector using Sfi 1

The Fab fragment and vector were digested with Sfi 1 in New England Biolabs, Buffer 2 (10 mM Tris–HCl, 50 mM NaCl, 10 mM $MgCl_2$ and 1 mM DTT)

Component	**PComb3XSS**	**Fab fragment**
Buffer	1X	1X
BSA	1X	1X
Sfi 1	200 units	300 units
DNA	28 µg	8 µg
H_2O	Up to 100 µl	Up to 200 µl

The digest was run for 5 hours at 50°C. The vector, stuffer fragment and Fab fragment were gel purified and quantified.

2.4.10 Ligation of Fab gene into pComb3X

Purified digests of Fab, vector and stuffer fragment were ligated at a DNA : vector ratio of 1:1 and a 1 / 20 dilution of T4 DNA Ligase at 16°C overnight.

2.4.10.1 Preparation of Electrocompetent XL - 1 Blue cells with high transformation efficiency.

Electroporation is the most efficient method for obtaining high transformation efficiency cells. A single XL – 1 Blue colony was grown overnight in 5 ml SB (Super Broth) plus 30 μg / ml tetracycline at 37°C and 220 rpm. 1.5 ml of this overnight culture was seeded into 500 ml SB, 1% (w/v) glucose, 5 ml $MgCl_2$ and no antibiotics. This culture was grown at 37°C and 220 rpm until the OD at 600nm had reached 0.8. The culture flasks and centrifuge bottles were chilled at 4°C for 15 min. 10% (v/v) glycerol was prepared and stored at 4°C. From this point onwards all steps were performed as rapidly as possible and kept at 4°C. The cultures were centrifuged in chilled bottles at 4000 rpm and 4°C for 20min. The supernatant was poured off and the pellet was resuspended in 10% (v/v) glycerol and centrifuged again at 4000 rpm, 4°C for 20min. The last step was repeated one more time. The final pellet was resuspended in 25 ml 10% (v/v) glycerol and transferred into pre-chilled 50 ml polypropylene tubes and centrifuged at 3500 rpm, 4°C for 20min. Twenty 1.5 ml screwcap microcentrifuge tubes were set up in a dry ice / ethanol bath. The supernatant was carefully discarded leaving 2 ml covering the pellet. The pellet was resuspended in this remaining 2ml volume and stored at -80°C in 300 μl aliquots until required for use.

2.4.10.2 Transformation of E. coli XL – 1 Blue with vector plus insert

The ligation mixture was precipitated with ethanol in order to remove any excess salt, which may cause arcing, prior to electroporation. The competent cells were thawed on ice along with the desalted ligation mixture. The DNA and competent cells were mixed and transferred to 2mm Gene Pulser ® Cuvettes (Bio - Rad Cat no # 165 – 2086). The cells were pulsed at 2500 V, 200 Ώ. 5 ml of SOC media was immediately added to the cells and transferred to a 15 ml polypropylene tube. The culture was incubated at 37ºC and 200 rpm for 1 hour. Cells were plated on LB agar plates with carbenicillin and grown overnight at 37ºC. Plates were scraped using LB liquid media, library stocks were prepared with the addition of 20 % (v/v) glycerol and flash frozen in liquid nitrogen and stored at – 80ºC.

2.5 Biopanning of a recombinant antibody library against amphetamine.

2.5.1 Rescue of Fab displaying phage

Initial library rescue was performed by inoculating 100ml SB with 50 µg/ml carbenicillin and 1% (w/v) glucose, with 100 µl frozen library stock. This was grown at 37ºC at 200 rpm until the OD at 600nm reached 1.0. The culture was centrifuged at 4000 rpm, 4ºC for 10 mins and the pellet resuspended in the absence of glucose in 200ml SB (plus 50 µg/ml carbenicillin). The culture was then infected with 6 x 10^{11} M13KO7 helper phage and allowed to grow at 37ºC at 220 rpm for 2 hours. 70 µg/ml kanamycin was added to the culture which was then incubated overnight at 37ºC at 220 rpm.

2.5.2 PEG / NaCl precipitation of phage

The 200 ml overnight rescued library was centrifuged in sterile centrifuge bottles at 4000 rpm at 4ºC for 20 min. The supernatant was poured into a fresh sterile bottle and 8 g PEG and 6 g NaCl were added and allowed to dissolve for 5 min at 37ºC. The supernatant mix was allowed to stand on ice for 30 min. It was then centrifuged, with the brake turned off, at 9000 rpm at 4ºC for 15 min. The supernatant was carefully decanted and the phage pellet was allowed to air-dry for 10 min at room temperature. The phage pellet was resuspended in cold sterile filtered 1% (w/v) BSA. This phage preparation was ready for immediate biopanning. Alternatively it can be stored in 1% (w/v) sodium azide (handle sodium azide with care and PPE should be worn at all times) at 4ºC for future panning although it must be reamplified unless prepared fresh on the same day.

2.5.3 Panning of specific anti-amphetamine Fab – displaying phage

8 wells of a Nunc maxisorb plate were coated with amphetamine – BSA conjugate at 4ºC overnight. For initial rounds of panning 10 μg/ml coating concentration was used. This was reduced to 5 μg/ml and 2 μg/ml in further rounds of panning. The coating solution was discarded and the wells were blocked with 150 μl 3% (w/v) sterile filtered BSA for 2 hours at 37ºC. Meanwhile 2 x 2 ml XL – 1 Blue cultures were grown at 37ºC and 220 rpm until they reached an OD at 600 nm of 1.0. The blocking solution was discarded and the freshly prepared phage solution was added at 100 μl per well. The phage solution was left to bind for 2 hours at 37ºC. The wells were washed with repeatedly with PBS and PBST. The bound phage were eluted with 100 μl of 10 mg/ml sterile filtered trypsin at 37 ºC for 30 min. Alternatively, free antigen elution was employed in later rounds of panning. Elution time was increased to 1 hour for this strategy and the free antigen concentration was 100 μM. The solution in the wells was pipetted vigorously up and down in order to remove all bound phage and then added to a 2 ml XL – 1 Blue culture. The phage were allowed to infect for 20 min at room temperature. A sample of this infected culture was taken and diluted 100 – fold and plated on LB agar plus carbenicillin plates for output titering. The volume of the remaining infected culture was increased to 8 ml by addition of 6 ml SB (plus 50 μg/ml carbenicillin) and was incubated at 37ºC and 220 rpm for 1 hour. The culture was centrifuged at 4000 rpm and 4ºC for 10min. The pellet was resuspended in 1 ml SB and plated on LB plus carbenicillin. The plates were incubated overnight at 37ºC.

2.6 Screening of anti – amphetamine Fab - displaying phage

2.6.1 Preparation of soluble expressing clones for a Monoclonal ELISA and master plate construction

A 96 well sterile culture plate was filled with 200 µl of 2XTY, 1% (w/v) glucose, 100 µg/ml carbenicillin and 30µg/ml tetracycline. Each well was inoculated with a single colony from the phage titre plates, leaving two wells as non-inoculated control wells. The plate was incubated at 37ºC and 220rpm overnight. This was deemed the master plate and was frozen at -80ºC with 15% (v/v) glycerol. A second plate was prepared with 180 µl of 2XTY, 1% (w/v) glucose, 100 µg/ml carbenicillin and 30 µg/ml tetracycline. 20 µl from each well of the master plate was transferred to the corresponding well on this second plate and incubated at 37ºC and 220rpm for 10 hours. The plate was centrifuged at 2500 rpm for 15 min. 1mM IPTG was made up in 2XTY, 100 µg/ml carbenicillin and 30 µg/ml tetracycline and added to each well and the plate was incubated at 30ºC and 220rpm overnight.

2.6.2 Monoclonal ELISA

A plate was coated with 100 µl of 1 µg/ml amphetamine – BSA and incubated overnight at 4ºC. The coating solution was discarded and 200 µl of 5 % (w/v) MPBS was added to the wells, the plate was incubated at 37ºC for 1 hour. The plate was washed three times with PBS and PBST. The culture plate was centrifuged at 4000 rpm, 4ºC for 20 min. The supernatant was mixed 1 / 2 with 2 % (w/v) MPBST and 100 µl of this solution was added to corresponding wells on the assay plate. The individual clones were incubated on the plate at 37ºC for 1 hour. The solution was discarded and the plates were washed 3 times with PBS and PBST.

100 µl of anti – HA – HRP - labelled antibody was added to each well and incubated at 37ºC for 1 hour. The plate was washed 3 times with PBS and PBST. 100 µl of 3, 3`, 5`,

5`- Tetramethylbenzidine dihydrochloride (TMB) substrate, diluted to1 mg/ml in 0.05 M citric phosphate buffer, pH 5, was added to each well. The reaction was allowed to proceed for 15 min at which time it was stopped via the addition of 10 % (v/v) HCl. The absorbance was read at 450nm.

2.6.3 Soluble expression and lysate preparation of positive clones on small scale

Positive clones resulting from the monoclonal phage ELISA were plasmid prepared as outlined in section 2.6.1. One µl of the prepared DNA was electroporated into electrocompetent *Top 10 F'* cells, prepared as described in 2.6.3. 10 single colonies were picked into 5ml SB (plus 50 µg/ml carbenicillin) and grown all day at 37ºC and 220 rpm. 2mM IPTG was added to each culture and allowed to induce at 30ºC and 220 rpm overnight. Immediately following IPTG addition 10 µl of each culture was streaked on a plate for individual clone backup stocks. The next day the cultures were centrifuged at 4000rpm and 4ºC for 15 min.The pellets were resuspended in 300 µl PBS and were subjected to freeze / thaw 3 cycles in order to lyse the cells. The lysed cells were centrifuged at 14000 rpm and room temperature for 10min to eliminate cell debris from the cleared lysate.

2.6.4 ELISA on soluble expressed clones

A 96 – well microtitre plate was coated with 100 µl of 2 µg/ml amphetamine overnight at 4ºC. The plate was blocked with 200 µl 5% (w/v) MPBST at 37ºC for 1 hour. The plate was washed 3 times with PBS and PBST. The lysate was mixed 1 / 2 with MPBST and 100 µl was applied to the appropriate well on the assay plate and incubated at 37ºC for 1 hour. The plate was washed 3 times with PBS and PBST. 100 µl of anti-HA-HRP-labelled antibody was added to each well and incubated at 37ºC for 1 hour. The plate was washed 3 times with PBS and PBST. 100 µl of 3, 3' 5, 5`- Tetramethylbenzidine

dihydrochloride (TMB) substrate diluted 1 mg/ml in 0.05 M citric phosphate buffer, pH 5, was added to each well. The reaction was allowed to proceed for 15 min at which time it was stopped via the addition of 10 % (v/v) HCl. The absorbance was read at 450nm.

2.7 Antibody Expression and Purification conditions

2.7.1 Large scale expression of Fab fragments in pComb3X

The positive Fab clone was introduced into *E. coli Top 10 F'* (Invitrogen) via electroporation before plating on LB agar plus 100 μg/ml carbenicillin plates. Single colonies were inoculated in 10 ml SB, 1% (w/v) glucose and 50 μg/ml carbenicillin, which were incubated at 37ºC, 220 rpm overnight. 1.5 ml of the starter cultures was seeded into 500ml SB, 1% (w/v) glucose and 50 μg/ml carbenicillin and incubated for 8 hours at 37ºC and 220 rpm. Cultures were centrifuged at 4000 rpm and 4ºC for 20min. The pellets were re-suspended in fresh SB with 50 μg/ml carbenicillin with no glucose added. The cultures were allowed to recover at 30ºC for 1 hour prior to induction with 1mM IPTG. The induced cultures were incubated at 30ºC and 220 rpm overnight. Cultures were centrifuged at 4000 rpm and 4ºC for 20 min. The pellets were re-suspended in 25 ml column loading buffer consisting of 50 mM NaH_2PO_4; pH 8.0, 300 mM NaCl and 5 mM imidazole. The cell suspension was sonicated under the following settings, 5 sec pulses at 50% amplitude for 90 sec and 5 sec pulses at 70% amplitude for 20 sec. Each of the aforementioned protocols was performed twice. The lysed cell suspension was centrifuged at 11000 rpm, 4ºC for 30 min. The cleared lysate was semi – purified using immobilized metal affinity chromatography (Ni – NTA Qiagen)

2.7.2 Purification by IMAC

The 500 ml terrific broth culture of induced cells was centrifuged at 12,000 rpm for 10 minutes at 4ºC. The pellets were resuspended in 30 mls of sonication buffer (1 x PBS + 500 mM NaCl + 20 mM Imidazole). The resuspend pellet was aliquoted into thirty 2 ml centrifugation tubes and each sample sonicated on ice using the appropriate setting (Amp 40 for 45 seconds with 3 second intervals). The samples were centrifuged at

14,000 rpm for 10 minutes at 4ºC and the lysate was passed through a 0.2 μm filter to remove any additional cell lysate. Four mls of nickel NTA resin slurry (Qiagen) was added to a column. The column was equilibrated with 30 mls of running buffer (sonication buffer + 1 % (v/v) Tween). The filtered lysate was passed through the column once and the flow-through collected. The column was washed with 30 mls of running buffer to remove any non-specifically binding proteins. The recombinant antibody fragment was eluted with 20 mls of 100 mM sodium acetate solution, pH 4.4. The eluted antibody fragment was collected in 1.5 ml centrifugation tubes (final volume 500 μl in each tube) containing 50 μl 10 x PBS (filtered through a 0.2 μm filter) and 50 μl 100 mM NaOH.

2.7.3 Immunoblot analysis of protein purification

An Immunodot analysis was performed on each eluted fraction. A fraction volume of 2.5 μl was spotted onto Whatmann chromatography paper. The blot was blocked with 3 % (w/v) BSA for 1 hour at room temperature. The appropriate enzyme-labelled secondary antibody was added to the blot for 1 hour at room temperature. After washing the blot (3 x PBS Tween and 3 x PBS) the liquid substrate was added and each signal spot that developed signified the presence of the eluted recombinant antibody. These fractions were pooled together and added to a spin column with a 5000 Dalton MWCO (Vivaspin, Sartorious). This was centrifuged at 4,000 rpm at 4^{o}C until the sample was concentrated to a volume of 500 μl. 5 ml of filtered PBS was added to the column. This was stored overnight on ice overnight at 4^{o}C. The following day the sample was centrifuged at 4,000 rpm at 4^{o}C until the sample was concentrated to 500 μl aliquot. The concentration of protein was calculated on the nanodrop and a SDS-PAGE and Western blot performed. The recombinant antibody was stored in 20 μl aliquots at -20^{o}C until required.

2.7.4 Sodium dodecyl sulphate – polyacrylamide gel electrophoresis (SDS-PAGE)

SDS-PAGE analysis was used to assess protein purity and to determine the apparent molecular mass of proteins. Protein electrophoresis was performed using an Atto dual minislab AE-6450 gels under reducing conditions, by the method previously described by Laemmli (1970). Samples for analysis were diluted with the sample loading dye (4:1, sample: buffer) and boiled for 10 mins. The sample (20μl) was added to the gel and electrophoresed alongside appropriate molecular weight markers. Prestained molecular weights were also electrophoresed when the gels were being prepared for western blot analysis (See Section 2.7.4). Initially the gels were electrophoresed at 15mA per plate until the samples migrated through the stacking gel and electrophoresed at 30mA per plate until the sample had migrated to the end of the gel. SDS-PAGE gels were stained for 2 hours using Coomassie blue staining solution to allow visualisation of the protein bands, and then destained overnight in destaining solution (described in Table 2.7.3.1).

Table 2.7.4.1 Composition of buffers required for SDS- PAGE and Western blotting.

Buffer	**Composition**
30 % acylamide	29.2 g acrylamide
	0.8 g bis – acrylamide
	100mls dH_2O
	Store at 4 ºC
4x Separating buffer	75 ml 2M Tris – HCl, pH 8.8
	4 ml 10% (w/v) SDS
	21 ml dH_2O
	Store at 4ºC
4x Stacking buffer	50 ml 1M Tris – HCl, pH 6.8
	4 ml 10 % (w/v) SDS
	46 ml dH_2O
	Store at 4ºC
Ammonium persulphate	50 mg ammonium persulphate
	500 µl dH_2O
	Make fresh before each use
10 X Electrophoresis buffer	30 g tris base (25mM)
	14.4 g glycine (129mM)
	10 g SDS
	Make up to 1L with dH_2O

Sample buffer	0.6 ml 1M Tris – HCl, pH 6.8
	5 ml 50% (v/v) glycerol
	2 ml 10% (w/v) SDS
	0.5 ml 2- mercaptoethanol
	1 ml 1% (w/v) bromophenol blue
	0.9 ml dH_2O
	Store at -20ºC
Coomassie blue staining solution	500 mg Coomassie brilliant blue R-250
	125 ml methanol
	50 ml acetic acid
	Make up to 500ml with dH_2O
Destaining solution	150 ml methanol
	50 ml acetic acid
	300 ml dH_2O
Transfer buffer	50 ml 10X Electrophoresis buffer
	100 ml methanol
	350 ml dH_2O

2.7.4.2 Composition of SDS –PAGE Gels

Separating Gel 10ml / plate (15% (v/v))	2.5 ml 4x separating buffer 5.0 ml 30 % (v/v) acrylamide 2.5 ml dH_2O 150 µl ammonium persulphate 10 µl TEMED
Stacking Gel 5 ml / plate (5% (v/v))	1.25 ml 4x stacking buffer 833 µl 30 % (v/v) acrylamide 2.877 ml dH_2O 50 µl ammonium persulphate 10 µl TEMED

2.7.5 Western blot analysis

Proteins were transferred from SDS-PAGE gels to nitrocellulose membrane by electophoretic means using a BioRad semi-dry blotter. The SDS-PAGE gel, 1 piece of nitrocellulose and 6 pieces of Whatman chromatography paper were soaked in transfer buffer for 15 mins. The proteins on the gel were transferred to the membrane for 20 mins at 15V. The membrane was blocked with 5% (w/v) MPBST overnight at 4°C. The blocked membrane was then washed extensively three times with PBS and three times with PBST. An appropriate enzyme-labelled secondary antibody (see section 2.1.4), diluted to 1/2000, was added and the blot incubated and washed as before. Color development was then observed following addition of the appropriate substrate, and the reaction stopped by addition of 50mM EDTA.

2.8 ELISA analyses

2.8.1 Direct Enzyme-linked immunosorbent assay (ELISA).

Direct ELISA was performed according to standard ELISA protocol for recombinant antibodies (Barbas *et al.,* 2001) with the following modifications: the scFv and FAb were detected using anti-HIS-HRP (Qiagen) and anti-HA-HRP secondary antibodies, respectively. Specific antibody binding was detected using o-phenylenediamine (o-PD) ELISA substrate. Absorbances were read after 30 min at 450nm. This method was used to optimise antibody and coating antigen concentrations in a checkerboard ELISA format.

2.8.2 Competition Enzyme-linked immunosorbent assay (ELISA).

Competition ELISAs were performed separately for each antibody construct under conditions determined by direct ELISAs: microtitre plate wells were coated with 100µl/well drug-protein conjugate (2 µg/ml in PBS), overnight at 4^{o}C. These plates were then washed three times with PBS and PBST and blocked with 300µl/well PBS/M (PBS/5% (w/v) milk protein) for 1h at 37^{o}C. 50 µL scFv or FAb were then added to each well in the presence of serially-diluted (PBS/2% (w/v) milk marvel) concentrations of free analyte (50µl) and incubated at 37^{o}C for 1hour. Plates were then washed 10 times with distilled water and antibody binding detected, as described for direct ELISA.

2.9 Biacore assay conditions

Analysis was performed using Biacore 3000 instrument and data analysis was performed using BIAevaluation 3.0 (BIAcore, St Albans, Hertfordmidshire, UK). Research grade CM5 sensor chips were employed in all analyses with Hepes-buffered saline, pH 7.0, (HBS) (10m*M* Hepes, 150 m*M* NaCl, 3.4 *M* EDTA and 0.025% (v/v)

Tween 20) as running buffer. HBS was 0.2μm filtered, degassed and syringe filtered (0.45μm) immediately before use.

2.9.1 Preconcentration Studies

Immobilisation of hapten – conjugate to the sensor chip surface was optimised via a preconcentration step. This allowed the optimal pH conditions to be identified. The carboxymethylated suface of the chip is negatively charged at pH values above pH 3. The desired pH conditions for electrostatic immobilisation are such that result in the ligand possessing an overall positive charge. Therefore, a buffer with a pH lower than the pI of ligand is required. Sodium acetate buffer is used in preconcentration studies due to its low ionic strength thus maximising ionic interactions between ligand and chip surface. 100 μg/ml solutions of hapten – conjugate were made up in 10 mM sodium acetate at a range of varying pHs in the range 3.8 – 5.0. These were passed over the underivatised chip surface and the pH which gave the highest degree of electrostatic interaction was chosen as the optimal pH for immobilisations.

2.9.2 Immobilisation of hapten - conjugate on sensor chip surface.

M3G-OVA conjugate immobilization was carried out according to standard amine coupling chemistry.

2.9.3 Immobilisation of Hapten directly on sensor surface.

Direct immobilisation of M3G on the sensor chip surface was performed as follows: the carboxylmethylated dextran surface of the sensor chip was activated by mixing equal volumes of 0.1M NHS (*N*-hydroxy-succinimide) and 0.4M EDC (*N*-ethyl-*N*-(dimethyl-periplasaminopropyl) carbodiimide hydrochloride) and injecting the mixture over the sensor chip surface for 8 min at a flow-rate of 5 μl /min. The chip surface was then

capped with 1M ethylene diamine (pH 8.5) for 10 min (flow-rate 5 µl /min). M3G (100µg/ml diluted in EDC/NHS) was incubated at room temperature for 3 min., before injection over the chip surface for 20 min at a flow-rate of 10 µl /min. To complete the reaction, unreacted sites on the chip were capped with 1M ethanolamine. The surface was then regenerated 5 times with 40 mM NaOH prior to use.

2.9.4 Non – specific binding studies

Antibody samples were passed over proteins i.e. BSA or OVA immobilised on the sensor chip surface, in order to rule out non – specific binding to the conjugate in question and to ensure recognition was to the hapten and not the carrier or the conjugation linkage chemistry.

2.9.5 Inhibition studies

To prepare samples for Biacore sensor analysis, antibodies were diluted in HBS buffer (pH 7.4). Concentration standards of M3G (ranging from 318 to 1.25 x 10^6pg/ml) were then prepared in HBS buffer. When using the M3G-coated sensor surfaces, each concentration standard was incubated separately with an equal volume of a 1/60 dilution of the Fab (1/120 final dilution) and a 1/25 dilution of the scFv (1/50 final dilution) for 30 min at room temperature before being passed over the chip at a flow-rate of 5 µl/min to examine antibody binding profiles. Preparations of the Fab were diluted to 1/20 and the scFv to 1/8 for use on the M3G-OVA immobilized chip. Final antibody concentrations were pre-determined to provide a signal of approximately 300 RU on each respective surface, in the absence of competing antigen. M3G and M3G-OVA-chip surfaces were both fully regenerated using a single 15 second pulse of 40mM NaOH at a flow-rate of 20 µl /min. A control sample containing no M3G was included in each run to provide maximal signal for R/R_0 calculations. Analyses at each free M3G

concentration were carried out in triplicate on 3 separate occasions for assay variability studies.

2.9.6 Kinetic analysis of the binding of the anti – M3G scFv and anti – M3G Fab using Biacore.

Biacore analysis was performed to examine the binding kinetics of both scFv and Fab. Analyses were performed using a directly coupled M3G chip surface which generated a maximum resonance signal of 100RU when saturated with either scFv or Fab antibody fragments. Rmax of approximately 100RU, is designated by Biacore as optimal for kinetic studies. This provided an appropriate surface for comparison studies and was within the parameters recommended by Biacore for kinetic analysis. Individual samples consisting of 90µl of either IMAC-purified scFv or Fab were passed over the chip surface at a flowrate of 30µl/min. Following analysis, bound antibody fragments were eluted using 40mM NaOH until the resonance signal returned to baseline value. The sensogram obtained from injecting non-specific antibody fragment in PBS plus 25mM imidazole diluted in HBS (mimicking a nickel-purified antibody buffer preparation) was used to normalise the sensograms obtained from both Fab and scFv binding to M3G. The dilutions for both antibody fragments used were as follows; 1/10, 1/20, 1/40, 1/80, 1/160, 1/320 in HBS. At each concentration reference surface readings were subtracted and the data corrected automatically for baseline and then analysed using BIAevaluation. Apparent Kd constants were derived as those that were consistent over the analyte concentration ranges. Mass transfer limitations were determined to be negligible

2.10 Multimerisation Analysis

2.10.1 HPLC Assay conditions

Size exclusion HPLC analysis was carried out using the Phenomenex, BioSep – SEC – S – 3000, 300nm x 7.80nm. All assays were performed at a flowrate of 0.5 ml/min using an injection volume of 50 µl. The mobile phase was PBS (pH 7.4). All samples were examined at neat dilutions in PBS. Protein molecular weight standards for HPLC (Sigma) included bovine serum albumin (BSA), 66KDa; chicken egg albumin, 45KDa; crbonic anhydrase, 25KDa; and beta lactalbumin, 14.5 KDa.

2.10.2 Native polyacrylamide gel electrophoresis conditions

Antibody multimerisation was also examined by native polyacrylamide gel electrophoresis (Laemmli, 1970). In non-denaturing gel electrophoresis the molecular weight standards used were the same as those described for use with HPLC.

2.11 Kunkle-style mutagenesis of the anti-M3G fab fragment.

The mutagenesis strategy used is outlined in Kunkle *et al.,* (1990). Amendments to the procedure are outlined in sections 2.11.3.1 – 2.11.3.3.

2.11.1 Primer design.

M3G CDRH1-Fstop
ACTGGCTACACATTCAGTTAATAATAATAATAATGGGTAAAGCAGAGGCCT

M3G CDRH1-Rstop
AGGCCTCTGCTTTACCCAATTATTATTATTATTACTGAATGTGTAGCCAGT

M3G CDRL2-Fstop
TTCACTGGTCTAATAGGTTAATAATAATAATAATAATAAGGTGTTCCTGCCA
GATTC

M3G CDRL2-Rstop
GAATCTGGCAGGAACACCATTATTATTATTATTATTATTACCTATTAGACCA
GTGAA

M3G CDRL3-Fstop
GAGGCAATATATTTCTGTTAATAATAATAATAATAATAATAATAATTCGGTG
GAGGAACCAAA

M3G CDRL3-Rstop

TTTGGTTCCTCCACCGAATTATTATTATTATTATTATTATTAACAGAAAT
ATATTGCCTC

M3G CDRH1-Fmut

ACTGGCTACACATTCAGTNNSNNSNNSNNSNNSTGGGTAAAGCAGAGGCCT

M3G CDRH1-Rmut

AGGCCTCTGCTTTACCCASNNSNNSNNSNNSNNACTGAATGTGTAGCCAGT

M3G CDRL2-Fmut

TTCACTGGTCTAATAGGTNNSNNSNNSNNSNNSGCTCCAGGTGTTCCTGCC

M3G CDRL2-Fmut

GGTCTAATAGGTGGTACCNNSNNSNNSNNSNNSGGTGTTCCTGCCAGATTC

M3G CDRL2-Rmut

GAATCTGGCAGGAACACCSNNSNNSNNSNNSNNGGTACCACCTATTAGACC

M3G CDRL2-Rmut

GGCAGGAACACCTGGAGCSNNSNNSNNSNNSNNACCTATTAGACCAGTGAA

M3G CDRL3-Fmut

TTCTGTCTTCTATGGTACNNSNNSNNSNNSNNSTTCGGTGGAGGAACCAAA

M3G CDRL3-Fmut

GAGGCAATATATTTCTGTNNSNNSNNSNNSNNSAACCATTTGGTGTTCGGT

M3G CDRL3-Rmut

TTTGGTTCCTCCACCGAASNNSNNSNNSNNSNNGTACCATAGAAGACAGAA

M3G CDRL3-Rmut

ACCGAACACCAAATGGTTSNNSNNSNNSNNSNNACAGAAATATATTGCCTC

2.11.2 Preparation of dU-ssDNA

A single colony of CJ236 *E. coli*, containing the anti-M3G fab plasmid, was inoculated into 5ml 2XTY media (100µg/ml carbenicillin and 10µg/ml chloroamphenicol). The culture was grown overnight at 37^{o}C while shaking at 220rpm. The overnight culture was seeded at a 1/100 dilution into 2 ml 2XTY (100µg/ml carbenicillin and 10µg/ml chloroamphenicol) and grown at 37^{o}C while shaking at 120rpm until OD 0.5nm. When the OD had reached 0.5, 250µl of M13KO7 helper phage and 0.25µg/ml uridine was added and the volume was increased to 100ml. The 100ml culture was grown for 1 hour before addition of 50µg/ml kanamycin. The infected culture was grown overnight at 37^{o}C and 120rpm. The culture was centrifuged at 12,000rpm, 4^{o}C for 15min. The supernatant was decanted into fresh tubes and the phage was PEG/NaCl precipitated on ice for 45min. The suspension was centrifuged at 12,000rpm, 4^{o}C for 15min with the brake turned off. The supernatant was discarded and the phage pellet was resuspended in 2 ml sterile filtered PBS. All insoluble cell debris and endogenous DNA were removed by an additional 12,000rpm centrifugation step here. Single stranded DNA was purified from the phage prep using the Qiagen Spin M13 kit. The dU-ssDNA was quantified on the nanodrop.

2.11.3 In-vitro synthesis of heterduplex DNA

2.11.3.1 Phosphorylation of the oligonucleotide

Table 2.11.3.1.1 Components of phosphorylation reaction

Component	Concentration	Volume (µl)
Oligonucleotide	0.6µg	1
10X buffer	1X	2
ATP	10 mM	2
T4 polynucleotide kinase	20 units	2
H_2O	Up to 20 µl	x

Table 2.11.3.2 Reaction conditions

Temperature	Time (minutes)
37^oC	30
65^oC	10

2.11.3.2 Annealing the oligonucleotide to the template dU-ssDNA

Table 2.11.3.2.1 Components of annealing oligonucleotide/template reaction

Component	Concentration	Volume (µl)
Oligonucleotide	0.6µg	1
10X buffer	1X	1
dU-ssDNA	2 µg	x
H_2O	Up to 10 µl	y

Table 2.11.3.2.2 Reaction conditions

Temperature	Time (minutes)
90°C	10
Slowly cool to 20°C	
20°C	5

2.11.3.3 Enzymatic synthesis of covalently closed circular DNA (CCC-DNA)

The following is added to the annealed oligonucleotide/template reaction mix.

Table 2.11.3.3.1 Components required for the enzymatic synthesis of CCC-DNA

Component	Concentration	Volume (µl)
ATP	10mM	1
dNTP	10mM	5
DTT	5 mM	1
T4 DNA ligase	30 units	3
T7 DNA polymerase	30 units	3

Table 2.11.3.3.2 Reaction conditions

Temperature	Time (minutes)
4°C	5
25°C	5
37°C	240

2.11.3.4 Affinity purification and de-salting the CCC-DNA

This was carried out using the Qiagen Qiaquick nucleotide removal kit manufacturer's manual.

2.12 Sequence analysis of genes encoding specific antibody fragments

A single colony was grown overnight in LB media. The expression vector, containing gene of interest, was isolated and purified using Wizard Plus SV Miniprep kit, according to the manufacturers instructions. Plasmid DNA was sequenced by Qiagen. Raw data, forward and reverse sequences, was analysed using CHROMAS sequence analyser software. The DNA sequences were exported and analysed using a variety of web-based bioinformatics tools (see table 2.12.1)

Table 2.12.1 Source of web based bioinformatics tools used for sequence analysis of antibody fragments.

Tool	Source
CHROMAS	www.technelysium.com.au/chromas.html
Translate tool	www.expasy.org
BLAST	www.expasy.org
Swiss-model	http://swissmodel.expasy.org
Multialin	http://prodes.toulouse.inra.fr/multalin/multalin.html
Kabat Rules	www.//acrmwww.biochem.ucl.ac.uk/abs

Chapter 3

3.0 Generation of anti-amphetamine recombinant antibody fragments and their characterisation

3.1 Introduction

3.1.1 Factors influencing antibody phage display

A detailed description of the individual vector maps used in this work (pAK vector series and the pComb3x vector series) is given in section 1.9.3. Each component of the phagemid vector needs to be evaluated fully prior to the construction of an antibody phage display library. Each phagemid vector varies in a number of key characteristics, e.g. a different combination of enzyme tags, variance in display valency, use of pIII or pVIII display protein. Each of these has a significant influence on the panning approach employed and the final outcome of the experiment, although the target and recombinant antibody format (scFv or Fab) used is also an influency factor. While the scFv library construction and panning (section 1.9.5) is strongly facilitated by the smaller size and composition of a single polypeptide, Fab libraries are not afforded these fundamental advantages.

The ideal antibody phage display system will result in the production and purification of an antibody fragment that is, at least, comparable to IgG in terms of stability, affinity and compatibility with current diagnostic systems (Hust and Dubel, 2004). Small antibody fragments such as Fv or scFv are easily produced and the yield is often higher than that achieved in the production of Fab fragments (Pluckthun, 1991). However, scFv fragments can cause problems due to the formation of multimers (examined extensively in chapter four) while Fab fragments are stabilized by the presence of a disulphide bond between the heavy chain and the light chain (Hust and Dubel, 2004). One significant advantage of using the Fab antibody format in diagnostics is its superior stability compared to the far less rigid scFv fragment (Bradbury *et al.,* 2003) where the kinetic stabilization of a linker region is relied upon (Glockshuber *et al.,* 1990). In addition, the presence of a complete constant heavy chain in the Fab makes it

compatible for use with almost all secondary antibodies already generated and hence it can be used in most current detection platforms available.

Despite different opinions regarding the optimal recombinant antibody format for diagnostic and therapeutic applications the phagemid vector used is the one parameter that must be carefully considered. The phage display vector / vector series must provide robustness, vector stability, tight control of protein-gene III fusion, easy-to-use primer sets, a protein assembly strategy, enzyme restriction sites for directional cloning and contingent for soluble protein expression (Krebber *et al.,* 1997).

3.1.2 Phagemid vectors

Phage display vectors can be classified according to three characteristics (Barbas *et al.,* 2001).

1. The coat protein selected for display (pIII or pVIII)?

The two proteins involved in display of proteins on the phage particle are pIII (minor capsid protein) and pVIII (major capsid protein). pIII is the most commonly used capsid protein for phage display and while it only allows about 5 molecules to be displayed per single phage particle, it does package along with large fusion proteins very efficiently in comparison to pVIII.

2. The display of the recombinant proteins on all or only some of the coat proteins?

The pComb3x vector series used in this work is classified as a Type 3 + 3 vector (Smith and Petrenko, 1997). These phage typically display up to 5 copies of wild type pIII on their surface along with the fusion protein pIII from the phagemid, creating a competitive environment for incorporation into the virion during assembly. This process results in a low valency system, which favours selection of high affinity fusion proteins. Phage display vectors such as type 3 and type 8 + 8 exploit their high valency display and are used in the screening of low affinity target experiments such as anti-

carbohydrate antibodies (Scott and Smith, 1990). These phage can display up to 200 copies of the foreign peptide (Yau *et al.,* 2003).

3. The recombinant gene is cloned directly into the phage genome or on a separate phagemid vector?

The pComb3x vector series does not involve direct cloning into the phage genome, instead it contains a second plasmid, which also encodes a phage origin of replication. Two – gene display systems provide the opportunity to modulate the valency of the displayed fusion protein, (Barbas *et al.,* 2001), a key factor in antibody display for selection of the high affinity binders. This point is examined more extensively in chapter four.

3.1.2.1 pAK vectors; 100 and 400

This phagemid vector series (section 1.9.3), unlike the pComb series, consists of 6 different vectors and includes separate vectors for display and soluble expression. The pAK 100 vector is used for display of foreign peptides and is classified as a monocistronic vector as it encodes a single lacZ promoter and also utilizes a single leader sequence (pelB). The pAK 400 vector encodes an amber codon, which facilitates switching between display and soluble expression and a c-myc tag for detection, but it does not encode a convenient method for purification. However, the pAK 400 vector excludes the gene III and encodes a stronger Shine Dalgarno sequence ($SDT7_g10$) and a hexahistidine tag to allow use of IMAC purification methods and antibody detection.

3.1.2.2 pComb3x

Section 1.9.3 details this series schematically, however, there are some key points that require more in-depth discussion. The pComb vector series was modified so that it contains a single lacZ promoter and two leader sequences (OmpA and pelB). This bicistronic feature results in the translation of a both light and heavy chains of the antibody fragment from a single mRNA (Kirsch *et al.,* 2005). The importance of the

bicistronic vector is most evident in Fab fragment expression as it ensures that an equal ratio of heavy chain to light chain is achieved.

The human constant regions are sourced from the pComb3xTT vector, as mentioned in section 1.9.3. This vector contains a human anti-tetanus toxin Fab insert from which the human kappa light chain and human constant heavy chain can be amplified. In chapter four, where the anti-M3G Fab required the use of a constant lambda light chain, the pComb3xLamda-containing vector is used instead. This vector does not contain a functional antibody fragment insert. Instead it has a nonsense antibody with a human lambda constant region.

3.2 Rationale for the construction of anti-amphetamine recombinant antibody fragments from an IgG genetic template.

A number of groups have reported the construction and expression of small recombinant antibody fragments from the genetic backbone of target specific whole IgG. The fact that many anti-hapten antibodies rely primarily on the cavity shaped paratopes for antigen contact, a notion that is further developed in chapter five, implies that the rigidity and conservation of structure through constant chain scaffolding are vital to maintaining the specific anti-hapten antibody affinity. This leads one to question if an anti-hapten monoclonal antibody can be successfully converted into a smaller recombinant antibody fragment and if the cavity shaped antigen-binding site remains intact in the scFv and Fab structural formats.

In the study presented here, the effects of converting an anti-amphetamine IgG to, first a Fab and then, a scFv fragment were examined. The variable regions of the previously described IgG (Fanning, 2001) were re-engineered for the expression of these small recombinant fragments. The characteristics of the resulting Fab fragment were compared to the IgG using ELISA and Biacore. The scFv expression proved unsuccessful, holding true to the theoretical importance of structural scaffolding to the affinity of the IgG.

3.3 Results and Discussion

3.3.1 Construction of an anti-amphetamine Fab fragment from a monoclonal anti-amphetamine antibody-secreting hybridoma

3.3.1.1 Construction of chimeric anti-amphetamine Fab.

The anti-amphetamine construct was constructed using the anti-amphetamine secreting hybridoma, 4EP18E (Fanning, 2002). Variable heavy and light chains were amplified from the freshly prepared cDNA, using the primers listed previously in section 2.4.8. The human constant heavy and constant kappa domains were amplified from the pComb3XTT vector. The $MgCl_2$ concentration was optimized for each PCR reaction, keeping all other components constant. The concentrations varied from 1.5mM-6mM. The efficiency was assessed by running the PCR products side by side on a 1% (w/v) agarose gel and visually inspecting them. The V_H and V_L fragment ratio for the final SOE PCR was optimized by varying the ratio of each fragment while keeping all other components constant. This extensive optimization resulted in efficient amplification of the required bands with no non-specific bands being generated (Figure 3.3.1.1.1). It was necessary to amplify all chains V_L, V_H, C_L and C_H, separately, initially. Appropriate chains are then overlapped leading to the final Fab fragment construction.

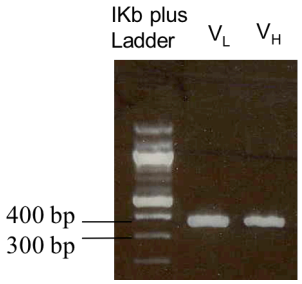

Figure 3.3.1.1.1 Variable light and variable heavy chain amplifications run on a 1% (w/v) agarose gel alongside an appropriate MWM; 1kb plus ladder. The mouse variable regions products are about 400bp in size. The correctly sized DNA bands are excised, purified and stored until required for the final Fab light and heavy chain splice by overlap extension (SOE).

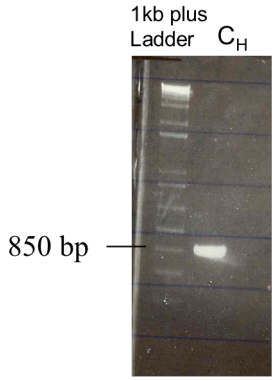

Figure 3.3.1.1.2 Constant light and constant heavy chains are amplified from pComb3XTT, which encodes a cloned human Fab template, run on a 1 % (w/v) agarose gel alongside a 1kb plus ladder. The chimeric light and heavy chain (shown here) products are about 850bp in size.

When all individual fragments are amplified each of the final heavy and light chains can be constructed using the appropriate overlapping primers. Each of the single fragment amplifications yielded approximately 200 ng/µl DNA when analysed at 260nm. Two SOE PCR's were carried out separately, the first for the construction of the chimeric light chain and the second for the chimeric heavy chain.

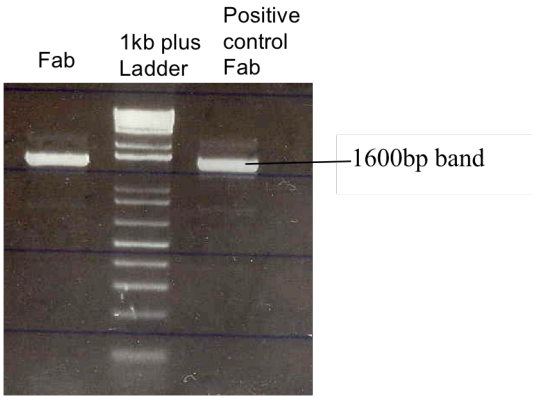

Figure 3.3.1.1.3 Final SOE PCR, combining the light chain and heavy chain of the anti-amphetamine antibodies yielding a 1600bp band. Samples were run on a 1% (w/v) agarose gel.

The pComb3x vector and the newly constructed anti-amphetamine Fab were digested with *Sfi* 1 and run on a 1% (w/v) agarose gel for assessment. The large-scale PCR reaction products were gel-extracted and purified via electro-elution, as a means of improving the efficiency of the gel purification system.

3.3.1.2 Bio-panning the anti-amphetamine Fab library

An anti-amphetamine monoclonal antibody-secreting clone was used as the genetic resource for this library construction and as a result the panning strategy is slightly different in comparison to that used with a large diverse immune or mutated library (chapter five and chapter six). The panning was designed so that it was just stringent enough to pull out the genotypically similar antibody to the original monoclonal but it did not need to be excessive. It was decided that two rounds of panning would be sufficient and following these a polyclonal phage ELISA was carried out. Low-level enrichment of positive signal from each round of panning was observed in tandem with good input and output titres from pan 0 to pan 2 (Table 3.3.1.2.1).

Table 3.3.1.2.1 Input and output titres for all rounds of panning for anti-amphetamine recombinant Fab library.

	Pan 0	**Pan 1**	**Pan 2**
Input	-	6×10^{11}	$1.8 \times ^{12}$
Output	6.3×10^{7}	4×10^{4}	1×10^{5}

3.3.1.3 Individual clone analysis

While the polyclonal phage ELISA confirmed the presence of amphetamine-specific phage, an "insert check" pick PCR was carried with random colonies picked from the round 2 output titre plates. This allowed conformation and visualization of the Fab insert. The same clones were grown and digested with the high frequency cutting enzyme Alu 1 to investigate the presence of any mutations. This digest was run on a 3% (w/v) agarose gel in order to achieve good separation of bands (Figure 3.3.1.3.1).

Figure 3.3.1.3.1 Single clones from round 2 panning output titre plates, were randomly chosen and digested with Alu 1 to determine the mutation rate in the library. It is clear from the gel picture that the digest pattern varies widely between each clone. This is indicative of a high number of mutations. This may be as a result of ligation of more than one specific light chain.

Ten colonies were picked, grown and induced with IPTG. The lysates were prepared as described in chapter 2. The 10 clones were screened in ELISA (Figure 3.3.1.3.2).

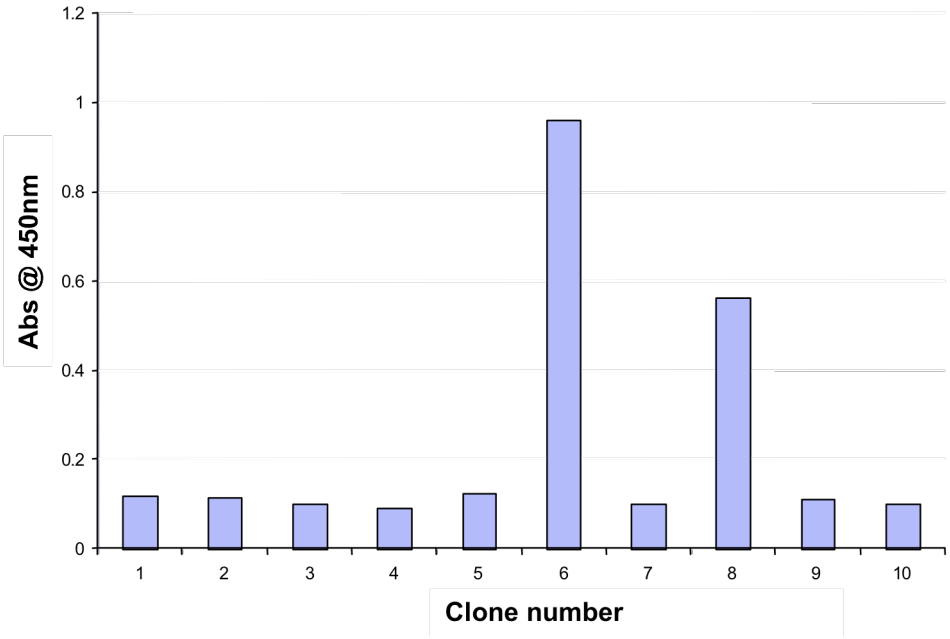

Figure 3.3.1.3.2 ELISA analysis carried out on 10 anti-amphetamine clone lysate preparations. 1 µg/ml amp-BSA was coated on the plate and binding was detected with an anti-HA-HRP secondary antibody. Data expressed as Abs (Absorbance). Two clones (6 and 8) demonstrated expression of anti-amphetamine Fab, with absorbance values 5 times over background absorbance.

Following identification of positive clones, no. 6 and no. 8 a competitive ELISA was carried out on the lysate preparations using a free drug range of 5000 - 1.6 ng/ml (Figure 3.3.1.3.3). This range allows identification of any clone expressing anti-amphetamine Fab capable of being displaced by free amphetamine.

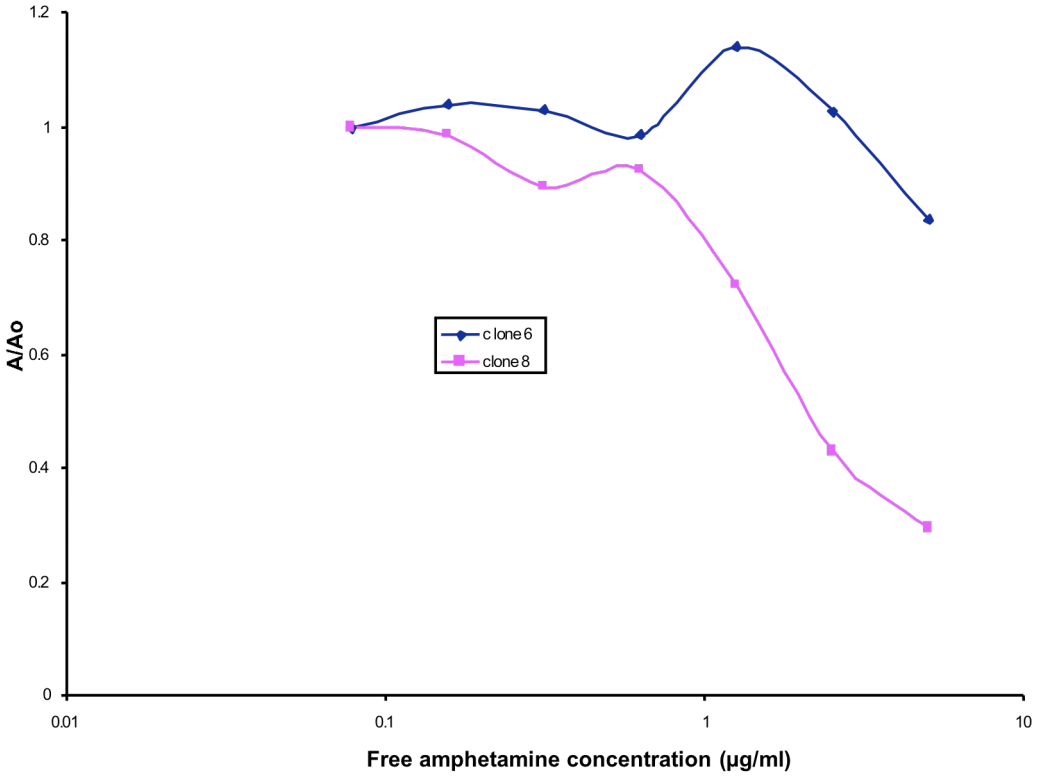

Figure 3.3.1.3.3 ELISA lysate-inhibition assay performed on Amphetamine-BSA-coated wells comparing the binding response of clone no. 6 (blue) and clone no. 8 (pink) versus free drug in the range of 1.6 - 5000 ng/ml. Data is expressed as A/Ao (i.e. signal at different free analyte concentrations are expressed as a proportion of signal in the presence of no competing analyte).

3.3.1.4 Characterisation of positive clone

The Fab from clone no. 8 was chosen for further characterisation and development due to its significantly better performance in the inhibition ELISA compared to clone no. 6. It was grown up on a larger scale (500 ml culture volume) and the anti-amphetamine Fab was purified using the IMAC system. The appropriate dilution of the Fab preparation for use in the inhibition ELISA was determined. The pComb3X vector adds a heamaglutanin (HA) tag to the antibody fragment which facilitated screening as the anti-HA secondary antibody is highly sensitive. However, it is also very expensive and so an alternative secondary antibody was investigated. The anti-amphetamine Fab is a C_{κ} construct. This permitted the use of an anti-human-kappa secondary antibody for screening which is less expensive. The activity of both secondary antibodies was compared and no significant difference between the two was observed. Hence, all anti-amphetamine Fab ELISA's were carried out with the anti-human-kappa antibody. The anti-amphetamine Fab titre showed that the ideal dilution of the Fab for use in inhibition analysis was 1 in 2000 of the purified antibody preparation. All assay conditions were optimized (data not shown) prior to the development of the inhibition ELISA (Figure 3.3.1.4.1). The ELISA was carried out, as outlined in section 2.8.9, with an amp-BSA coating concentration of 1 μg/ml. The anti-human-kappa secondary antibody was alkaline phosphatase-labeled and the substrate used to detect its presence was BCIP. The standard deviations were between 8% and 15.5%, which is the acceptable standard for many of the points.

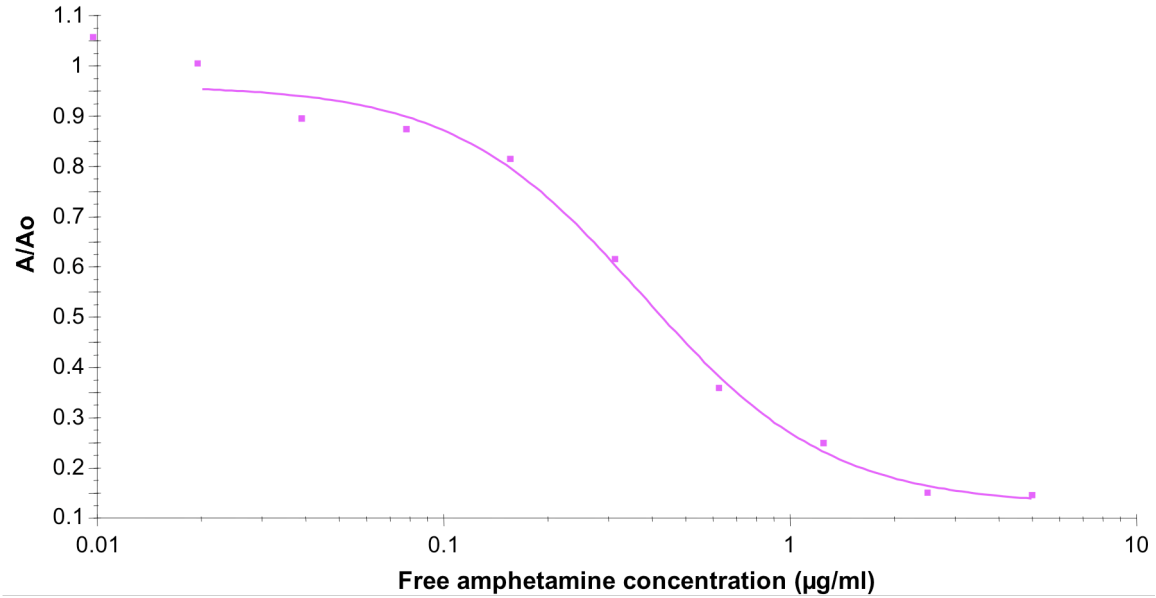

Figure 3.3.1.4.1 ELISA inhibition assay performed on amphetamine-BSA-coated wells comparing Fab binding response versus competing free amphetamine concentrations. Data is expressed as A/A_o (i.e. signals at different free analyte concentrations were expressed as a proportion of signal in the presence of no competing analyte). All analyse were carried out in triplicate on three separate occasions. Standard deviations at all points examined were between 8 -15% of total signal.

3.3.1.5 Biacore analysis

A Biacore™ competition assay was developed using an amphetamine-BSA-coated CM5 chip surface to determine the range of free amphetamine detection for the Fab. The same range of free drug, as used with the ELISA, was employed in all Biacore competition assays. The Fab displayed negligible non-specific binding to the BSA-coated chip surface negating the need for pre-incubation steps with BSA.

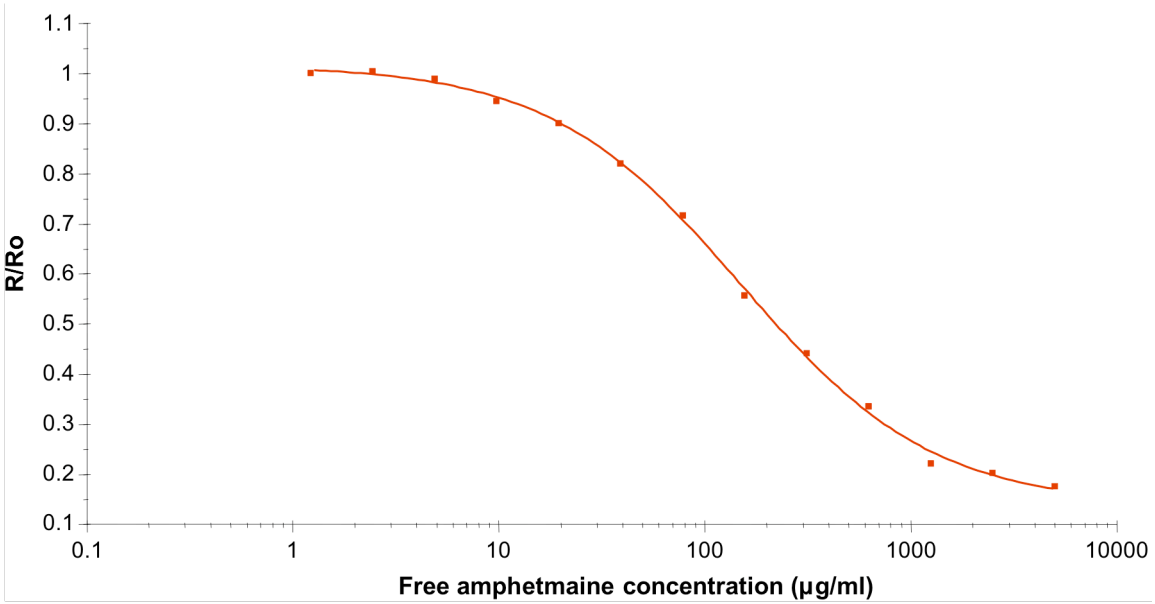

Figure 3.3.1.5.1 Biacore™ inhibition assays performed on an amphetamine-BSA-coated CM5 chip surface. Data was expressed as R/R_0 (i.e. signal at different free analyte concentrations are expressed as a proportion of signal in the presence of no competing analyte). All analyses were performed in triplicate on three separate occasions. Standard deviations at all points examined were less than 9% of signal, with a mean deviation of 3 % of signal.

The linear range of the Fab on ELISA was shown to be 1250 - 39 ng/ml, with an IC_{50} value of approximately 200ng/ml (Figure 3.3.1.5.1). The Fab construct was compared to the parent monoclonal anti-amphetamine antibody in an inhibition assay format (Figure 3.3.1.5.2). The monoclonal antibody, which has been previously described by Fanning (2001), demonstrated a similar linear range to that of the Fab and an IC_{50} of approximately 600 ng/ml. This data would indicate that the Fab is 2/3 fold more sensitive than the parent monoclonal.

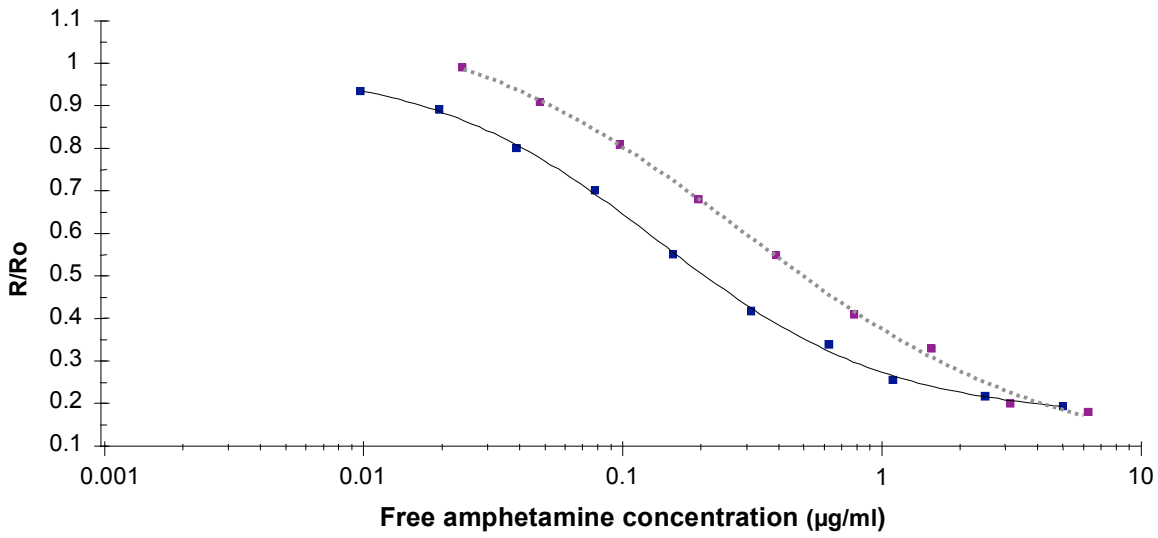

Figure 3.3.1.5.2 Biacore™ inhibition assays performed on an amphetamine-BSA-coated CM5 chip surface, comparing the binding response of the Fab (solid) and monoclonal antibody (dashed) versus competing free amphetamine concentration. Data was expressed as R/Ro (i.e. signal at different free analyte concentrations are expressed as a proportion of signal in the presence of no competing analyte). All analyses were performed in triplicate on three separate occasions. Standard deviation at all points examined was < 5% of signal.

3.3.1.6 Sequencing

The next stage of this work investigated the conversion of the Fab fragment to a scFv fragment. If the Fab was sequenced it would negate the need for mixed primer sets for variable heavy and light chain amplification, as the variable regions could be identified.Plasmid DNA was sent to MWG Biotec (Germany), for sequencing. Comfort reads were performed in triplicate using the primers ompseq (5` AAG ACA GCT ATC GCG ATT GCA G 3`) and pelseq (5` ACC TAT TGC CTA CGG CAG CCG 3`). The resulting nucleic acid sequence was analysed using the Chromaslite 200 software package, and the Expasy nucleic acid translation tool (http://www.expasy.org/tools/dna.html). Once the amino acid sequence had been obtained, it was inputted into the IgBlast search engine at the National Institutes of Health, National Centre for Biotechnology Information website (http://www.ncbi.nlm.nih.gov/igblast/). The CDR's were identified using Kabat rules.

Framework 1 CDRL1

V M T Q S P L S L P V S L G D Q A S I S C R S S Q S L V Y S N G N T Y L H W

Framework 2 CDRL2 Framework 3

Y L Q K P G Q S P K L L I H K V S N R F S G V P D R F S G S G S G T D F T L

CDRL3

K I I R V E A E D L G V Y F C S Q S T H V P F T F G S G T K L E L K .....

Framework 1 CDRH1

E V M L V E S G G G L V K P G G S L K L S C A A S G F T F S N Y A M S W V R Q T P D

Framework 2 CDRH2 Framework 3

K R L E W V S S I T S G G S T Y Y P D S V K G R F T I S R D N A R N M L Y L Q M S S

CDRH3

L R S E D T A M Y Y C T R E S H Y G R S Y D Y F D Y W G Q G T S V T V S S A S.....

Figure 3.3.1.6.1 Sequence analysis of the anti-amphetamine Fab fragment. Heavy and light chains CDR's are highlighted in red and framework regions are shown in black.

3.3.2 Conversion of the anti-amphetamine Fab to an scFv fragment.

3.3.2.1 Construction of anti-amphetamine scFv

It proved difficult to choose specific primers from the Krebber scFv primer set based on the Fab sequence obtained. However, after test reactions it was determined that light chain primers, LB5 and the LFmix, and the heavy chain mix primer set would be most suitable for the amplification of an scFv from the Fab template. A large non-specific smear was evident in the SOE PCR product after visualization on a 1% agarose gel. After a number of optimization strategies, DMSO was added to the reaction at varying concentrations. Figure 3.3.2.1.1 (a) and (b) illustrate the influence of selection of the optimal DMSO concentration followed by $MgCl_2$ concentration optimisation.

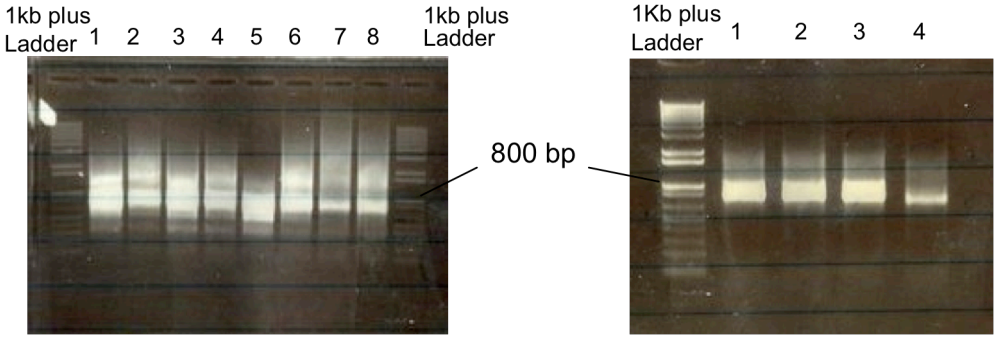

Figure 3.3.2.1.1 SOE PCR conditions were optimized through varying concentrations of DMSO and $MgCl_2$. In gel picture (a), 100 ng/ml of each fragment, V_H and V_L, were included in the reaction. Reactions in lanes 1 - 4 contain no DMSO and varying concentrations of $MgCl_2$; 1.5 - 4mM, respectively, lanes 5 - 8 contain 5% (v/v) DMSO with varying concentrations of $MgCl_2$; 1.5 - 4mM, respectively. Gel picture (b) represents further optimization carried out on the same SOE PCR using 50 ng/ml of each fragment, V_H and V_L. All other components, including 5% (v/v) DMSO, were kept constant except $MgCl_2$, lanes 1 - 4; 1.5mM - 4mM $MgCl_2$, respectively.

3.3.2.2 Bio-panning and analysis of clones

The anti-amphetamine scFv library size was determined to be 5.1 x 10^7, all library construction controls were included and examined prior to continuing to bio-panning. The panning strategy used here mimicked the strategy outlined in section 3.3.2 as a similar theory applies here. It is more of a conversion than a full-scale diverse library building. Therefore, an extensive panning strategy was not necessary.

Following two rounds of solution phase panning, a polyclonal phage ELISA was carried out resulting in low signal from each round of panning. A monoclonal phage ELISA was carried out on the round 2 output colonies to confirm the presence of specific anti-amphetamine scFv-displaying clones (Figure 3.3.2.2.1 (a)). Despite the low overall signal this result was indicative of a potentially positive anti-amphetamine scFv library, therefore, the library was cut, ligated into pAK 400 and transformed into *Top 10 F'* for soluble expression and further analysis. A soluble expression monoclonal ELISA was carried out according to section 2.6.2. (Figure 3.3.2.2.1 (b))

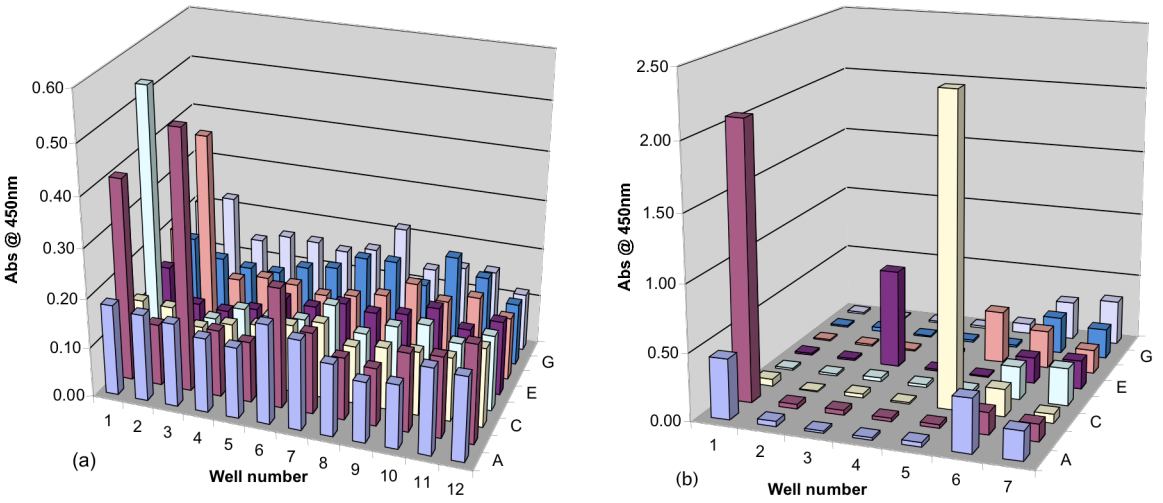

Figure 3.3.2.2.1 (a) Round 1 monoclonal phage ELISA results on 92 clones. Positive clones are those observed as having 2 times signal over the control signal. Binding was detected with an anti-M13-HRP labeled secondary antibody. (b) ELISA on soluble expressed scFv fragments. Positive clones are those observed as having 2 times signal over the control signal. Binding was detected with an anti-HA secondary antibody. Signal developed using TMB chromogenic substrate and monitored by optical density at 450nm. Data is expressed as absorbance read.

Four clones were taken on to the next stage, grown and expressed. Based on the outcome here (Figure 3.3.2.2.1(b)), clones ASR12, ASR121, ASR135, ASR138 were grown in 5ml cultures and expression was induced with IPTG. Competitive analysis revealed clone number ASR121 was displaced by concentrations of free amphetamine.

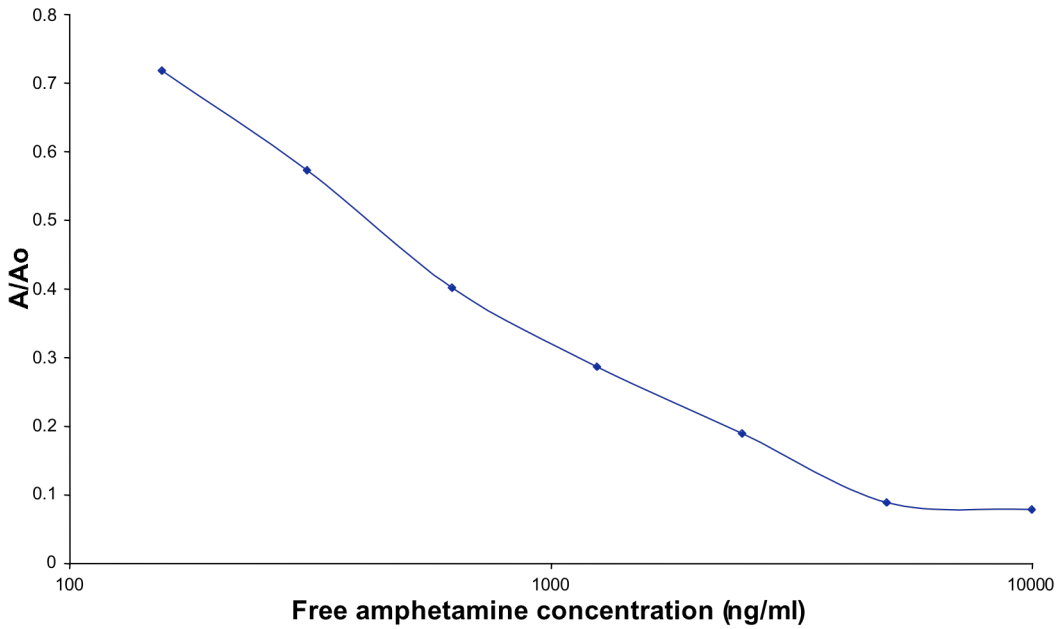

Figure 3.3.2.2.2 ELISA inhibition assay performed on amphetamine-BSA-coated wells comparing scFv ASR121 lysate binding response versus competing free amphetamine concentration (156 - 10000 ng/ml). Data is expressed as A/A_o.

In direct ELISA the His purified antibody fragment provided a titre of 1/1000 (Figure 3.3.2.2.3). However, uniform signal was observed across all concentrations of free amphetamine drug. The assay was repeated on three separate occasions and the result remained negative. This presented a problem as the clones had demonstrated some inhibition, albeit low levels (Figure 3.3.2.2.3), when assayed in lysate rather than purified antibody fragments.

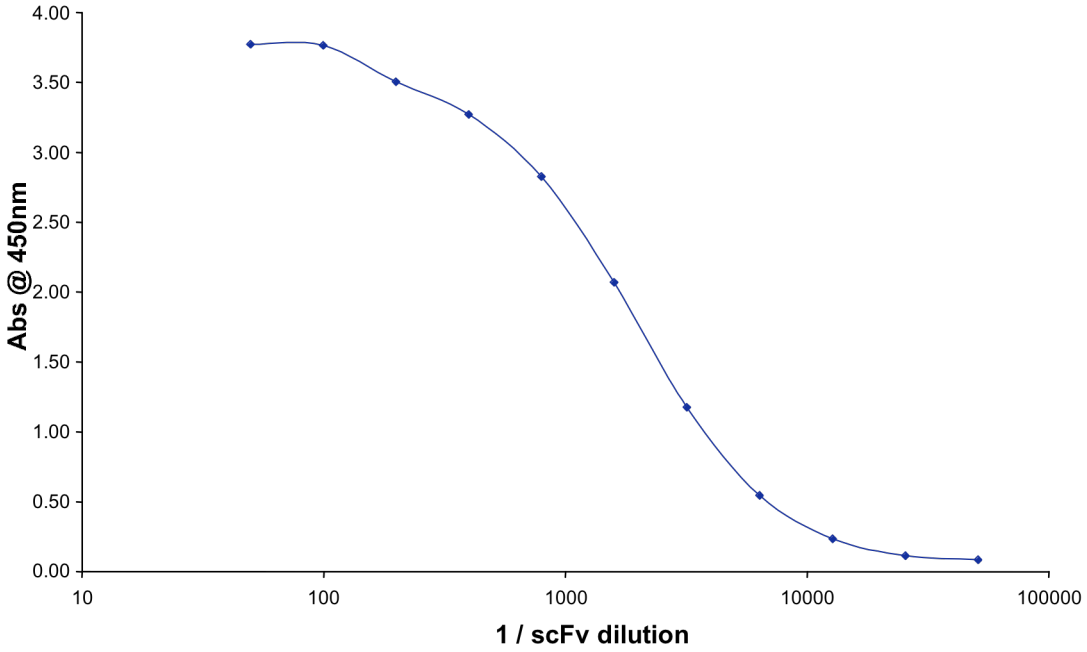

Figure 3.3.2.2.3 Direct ELISA of the His purified anti-amphetamine scFv fragment on an amphetamine-BSA coated surface. Signal developed using OPD chromogenic substrate and monitored by optical density at 450nm. Data is expressed as absorbance (nm).

Upon further investigation, many publications have eluded to the importance of structure and rigidity of an anti-hapten scFv rather than the more traditional notion of the importance of the CDRH3 for high affinity binding. It is thought that the antibody-hapten interaction may be primarily dependant on the binding cavity (Persson *et al.,* 2008) created by the rigidity of the structure.

This theory holds true for the problems encountered in the conversion of an IgG / Fab to an scFv fragment in this work. The recombinant Fab fragment demonstrated binding characteristics comparable albeit at a 3 fold higher affinity to that of the parent monoclonal antibody. However, the parent clone was essentially screened and selected for its ability to bind free amphetamine in the presence of the large, rigid and monomeric binding structure that is characteristic of an IgG. The direct conversion of

this antibody to a Fab fragment was successful as the Fab structure retains a certain level of that rigidity and scaffolding via the remaining constant heavy and light chains.

When the genetic material was converted and expressed as an scFv fragment and screened via phage display it is valid to assume that the loss of any scaffolding and the resulting expression of "floppy" scFv fragment will result in a binding event starkly different to that of the monoclonal antibody and Fab antibody fragment and that the optimal light chain-heavy combination may not be present for this format. Figure 3.3.2.2.2 indicates displacement of the unpurified lysate by free amphetamine. The purified antibody was titred successfully against amphetamine-BSA (Figure 3.3.2.2.3) however; any inhibition characteristics of the scFv were lost (Figure 3.3.2.2.2).

In order to conclude that the unsuccessful production of an scFv fragment was not vector-dependant and explore each available resource in the lab the scFv was ligated into the pComb3x vector for a second round of panning.

However, similar results were observed as with the pAK system and no soluble expressing scFv fragment was obtained. Two clones from each panning strategy were sent for sequencing and the light chains were compared to the parent Fab fragment.

3.5 Conclusion

This research described the construction of a Fab and an scFv fragment from the cDNA of a positive anti-amphetamine-secreting clone previously described by Fanning (2002). This monoclonal anti-amphetamine antibody exhibited an IC 50 of 600ng/ml. It is vital to the success of the project that the most sensitive and specific antibody is ultimately applied to the biochip platform. It was thought that constructing a genetically derived antibody fragment from this parent clone would allow improvements in affinity. The Fab construct displayed a 3-fold improvement in affinity compared to the IgG with an IC 50 of 200ng/ml. Using the Fab as the genetic template, the scFv expression was unsuccessful. This is strongly conclusive of the structural rigidity dependence on the particular light-heavy chain combination of the IgG secreted from clone 4EP18E (Fanning, 2002). It is highly likely that in order to successfully express the anti-amphetamine scFv fragment, in-vitro affinity maturation steps would be required. In light of the dependence on structural rigidity, light chain shuffling may permit the optimal combination required for success. Albeit a heavy workload, construction of an anti-amphetamine immune library would be recommended as the next course of action.

Chapter 4

4.0 Anti-Morphine-3-Glucuronide Recombinant Antibody Engineering - the implications of using an scFv or a Fab fragment

4.1 Introduction

4.1.1 Biosensors

A biosensor is a device which couples a biological sensing element (tissue, enzyme, antibody, nucleic acid, cells or whole organisms) with a transducing mechanism (amperometric, potentiometric, calorimetric, acoustic or optical), as mentioned briefly in section 1.2.1.2. When biological molecules interact a change occurs in one or more of the parameters associated with the interaction event. These changes can be monitored and translated by the transducer. The response of the biological component is translated to a readable signal by the transducer (Rogers, 2000). A biosensor can be divided into 4 main categories electrochemical, optical, piezoelectric and thermal sensors (Rodriguez-Mozaz *et al.,* 2005). Specificity and sensitivity are the primary properties of any proposed biosensor (Marazuela *et al.,* 2002). The specificity depends entirely on the properties of the biological component as it must recognize the analyte in order for an interaction to take place. However, the sensitivity is dependant on a combination of both the nature of the biological component and the type of transducer in use for detection (Byfield *et al.,* 1994)

4.1.2 Choosing the appropriate biosensor

The continuing quest for a rapid, sensitive, selective, simple, rugged, and multi-analyte testing device is driving biosensor development research. Antibody-based biosensors are very versatile with antibodies which have been specifically selected for their affinity to the particular antigen or group of antigens of interest (Rogers, 2006). However, of equal importance, in the design of a biosensor for illicit drug detection, is the transducer used. Optical biosensors, such as surface plasmon resonance-based biosensors, are ideal as they allow direct ‘label-free’, ‘real-time’ detection of illicit drugs Several commercial

biosensors have used surface plasmon resonance as there detection method and have been successfully developed for application in small molecule analysis (Brennan *et al.,* 2003; Dillon *et al.,* 2003; Redshaw *et al.,* 2007).

4.1.3 Surface Plasmon Resonance (SPR)

The majority of SPR-based biosensors have been developed based on the Kretschmann configuration. The Biacore™ was used in this work and so the principal of SPR will be explained using the Biacore™ system as reference. The most common geometric set up (the Kretschmann configuration) is shown in figure 4.1.3.1.

SPR is an optical phenomena which occurs as a result of total internal reflection of light at a metal-liquid interface. The SPR system basically consists of a monochromatic and p-polarized light source, a glass prism, a thin metal (gold) film at the base of the prism and a photodetector. SPR is achieved when the incident p-polarised light is directed into a glass prism at a fixed wavelength and at an angle equal to or greater than the critical angle. Under these conditions total internal reflection occurs. A small amount of light leeches through the boundary between the glass prism (high refractive index) and the sample media (low refractive index) and an evanescent field is generated. As this evanescent wave moves further away from the interface it decays exponentially.

In the case of Biacore™, where the interface between the lower refractive index and higher refractive index is coated with gold, the evanescent wave, which passes through the metal surface causes the plasmons to resonate. The resulting loss in energy from the incident light creates a dip in the intensity of the reflected light , the angle at which this occurs is known as the SPR angle (θ). The SPR angle is dependant on the properties of the metal film, the wavelength and polarization of the incident light and the refractive index of the media on each side of the metal film. In Biacore™ these factors are kept

constant, therefore, the SPR signal can be used to measure the biological interactions occurring within the evanescent field.

When the refractive index of the sample medium is changed, i.e. when a mass change on the surface occurs, within this evanescent field (200-300 nm), the angle of reflected light changes, (θ_2), (Figure 4.1.3.2). The difference between these two angles is measured and interpolated as a sensorgram (Figure 4.1.3.3).

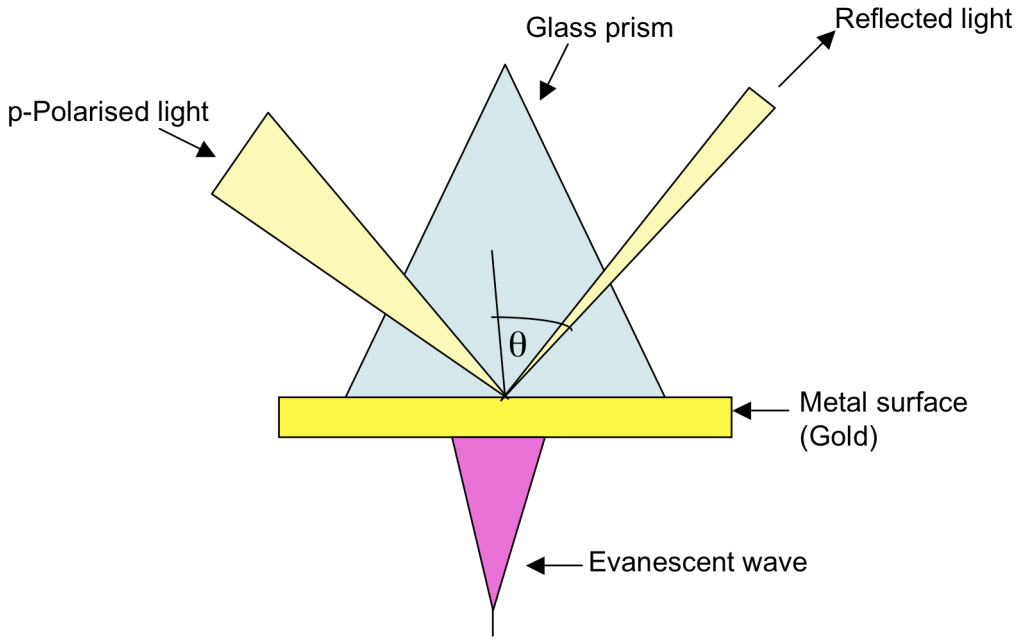

Figure 4.1.3.1 The basic "Kretschmann configuration". Under conditions of total internal reflection at a metal-coated surface, the p-polarized light is directed into a an area of high refractive index (glass prism) and an evanescent wave propagates into the medium of lower refractive index (sample buffer) and decays exponentially.

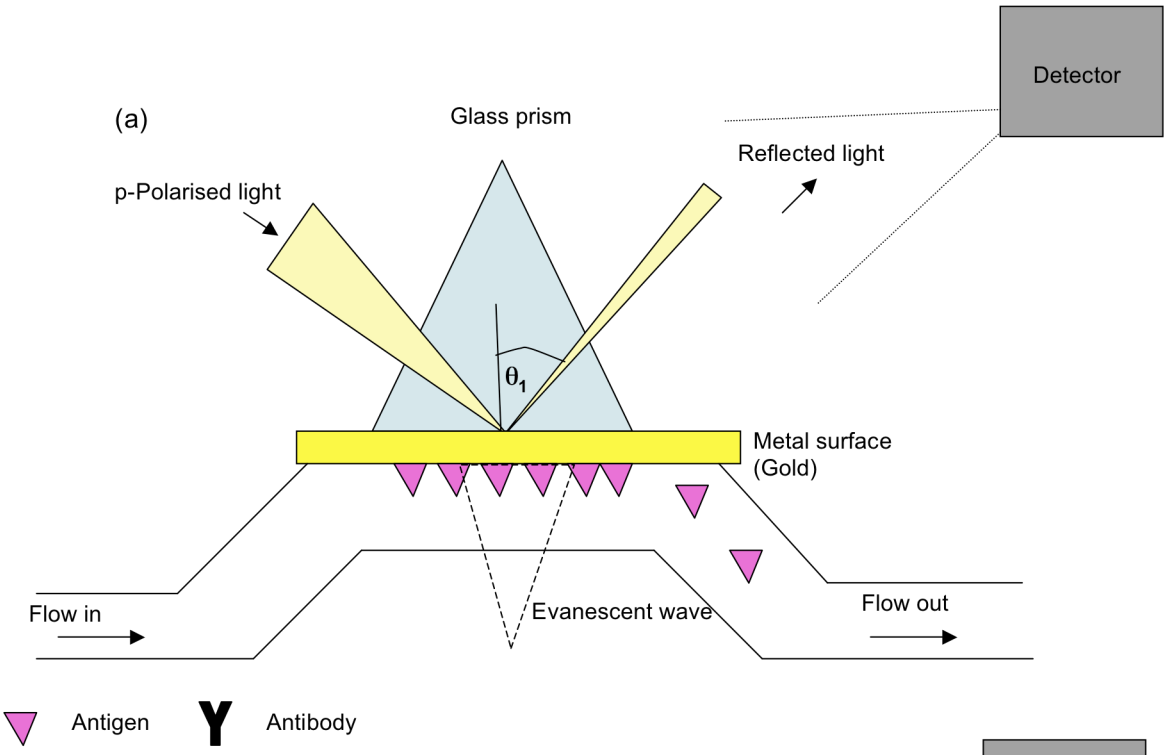
(a)
Glass prism
Detector
Reflected light
p-Polarised light
θ1
Metal surface
(Gold)
Flow in
Evanescent wave
Flow out
Antigen
Antibody

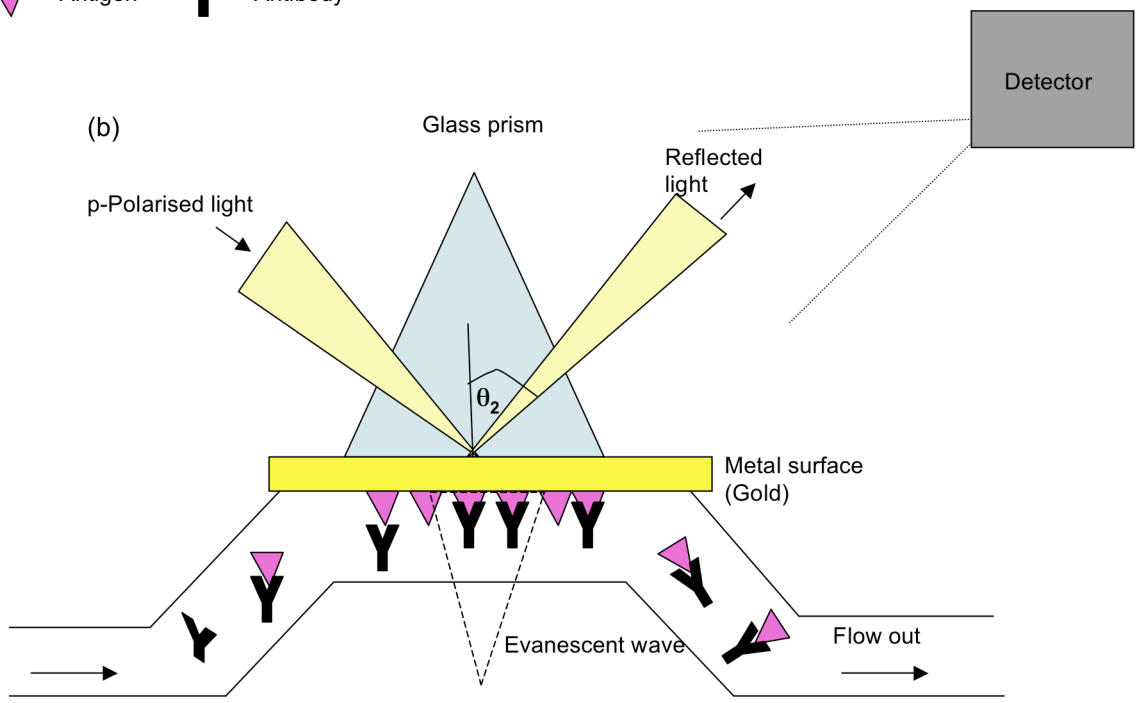
(b)
Glass prism
Detector
Reflected
light
p-Polarised light
θ2
Metal surface
(Gold)
Evanescent wave
Flow out

Figure 4.1.3.2 Shows the working principle of SPR in the Biacore™ instrument. Antigen is immobilized on the chip surface using standard EDC / NHS amine coupling chemistry (a). Light is focused on the gold surface by means of a prism under conditions of total internal reflection. When the antibody / antigen mixture is injected over the surface a mass change occurs thus causing a refractive index change within the evanescent field (b). This change results in a shift in the SPR angle which can be measured and relayed as a sensogram to the user

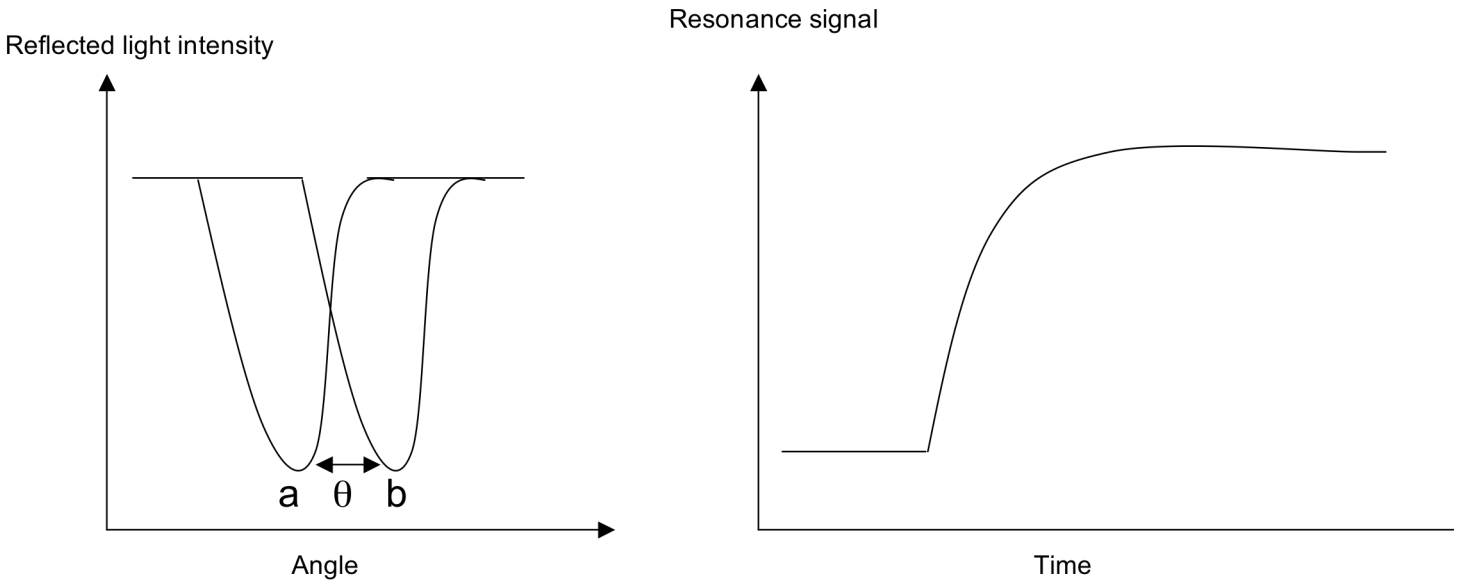

Figure 4.1.3.3 The SPR angle is seen as a dip in the intensity of the reflected light. Changes in θ are displayed as a sensogram and bimolecular interactions within the evanescent field result in an increase in the SPR angle and thus displayed as an increase in the signal of the sensogram. The "real-time" difference between the two angles (θ_a and θ_b) is plotted as arbitrary response units (RU) against time in seconds.

4.1.4 CM5 sensor chip

A key component in the Biacore ^{TM} system, is the sensor chip. The CM5 chip (Figure 4.1.4.1) consists of three layers: glass slide, thin gold film coating and a carboxymethylated dextran surface. Gold is used as the metal component as it possesses good SPR response. This carboxymethylated dextran matrix permits covalent immobilisation of analytes onto the sensor chip surface.

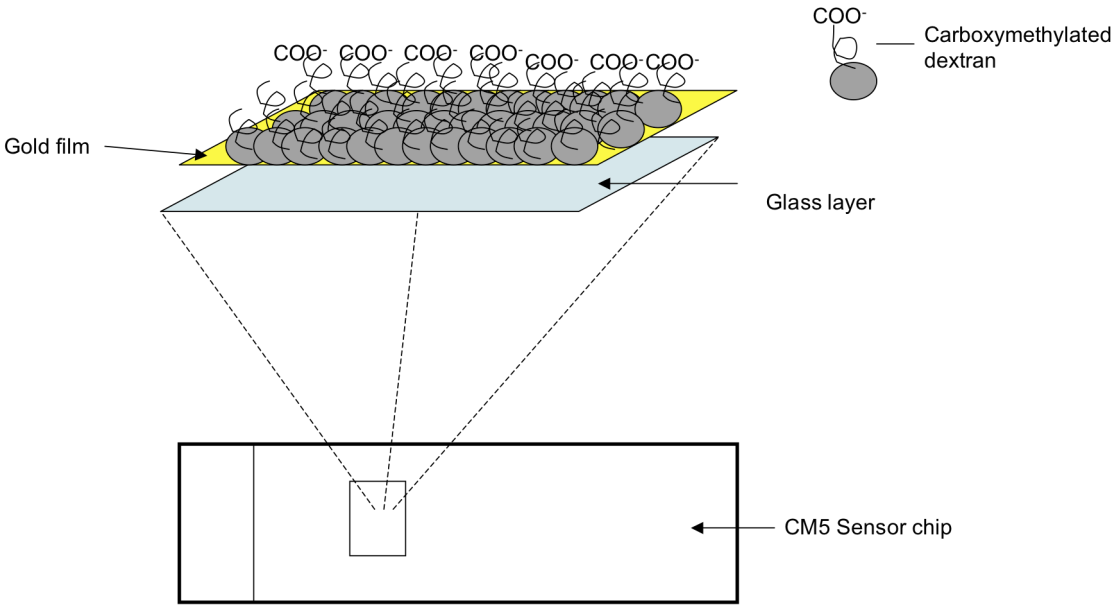

Figure 4.1.4.1 Schematic illustration of the surface of the Biacore^{TM} CM5 sensor chip. The 3 distinct layers are shown, the glass slide, the thin gold film and a carboxymethylated dextran layer. This layer facilitates standard carboxyl-amine coupling.

4.1.5 Application and considerations of SPR technology for detection of small haptens i.e. drug molecules

In SPR the changes in refractive index are dependant on mass, thus, the capabilities of the biosensor are pushed to the limit when dealing with small molecules such as illicit drugs. However, the label-free approach of SPR, reduces time and cost and compared to fluorescent tags, it also reduces false negatives and positives caused by the label occluding the binding site and the hydrophobicity of the tag, respectively (Karp *et al.,* 2005). When developing a Biacore^{TM}-based assay for the detection of small molecules such as illicit drugs, the assay format favoured is the inhibition assay and not the capture method employed in the detection of larger molecules (Leonard *et al.,* 2007).

A number of SPR-based assays have been reported for the successful detection of small molecules such as the mycotoxins (Daly *et al.,* 2000) and illicit drugs (Dillon *et al.,* 2003; Townsend *et al.,* 2006). The solubility of illicit drugs presents another problem for SPR as dimethlysufide (DMSO) is often included in preparations to aid solubility (Lipsinki *et al.,* 1997). DMSO has a high refractive index, which results in large signal change in the sensogram known as a "bulk effect". One method of overcoming this issue is a recently developed "bulk effect" calibration method (Frostell-karlsson *et al.,* 2000; Ahmad *et al.,* 2003). However, this method was analysised and validated by Karp *et al.,* (2005) and it was concluded that simple control surface extraction was the most efficient method of correction as outlined in this work (section 4.3.3.2 and Figure 4.3.4.4.1(b)).

4.2 Rationale for the conversion of the anti-M3G scFv to a Fab format

The laborious techniques used in traditional antibody production have led several research groups to investigate the use of recombinant antibody technology, to produce scFv and Fab antibody fragments (Tout *et al.* 2001; Li *et al.* 2000; Rau *et al.* 2002; Brennan *et al.* 2003) with high-affinity for small molecules. ScFv's are the most commonly used recombinant antibody format as it can be rapidly constructed, typically well expressed in *E. coli* and can exhibit high affinity and stability (Barbas *et al.* 2001). Most scFv molecules are designed with an Fv-region linking peptide based on glycine-serine repeat sequences of 15-20 residues, which typically lead to scFv molecules which are labelled 'monomeric'(Maynard and Georgiou 2000), but in the bacterial periplasm a portion of the scFv typically dimerizes, resulting in a mixture of monomeric and dimeric fragments (Mc Gregor *et al.,* 1994).

A number of groups have engineered the variable regions of scFvs for the expression of monovalent Fab fragments (Arndt, 1998) and Fab constructs have been used specifically to determine the true affinities of scFv fragments which had been modified for increased affinity (Rau, 2002). However, none of the above mentioned studies has specifically addressed the issues of SPR surface chip chemistry in relation to different antibody structural formats and whether it is appropriate to convert scFvs to Fab format, to ensure a monovalent binding population for use in SPR analyses.

Monovalent antibodies are frequently used to measure binding constants (George *et al.,* 1995) as monovalency prevents the formation of antigen-bridge complexes, which result in an increase in binding avidity (Mac Kenzie *et al.,* 1996). The monovalency of binding ligand interaction is especially important with regard to kinetic analysis on Biacore and, thus, also in cases where new antibody panels are ranked according to affinity (Li *et al.* 2000; Lu *et al.* 2003; Stacy *et al.* 2003, Fredericks *et al.* 2004). Kinetic characterization reveals the rate at which the immune complex both associates and

dissociates, thereby providing a stringent measure for tailoring and selecting reagents (Quinn and O'Kennedy, 2001). The interaction between a soluble, monovalent analyte and an immobilized monovalent ligand can be interpreted in terms of pseudo-first-order kinetics, but heterogenicity of the binding ligand and possible multivalency can cause deviations from pseudo-first-order behaviour (O' Shannessy *et al.* 1996)

In the study presented here, the effects of SPR chip surface chemistry and antibody valency on the function of a model anti-morphine-3-glucoronide SPR assay is investigated. The variable regions of a previously described anti-M3G scFv (Brennan, 2003), were re-engineered for the expression of monovalent Fab fragments. The characteristics of the resulting scFv and Fab fragments were then compared using ELISA, SDS-PAGE, HPLC and Biacore^{TM}.

4.3 Results and Discussion

4.3.1 Construction and expression of anti – M3G Fab

After electroporation of *E. coli* XL-1 Blue, the finished anti-M3G C_κ-Fab construct gave 3.1 x 10^7 total transformants, with a vector self-ligation background of < 0.1%. After the biopanning process had been performed, very poor signal was observed in phage ELISA against M3G-OVA. In subsequent ELISA characterization of soluble antibody, the C_κ-Fab demonstrated high sensitivity when used at a 1/200 dilution and exhibited a range of detection (IC_{50} of 1.4ng/ml), which was similar to that of the parent scFv (Figure 4.3.1.1).

When this C_κ-Fab construct was examined using Biacore, no binding was observed to either the M3G surface or to the reference (OVA) surface. The scFv was analysed on the same surface and demonstrated a strong binding response. This was indicative of a problem with the Fab construct and not in the assay itself. On examination of the parent scFv sequence/gene, it was discovered that the antibody fragment was constructed with a lambda variable light chain. It was thought that expression may be improved by the more compatible constant and variable light chains.

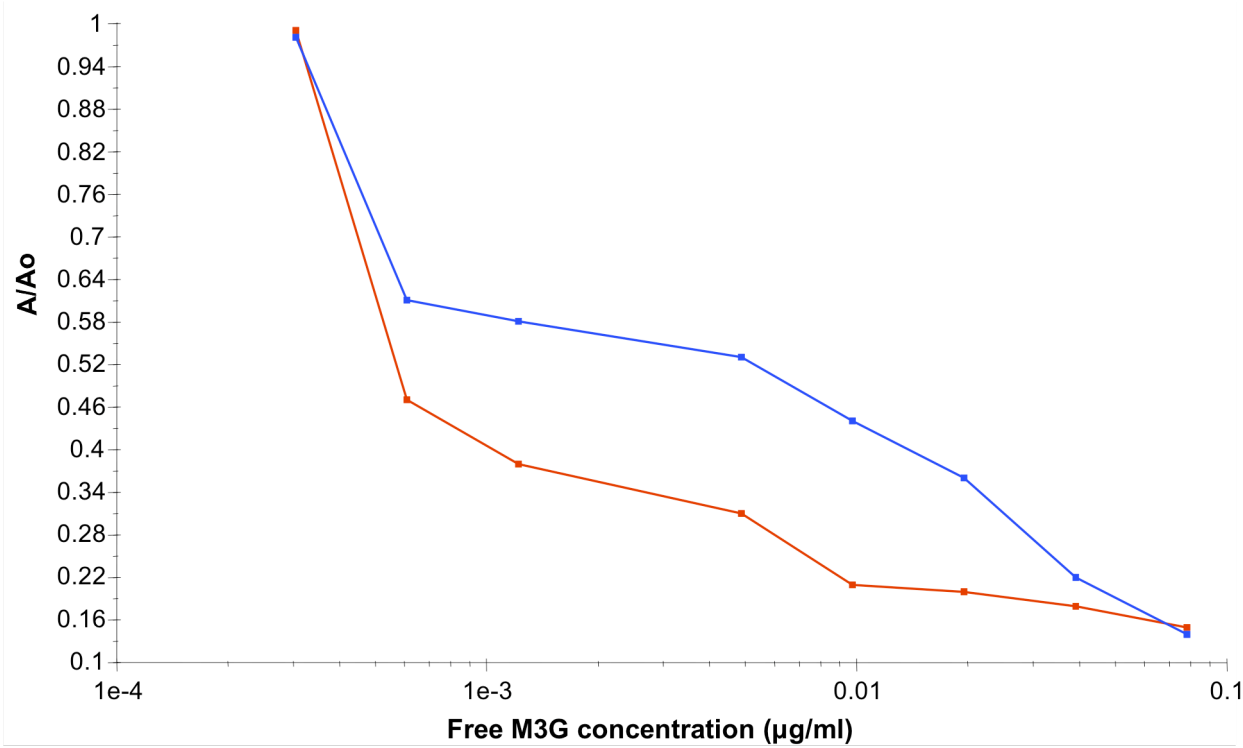

Figure 4.3.1.1 ELISA inhibition assay performed on M3G-OVA-coated wells comparing Fab (blue) and scFv (red) binding response versus competing free M3G concentration. Signal developed using OPD chromogenic substrate and monitored by optical density at 450nm. Data expressed as A/A_0 (i.e. the signal at different free analyte concentrations are expressed as a proportion of signal in the presence of no competing analyte). All analyses were preformed in triplicate on three separate occasions. Standard deviations at all points examined were $\leq 10\%$.

The C_κ-Fab was therefore converted to a C_λ-Fab construct, as it was postulated that use of a more compatible pairing of light chain constant and variable regions might improve the structural stability, secretion and, therefore, overall activity of the final Fab product. In the second Fab panning series, a strong ELISA signal was observed by the second round for the C_λ-Fab construct. No concomitant increase in signal was observed against control antigen (OVA).

4.3.2 Anti - M3G scFv and Fab comparison studies prior to application to Biacore™

When expressed in parallel, both the scFv and the C_λ-Fab produced large quantities of high titre, high activity antibody. In western blot analyis the Fab and scFv ran in parallel due to the denaturing properties of the SDS-PAGE (Figure 4.3.2.1). In direct ELISA, the His-purified and concentrated (to 1ml final volume) antibody preparations provided titers of 1/81,000 and 1/20,000 for scFv and Fab, respectively. ELISA conditions for each antibody were optimized for maximal sensitivity (data not shown) and for both scFv and Fab, the optimal well coating concentration was determined to be 3 μg/ml M3G-OVA. At an optimal dilution of 1/15,000, the scFv was shown to have a detection range for free M3G of 305 - 312,500 pg/ml, with an IC_{50} value of 30,000pg/ml (Figure 4.3.2.2). The anti-M3G C_λ-Fab was used at a 1/5000 dilution, therefore, having several times more specific activity than that observed for the similarly expressed and purified C_κ-Fab. The C_λ-Fab was further shown to have a detection range of 152 - 19,500 pg/ml, with an IC_{50} value of 1.4ng/ml (Figure 4.3.2.2).

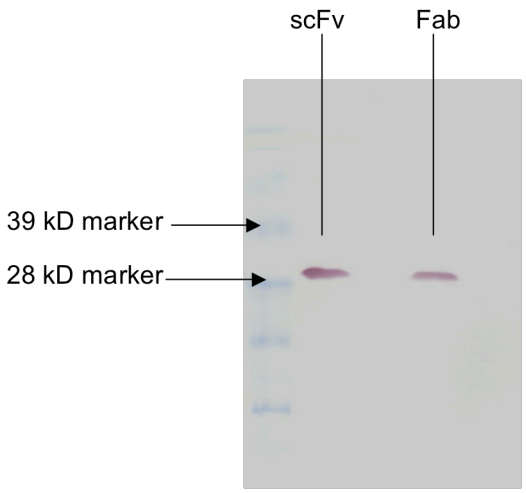

Figure 4.3.2.1 Western blot analysis of the immobilised metal affinity chromatography (IMAC)- purified Fab and scFv fragments. The 28 kD and 39kD bands are highlighted above.

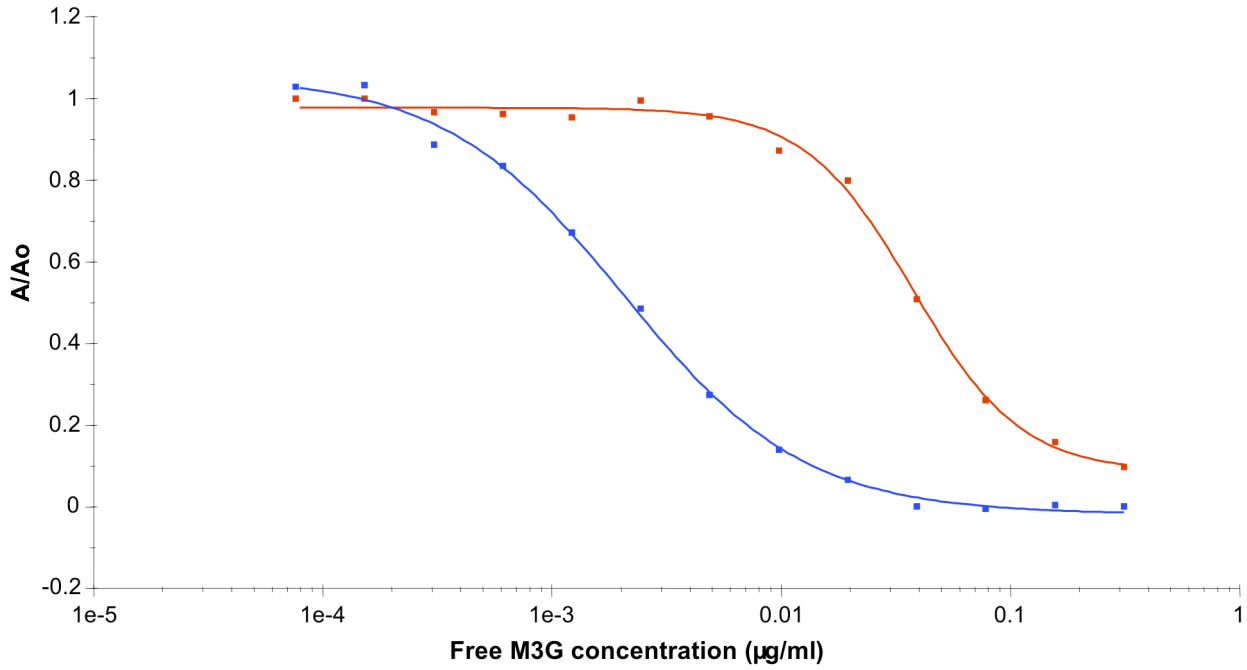

Figure 4.3.2.2 ELISA inhibition assay performed on M3G-OVA-coated wells comparing Fab (blue) and scFv (red) binding response versus competing free M3G concentration. Signal developed using OPD chromogenic substrate and monitored by optical density at 450nm. Data expressed as A/A_0 (i.e. signal at different free analyte concentrations are expressed as a proportion of signal in the presence of no competing analyte). All analyses were preformed in triplicate on three separate occasions. Standard deviations at all points examined were $\leq 10\%$.

In a number of previously described chimeric Fab library construction methodologies, the light chain V regions (both κ and λ) of mice (Barbas *et al.,* 2001), rabbits (Rader *et al.,* 2000) and chickens (Andris-Widhopf *et al.,* 2000) are spliced onto a single human C_κ region. This is presumably due to the dominance of the V_κ in the immunoglobulin repertoires of mice and rabbits (Barbas *et al.,* 2001; Popkov *et al.,* 2003), meaning that V_λ clones are likely to be infrequent in resulting immune recombinant antibody libraries. However, the observation outlined here that Fab light chain function and

overall antibody binding activity were improved by combining the V_λ region (isolated from a murine scFv library) with a C_λ region, as opposed to C_κ, implies that the use of a C_λ scaffold in Fab library construction might improve the isolation of lambda-associated Fabs.

4.3.3 Biacore analysis of constructs

Having established a functional anti-M3G FAb construct, Biacore™ competition assays were then developed, using both M3G-OVA and M3G - coated SPR surfaces, to determine the range of free M3G detection of both the Fab and scFv.

4.3.3.1 Preconcentration studies

A preconcentration step is necessary prior to immobilisation of the drug-protein conjugates to the carboxymethylated dextran chip surface. This step ensures maximum efficiency of the immobilisation method. 10mM sodium acetate solutions were made up to different pH's with 10% (v/v) acetic acid. The pH range used in this study was 3.8 - 5.0. Solutions of M3G-OVA were made up in each pH buffer and injected over an underivatised flow cell at a flow rate of 5 μl / min for 2 minutes. The results of the preconcentration step are shown in Figure 4.3.3.1.1. The optimal pH for M3G-OVA immobilisation was determined to be 4.0.

Immobilisation strategies were carried out as outlined in section 2.9.2 and 2.9.3. The M3G-OVA flow cell and reference OVA flow cell immobilisation profiles are shown in Figure 4.3.3.1.2 and Figure 4.3.3.1.3.

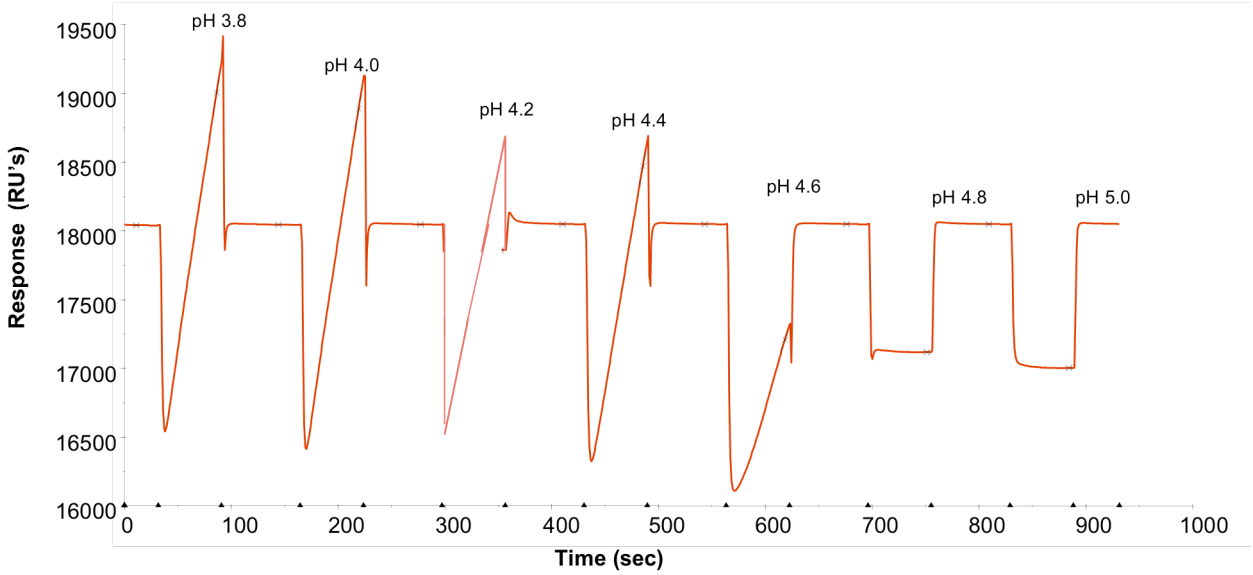

Figure 4.3.3.1.1 Biacore based analysis of the preconcentration of the M3G – OVA conjugate to the surface of the CM – dextran chip surface. The low ionic strength of sodium acetate buffer favours electrostatic interaction between the positively charged protein (below the proteins pI) and the negatively charged dextran layer. The optimal pH for the immobilisation of the M3G – OVA conjugate was found to be pH 4.0.

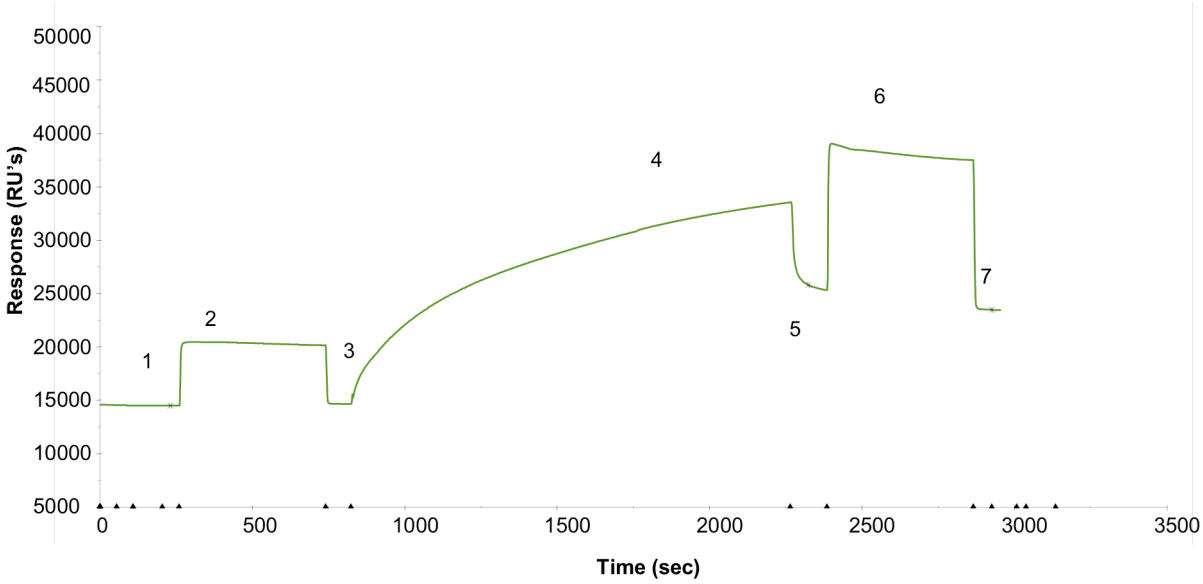

Figure 4.3.3.1.2 Sensogram respresenting the immobilisation of M3G-OVA onto a CM5 dextran chip surface

(1) – HBS buffer injection and baseline measurement recorded.

(2) – The carboxymethylated surface was activated when a mixture of EDC and NHS (0.02M and 0.05M, respectively) was injected over the flow cell at a flow rate of 5 µl / min for 7 minutes.

(3) – HBS injection. Activation was confirmed by the increase of ~ 150 RU from baseline (1)

(4) – A solution of 100 µg / ml of M3G-OVA in sodium acetate buffer, pH 4.0, was injected over the flow cell at a flow rate of 5 µl / min for 20 minutes.

(5) – A HBS injection removed all unbound conjugate and the quantity of immobilised M3G-OVA was recorded as the change in response units from (3)

(6) – The flow cell was capped / deactivated with an injection of 1M ethanolamine, pH 8.5. All non-covalently attached conjugate was also removed at this injection point.

(7) A HBS injection permited the recording of the new (immobilised surface) baseline. Approximately 11,000 RU's of M3G-OVA were immobilised on the flow cell.

4.3.3.2 Inhibition assay development

A similar range of free M3G was employed as in the ELISA inhibition assay, with samples being injected over each chip in a pre-programmed order and each injection followed by a regeneration step. Both antibodies displayed negligible non-specific interactions with immobilized OVA and the modified CM-dextran surface, negating the need for pre-incubation steps of antibodies with either OVA or activated CM-dextran. The linear range of detection for the scFv was found to be 39 - 156 ng/ml (IC_{50} of 117 ng/ml) on the M3G-OVA surface and 9.8 - 78 ng/ml (IC_{50} of 30 ng/ml) on the M3G - coated surface (Figure 4.3.3.2.1 and Figure 4.3.3.2.2). The linear range of detection for the Fab was found to be 4.8 - 39 ng/ml (IC_{50} 19 ng/ml) and 4.8 - 78 ng/ml (IC_{50} 14 ng/ml) on M3G-OVA and M3G surfaces, respectively (Figure 4.3.3.2.1 and Figure 4.3.3.2.2).

The data described above suggest that the Fab fragment is consistently more sensitive in measurement of free M3G than the scFv fragment in SPR assay, where it is ~2 to 6-fold more sensitive (Figure 4.3.3.2.1 and Figure 4.3.3.2.2) and also in ELISA assay where it is 11.5-fold more sensitive (Figure 4.3.2.2). The respective sensitivities for Fab and scFv in ELISA analysis and SPR assay were highly similar, suggesting that an SPR assay for M3G can be designed which is as sensitive and reproducible as an optimised plate assay. These data also suggest that the differences observed between Fab and scFv responses in ELISA were not mediated by the different secondary antibodies used to detect binding. The use of direct M3G conjugation on the SPR surface appears to be more effective and reliable than an M3G-OVA surface as it promotes greater linearity in scFv competition assay response (Figure 4.3.3.2.1 and Figure 4.3.3.2.2). The surface directly coated with M3G also gave the most sensitive and highly correlated recognition of free M3G, by both constructs. Indeed, logit transformation of the data and subsequent two-tailed t-test showed that on the surface directly coated with M3G, values for Fab and scFv were not significantly different ($p > 0.05$) whereas, the values for both constructs differed greatly on the M3G-OVA surface ($p < 0.001$).

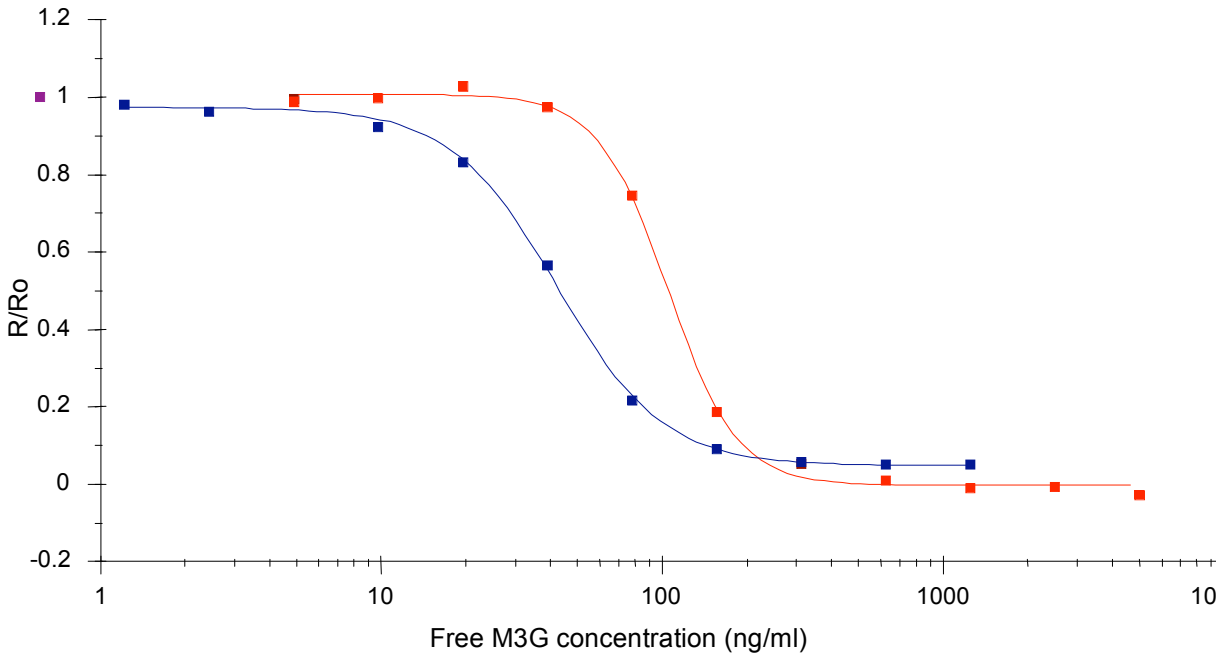

Figure 4.3.3.2.1 Biacore inhibition assays performed on an M3G-OVA-coated CM5 chip surface, comparing Fab (blue) and scFv (red) binding response versus free M3G concentration. Data expressed as R/R_0 (i.e. signal at different free analyte concentrations are espressed as a proportion of signal in the presence of no competing analyte). All analyses were preformed in triplicate on three separate occasions. Standard deviations at all points examined were < 5% (mean deviation scFv = 1.2%; mean deviation Fab = 0.8%).

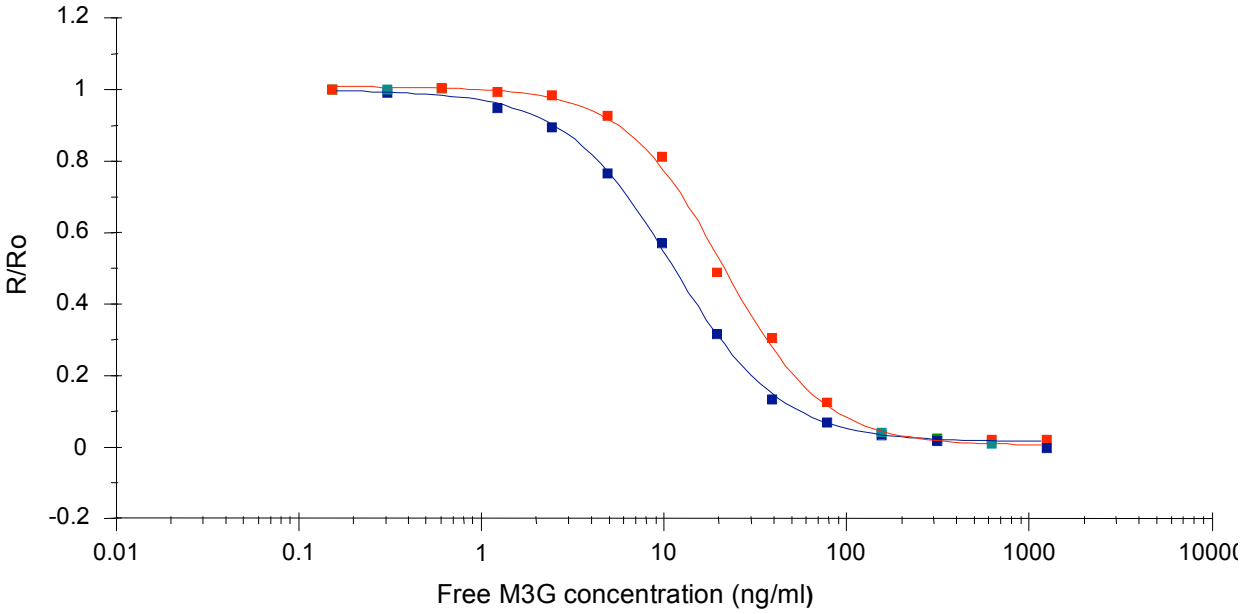

Figure 4.3.3.2.2 Biacore inhibition assays performed on an M3G-coated CM5 chip surface, comparing Fab (blue) and scFv (red) binding response versus free M3G concentration. Data expressed as R/R_0 (i.e. signal at different fee analyte concentrations are espressed as a proportion of signal in the presence of no competing analyte). All analyses were preformed in triplicate on three separate occasions. Standard deviations at all points examined were < 5% (mean deviation scFv = 1.9%; mean deviation Fab = 1.1%).

This further suggests that direct hapten-labelled SPR surfaces may be more appropriate for the comparative analysis of the assay sensitivities of different antibody constructs. Interestingly, in both the Fab and scFv assays a lower concentration of antibody was required for use on the directly immobilized M3G chip surface. This surface also exhibited much greater stability after regeneration, with only 50 regenerations possible for the conjugate surface, as previously observed (Brennan *et al.,* 2003), but over 200 regenerations possible when using the directly immobilized chip, suggesting that the directly immobilized M3G surface will be more appropriate for 'real-world' assay conditions.

While carrying out the comparative ELISA and Biacore competition assays described above, it was observed that not only do the anti-M3G Fab and 'monomeric' scFv preparations have considerably different IC_{50} values, but they also exhibit considerably different dose-response profiles in both ELISA and Biacore (depending on the sensor surface type). When examined on the M3G-OVA surface, the two antibody constructs do not exhibit parallelism in their ranges of response, with only the Fab giving a clearly linear profile (Figure 4.3.3.2.1). However, their parallelism, linearity and sensitivity become highly similar when the same assays are performed on the M3G surface (Figure 4.3.3.2.2). Given that scFv molecules have been shown to be prone to the formation of multimeric intermediates (Griffiths *et al.,* 1993; Kortt *et al.,* 1997), while Fabs are obligately monomeric (Borrebaeck *et al.,* 1992), we therefore examined the scFv and Fab preparations by HPLC and non-reducing SDS-PAGE to investigate the extent of antibody fragment multimerisation.

4.3.4 scFv multimerisation studies

4.3.4.1 Native SDS-PAGE and Western blot analysis

There was a concern that the assumed monomeric scFv purified samples may contain some dimeric binding characteristics, as shown in the Biacore data. The first stage in examining the degree of multimerisation of the scFv compared to the Fab was non-denaturing gel electrophoresis. Urea and sodium dodecyl sulfate cause the denaturation of proteins through dissociation of oligomers to their subunits. Excluding the β-mercaptoethanol ensures the disulphide bonds between the chains are kept intact and excluding SDS allows migration of the proteins based on their native charge. If there is more than one protein fragment present, as determined from the SEC-HPLC, they should show up as separate bands on a native gel (Figure 4.3.4.1.1). The Fab sample revealed a single band while the scFv sample revealed 2/3 separate bands. These bands

were not seen in the non native SDS-PAGE. A western blot was carried out on a duplicate gel and all antibody fragments where detected with the secondary antibody, indicating that the tag was intact in all fragments.

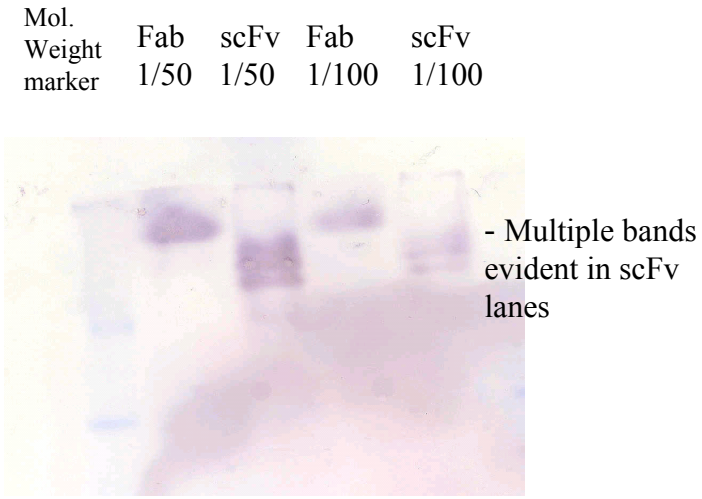

Figure 4.3.4.1.1 Western blot of both scFv and Fab fragments transferred from a native gel indicating multiple bands in the Fab land and only one in the scFv lane at 2 different dilutions. Antibody fragments were detected with anti-His HRP-labeled secondary antibody and developed with TMB liquid substrate.

4.3.4.2 Size exclusion chromatography

Size exclusion chromatography permits the examination of various sized proteins in a sample. It works on the principal that smaller molecules pass through tiny pores in the column thus having a longer retention time than larger molecules not permitted through the pores which pass through the column at a faster rate. All assays were performed at a flowrate of 0.5ml/min with an injection volume of 50µl. The mobile phase was phosphate buffer saline (PBS). Both scFv and Fab antibody fragments were examined at stock dilutions in PBS. Standards to ensure the efficiency of the column were employed (Table 4.3.4.2.1)

Table 4.3.4.2.1 Molecular weight markers were run through the Phenomenex, BioSep-SEC-S-3000, 300nm x 7.80nm column at a flowrate of 0.5 ml/min with an injection volume of 50 µl. Individual molecular weights and retention times are listed above.

Protein	**Molecular Weight**	**Retention time (min)**
BSA	66kD	16.0
Trypsin	29kD	18.8
Carbonic anhydrase	24kD	18.0
Cytochrome C	12kD	21.8

The molecular weight of an scFv is ~ 30kD while the molecular weight of a Fab fragment is close to double this at ~ 60kD. Only one clear peak would be expected in both cases as the samples were previously IMAC purified via the His-tag in each antibody fragment (Figure 4.3.2.1). However, the chromatographs obtained for the scFv indicate a second distinct peak with a shorter retention time than that of the primary peak. This second peak has a retention time in between that of the Fab and the scFv

(Table 4.3.4.2.2 and Figure 4.3.4.2.1). This was strongly indicative of the spontaneous formation of multimers within a monomeric scFv population.

Table 4.3.4.2.2 Antibody fragments were run through the column at a flowrate of 0.5 ml/min with an injection volume of 50 µl. All retention times are listed above.

Sample	Peak number	Retention time (min)
scFv	1	16.96
	2	18.15
Fab	1	17.35

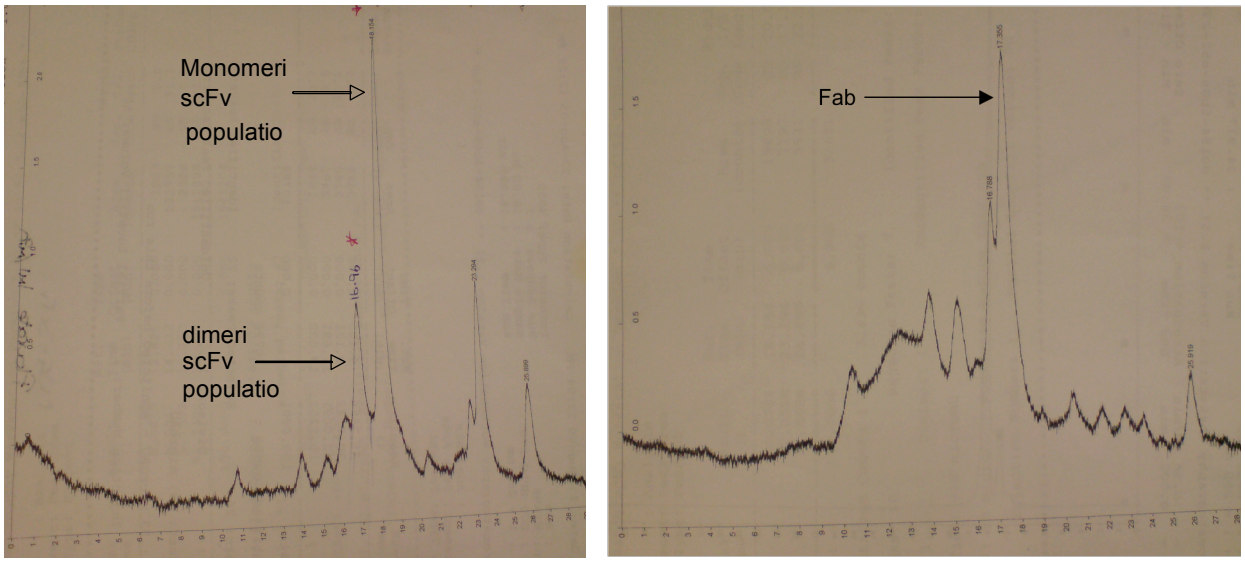

Figure 4.3.4.2.1 Antibody fragments were run through the column at a flowrate of 0.5 ml/min with an injection volume of 50 µl. The scFv population is clearly a mixture of monomeric and dimeric antibody fragments

4.3.4.3 ELISA analysis of size exclusion chromatography (SEC) fractions

The possibility that these additional peaks and bands merely represent aggregated inactive protein had to be investigated. For this purpose an ELISA was performed on HPLC output fractions collected at 1min intervals (Figure 4.3.4.3.1).

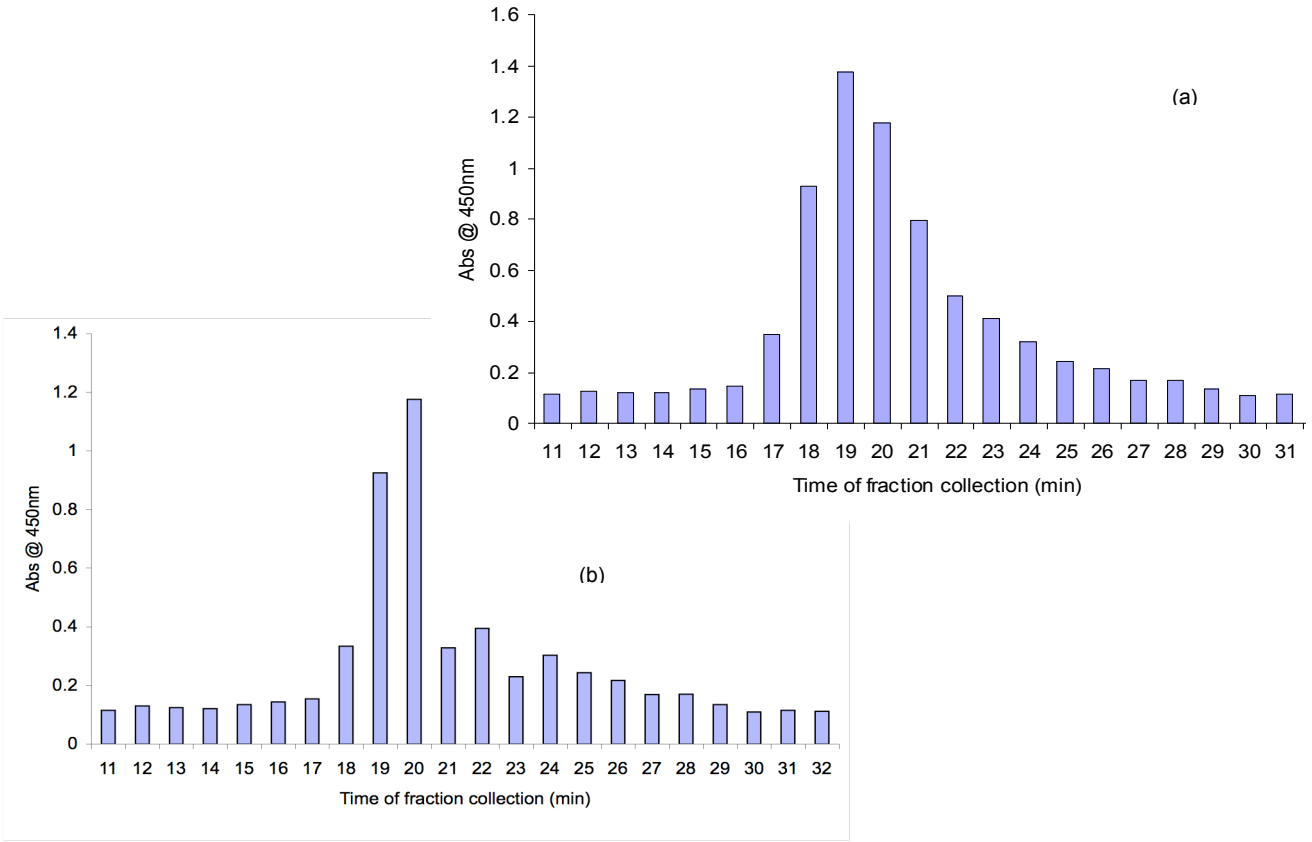

Figure 4.3.4.3.1 ELISA assay performed on M3G-OVA coated wells comparing scFv (a) and Fab (b) samples collected from HPLC. Samples for analysis were collected from the HPLC column at 1 min intervals. Antibody activity was examined via detection of binding of each sample to the M3G – OVA coated surface. Signal developed using TMB chromogenic substrate and montitored by optical density at 450nm. Data is expressed as absorbance read.

The figure above clearly illustrates activity spanning 4 minutes, thus covering the exact time at which the two significant peaks are seen on the chromatograph. This would indicate that the scFv has spontaneously multimerised and has retained activity in these

multimeric forms, while the Fab is inherently monomeric. The apparent time difference observed between the HPLC and ELISA samples is an effect of the manual sample collection.

4.3.4.4 Influence of the scFv multivalency on SPR analysis

To compare the influence that multimerisation (and therefore multivalency) might have on the Biacore profiles of the scFv and Fab constructs, kinetic analysis was performed for each construct. Kinetic analyses were performed on the directly immobilised M3G surface rather than the M3G-OVA surface. For the purpose of kinetic analysis, the immobilised surface used and the concentration of antibody injected over the surface is sufficient only to obtain an RU_{max} = 100RU

Under the optimised competition assay conditions on the M3G-OVA surface, the Fab exhibited faster association and dissociation rate constants than the scFv (Figure 4.3.4.4.1(a)). In kinetic analyses the contrast between the two constructs was even more noticable, with the scFv exhibiting a considerably different dissociation profile to that of the the Fab (Figure 4.3.4.4.1(b)). Although rates of association are similar for both antibody constructs, the anti-M3G Fab fragment shows a significantly faster dissociation rate 4.8×10^{-2}, when compared to 1.03×10^{-3} for the anti-M3G scFv.

These observations are of particular interest in the context of anti-hapten recombinant antibody development. Recombinant antibody technology can lead to the rapid development of large panels of antigen-specific antibodies of differing sensitivity. To accelerate the screening of these panels, several groups have employed kinetics screening of initial cones by SPR, to rapidly identify the highest affinity binders (Li *et al.,* 2000, Lu *et al.,* 2003, Stacy *et al.,* 2003, Fredericks *et al.,* 2004). However, the

purpose of this SPR screening is typically to identify antibodies for subsequent use in competition assays, which rely on antibody recognition of free molecule in solution.

It has been previously shown that 'monomeric' antibody fragments (scFv, ~90 % monomeric) demonstrate a more rapid dissociation profile than 'dimeric' (~90 % dimerized) fragments. However, our observations suggest that a predominantly monomeric scFv form can still exhibit a considerably slower dissociation rate than a truly monomeric Fab fragment. Due to the common occurrence of antibody concentration and/or pH-based multimerisation in scFv populations (Arndt *et al.,* (1998)), any individual scFv sample is likely to contain an unknown proportion of dimeric antibody, which is functionally bivalent and can lead to a profound change in off rate kinetics profiles. Indeed, it has been shown that different antibodies with linkers of the same length may dimerise to different extents (Griffiths *et al.,* 1993, Raag and Whitlow 1995, Wu *et al.,* 1996). It is therefore arguable, that the ranking of scFv molecules by off-rate kinetics on hapten-coated SPR surfaces may be misleading and may give an unreliable estimation of binding affinity for free hapten, even under the stringent SPR conditions designed for kinetics analyses.

Therefore this poses a question that must be addressed: is it possible that avidity masks the true affinity in multimeric scFv populations?

(a)

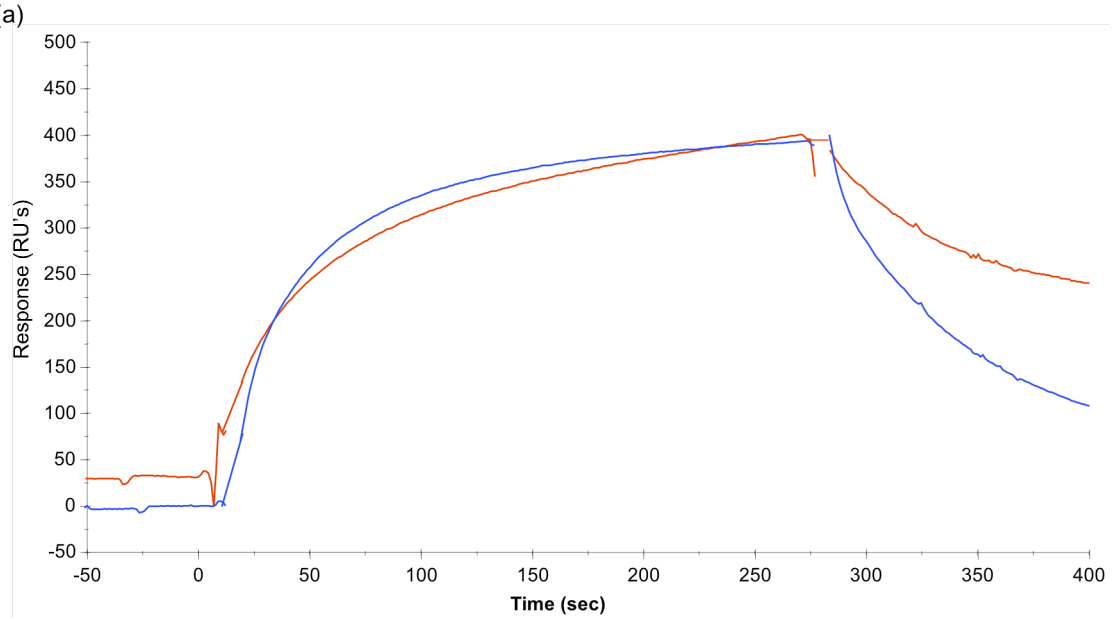
Response (RU's)
500
450
400
350
300
250
200
150
100
50
0
-50
-50
0
50
100
150
200
250
300
350
400
Time (sec)

(b)

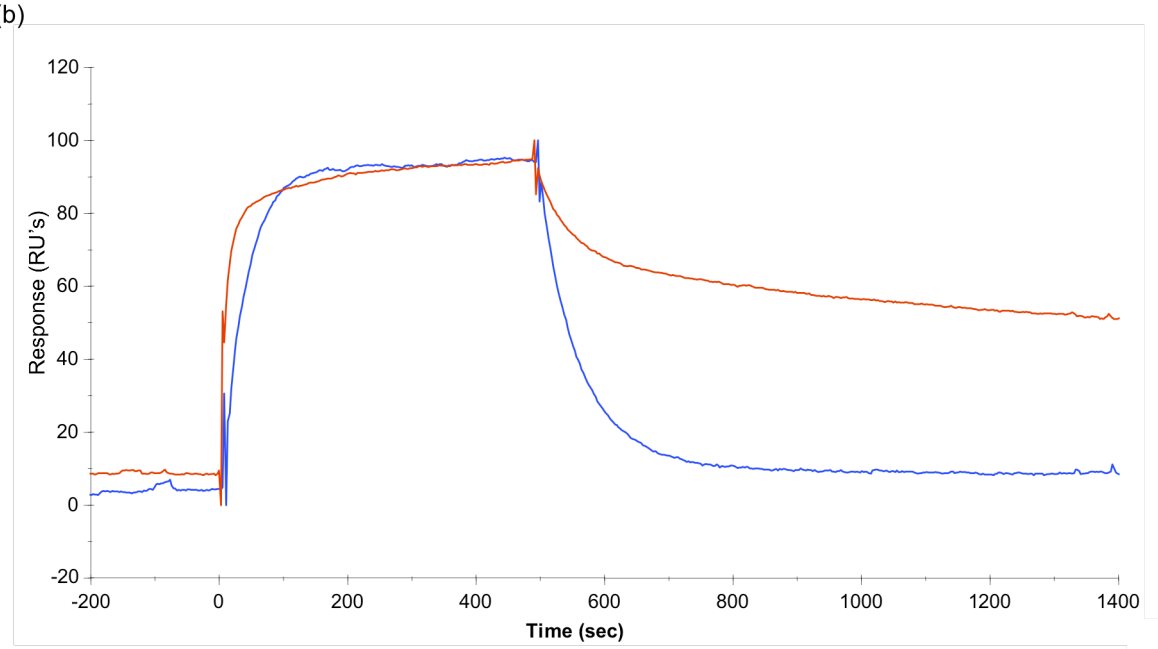
Response (RU's)
120
100
80
60
40
20
0
-20
-200
0
200
400
600
800
1000
1200
1400
Time (sec)

Figure 4.3.4.4.1 (a) Representative sensogram demonstrating the difference between Fab (Red) and scFv (Blue) binding response under normal assay conditions described previously, when examined on the M3G-OVA-coated CM5 chip surface. On-line reference subtraction was performed against a flow-cell coated with OVA. An antibody sample buffer mimic, containing no anti-M3G, was used as a secondary negative control. (b) Kinetics sensograms demonstrating the difference between Fab (dark) and scFv (light) binding response when examined on the M3G – coated surface. 'On-line' reference subtraction was performed against a flow cell, which was activated and capped as for the M3G-coated cell. An antibody sample buffer mimic, containing no anti-M3G, was used as a secondary negative control.

4.3.5 Sequencing

Plasmid DNA was sent to MWG Biotec (Germany), for sequencing. Comfort reads were performed in triplicate using the primers ompseq (5' AAG ACA GCT ATC GCG ATT GCA G 3') and pelseq (5' ACC TAT TGC CTA CGG CAG CCG 3'). The nucleic acid sequences were analysed using the chromaslite 200 software package and the expasy nucleic acid translation tool (http://www.expasy.org/tools/dna.html). The CDR's were identified (Figure 3.3.5.1) using Kabat rules for identifying antibody CDR regions from linear amino acid sequences, which are summarized at http://www.rubic.rdg.ac.uk/abeng/cdrs.html. The final demonstration in this comparison between the Fab and scFv constructs is the sequence alignment of the two V_H and V_L sequences. Figure 4.3.5.2, illustrates the almost 100% homology between the two purified clones. This further demonstrates the influence of antibody structure on SPR analysis.

Figure 4.3.5.1 Sequence analysis of anti-M3G Fab fragment. Both heavy and light chain CDR's are highlighted in Red and Framework regions are in black.

```
ScfvVH   EVQLQQSGAELMKPGASVKISCKATGYTFSRYWIEWVKQRPGHGLEWIGEILPG
FabVH    EVQLQESGAELMKPGASVKISCKATGYTFSRYWIEWVKQRPGHGLEWIGEILPG

Cons     ***** ************************************************

ScfvVH   SGSTKYNEKFKGRATFTADTSSNTVYMQLSSLTSEDSAVYHCARWSQVHVMDYW
FabVH    SGSTKYNEKFKGRATFTADTSSNTVYMQLSSLTSEDSAVYHCARWSQVHVMDYW

Cons     ************************************************************


ScfvVH   GQGTTVTVSSAS
FabVH    GQGTTVTVSSAS

Cons     ************
```

Figure 4.3.5.2 Alignment of anti-M3G scFv (Brennan *et al.,* 2003) and anti – M3G Fab variable heavy chain regions demonstrating almost 100% homology.

4.4 Conclusion

If kinetic ranking of recombinant anti-hapten antibody fragments assumes monomeric binding interaction, and the ranking is performed to rapidly isolate antibodies which are good for competition assay, then this method will only be truly reliable for Fab constructs, where monomeric binding status is guaranteed. The influence of multimeric scFv is starkly illustrated in Figure 4.2.4.4.1(a), where the off-rate apparent in the kinetics sensorgrams of the Fab and scFv constructs are strikingly different, leading to a 40-fold difference in calculated off-rate values. This suggested higher affinity of the scFv for M3G is not borne out, however, on subsequent assay development, as the Fab can actually out-perform the scFv molecule in both plate and SPR assay formats (Figure 4.2.2.2 and Figure 4.3.3.2.1). Moreover, the scFv and Fab constructs are found to have highly similar affinity for the free M3G molecule under optimised assay conditions (Figure 4.3.3.2.2).

This research described the development of an immunoassay using an alternative genetically derived Fab antibody fragment, for the detection of M3G, constructed from a previously described scFv (Brennan *et al.,* 2003). The Fab construct displayed a marginal improvement in affinity for the free drug. During Biacore assay development it became evident that the directly labelled hapten SPR surface may be more appropriate for comparative analysis of different constructs i.e. scFv and Fab. It was shown that the Fab construct performed better in ELISA and Biacore assay formats, through, either the changes in valency when using the Fab format or through the increased rigidity of the V regions. The influence of increased rigidity and scaffolding on anti-hapten antibody binding is further examined and exploited in chapter 5 (mutagenesis).

Chapter 5

5.0 Generation of anti-tetrahydrocannabinol recombinant antibodies and their application, in conjunction with other anti-drug antibodies, on a multi-drug detection platform

5.1 Introduction

5.1.1 Species selection

The antibodies described previously were generated using murine genetic template material. This was primarily because there were pre-existing murine IgG structures available. However, in the case of tetrahydrocannabinol, there were no pre-existing antibodies available in the laboratory nor are there any reports of successful generation or application of anti-THC recombinant antibodies currently in the public domain. With this in mind it presented the ideal opportunity to investigate the benefits of using a leporine model in place of the typical murine model for the generation of anti-tetrahydrocannabinol recombinant antibodies.

5.1.1.1 Leporine immune response

Rabbits have a limited V(D)J gene repertoire formed primarily by the rearrangement of a single V_H gene (V_H1). The crucial first stage of a functional immune response is the generation of a primary antibody response sufficiently diverse so as to recognise a vast array of antigens (Crane *et al.,* 1996). This is also true for the generation of a functional recombinant antibody immune library. Most species form a diverse primary response via the combinatorial joining of multiple V, D and J segments (section 1.9). However, combinatorial recombining only has a very limited impact on the diversity of the rabbit response. Rearrangment is minimal and the same V_L and J_L genes are used in all B cells. A very limited number of V_H, J_H and D_H gene combinations are also utilised. The leporine system utilises a mechanism known as somatic gene conversion, as do chickens, the only difference being that somatic gene conversion occurs in chickens before they are born while it occurs after birth in rabbits.

At the loci of both the heavy and light chains there are upstream families of psuedogenes that lack the necessary functional recombination signal sequences required to undergo rearrangment. However they can donate sequences to the functionally recombined VJ_L and VDJ_H genes. Somatic gene conversion is a powerful tool in the

generation of antibody repertoires (Ratcliffe, 2006). This notion was first described by Reynaud *et al.* (1987) in relation to the avian immune response. The upstream donor remains un-altered, in that it donates gene segments but does not receive any in return thereby acting as a resevoir of diversity for the recombined gene segments (VJ and V(D)J).

5.2 Rationale for the construction of an anti-tetrahydrocannabinol scFv recombinant antibody

Previous chapters have discussed the benefits of Fab construction from IgG genetic templates. The implication of using a Fab instead of an scFv fragment were described in chapter four. However, the work described herein, involved the construction of a scFv, from a leporine immune library, in preference to a Fab fragment. The generation of an scFv is less laborious than a Fab and it displays significantly better on phage (Barbas *et al.,* 2001). Rabbit variable chains have been shown to be unstable and often require the stablising impact of the presence of the disulphide linkage which is available in the scFv construct (Rader *et al.,* 2003). Also, taking into consideration, the findings in earlier chapters (Chapter three and four) that the structural conversion of a Fab to an scFv is more difficult than the converse, it was decided that an anti-THC scFv would be constructed.

Aside from the obvious construction and display advantages of the development of an anti-THC scFv fragment, the future potential to convert it to alternative recombinant structures such as a Fab fragment is also provided. The generation of an anti-THC recombinant antibody fragment is the last of the three anti-drug antibodies to be constructed in the work outlined in this thesis. Both the anti-amphetamine and anti-M3G antibodies are in the Fab format, thus it was ideal to have alternative antibody structural formats for eventual application to a multi-drug detection platform. This is important where the antibodies developed have the potential to be applied to a number of assay platforms.

5.3 Results and Discussion

5.3.1 Production of a recombinant antibody library against Tetrahyrdocannabinol

5.3.1.1 Serum analysis and cDNA synthesis

The standard rabbit immunisation sechedule was followed here (Section 2.3.3). A direct ELISA was carried out to determine if the antiserum was of sufficiently high titre prior to sacrifice and collection (figure 5.3.1.1). The antibodies that were raised against THC-BSA were screened against THC-BTG so as to eliminate false positives as a result of non-specific binding to the carrier protein. The serum titred out at approximately a 1 in 300,000 dilution of neat serum. A pre-immunisation serum sample was included as a control. The RNA was extracted (total RNA extracted was approximately 10mg), the cDNA was synthesised and the scFv gene was amplified according to the protocols outlined in section 2.4.1, 2.4.2 and 2.4.8, respectively.

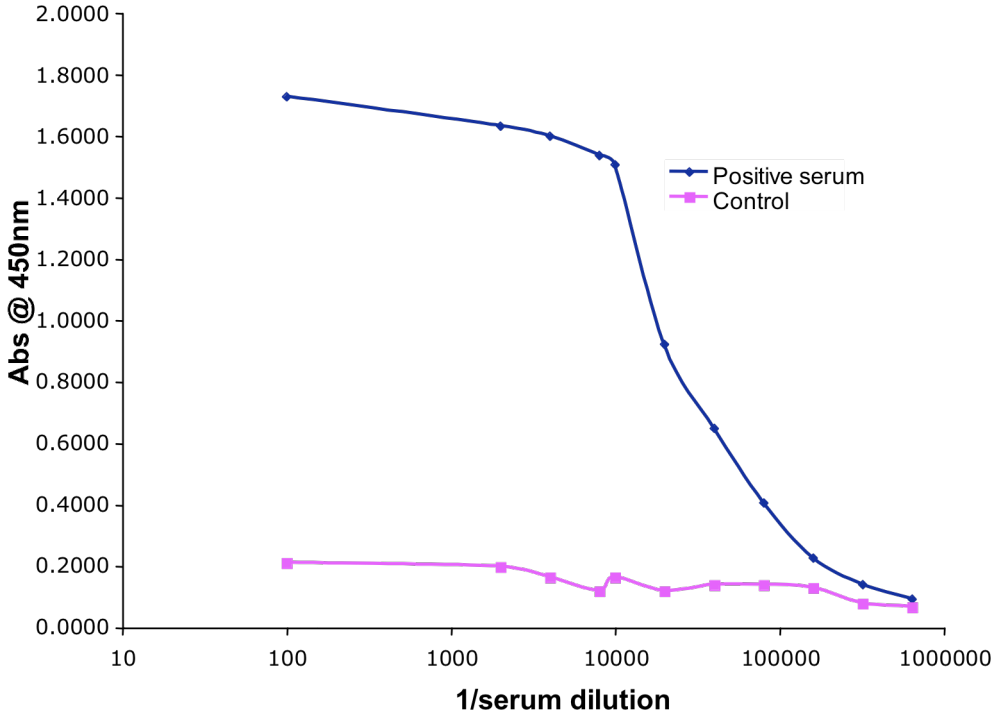

Figure 5.3.1.1 Titre of antibody from rabbit immunised with THC-BSA. The antibody was titred against THC-BTG in 1% (w/v) BSA to eliminate any antibodies specific to the carrier protein. Pre-immunised serum was included as a control. Bound antibodies were detected using a peroxidase-labelled anti-rabbit secondary antibody and signal was developed using a TMB chromogenic substrate. Absorbance was read at 450nm.

5.3.1.2 Isolation of scFv fragments from rabbit library

5.3.1.2.1 Digestion and ligation of scFv and vector fragments

The scFv fragment and the pComb3x vector were digested with *Sfi 1* in parallel and a 1:2 ratio of antibody DNA to vector DNA was included in the ligation reaction. After ethanol precipitation to concentrate the DNA, two full-size electroporations were prepared (section 2.4.10.2). The transformed library was titred and yielded a library size of 1.06×10^8 which was sufficently large for this work.

5.3.1.2.2 Bio-panning

The bio-panning strategy employed here was in accordance with the protocal 10.5 in the Barbas manual (Barbas *et al.,* 2001) with the exception that immunotubes were used in place of immunosorbent wells for the first two rounds. An elevated concentration of the drug (50µg/ml) was used in the early rounds of the panning process to ensure that no loss of positive phage occurred as a result of the inaccessibility of this particularly difficult target antigen due to its solubility issues.

In rounds one and two phage were incubated on immunotubes coated with 20µg/ml THC-BTG for 2.5 hours and 1.5 hours, respectively. In rounds three and four duplicate immunosorbent wells replaced the use of immunotubes for phage incubation. The smaller surface area, in conjunction with a more extensive washing steps (15 x PBS followed by 15 x PBST) led to an increase in the panning stringency. Input and output titres were analysed after round four to assess the enrichment of the phage population prior to moving onto a further round of panning. Input and output titres, plotted in figure 5.3.1.2.2.1, indicated appropriate enrichment of phage after each round and also that an enrichment plateau had not yet been reached. Phage were incubated for 45 min on a single immunosorbent well in round five and the washing steps were 15 x PBS followed by 15 x PBST.

5.3.1.2.3 Single clone analysis of the panned library

A polyclonal phage ELISA was carried out for all five rounds of selection. An anti-M13-HRP-labelled secondary antibody was used for detection. Figure 5.3.1.2.3.1 illustrates the enrichment of positive anti-THC-binding phage after round two. There is a slight decrease of approximately 10% in signal between round three and round five, therefore, it was concluded that the maximum tolerable stringency had been reached and that colonies would be selected randomly from rounds three, four and five for monoclonal analysis.

Single colonies from each round were chosen at random and seeded for use in single clone soluble analysis, as described in section 2.6.4. Two 96-well microtitre plates were inoculated and each plate included the appropriate control wells. A high, relatively uniform, signal was produced across the two plates (data not shown). Twenty random clones were selected to assess single clone target specificity further. These 20 clones were grown in 5 ml culture volumes, induced and lysed via three rounds of freeze/thawing. Each lysed preparation was applied to the plate at a final 1 / 4 dilution and incubated with 3 different concentrations of free THC (10 μg/ml, 1 μg/ml and 100 ng/ml) to investigate the competition properties of the expressed antibodies. The results are illustrated in figure 5.3.1.2.3.2. Four out of twenty clones demonstrated displacement by free THC and also showed an increase in signal intensity inversely proportional to a decrease in THC concentration.

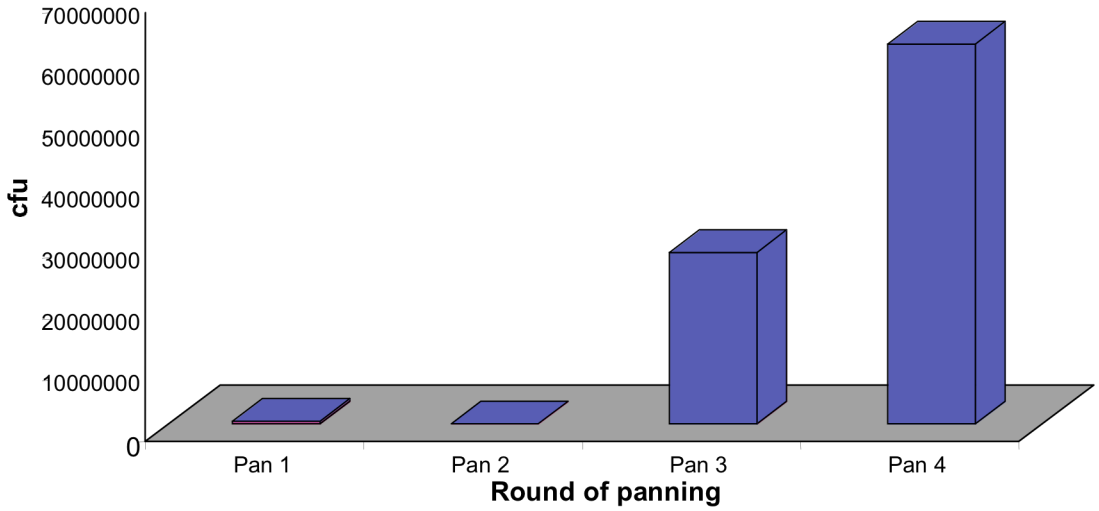

Figure 5.3.1.2.2.1 The number of colony forming units formed after each round of panning of the rabbit anti-THC scFv library. Panning stringency was increased with each successive round with significant enrichment of potential positive clones evident in rounds three and four.

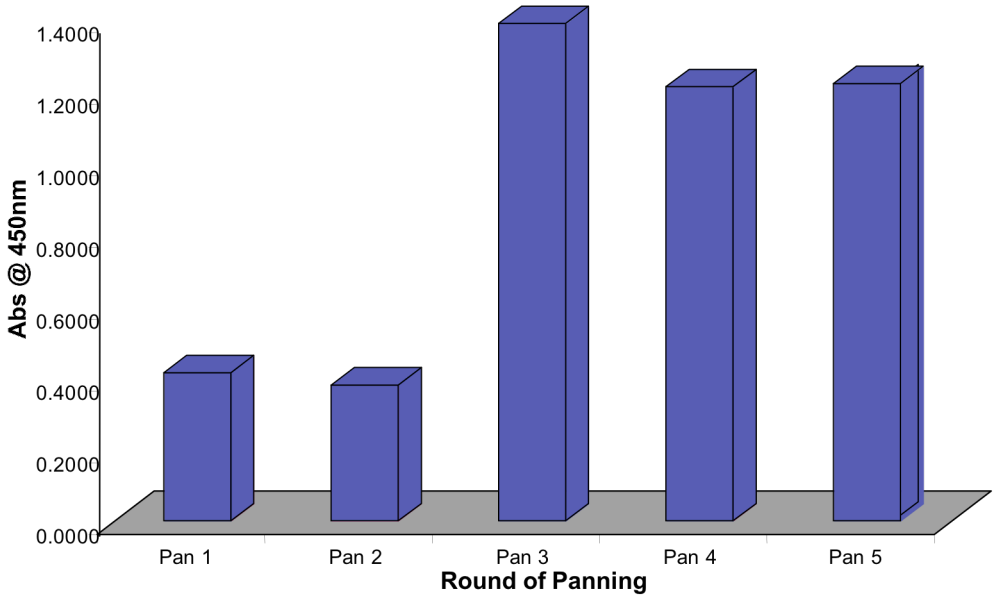

Figure 5.3.1.2.3.1 Results of a polyclonal phage ELISA following five sucessive rounds of panning of the rabbit anti-THC scFv library. Phage binding was detected with an anti-M13-HRP-labelled secondary antibody.

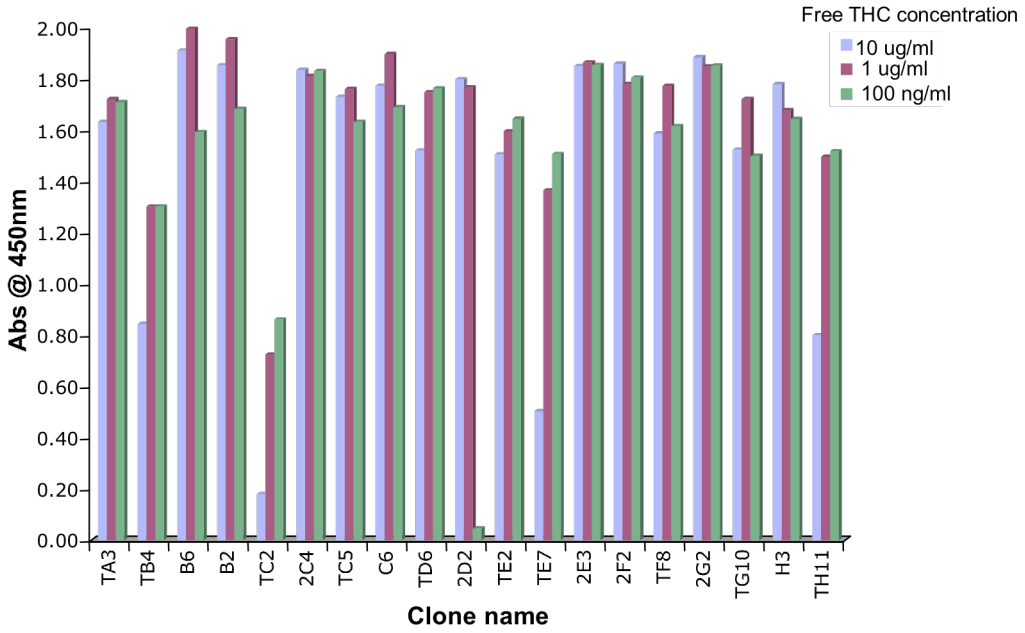

Figure 5.3.1.2.3.2 Representation of single clone soluble expression analysis via an inhibition ELISA performed on THC-BTG-coated wells. Data is expressed as absorbance.

5.3.2 Characterisation of positive clones

5.3.2.1 Sequence analysis and inhibition ELISA

A competitive ELISA was performed with the four positive clones TB4, TC2, TE7 and TH11. This competitve ELISA incorporated a larger range with smaller increments in free THC concentration, (10,000 – 9.7 ng/ml). An antibody dilution factor of 1/ 2 final concentration was used for each clone (figure 5.3.2.1.1). Clone TB4, did not demonstrate any displacement when analysed and as such it was eliminated from further analysis. All three remaining clones displayed similar displacement profiles with IC50's of approximately 600 ng/ml. A pick PCR was carried out to confirm the presence of the correct size DNA band using the standard pComb scFv amplification primers. The correct 800 bp band was amplified for the three clones TC2, TE7 and TH11 (figure 5.3.2.1.2). Each of the three clones was sequenced and it was revealed that each was the same clone (figure 5.3.2.1.3).

The anti-THC scFv was grown in large-scale and purified via metal affinity chromatography as outlined in sections 2.7.1 and 2.7.2. In direct ELISA, the IMAC-purified and concentrated (to 750µl final volume) antibody preparation provided a titre of 1/64,000. ELISA conditions for the antibody were optimized for maximal sensitivity (data not shown). At an optimal dilution of 1/8,000 the scFv was shown to have a detection range of 156 – 1,250 ng/ml for free THC, with an IC_{50} value of 600 ng/ml (figure 5.3.2.1.4).

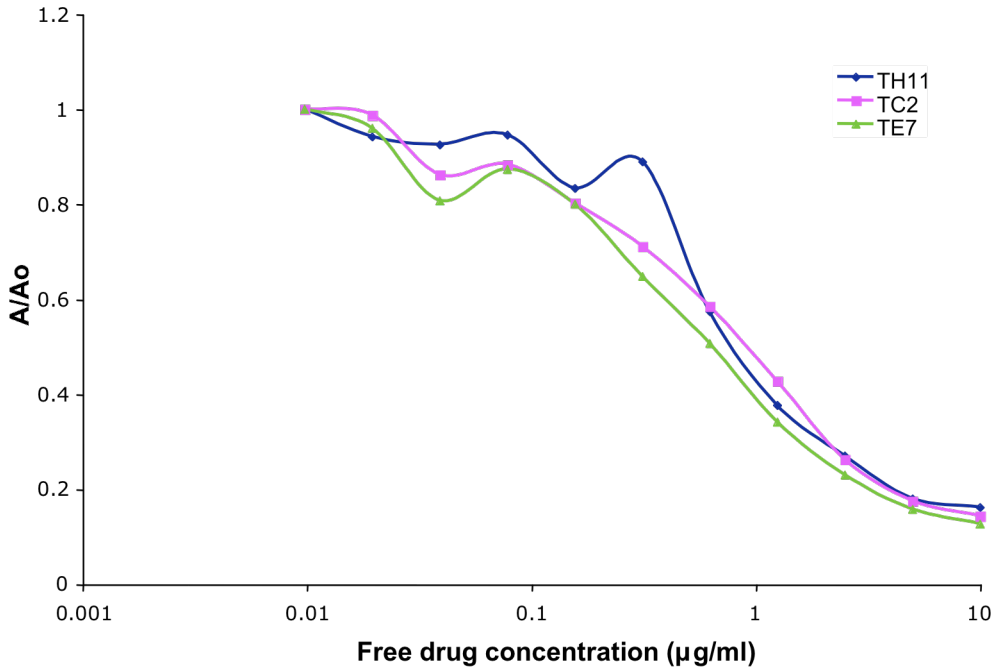

Figure 5.3.2.1.1. An ELISA inhibition assay was performed on THC-BTG-coated wells comparing TH11 (blue), TC2 (purple) and TE7 (yellow) binding response versus competing free THC concentration. Signal developed using TMB chromogenic substrate and monitored by optical density at 450nm. Data is expressed as A/A_0 (i.e. the signal at different free analyte concentrations are expressed as a proportion of signal in the presence of no competing analyte).

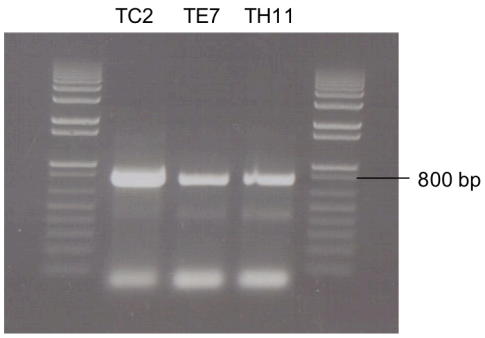

Figure 5.3.2.1.2 A colony pick PCR using standard scFv amplification primers and conditions revealed the presence of an 800bp band in each of the three clones TC2, TE7 and TH11.

```
                                                CDRL1                   CDRL2
TC2     QAAELDLTQTPASVEVAVGGTVTIKCQASQSISSRLAWYQQKPGQPPKLLIYAASTLESG
TH11    QAAELDLTQTPASVEVAVGGTVTIKCQASQSISSRLAWYQQKPGQPPKLLIYAASTLESG
TE7     QAAELDLTQTPASVEVAVGGTVTIKCQASQSISSRLAWYQQKPGQPPKLLIYAASTLESG
        ************************************************************

                                                CDRL3                   LINKER
TC2     VPSRFRGSGSGTDFTLTISGMKAEDAATYYCQSADASTVAFGAGTNVEIKSSGGGGSGGG
TH11    VPSRFRGSGSGTDFTLTISGMKAEDAATYYCQSADASTVAFGAGTNVEIKSSGGGGSGGG
TE7     VPSRFRGSGSGTDFTLTISGMKAEDAATYYCQSADASTVAFGAGTNVEIKSSGGGGSGGG
        ************************************************************
                                                CDRH1
TC2     GGGSSRSSQSLEESGGRLVTPGTPLTLTCTASGFSLTSNVVTWVRQAPGEGLEWIGTIAY
TH11    GGGSSRSSQSLEESGGRLVTPGTPLTLTCTASGFSLTSNVVTWVRQAPGEGLEWIGTIAY
TE7     GGGSSRSSQSLEESGGRLVTPGTPLTLTCTASGFSLTSNVVTWVRQAPGEGLEWIGTIAY
        ************************************************************

         CDRH2                                                  CDRH3
TC2     GAATYYATWAKGRFTISKTSTTVDLKITSPTTEDTATYFCARGYPGHIAADIWGPGTLVT
TH11    GAATYYATWAKGRFTISKTSTTVDLKITSPTTEDTATYFCARGYPGHIAADIWGPGTLVT
TE7     GAATYYATWAKGRFTISKTSTTVDLKITSPTTEDTATYFCARGYPGHIAADIWGPGTLVT
        ************************************************************


TC2     VSLGQPKAPSVTSGQAGQHHHHHH
TH11    VSLGQPKAPSVTSGQAGQHHHHHH
TE7     VSLGQPKAPSVTSGQAGQHHHHHH
        ************************
```

Figure 5.3.2.1.3 T-coffee alignment of three anti-THC scFv clones; TC2, TE7 and TH11. Sequence analysis revealed that all three clones were identical. The individual CDR's are highlighted in bold and labelled in pink,. The serine-glycine linker is labelled in pink also.

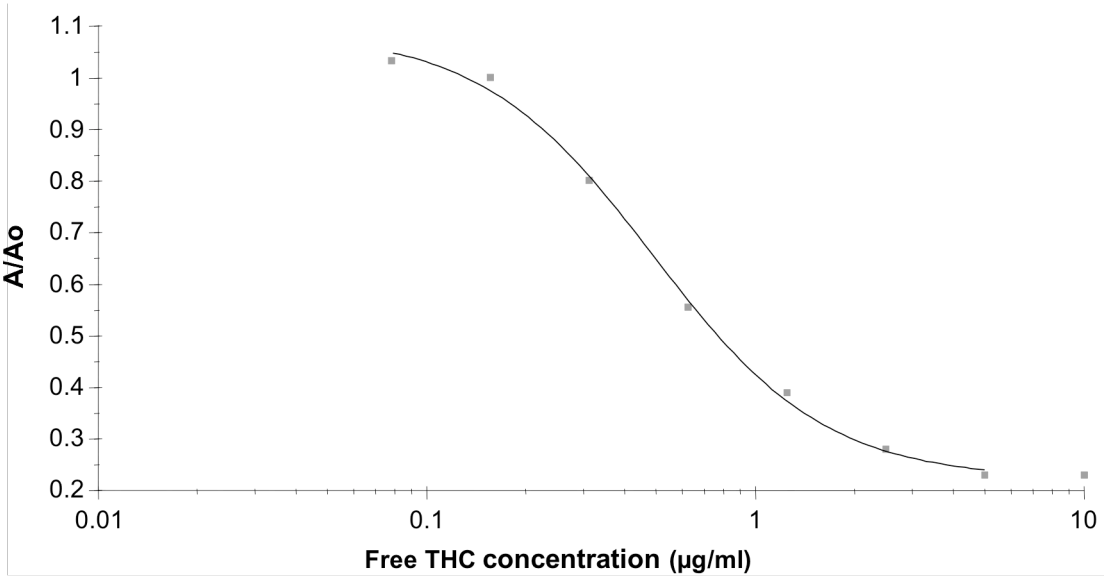

Figure 5.3.2.1.4 ELISA inhibition assay performed on THC-BTG-coated wells showing the scFv's binding response versus competing free THC concentration. Data is expressed as A/A_0. All analyses were preformed in triplicate on three separate occasions.

5.3.3 Comparative studies on the performance characteristics of the anti-THC recombinant scFv and a commercially available anti-THC monoclonal antibody.

The scFv's performance in ELISA was compared to that of the commercially available monoclonal anti-THC antibody (Europa Bioproducts Ltd). The data suggested that the anti-THC scFv is two fold more sensitive on ELISA when compared to the anti-THC monoclonal antibody (figure 5.3.3.1). The scFv has a significantly more reproducible linear range of detection (figure 5.3.2.4.4), a factor that becomes extremely important in a situation where the accurate detection limits have legal consequences. It was concluded that the scFv was more suitable for use in the development of a biacore inhibition assay due to its higher affinity for the free molecule, its reproducibility (low standard deviations) and its cost effective 'in-house' expression and purification. Although it was clear at this point that there would be issues with the stability of the

free drug in solution, the results obtained for the monoclonal antibody were less reproducible than those for the scFv. The platforms in this study utilized an aqueous solution and as such a highly lipophilic target causes problems. THC naturally adheres to the glass or plastic vessel in which it is stored for the duration of the assay. The inclusion of solvent in the assay resulted in significantly reduced reproducibility and was therefore eliminated as a possible solution to the problem. Furthermore, in view of the aim of developing a multi-analyte detection platform it is ideal to have all antibodies functioning in the same storage and analysis buffer (PBS).

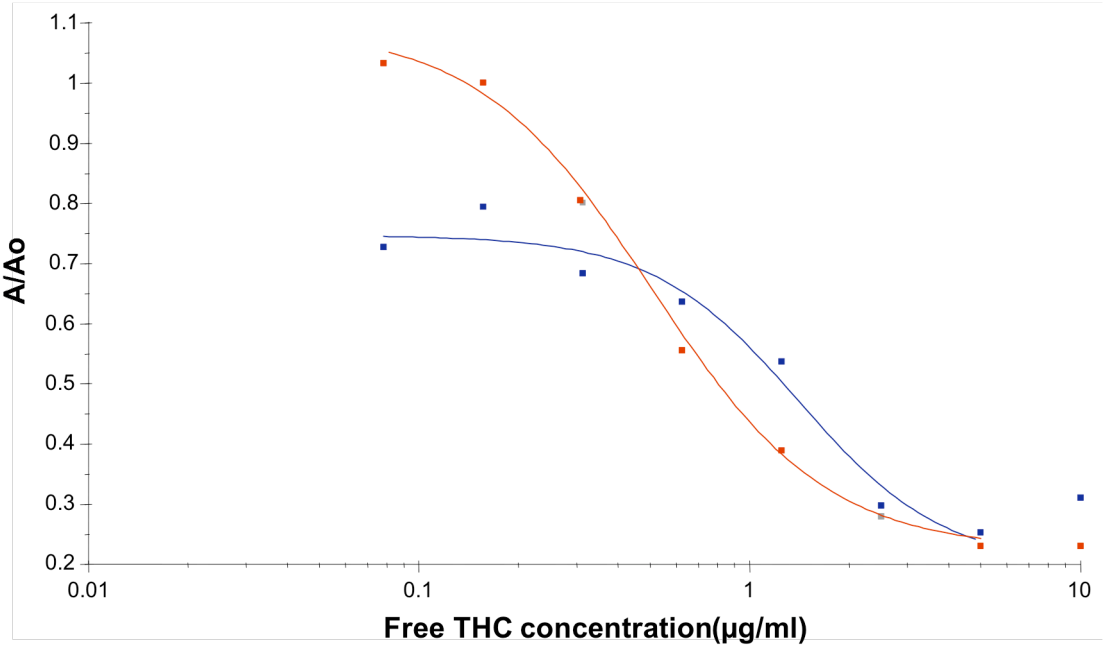

Figure 5.3.3.1 ELISA inhibition assay performed on THC-BTG-coated wells comparing monoclonal antibody (blue) and scFv (brown) binding response versus competing free THC concentration. Data is expressed as A/A_0 (i.e. signal at different free analyte concentrations are expressed as a proportion of signal in the presence of no competing analyte).

5.3.4 Biacore analysis of constructs

5.3.4.1 Preconcentration analysis and immobilisation

The pH range used in this study was 3.8 - 5.0. Solutions of THC-BSA were made up in each pH buffer and injected over an underivatised flow cell at a flow rate of 5 µl / min for 2 minutes. The optimal pH for THC-BSA immobilisation was determined to be 4.0 and immobilisation strategies were carried out as outlined in section 2.9.2 and 2.9.3.

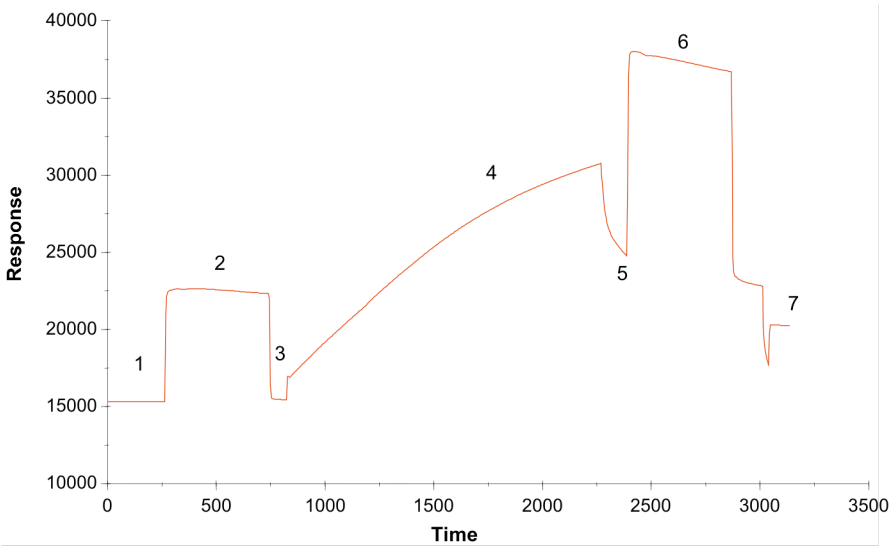

Figure 5.3.4.1.1 Sensogram respresenting the immobilisation of THC-BSA onto a CM5 dextran chip surface. (1) HBS buffer injection and baseline measurement recorded. (2) The carboxymethylated surface was activated when a mixture of EDC and NHS was injected over the flow cell at a flow rate of 5 µl per min for 7 minutes. (3) HBS injection. Activation was confirmed by the increase of ~ 150 RU from baseline (1). (4) A solution of 100 µg / ml of THC-BSA in sodium acetate buffer, pH 4.0, was injected over the flow cell at a flow rate of 5 µl / min for 20 minutes. (5) A HBS injection removed all unbound conjugate and the quantity of immobilised THC-BSA was recorded as the change in response units from (3). (6) – The flow cell was capped / deactivated with an injection of 1M ethanolamine, pH 8.5. All non-covalently attached

conjugate was also removed at this injection point. (7) A HBS injection permited the recording of the new (immobilised surface) baseline. Approximately 8,000 RU's of THC-BSA were immobilised on the flow cell.

5.3.4.2 Inhibition assay development

A similar range of free THC (10,000-9.7ng/ml) was employed as in the ELISA inhibition assay, with samples being injected over each chip in a pre-programmed order and each injection followed by a regeneration step. Both antibodies displayed negligible non-specific interactions with immobilized BSA and the modified CM-dextran surface, negating the need for pre-incubation steps of antibodies with either BSA or activated CM-dextran. The linear range of detection for the scFv was found to be 156 – 2500 ng/ml (IC_{50} of 625 ng/ml) on the THC-BSA surface (figure 5.3.4.2.1).

The sensitivity of the scFv is highly similar in both ELISA (figure 5.3.2.4.4) and Biacore assays (figure 5.3.4.2.1). This would suggest that there is potential to develop and validate an SPR assay similar to the work carried out in chapter four with the anti-M3G antibody fragments. While the inhibition curves are highly comparable and reproducible across replicate assays there is an inherent issue with the solubility of the free drug. With aggregation observed in the free drug stock, it is highly possible that the antibodies described have a higher affinity than the data observed and reported here. Further analysis and exact concentration determination of the THC by the forensics laboratory is an essential next step

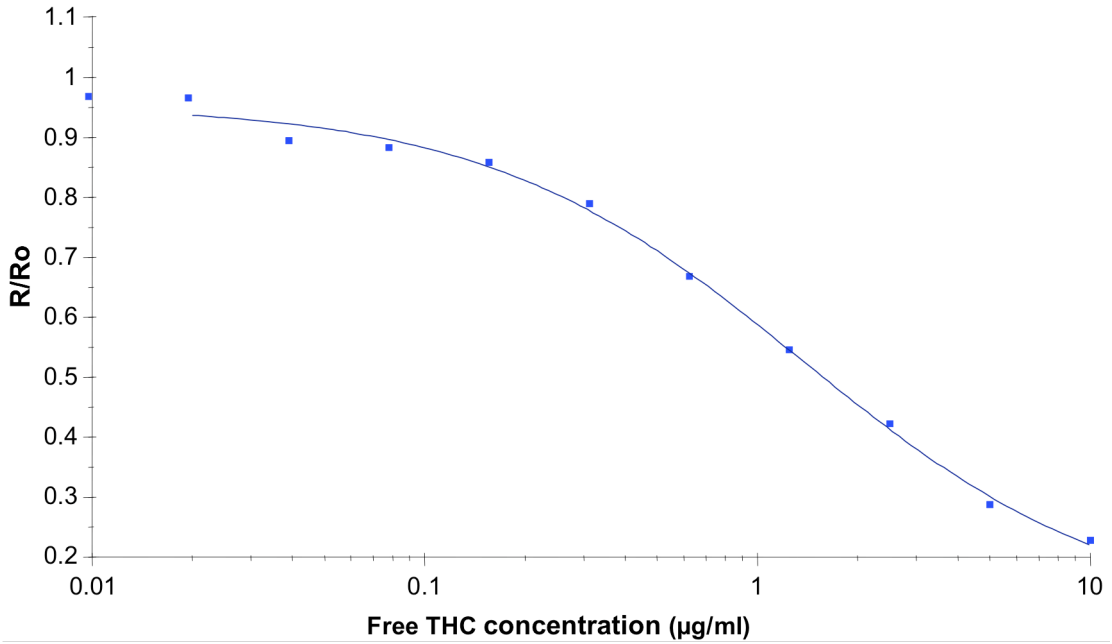

Figure 5.3.4.2.1 Biacore inhibition assays performed on an THC-BSA-coated CM5 chip surface, comparing the scFv's binding response versus free THC concentration. Data is expressed as R/R_0 (i.e. signal at different free analyte concentrations are expressed as a proportion of signal in the presence of no competing analyte). All analyses were preformed in triplicate on three separate occasions.

This research described here has focused on the generation of the third anti-drug recombinant antibody fragment. At this stage each of the three antibodies (anti-M3G, anti-amphetamine and anti-THC) were fully characterized on both ELISA and Biacore assay formats. The next phase of the work entailed the application of the antibodies generated to a multi-analyte detection assay. This is an important step in research of this kind, where the detection of the target antigens is necessary to counteract anti-social or illegal behavior etc., moreover, the application of these antibodies to a multi-drug detection assay was vital to the successful completion of the aims of the research grant.

5.4 Multi-drug chip-based SPR inhibition assay

5.4.1 Rationale for the development of a mutli-drug detection assay

The previously developed and well-defined immunoassay strategies, such as those mentioned in section 1.4, have paved the way for recombinant antibody microarrays in terms of the major issues such as methods of immobilization and detection. There is a major need for the development of a cost-effective, reliable and sensitive test to screen for drugs of abuse. The use of recombinant antibodies offers greater sensitivity and specificity, as illustrated in chapters three, four and earlier in this chapter. Furthermore, the feasibility of applying affinity maturation methods to these antibodies is demonstrated in the work outlined in chapter six. Microarrays have already been exploited in the fields of both proteomics and genomics, however, they are a potential lead-technology in point-of-care diagnostics. Biochips may be generated via spotting low-density antibody-arrays onto plastic chips. This technology can be produced for multiple illicit drug detection. Signals are generated on the chip through enhanced signal amplification e.g. fluorescence. This type of assay is particularly advantageous, as it offers high sensitivity, large sample throughput and low cost analysis. Testing is still very much biased towards the more classical quantification techniques e.g. GC-MS, despite the requirement of expensive equipment, highly trained personnel and laborious sample preparation. Currently despite their performance such novel screening methods are still only regarded as preliminary tests requiring further verification. Here an SPR based assay was chosen as a proof of concept platform for the detection of three alternative drugs on a single platform. This SPR-based assay was designed to determine if the antibodies developed and characterized specifically for their application in a multi-drug detection assay could perform as intended. It also provides a comparative study between their performance in a single-drug assay and a multi-drug assay.

5.4.1.1 Influencing factors on assay design

The feasibility of a multi-analyte assay was examined using the three recombinant antibody fragments developed against the targets; morphine-3-glucuronide, amphetamine and tetrahydrocannabinol. They were optimized in both plate and SPR assay formats. There are a number of parameters to consider when designing any multi-analyte detection method.

The antibody storage buffer:

Each of the antibodies produced in this work (anti-amphetamine Fab, anti-M3G Fab and anti-THC scFv) are stable in PBS. Each of the antibodies have been buffer exchanged and concentrated to storage volumes of less than 1 ml and therefore, are used at high dilution factors (1 in 8000, 1 in 5000 and 1 in 8000, respectively). This eliminated any potential problems when preparing a single, multi-analyte solution.

Antibodies performance in a single analyte assay:

The antibody fragments described have been assayed in an inhibition format rather than a competitive format, i.e. all analyses were performed on an antigen immobilized surface and the antibody / free drug mix was passed over it. Also, all antibodies had a linear range of detection on the Biacore assay format in the region of 1.22 – 1250 ng/ml, and, as a consequence, a single concentration range of drugs can be used in a multi-drug assay.

Cross reactivity:

None of the antibodies demonstrate any problematic cross reactivity towards the non-target drugs when assayed in a single analyte assay. However, this must be included as a control on the multi-analyte chip where all three antibodies and all three drugs are mixed in a single solution.

The solubility of the free drugs (M3G, Amp and THC):

The solubility of the amphetamine and MG3 has never been an issue when designing single drug assays. The THC molecule has proven to be extremely problematic in every aspect of analysis unless in its conjugated form. It is difficult to maintain a precise concentration range as the drug has a tendency to fall out of solution when diluted in PBS prior to assaying. In a single analyte assay it is possible to address the insolubility issues via the inclusion of small concentrations of solvents etc. However, in this case, where the THC molecule will be mixed with an assortment of other antigens and antibodies prior to the binding event it is not as simple. Further investigation would be required on the stability and solubility of the drug prior to assay validation.

5.4.1.2 Chip design and assay conditions

The multi-drug assay was designed based on the formats used in the single-drug detection assays described throughout this work (chapters 3, 4 and 5). This involved the immobilisation of the three drug conjugates on three flow cells on a single CM5-sensor chip along with BSA immobilised on a reference flow cell as a control (figure 5.4.1.2.1). BSA was chosen as the reference because both the THC and amphetamine drugs are conjugated to BSA and although the M3G molecule is linked to ovalbumin the antibody has not demonstrated any non-specific binding to the protein used in the conjugation (section 4.3.3.2).

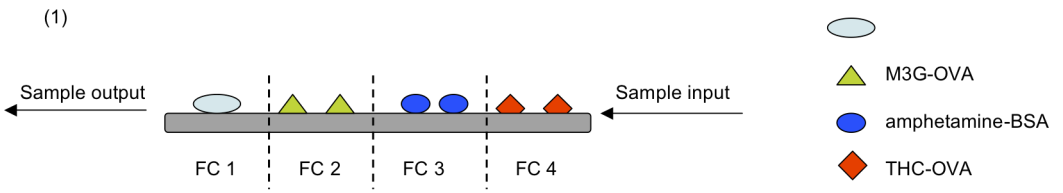

Each drug-conjugate, M3G-OVA, amphetamine-BSA and THC-BSA, is immobilised onto flow cells 2,3 and 4, respectively. BSA is immobilised on flow cell 1 to facilitate reference subtraction.

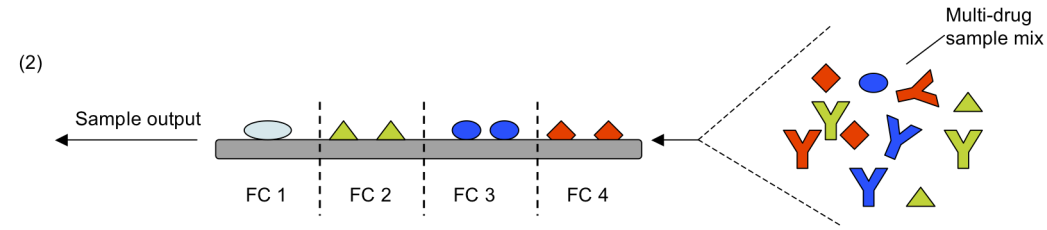

The assay sample, containing the anti-M3G Fab, anti-amphetamine Fab, anti-THC scFv and thee three corresponding free drug compounds, is prepared. Each antibody is present at a single (optimised concentration) and each of the free drugs are included at a concentration range of 10,000 - 9.7 ng/ml. The flow path is 4-3-2-1 over the sensor chip surface.

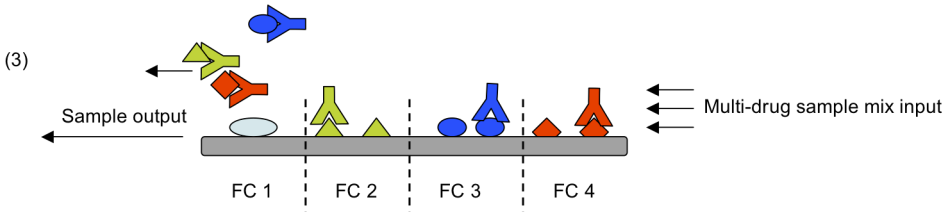

The assay sample is injected across all four flow cells of the CM5 sesor chip surface. Each sample, containing different concentrations of free drug is passed over separately and recorded in a single file. Unbound antibodies and antibody-antigen complexes are washed away. Bound antibody is detected and measured as a mass change on the chip surface.

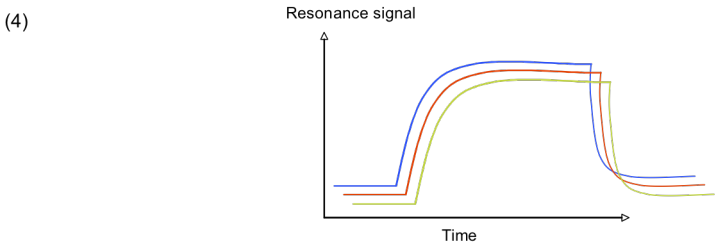

This mass change recorded as a result of antibody binding antigen on the surface of the chip, with respect to each flow cell, is recorded and translated into sensograms.

Figure 5.4.1.2.1 Diagramatic representation of mult-drug assay on a Biacore CM5 sensor chip. Section 1-4 illustrate the functionalitly of the chip and the generation of responses on Biacore.

5.4.2 Results

Each antibody was passed across each flowcell to determine its specificity for its corresponding conjugate. After extensive optimisations assay conditions were determined and the sample mix containing the three antibodies (anti-M3G, anti-amphetamine and anti-THC) and the three drug compounds was prepared for the Biacore inhibition assay (figure 5.4.1.2.1).

The inhibition curves produced as a result of the multi-analyte detection assay (figure 5.4.2.1(a), (b) and (c)) were comparable to the performance of the antibodies when analysed in individual detection assays as illustrated in previous chapters and sections. In short, no decrease in sensitivity or comprise in detection range was observed when the antibodies were applied to the multi-drug detection assay compared to those results achieved in the single-analyte assay.

This result is indicative of the potential use of the antibodies produced in this project on a multi-analyte assay format. All three antibodies proved to be appropriately stable and specific for their intended use. The biacore assay presented here may also be viewed as a proof of concept and is illustrative of the practical opportunities for using these three recombinant antibodies on a single mutli-drug detection platform in the future.

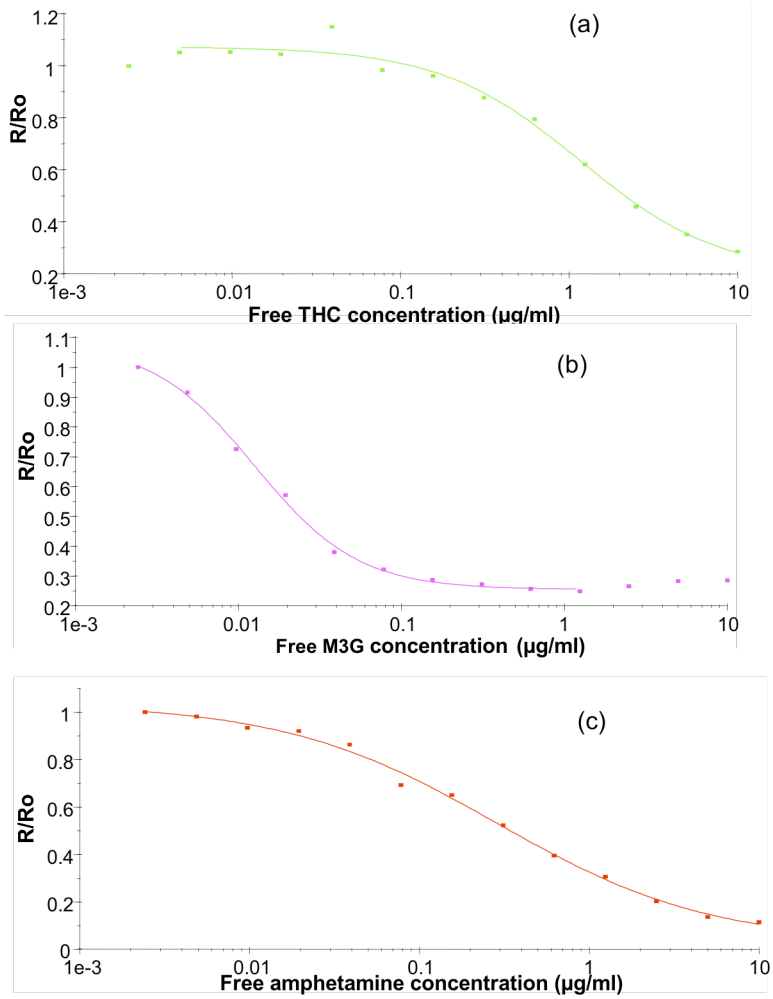

Figure 5.4.2.1 Each data point on the curves represents a sample taken from a mixed solution containing free THC, amphetamine, M3G and antibody fragments specific for THC, amphetamine, M3G. (a) Biacore inhibition assays performed on a THC-BSA-coated CM5 flow cell surface, comparing the anti-THC scFv's binding response versus free THC at various concentration. (b) Biacore inhibition assays performed on a M3G-OVA-coated CM5 flow cell surface, comparing the anti-M3G Fab's binding response versus free M3G. (c) Biacore inhibition assays performed on a AMP-BSA-coated CM5 flow cell surface, comparing the anti-Amp Fab's binding response versus free amphetmaine. Data expressed as R/R_0. All analyses were preformed in triplicate on three separate occasions.

5.5 Conclusion

Previous work in this area reported serious problems in obtaining soluble anti-THC scFv fragments. Brennan (2004, unpublised data) reported on the difficulties developing recombinant antibodies against THC. While phage-bound scFv's were described, there was no success in generating soluble recombinant antibody fragements with potential for assay application reported. However, this chapter has described the successful production and characterisation of an anti-THC scFv fragment on ELISA and Biacore. The resultant scFv out-performed commercially available monoclonal antibody with respect to its detection of THC. Furthermore its application to a multi-analyte assay has been demonstrated. The linear range of detection was found to be 156 – 1250 ng/ml in both ELISA and Biacore analysis.

The influence of the lipophilic nature of the drug on the assay and the limits of detection requires further investigation in order to validate this method of detection. The exact concentration of the drug present in samples over the course of an assay must be determined to ensure accurate reproducible results, especially, if the intended outcome were to commercialise such an antibody. It is also very possible that the anti-THC scFv is more sensitive than is reported here due to the fact that the drug readily falls out of solution and adheres to the side of the glass or plastic receptacle in which the assay is performed.

In chapter six, the genetic engineering via *in-vitro* mutagenesis of the anti- M3G Fab fragment was described. This anti-THC scFv is an ideal candidate for affinity maturation based on a number of important factors. Unlike the anti-M3G Fab it was not derived from a monoclonal parent but instead selected from an immune library, as such it may be more susceptable to *in-vitro* maturation as it did not undergo significant functional optimisation *in-vivo* prior to selection.

Secondly, based on the findings in chapters three and four, the structural conversion of this anti-THC scFv to a Fab fragment may also influence the sensitivity of the the recombinant antibody fragment. In previous chapters this affinity improvement has been

attributed to the link between the increased structural rigidity of the anti-hapten Fab and its affinity for the target.

Finally, the anti-THC scFv along with antibodies described in chapter's three and four were characterised with regard to their application to a multi-drug detection assay. While the primary goal was to develop an assay in collaboration with the optical-sensory group, due to differences is project time-lines etc. this became unfeasible at this time.

There are a number of lateral flow based multi-drug test kits comercially available, for example, oratect (BMC™), a lateral flow based assay with a testing time of 15 minutes. Intercept® (Orasure technologies inc.), an EIA based test and also the Ontrack oratube (Varian inc.), based on GC/MS assay techniques, both of which require a number of days to obtain results. All of these test kits yield a positive / negative result for the presence or absence of the individual drugs but do not provide any quantitative data. However, the demonstration of a successful biacore based multi-drug inhibition assay illustrates the capabilities of the antibodies developed and described throughout this work for use in such a multi-analyte assay. A quantitative result would be extremely useful where very low levels of the drug are detected as a result of ingestion of over-the-counter medication and is not indicative of substance abuse. The high specificity observed in this assay is strongly indicative of their potential application to a rapid, sensitive, specific and cost effective low-density microarray that will be developed in future collaborations.

Chapter 6

6.0 Antibody engineering - mutagenesis of the anti-Morphine-3-Glucuronide Fab fragment.

6.1 Introduction

The immune system is the fundamental mechanism used for generating novel, multiple affinity antibodies against almost any target imaginable. The first phase of the response results in the selection of moderate affinity antibodies displayed on the surface of B cells. Thus, the B cell represents a single entity comprising both the phenotype and the genotype of the particular antibody in question. The principles of phage display, described previously in chapters 1, 3 and 4, illustrate the likeness between the natural immune system and phage display technology. The second phase of the response involves the affinity maturation of specific antibodies via somatic hypermutation and class switching. All *in – vitro* antibody engineering strategies to date are in some way modeled on the natural functioning of the immune system and its ability to affinity mature specific antibodies.

The immune system naturally selects for the highest affinity binders after somatic hypermutation through class switching. After this first somatic affinity maturation step the antibodies are switched from the multivalent IgM to the bivalent IgG. This class switch enhances the selection bias towards higher affinity antibodies, as selection cannot rely on avidity when in an IgG format.

Recombinant antibody technology is continuously developing and new ways to mimic and improve on the natural immune system are being discovered. In B cells, antibodies undergo successive rounds of mutation and affinity selection. The concept of improving or modifying recombinant antibody affinity *in vitro* is examined throughout this chapter. There are numerous methods of affinity maturation, each of which is explained in section 6.1.1.

6.1.1 Methods for the affinity maturation of antibodies.

A number of techniques have been used for the successful mutagenesis of antibodies against many different targets. These include the use of bacterial mutator strains (Coia

et al., 2001), error prone PCR (Daugherty *et al.,* 2000), DNA shuffling / chain shuffling (Boder *et al.,* 2000) and site directed mutagenesis (Zimmerman *et al.,* 2006).

6.1.1.1 Bacterial mutator strains

The use of bacterial mutator strains for affinity maturation of proteins is often used as a starting point for random mutagenesis. After the clone of interest is infected into the mutator strain the culture is grown and re-inoculated repeatedly until the desired number of rounds of replication is achieved. The choice of growth media used is a key factor in the rate of mutation with a 10^5 fold difference between growth in minimal media compared to rich media (Cox, 1976), the latter achieving the highest rate of mutation. Low *et al.* (1996) reported the improved affinity of an anti-hapten scFv (anti-2-phenyl-5-oxazolone) through a 100-fold decrease in the off-rate. This was achieved predominantly via mutations in the CDR loops and to a lesser extent in the framework regions. The improvements are attributed to, but not limited to, mutations in the CDRH1 and CDRL2 while no improving mutations in the CDRH3 are reported. However, a significant disadvantage with this system is the introduction of mutations in the entire phagemid and not just in the antibody encoding region of the gene. Hence, a large library would be required to get a good representation of all positive mutations. In this case large library construction is dependant on transformation efficiency of the *E. coli.*

6.1.1.2 Error prone PCR

Error prone PCR is a method used to introduce random sequence copying mutations through imprecise reaction conditions along with the addition of Mn^{2+} and Mg^{2+} to the reaction. Error prone PCR is commonly used with previously randomised libraries or in combination with a second mutagenesis technique (Dong *et al.,* 2002; Zahnd *et al.,* 2004 and Razai *et al.,* 2005). These random insertions, deletions or substitutions are

often deliterious, but increases in affinity can result. The merits of the technique were investigated by Daugherty *et al.* (2000) who reported on the unexpectantly high number of functional clones obtained from a hypermutated library and also on the distance of the majority of these positive mutations from the antigen binding site (ABS).

6.1.1.3 DNA shuffling and chain shuffling

DNA shuffling is a method in which the gene of interest is enymatically digested with a high frequency cutting enzyme, DNase I. The DNA fragment is repaired via several rounds of PCR in the absence of any specific oligonucleotides. A full length fragment is achieved via site-specific-recombination of the individual 100bp fragments. Chain shuffling is a method which involves the sequential recombination of different light chains with a single specific heavy chain resulting in the selection of mutants comprised of V_H genes which are target specific and random light chains and vice versa. Chain shuffling has facilitated the investigation of the impact of substituting non-specific light chains in order to reduce cross reactivity, reduce immune responses in therapy and improve affinity (Parks *et al.,* 2000).

6.1.1.4 Site-directed mutagenesis

Site directed mutagenesis is the chosen method in this work. It requires knowledge of the gene of interest. This permits substitutions of specific amino acids or groups of amino acids in specific locations on any one of the CDR's in order to achieve a higher affinity antibody. Extensive research was carried out in this area since it was first discovered by Smith in 1993. A 16 – fold increase in antibody affinity was observed by Schier *et al.,* (1996), following sequential introduction of random substitutions into the CDR's of an anti-c-erbB-2 scFv using standard primer-directed mutagenesis. After selection, the highest affinity mutant was subjected to heavy chain randomization. This led to a 1200 - fold improvement in antibody affinity.

Generally, segmental mutagenesis is performed using oligonucleotides synthesized with degeneracy's at the position where randomization is desired. The most common oligonucleotide doping strategies use NNK or NNS where N is an equal mix of G and C, K is a mix of G and T and S is a mix of G and C. Both strategies encode all 20 amino acids and a single amber stop codon within a total of 32 codons. In order to facilitate

sequencing the NNK strategy is preferred to the NNS due to the higher G/C content which can complicate DNA sequencing (Barbas *et al.,* 2001).

For example, randomizing 5 codons will give a peptide diversity (20^n) 3.2 x 10^6, DNA diversity 32^n 3.4 x 10^7 and would require 1.6 x 10^8 transformants. These figures give a 99% confidence rating of obtaining at least one copy of a rare polypeptide sequence (Table 6.1.1.1).

Table 6.1.1.1 Number of transformants required to represent a degenerate library mutated with either NNK or NNS at a given number of codons (ή). These confidence values and table are based on the Poisson distribution calculation of Lowman and Wells (1991) and sourced from Barbas *et al.* (2001).

No. codons ή	Peptide diversity (20^n)	DNA diversity (32^n)	Transformants required for 90% confidence	Transformants required for 99% confidence
1	20	32	74	149
2	400	1.0×10^3	2.4×10^4	4.8×10^4
3	80×10^3	3.3×10^4	7.6×10^4	1.5×10^5
4	1.6×10^5	1.1×10^6	2.4×10^6	4.9×10^6
5	3.2×10^6	3.4×10^7	7.7×10^7	1.6×10^8
6	6.4×10^7	1.1×10^9	2.5×10^9	5.0×10^9
7	1.3×10^9	3.4×10^{10}	7.9×10^{10}	1.6×10^{11}
8	2.6×10^{10}	1.2×10^{12}	2.5×10^{12}	5.1×10^{12}
16	6.6×10^{20}	1.2×10^{24}	2.8×10^{24}	5.6×10^{24}

There are two strategies of CDR walking; in parallel and in sequence. Parallel walking involves several CDR's targeted at the same time and all mutated CDR's are combined to give the best antibodies, assuming avidity. Sequential involves any improvements generated from one CDR library selection being incorporated into the antibody sequence before constructing the next CDR library. In both strategies, free energy changes are expressed:

$$\Delta\Delta G_{AB} = \Delta\Delta G_A + \Delta\Delta G_B + \Delta\Delta G_I$$

where:

$\Delta\Delta G_A$ and $\Delta\Delta G_B$ are free changes in the free energy of CDR mutants A and B.

$\Delta\Delta G_I$ represents the change in interaction energy between the two residues.

$\Delta\Delta G_{AB}$ is the change in free energy of the protein encompasing the two mutated CDR's

Parallel and sequential differ in their dependence on combined mutants $\Delta\Delta G_1$. Parallel assumes $\Delta\Delta G_1$ is negligible while sequential takes into account that $\Delta\Delta G_1$ may not always be negligible and that optimal binding may result from the interdependence of CDR loops.

In the absence of structural data, as is often the case, site directed 'random' mutagenesis may be employed on all or just specifically chosen CDR loops. Valjakka *et al.* (2002) reported a 40-fold increase in affinity when an anti-testosterone monoclonal antibody was subjected to random mutagenesis of the CDR regions. Mutations in CDRL1 and CDRH3 are considered to have been involved in the improvements observed. This will be discussed later in the chapter.

6.2 Rationale of mutagenesis strategy adopted

The natural immune system can produce antibodies against an enormous range of foreign molecules from a relatively restricted set of germ-line segments. The "lock and key' theory was used to describe antibody - antigen interactions. However, the realization that there is a vast population of polyreactive antibodies in the primary immune response suggests that this concept needs to be very critically assessed. (Notkins, 2004). It was suggested that these antibodies produced as a result of the primary response are capable of binding multiple targets due to their ability to form more than one antigen-combining site (Wedemayer *et al.,* 1997). Their flexibility permits recognition of self and non – self antigens albeit at low affinities (Comtessa *et al.,* 2000). It is thought that antibody evolution alters the conformation of the antibody rendering it more rigid and restricted in structure producing specific higher affinity antibodies.

The specificity of the antibody is determined by the structure of its antigen - binding site which is formed by the 3 CDR's from both the heavy and the light chains acting together by heterodimerisation (Padlan *et al.,* 1994). This binding site results from 6

hypervariable loops converging. *In vivo* diversity in antibody binding sites is initially encoded in the germ-line by multiple variable (V) diversity (D) and joining (J) gene segments. CDR1 and CDR2 of the heavy and light chains are encoded within the V regions. Light chain CDR3 is produced by the genetic recombination of V and J regions while the heavy chain CDR3 is formed by the recombination of V, D and J regions. The heavy chain CDR3 can carry from between 2 – 26 amino acids.

This chapter describes two alternative strategies for mutating anti-M3G Fab, an anti-hapten recombinant antibody fragment, and the impact each strategy has on the affinity of the antibody for its target. There are a number of reports indicating that the CDRH3 is the most relevant region for antigen binding due to its huge diversity. Therefore, this was the first target for mutagenesis. However, it is apparent that regions outside of the antigen-binding site could have an impact on the affinity of an anti-hapten antibody (Daugherty *et al*., 2000; Persson *et al.,* 2006; Zimmermann *et al*., 2006 and Low *et al.,* 1996).

The second strategy changed focus, moved away from looking at the highly evolved CDRH3 and targeted the CDRL2, CDRL3 and CDRH1 all of which have been reported by various groups as having significant importance in anti-hapten antibody binding. A vital element in antibody affinity maturation is in understanding the difference between anti-hapten antibodies and anti-protein/peptide antibodies. Herein the key question of the impact of forcing mutations into the primary point of antigen contact is examined. This is then followed through with an investigation of site directed mutagenesis in the more peripheral regions of the fragment relative to the binding sites.

6.3 Results and Discussion

6.3.1 Mutagenesis strategy 1: CDR walking

6.3.1.1 Primer design for CDR walking

Sequence analysis of the anti-M3G Fab revealed the CDR3 of the light chain to be 9 codons in length (section 4.3.5). It was decided to introduce random mutations into the central 5 codons and to keep the two flanking codons constant. M-VH1-RAN-F introduces this randomized gene segment (NNK X 5) into CDR3 – 5` GAC TCT GCC GTC TAT CAC TGT GCA AGA TGG TCC NNK NNK NNK NNK NNK GAC TAC TGG GGT C 3`. The second primer, M-VH1-FR3-B, was designed to contain a 27 bp overlap with the forward primer – 5` TCT TGC ACA GTG ATA GAC GGC AGA GTC 3`. Using this overlap in sequence only two PCR steps were required to amplify the mutated gene. The other two primers, Ompseq and g-back are common to the pComb3X vector.

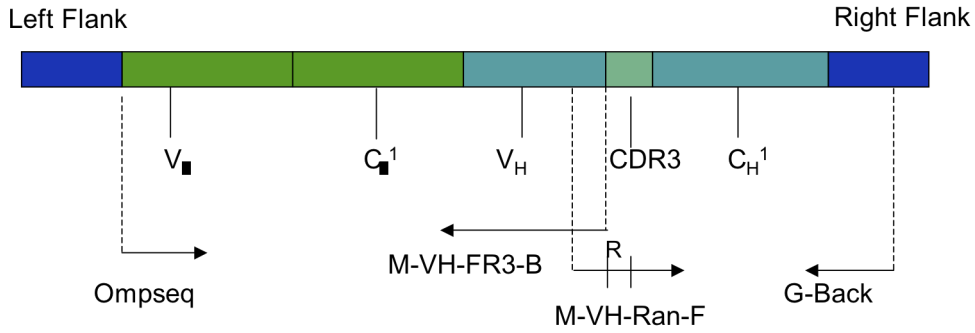

Figure 6.3.1.1.1 Site-directed mutagenesis in the CDRH3, of the anti-M3G Fab fragment in pComb3X, showing the randomized and overlapping regions of the gene. Ompseq and M-VH-FR3-B are used to amplify the light chain with an overlapping region of 27bp's into the variable region of the heavy chain. M-VH-Ran-F and G-Back are used to amplify the heavy chain. The forward primer M-VH-Ran-F introduces the randomized gene segment into the CDR3 of the variable heavy chain.

The CDR3 was targeted as the first step in a series of sequential mutating steps as the CDR3 of both the heavy and light chains have been shown to contain the hypervariable joints of the V/J and V/J/D gene arrangements. These regions participate in direct antigen contact in many studied antigen / antibody complexes (Wilson and Stanfield, 1993).

6.3.1.2 Amplification of anti- M3G mutant gene

The PCR's were carried out using high fidelity polymerase taq to encourage specific binding. This is more important when using heavily mutating primers such as in this case. There were only two PCR steps required to amplify the mutated gene. The first amplified each of the heavy and light chains, including the new randomized region in the CDR3 of the heavy chain. The second PCR overlapped the whole Fab fragment.

Table 6.3.1.2.1 Basic PCR mix used in all CDR walking amplifications

Component	**Concentration**
Template DNA	100ng (of each chain)
Primers	50 pmol of each
10x HIFI buffer	1X
10mM dNTP	0.2 mM
50mM $MgSO_4$	2mM
Platinum Taq	5 U / reaction
Molecular grade H_2O	Up to 50 µl

It was deemed necessary to eliminate any background amplification, selection or expression of the parent clone due to its high affinity and good expression characteristics. The method outlined to achieve this was to select a new template clone that encoded the anti-M3G Fab with the exception of the mutated CDR3 and one that

expressed in *E. coli* but one that did not recognize the target antigen. The first round of amplifications would be carried out and the new template would be selected based on ELISA (target recognition analysis) and western blot (expression analysis).

The first round of amplifications were completed and the library was transformed into XL-1 Blue, as normal. Random clones were chosen for pick PCR and all selected clones revealed the amplified band to be the expected 1600bp.

The vector was digested as before however, the gel was run for 2 hours 30min to ensure sufficient separation of the stuffer from the cut vector thus avoiding stuffer fragment contamination. A pick PCR was carried out throughout the process, at various stages, acting as the control.

Random clones were picked and examined on western blots (figure 6.3.1.2.1), ELISA (data not shown) and further test PCR's (data not shown). The western blot confirmed the expression of a Fab fragment from clone no. 2 and the ELISA demonstrated this clones inability to bind the target through the lack of any positive signal when assayed on a plate coated with M3G-OVA. The combination of both the ELISA and western blot confirmed the presence of a non-parental anti-M3G Fab fragment expressed in clone no. 2. This was used as the new template for the construction of the mutated anti-M3G Fab library.

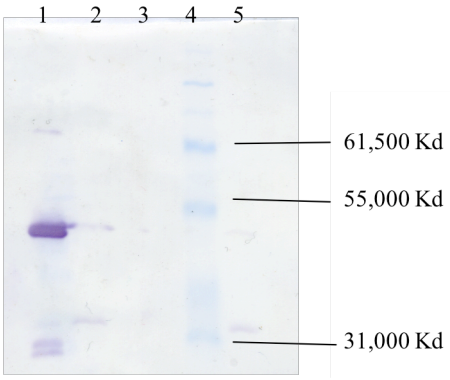

Figure 6.3.1.2.1 Western blot performed on small-scale induced clones. Binding was detected with anti-HA HRP-labelled secondary antibody. Lane 1: positive control (parent antibody), Lane 2: clone no. 7, Lane 3: clone no. 10, Lane 4: pre-stained molecular weight marker, and Lane 5: clone no. 11.

6.3.1.3 Construction of mutated library: Using clone no. 2 as template DNA in place of wild-type gene

After library construction and before panning the transformed library was examined using pick PCR and Alu 1 digest to ensure the stuffer had not contaminated the process again. All clones examined amplified bands of the correct size with no extra bands on the gels indicating that the correct Fab fragment was present. The resulting gel demonstrated that using the new template eliminated the non - specific amplification of the stuffer fragment (figure 6.3.1.3.1). Additionally, 5 random clones were picked from the library titre plates for sequencing to ensure the library was mutated in the correct regions (figure 6.3.1.3.2). The data revealed conservation of all sequences outside of the 5-codon region of the CDRH3 that was intentionally randomized via NNK doping strategies. The bio-panning strategy was then carried out with confidence that the library had been mutated successfully.

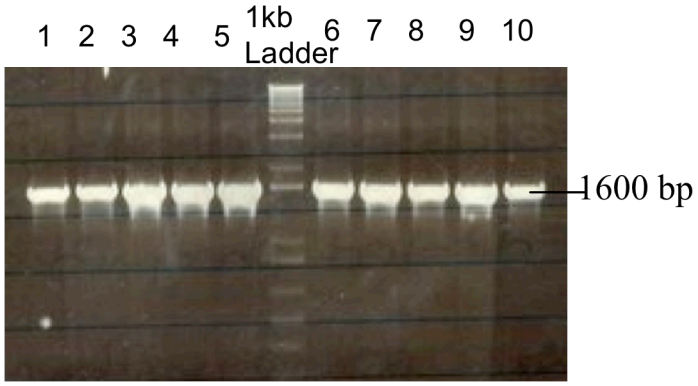

Figure 6.3.1.3.1 PCR verification of Fab insert using randomly picked clones from library transformation plates. Ompseq and gback primers were used along with standard Fab amplification PCR reaction conditions. Lanes 1-10: random clones picked from titre plates.

```
M3G-Mutated 1:
GTGCAAGATGGTCCCATGCTGTTACGTTTGACTACTGGGGTCAAGGAACCACGGTCACCG
GTGCAAGATGGTCCCAAGTGCATGTTATGGACTACTGGGGTCAAGGAACCACGGTCACCG
*************** *    *    * ********************************
M3G-Mutated 2:
GTGCAAGATGGTCCCGTGCTAATCGGTGTGACTACTGGGGTCAAGGAACCACGGTCACCG
GTGCAAGATGGTCCCAAGTGCATGTTATGGACTACTGGGGTCAAGGAACCACGGTCACCG
*************** *   **      ********************************

M3G-Mutated 3:
GTGCAAGATGGTCCTTGGGTTGGTGTAGGGACTACTGGGGTCAAGGAACCACGGTCACCG
GTGCAAGATGGTCCCAAGTGCATGTTATGGACTACTGGGGTCAAGGAACCACGGTCACCG
**************   *       ** ********************************

M3G-Mutated 4:
GTGCAAGATGGTCCGCTAATCGGGTGATGGACTACTGGGGTCAAGGAACCACGGTCACCG
GTGCAAGATGGTCCCAAGTGCATGTTATGGACTACTGGGGTCAAGGAACCACGGTCACCG
***************      *  ** ********************************

M3G-Mutated 5:
GTGCAAGATGGTCCGGGGTTGCGCGTCA-GGACTACTGGGGTCAAGGAACCACGGTCACC
GTGCAAGATGGTCCCAAGT-GCATGTTATGGACTACTGGGGTCAAGGAACCACGGTCACC
**************   ** **  ** * ********************************
```

Figure 6.3.1.3.2 The conserved regions of the CDRH3 are maintained through the use of primers M-VH1-Ran-F and M-VH1-FR3-B and are highlighted in blue. The sequence mismatches in the CDRH3 are highlighted in pink, spanning a 5 codon length of sequence. Underlining indicates those bases that are present in 4/5 of the mutated antibody.

6.3.1.4 Bio-panning

The first round of panning was carried out in accordance to protocol 10.5 in the Barbas manual after which a different panning strategy was employed based on work carried out by Lu *et al.* (2003), this strategy is outlined in table 6.3.1.4.1. The inclusion of the extra free drug incubation and washing step after the first round helped to eliminate any parental clone contamination, which would naturally exist in such a library. This panning strategy was established with the aim of pushing the selection to the limits of the wild-type anti-M3G Fab fragment. The IC50 of the parent clone (Chapter 4) was determined to be ~ 8 nM and so each successive round of selection included various concentrations and increased washing times of free M3G. The input and output titres of the panning process are given in Table 6.3.1.4.2.

Table 6.3.1.4.1 Panning strategy for selection of positive clones from the CDRH3 mutated anti-M3G Fab library. All rounds of selection were carried out in 300µl capacity immunosorbent wells and 100µl volumes are incubated at each step except during the washing steps where the wells are filled to capacity.

Parameter	Round 1	Round 2	Round 3	Round 4	Round 5
M3G-OVA conc.	9 μg/well	3μg/well	3μg/well	3μg/well	3μg/well
Input phage binding	2 hours	2 hours	1 hour	1hour	1 hour
Washes (PBST + PBS)	5 + 5	5 + 5	10 + 10	10 + 10	10 + 10
Extensive washes with M3G	0 min 0μM	15min 0.1μM	30min 0.1μM	3 hours 1μM	24 hours 1μM
Washes (PBST + PBS)	0	0	5 + 5	5 + 5	5 + 5
Trypsin elution (30 min)	10 μg/ml	10 μg/ml	10 μg/ml	10 μg/ml	10 μg/ml

Table 6.3.1.4.2 Input and output titres for all rounds of panning of the anti-M3G mutated Fab library.

	Pan 0	Pan 1	Pan 2	Pan 3	Pan 4
Input	-	3.3×10^{11}	1.9×10^{11}	2.2×10^{12}	1.0×10^{11}
Output	8.8×10^{8}	3.16×10^{6}	1.5×10^{5}	6.1×10^{5}	2.0×10^{4}

Pan 4 was the final round of selection calculated as there were no colonies on titre plates after round 5. This was mostly likely due to the stringency of the final round of selection. The next stage in the process was to assess single colonies from the panned

population. Single colonies were picked at random from rounds 3 and 4 and a monoclonal ELISA displayed zero positives from either round. This prompted the assaying of round 1-output colonies in order to determine whether or not the selection process had been so stringent as to eliminate all potential binders early on in the selection.

The monoclonal soluble expression ELISA on 2 x 96 well plates of single clones revealed a very poor result with only 4.5 % positive binders. This combined with a very low signal from the polyclonal phage ELISA caused concern. Nevertheless, each of the 5 positive clones from round 1 (P18H, P211H, P21B, P22A and P29C) were grown in 10ml cultures, induced and subjected to lysis via multiple freeze - thaw steps. A direct ELISA was carried out. However, uniform low signal was observed. Round one was examined via monoclonal phage ELISA and the result revealed a lack of M3G binders even at that early stage in the panning process.

This final result forced a re-examination of the mutagenesis strategy employed. It was possible to conclude that while the panning strategy may have been at its maximum possible stringency the presence of no target specific clones in the first round indicated that targeting the CDRH3 of the anti-M3G Fab fragment resulted in the complete loss of antigen recognition.

The CDRH3 is widely reported as being the dominant region of antigen – antibody contact. Persson *et al.* (2006) reported that anti-hapten antibodies have 5 less contact points than those antibodies raised against peptides or proteins. If this is the case, targeting the CDRH3 of the anti-M3G Fab fragment could very possibly have knocked out the entire antigen-binding site. This implied that this particular Fab relies very heavily on the CDRH3 and alternative regions of the antibody should be targeted for *in vitro* affinity maturation. Furthermore, Daugherty *et al.* (2000) commented on the lower tolerance of an antibody to mutation directly in the binding site. It is possible that similar conclusions may be drawn here in this work. The wild type has come from a monoclonal antibody, which is of relatively high affinity and would have undergone functional optimisation *in vivo*. It was also reported that the majority of the affinity

improving mutations in the scFv were residues located at a certain distance from the antigen-binding site (Daugherty *et al.,* 2000).

Spiking of the wildtype Fab fragment into this mutant library could act as an additional control for the assessment of the panning stringency. Without this "wild-type spiking", the severe stringency of the panning strategy must also be considered as an influencing factor in loss of binding of the polyclonal library population.

A new approach was adopted. This focused on CDR's / residues that are not directly involved with the antigen point of contact and instead they may play a role in the rigidity of the structure. Initially, the most logical option was mutating the CDRH3, as this is the CDR primarily involved in antigen contact. Zimmerman *et al.* (2006) reported that while increasing the affinity of an antibody, through restricting its conformation to fit the antigen, such as in somatic evolution, has yielded high affinity and high expressing antibodies it has not yet been optimised. In this strategy for mutating the anti –M3G Fab antibody the CDR3 of the heavy chain was to be retained as wild-type, while the CDR1 of the heavy chain and the CDR2 and CDR3 of the light chain were mutated, using similar NNK doping strategies to those described earlier in this chapter.

6.3.2 Mutagenesis strategy 2: site directed mutagenesis - Kunkel style

Kunkle (1985) proposed a method of site directed mutagenesis, which eliminated the use of PCR and resulted in greater transformation efficiency, and the method was used successfully for mutating anti-peptide antibodies (Sidhu *et al.,* 2000). It was proposed that improvements in affinities of anti-hapten antibodies may be mediated by changes in the rigidity of the antibodies structure and not by the formation of new antigen contact points (Zimmermann *et al.,* 2006). It is possible that focused mutagenesis on CDR's other than the primary point of contact, the CDRH3, will have a beneficial effect on the anti-M3G Fab. Zimmermann (2006) reported on mutations, that pushed the antibody into a single conformation fitting tightly around the antigen compared to the looser wild type conformation.

While the CDRH2 is important in antigen recognition (Persson *et al.,* 2006), the sheer length of this CDR made it unattractive as a target in this case. Persson and coworkers had access to extensive modeling facilities which allowed them to focus on particular residues within the lengthy CDR. The majority of academic laboratories do not have access to such facilities. It was therefore, decided not to include the CDRH2 in this study. In that same study carried out by Persson *et al.* (2006), the CDRH1 was targeted for the construction of a focused anti-hapten library and it was both feasible and desirable to include it here also. CDRL2 rarely contributes towards antigen binding (Wilson and Stanfield. 1994), however, based on findings by Zimmerman *et al.* (2006) it is probable that the CDRL2 located in the periphery, would have potential in altering the affinity of the antibody. Improvements may be seen by changing the overall rigidity of the antibody and stabilizing the antigen-binding site. Alternative mutagenesis strategies outlined by Daugherty *et al.* (2000), reported that affinity improving amino acid substitutions were not found in regions that came in direct contact with the target but instead they were located in peripheral CDR's and also in framework residues. In this study the framework regions were considered to be important to the structural integrity of the antibody and therefore, they would not be mutated.

It was highlighted in the first section of this chapter that targeting the CDRH3 may have proved to be too severe with respect to engineering this antibody. It indicated that the central combining site was already highly evolved. Hence it was decided that the CDRL3 would be targeted in this second strategy. However as it may also be heavily evolved with the potential to knock out antigen recognition entirely it was included in the strategy but not forced to mutate as with the CDRH3 CDR walking method. Of the three CDR's that were targeted only the CDRL2 was first mutated to a "stop" coding mutant (section 6.3.2.3). This provided a control on the severity with which the highly evolved CDR's such as CDRL3 would be mutated. While mutations in the CDRL2 would be required in order to achieve functional antibodies from the library, mutations in the CDRL3 and CDRH1 would only be retained if they were improvements or at

minimum null mutations. Any mutations in these regions that were detrimental to the antibodies activity would then be lost in the selection process.
With this in mind primers were designed to target CDRH1, CDRL2 and CDRL3.

6.3.2.1 Primer design

In the CDR walking strategy (section 6.3.1) parental DNA contamination was eliminated via selection of a non-wild type template. This was achieved by:

a) Early sequencing and selection of a non-wild type gene for library template.
b) Confirmation of protein expression via western blot analysis.
c) Confirmation of the lack of target recognition via ELISA analysis.

The approach taken in this second strategy to wild type elimination was the construction of a stop mutant template. Based on the CDR sequences obtained for the anti-M3G Fab fragment (figure 6.3.2.1.1) oligonucleotides encoding stops (TAA) in place of the functional codons in each of the targeted CDR's were designed (Table 6.3.2.1.1). The anti-M3G antibody was originally derived by phage display and expresses very well in *E. coli.* Without a stop-mutant template wild type carryover can outgrow and dominate selections (Yang *et al.,* 1995 and Lee *et al.,* 2004).
The mutating oligonucleotides were designed to incorporate full-length CDR mutations in the CDRL3, CDRL2 and CDRH1. The CDRL2 and L3 were 7 codons and 9 codons, respectively, in length and the CDRH1 was 5 codons in length (figure 6.3.2.1.1). It was essential for the success of this strategy that the correct strand of dsDNA was packaged. Since M13 packages only lead strand DNA it was necessary to confirm that the lead strand in the pComb3x vector was indeed the forward strand and so two sets of primers were designed for each step (a forward and a reverse primer) (Table 6.3.2.1.1).

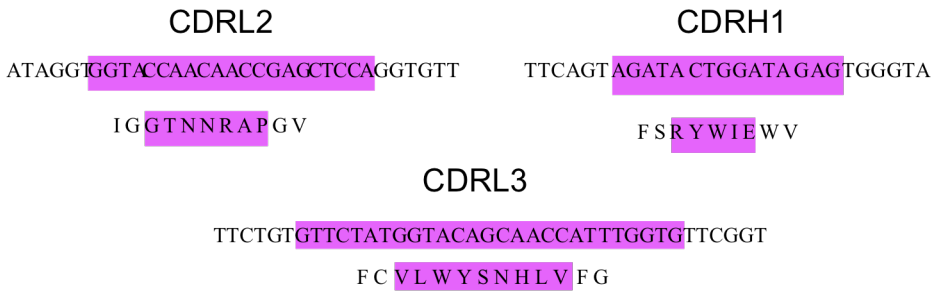

Figure 6.3.2.1.1 Sequence analysis of the antibody binding regions CDRL2, L3 and CDRH1 of the wild type anti-M3G Fab fragment. CDRL2 and CDRL3 contain 7 and 9 codons, respectively, while the CDRH1 is formed by 5 codons. CDR's are highlighted in purple with framework regions flanking each.

Table 6.3.2.1.1 Primers designed for Kunkel style mutagenesis strategy focused on CDRL2, CDRL3 and CDRH1. Forward stand and reverse strand primers were synthesized in order to confirm lead strand on the vector. Stop oligonucleotides were designed to eliminate wild type antibody contamination.

Primer name	Primer sequence
CDRH1-Fstop	ACTGGCTACACATTCAGTTAATAATAATAATAATGGGTAAAGCAGAGGCCT
CDRH1-Rstop	AGGCCTCTGCTTTACCCAATTATTATTATTATTACTGAATGTGTAGCCAGT
CDRL2-Fstop	TTCACTGGTCTAATAGGTTAATAATAATAATAATAATAAGGTGTTCCTGCCAGATTC
CDRL2-Rstop	GAATCTGGCAGGAACACCATTATTATTATTATTATTATTACCTATTAGACCAGTGAA
CDRH1-Fmut	ACTGGCTACACATTCAGTNNSNNSNNSNNSNNSTGGGTAAAGCAGAGGCCT
CDRH1-Rmut	AGGCCTCTGCTTTACCCASNNSNNSNNSNNSNNACTGAATGTGTAGCCAGT
CDRL2-Fmut	TTCACTGGTCTAATAGGTNNSNNSNNSNNSNNSGCTCCAGGTGTTCCTGCC
CDRL2-Fmut	GGTCTAATAGGTGGTACCNNSNNSNNSNNSNNSGGTGTTCCTGCCAGATTC
CDRL2-Rmut	GAATCTGGCAGGAACACCSNNSNNSNNSNNSNNGGTACCACCTATTAGACC
CDRL2-Rmut	GGCAGGAACACCTGGAGCSNNSNNSNNSNNSNNACCTATTAGACCAGTGAA
CDRL3-Fmut	TTCTGTCTTCTATGGTACNNSNNSNNSNNSNNSTTCGGTGGAGGAACCAAA
CDRL3-Fmut	GAGGCAATATATTTCTGTNNSNNSNNSNNSNNSAACCATTTGGTGTTCGGT
CDRL3-Rmut	TTTGGTTCCTCCACCGAASNNSNNSNNSNNSNNGTACCATAGAAGACAGAA
CDRL3-Rmut	ACCGAACACCAAATGGTTSNNSNNSNNSNNSNNACAGAAATATATTGCCTC

6.3.2.2 Strategy overview

This strategy utilises an *ung* $^{-}$ *E. coli* strain CJ236 which was obtained from NEB. Its genotype is listed as:

FΔ(HindIII)::cat (Tra+ Pil+ CamR)/ ung-1 relA1 dut-1 thi-1 spoT1 mcrA

Upon addition of uracil to the overnight growth culture, this *ung*- strain allows uricil to exist instead of thymine in plasmid DNA. This permits the accurate mutatgenesis of the lead strand and the generation of heteroduplex CCC-DNA, as illustrated schematically in figure 6.3.2.2.1. However, when the plasmid is transformed into a non-suppressor *ung*$^{+}$ strain of *E. coli* the dU-ssDNA is destroyed and only the mutated lead strand ssDNA is replicated. The resulting mutated plasmid was then subjected to numerous rounds of selection to pull out the optimal mutant clone.

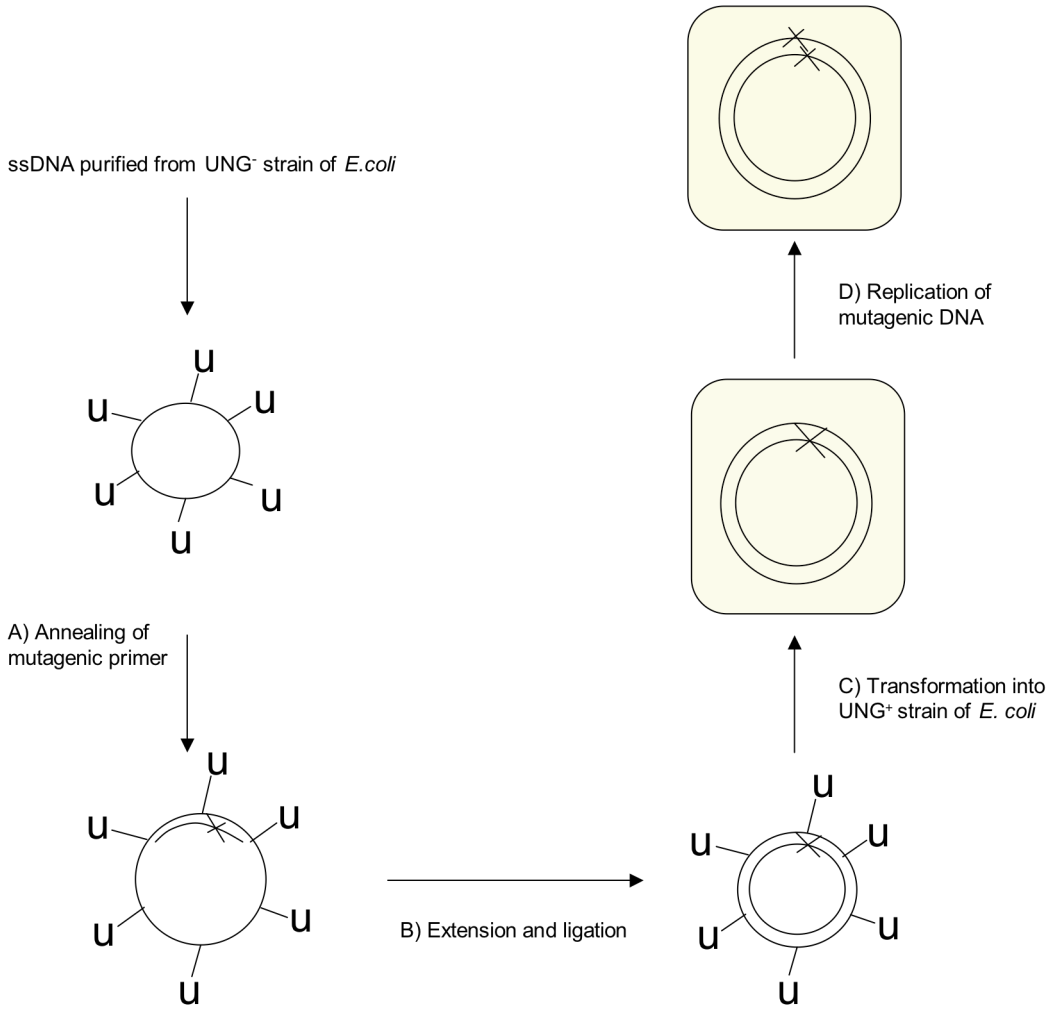

Figure 6.3.2.2.1 Kunkle-style strategy: The phagemid replicates, in the ung$^-$ *E. coli* host, as double – stranded plasmid. On co-infection with a helper phage (M13 in this case), single – stranded DNA replication is initiated and the phagemid ssDNA is preferentially packaged into the phage particles. This ssDNA is purified from phage, allowing production of large quantities of ssUracil-DNA which can be mutated using complimentary oligos, containing randomised codons. Filling in the rest of the complementary strand using T7 or T4 polymerase creates covalently-closed circular DNA When heteroduplex CCC-DNA is introduced into an ung$^+$ strain, the dU-ssDNA strand is preferentially destroyed and the synthetic strand is replicated.

6.3.2.3 Generation of stop mutant genetic template

CDRL2 was used to generate the stop mutant to be used as the genetic template for mutant library construction in place of the wild type clone. The individual stages in this strategy are outlined in section 2.11.2 – 2.11.3.4. Figure 6.3.2.3.1 illustrates the conversion of purified dU – ssDNA to CCC-DNA incorporating the uricil containing strand and the stop mutant lead strand. Confirmation that the lead strand is in fact the forward strand was achieved via sequence analysis (figure 6.3.2.3.2). Only the forward strand had the "stop" codons substituted into the replicated strand while the reverse strand remained as wild type.

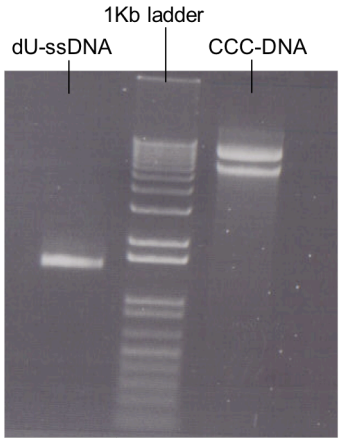

Figure 6.3.2.3.1 The complete conversion of ssDNA to CCC-DNA is demonstrated in this gel. Lane 1: the dU-ssDNA runs at ~1200bp. Lane 2: 1Kb ladder. Lane 3: the covalently closed circular DNA runs alongside the top of the ladder. An exact size is unattainable as the DNA is running as circular.

Wild Type anti – M3G Fab light chain:

A V V T Q E S A L T T S P G E T V T L T C R S S T G A V T T S N Y A N W V Q E K P D H L F T G
L I G **G T N N R A P** G V P A R F S G S L I G D K A A L T I T G A Q T E D E A I Y F C V L W Y S
N H L V F G G G T K L T V L G Q P K

Wild Type anti – M3G Fab heavy chain:

E V Q L Q E S G A E L **M** K P G A S V K I S C K A T G Y T F S R Y W I E W V K Q R P G H G L E
W I G E I L P G S G S T K Y N E K F K G R A T F T A D T S S N T V Y **M** Q L S S L T S E D S A V
Y H C A R W S Q V H V **M** D Y W G Q G T T V T V S S A S

Forward mutant 2; light chain:

A V V T Q E S A L T T S P G E T V T L T C R S S T G A V T T S N Y A N W V Q E K P D H L F T G
L I G **S S S S S S S** G V P A R F S G S L I G D K A A L T I T G A Q T E D E A I Y F C V L W Y S N
H L V F G G G T K L T V L G Q P K

Forward mutant 2; heavy chain:

E V Q L Q E S G A E L **M** K P G A S V K I S C K A T G Y T F S R Y W I E W V K Q R P G H G L E
W I G E I L P G S G S T K Y N E K F K G R A T F T A D T S S N T V Y **M** Q L S S L T S E D S A V
Y H C A R W S Q V H V **M** D Y W G Q G T T V T V S S A S

Reverse mutant 4; light chain:

A V V T Q E S A L T T S P G E T V T L T C R S S T G A V T T S N Y A N W V Q E K P D H L F T G
L I G **G T N N R A P** G V P A R F S G S L I G D K A A L T I T G A Q T E D E A I Y F C V L W Y S
N H L V F G G G T K L T V L G Q P K

Reverse mutant 4; heavy chain:

E V Q L Q E S G A E L **M** K P G A S V K I S C K A T G Y T F S R Y W I E W V K Q R P G H G L E
W I G E I L P G S G S T K Y N E K F K G R A T F T A D T S S N T V Y **M** Q L S S L T S E D S A V
Y H C A R W S Q V H V **M** D Y W G Q G T T V T V S S A S

Figure 6.3.2.3.2 Sequence analysis of random clones picked from transformation plates. Heavy chain CDR's are highlighted in blue, light chain CDR's are highlighted in pink and mutated sections are underlined (bold). The wild type (wt) is included as it is illustrative of the comparison between the mutated sequences and the original unaltered sequence. The forward mutant shows the mutated region in CDRL2 which is completely mutated with 7 stop codons (S). The reverse mutant illustrates no mutations in the CDRL2 as it is NOT the lead strand and was not packaged by the M13.

6.3.2.4 Generation of small scale CDRL2 mutant library.

Once the first set of CDRL2 primer reactions were performed random clones were sent for sequencing to confirm the replacement of stop codons for sense codons using the mutagenic primers (figure 6.3.2.4.1). The results demonstrated the requirement to eliminate the possibility of wild-type carry over in the construction of a mutated antibody library. It can be clearly seen (below) that one of the clones sequenced, CDRL2-P1C has retained the stop codons in the CDR and was not effected by the mutagenic primers. This indicated how the final library would contain a percentage of this type of sequence. The consequence of this inclusion in the library would have been significant if the wild type had not been eliminated by the generation of a stop template instead. This is especially important in a case like this one where the wild-type is a very strong expresser with a high affinity for the target and could potentially take over the selection process. Figure 6.3.2.4.1. also illustrates the diversity seen from two of the other clones sequenced.

```
                                          CDRL1
CDRL2_P2B         AVVTQESALTTSPGETVTLTCRSSTGAVTTSNYANWVQEKPDHLFT
WILDTYPE_STOP     AVVTQESALTTSPGETVTLTCRSSTGAVTTSNYANWVQEKPDHLFT
CDRL2_P2C         AVVTQESALTTSPGETVTLTCRSSTGAVTTSNYANWVQEKPDHLFT
CDRL2_P1C         AVVTQESALTTSPGETVTLTCRSSTGAVTTSNYANWVQEKPDHLFT
                  ********************************************

                     CDRL2                                    CDRL3
CDRL2_P2B        GLIGVNGNSAPGVPARFSGSLIGDKAALTITGAQTEDEAIYFCVLWYSNHLVFGGG
WILDTYPE_STOP    GLIGSSSSSSSGVPARFSGSLIGDKAALTITGAQTEDEAIYFCVLWYSNHLVFGGG
CDRL2_P2C        GLIGTRKALAPGVPARFSGSLIGDKAALTITGAQTEDEAIYFCVLWYSNHLVFGGG
CDRL2_P1C        GLIGSSSSSSSGVPARFSGSLIGDKAALTITGAQTEDEAIYFCVLWYSNHLVFGGG
                 ****     :.******************************************
```

Figure 6.3.2.4.1 T-coffee alignment of 3 random clones from the small scale mutagenesis of the CDRL2 and the wild type stop template. The mutated CDR of clone P1C is highlighted in green, all other mutated CDR's are highlighted in pink and the unchanged are highlighted in blue. The retention of the stop codons in clone P1C shown here is illustrative of the impact of wild-type carry-through in a library.

6.3.2.5 Sequence analysis of final large scale library.

It is possible to generate large libraries using the library construction method outlined in section 6.3.2.2 (Sidhu *et al.,* 2000) and this is one of the reasons that made it an attractive technique. In order to sample the diversity created by a mutagenesis strategy such as the one outlined here it was important to create a large enough library to incorporate the number of codons targeted. The method outlined here may at first glance appear to use the mutation in parallel theory, as discussed previously (section 6.1.1.4), a theory that is not ideal given the additive affects of mutating multiple CDR's. However, when the displacement activity of the polymerase is taken into account it becomes apparent that the strategy may actually be biased towards targeting one, two or all three CDR's. This is illustrate in figure 6.3.2.5.1, where in just five clones analyzed clone no.5 was mutated in CDRL2 and CDRH1 but CDRL3 remains unchanged by the mutating primer.

The large scale library was constructed so as to include mutagenic regions in CDRH1, CDRL2 and CDRL3. Figure 6.3.2.5.1 illustrates the sequence analysis of the library population prior to biobanning. These sequences confirm the vast diversity that was introduced into the targeted regions.

Light chain alignment:

```
clone_1   AVVTQESALTTSPGETVTLTCRSSTGAVTTSNYANWVQEKPDHLFTGLIGGTAFAARGVP
clone_3   AVVTQESALTTSPGETVTLTCRSSTGAVTTSNYANWVQEKPDHLFTGLIGLVFLGAPGVP
wildtype  AVVTQESALTTSPGETVTLTCRSSTGAVTTSNYANWVQEKPDHLFTGLIGGTNNRAPGVP
clone_5   AVVTQESALTTSPGETVTLTCRSSTGAVTTSNYANWVQEKPDHLFTGLIGGTESLSLGVP
          ************************************************     ***

clone_1    ARFSGSLIGDKAALTITGAQTEDEAIYFCGALSRNHLVFGGG
clone_3    ARFSGSLIGDKAALTITGAQTEDEAIYFCGQRELSNNVFGGG
wildtype   ARFSGSLIGDKAALTITGAQTEDEAIYFCVLWYSNHLVFGGG
clone_5    ARFSGSLIGDKAALTITGAQTEEEAIYFCVLWYSNHLVFGGG
           **********************:******     ********
```

Heavy chain alignment:

```
clone_5   EVQLQESGAELMKPGASVKISCKATGYTFSRVRWRWVKQRPGHGLEWIGEILPGSGSTKY
wildtype  EVQLQESGAELMKPGASVKISCKATGYTFSRYWIEWVKQRPGHGLEWIGEILPGSGSTKY
clone_1   EVQLQESGAELMKPGASVKISCKATGYTFSRRGSLWVKQRPGHGLEWIGEILPGSGSTKY
clone_3   EVQLQESGAELMKPGASVKISCKATGYTFSGGARMWVKQRPGHGLEWIGEILPGSGSTKY
          ****************************     ************************

clone_5   NEKFKGRATFTADTSSNTVYMQLSSLTSEDSAVYHCARWSQVHVMDYWGQG
wildtype  NEKFKGRATFTADTSSNTVYMQLSSLTSEDSAVYHCARWSQVHVMDYWGQG
clone_1   NEKFKGRATFTADTSSNTVYMQLSSLTSEDSAVYHCARWSQVHVMDYWGQG
clone_3   NEKFKGRATFTADTSSNTVYMQLSSLTSEDSAVYHCARWSQVHVMDYWGQG
          **************************************************
```

Figure 6.3.2.5.1 Sequence analysis of random clones picked from the transformation plates of the large scale library prior to panning. Mutated CDR's are highlighted in pink and unaltered CDR's are highlighted in blue. The wild type (wt) is included as it is illustrative of the comparison between the mutated sequences and the unaltered sequence.

6.3.2.6 Biopanning

The panning strategy was carried out in general accordance to section 6.3.1.4, with the exception that an immunotube was used in the first and second round of panning, only switching to an immunosorbent well for the third and final rounds. We were unable to generate the optimal large library and a library size of 2×10^7 was achieved. Very large libraries are not generally achieved in academic laboratory environments and this type of mutagenesis strategy in particular has not been attempted in laboratories outside of large institutes such as Genentech (Sidhu *et al.,* 2000) and the Scripps Institute. In order to sample the entirety of this moderately sized library we were required to calculate the desired inoculum volume needed for infection to facilitate the display of the maximum diversity that the library could offer in the selection process. This was determined based on the cell density of the initial transformed library stocks, which allowed the calculation of the amount of cells and therefore volume of that stock required to over-represent the theoretical diversity of the library 10-fold. Even where large libraries have been constructed it is not often that the entire diversity is sampled in the biopanning process. Despite the moderate size of the library used in this study, ever effort was made to ensure maximum possible display of its diversity, although it must be taken into account that targeting 3 CDR's and with a total combined length of 21 codons would require a library size of $>1 \times 10^{30}$. The input and output titres of the panning process are outlined in Table 6.3.2.6.1.

Table 6.3.2.6.1 Input and output titres for all rounds of panning for anti-M3G mutated Fab library.

	Pan 0	**Pan 1**	**Pan 2**	**Pan 3**	**Pan 4**
Input	-	2.5×10^{11}	7.2×10^{11}	3.2×10^{11}	1.9×10^{12}
Output	1×10^7	5×10^5	1.5×10^5	1.2×10^4	4.9×10^5

6.3.2.7 Single clone analysis of the panned library

Single colonies from Pan 4 output plates were grown and induced in small scale in microtitre wells. Two 96-well plates were seeded and used for single clone direct ELISA analysis on plates coated with 5µg/ml free M3G (figure 6.3.2.7.1(a) and (b)). Five clones demonstrated absorbance above 0.2. This was above the background signal of approximately 0.1, as determined by a control well demonstrating binding between the bound M3G-OVA and an anti-amphetamine Fab fragment. There were 6 clones, which expressed antibody that resulted in a high signal; P1C5, P1G4, P1H12, P2C2, P2C3 and P2E7. The maximum signal observed was that of P2C3 at >0.9. The same set of clones were then carried forward for a "single concentration" competition ELISA using 5µg/ml competing free M3G concentration across all wells (figure 6.3.2.7.2 (a) and (b)). Total background signal remained <0.1 while each of the 6 clones showed competitive inhibition with free M3G. It was concluded at this point that a number of clones (six) were expressing at a good rate and also demonstrated good inhibition when incubated with free M3G at the relatively high concentration of 5µg/ml.

Each of the positive binders was grown up in 10ml cultures, induced and an expression titre was carried out to investigate each clone for false positives and expression characteristics (figure 6.3.2.7.3). Five of the 8 clones examined proved to be false positives and three, P1C5, P2E7 and P2C3, were carried on for further analysis.

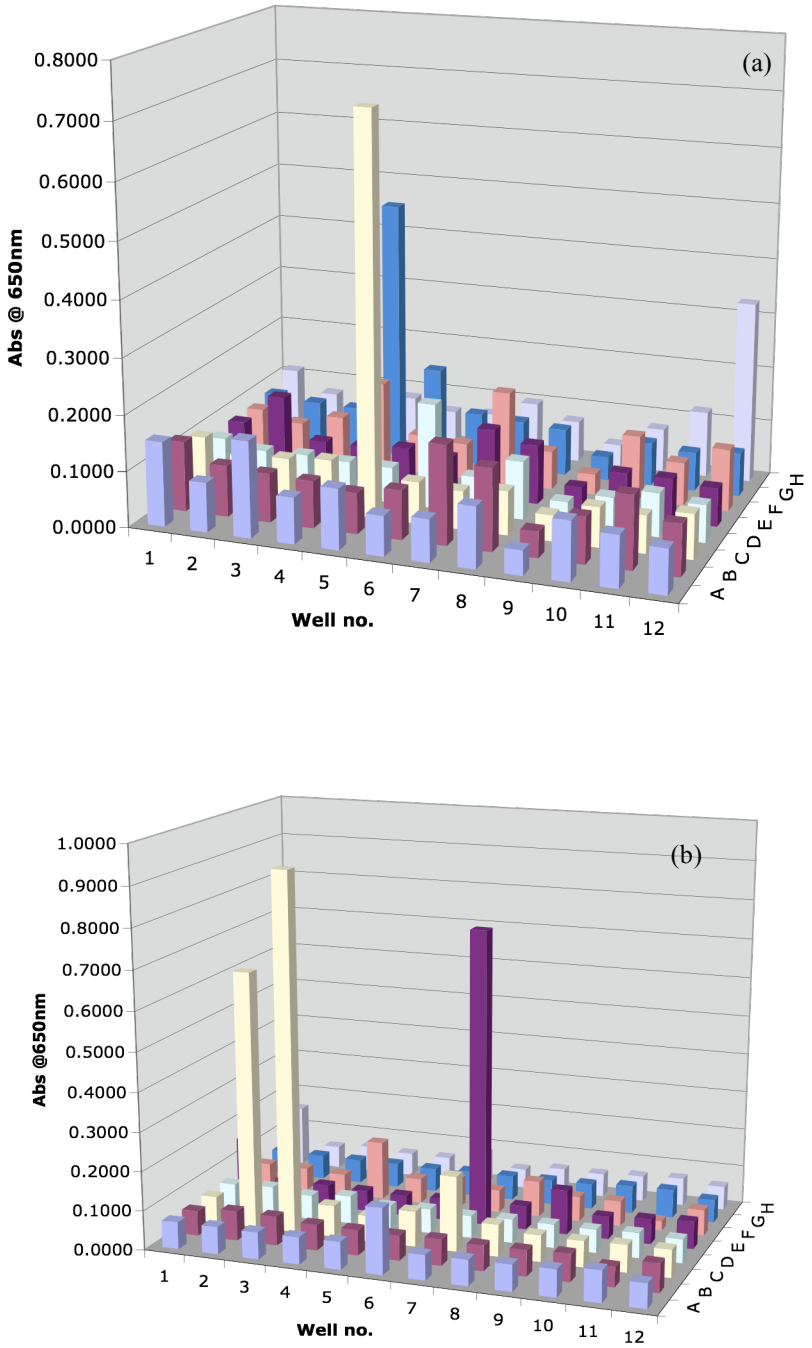

Figure 6.3.2.7.1 (a) and (b) represent the single clone (pan 4) soluble expression ELISA performed on M3G-OVA-coated wells. Data was expressed as absorbance (Abs).

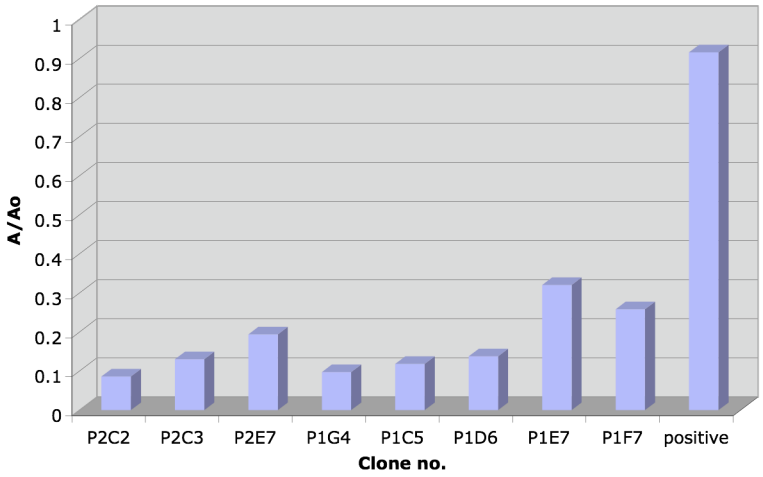

Figure 6.3.2.7.2 Inhibition ELISA assay performed on M3G-OVA-coated wells. Data was expressed as absorbance.

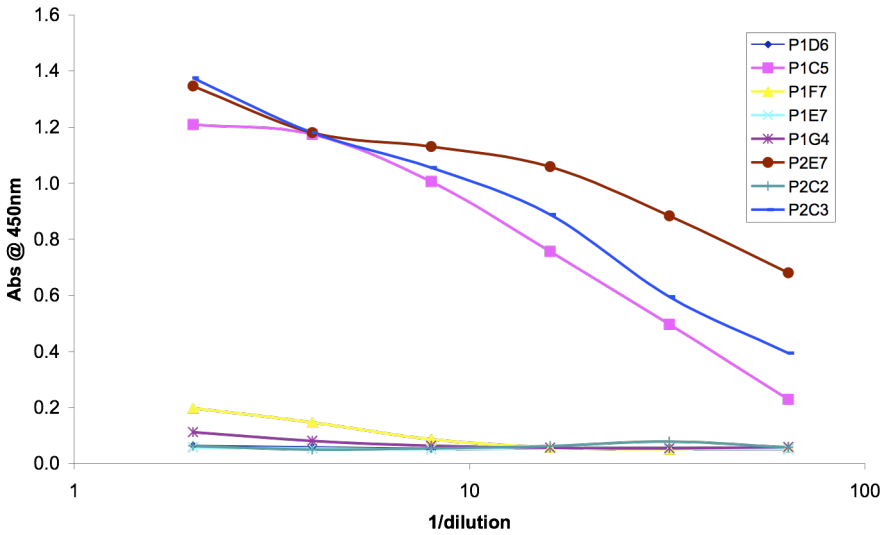

Figure 6.3.2.7.3 Direct ELISA performed on M3G-OVA-coated wells performed to calculate the titre of the P2C3 Fab fragment. Data was expressed as absorbance.

6.3.2.8 Characterisation of positive clones

A pick PCR was carried out in order to confirm the presence of a 1600 bp band using the standard Fab amplification primers (Chapter 3). A clean 1600 bp band was amplified from P2C3. However, there was no correct fragment size amplified from the P1C5 plasmid and there were multiple bands amplified along with the 1600bp band from the P2E7 plasmid. Hence, it was decided that while all three clones would be sent for sequencing (figure 6.3.2.8.1), only P2C3, would be further characterised, expressed and purified on a larger scale.

The sequence results for the three clones were of mixed quality and only P2C3 could be interpreted with any success. The poor sequence quality of the clones was confirmed with the mixed amplification pattern (data not shown) and as such the sequence quality was not queried. It can be concluded that the positive clones, other than P2C3, contained contaminating DNA and did not contain pure anti-M3G fab fragment genetic material.

The sequence analysis of the clone P2C3 revealed that two amino acids had been mutated compared to the wild type anti-M3G Fab fragment. These two amino acids are located in the CDR2 of the light chain (figure 6.3.2.8.1). Two asparagines are located at position 2 and 3 of the 7-base CDRL2 in the wild-type, these have been mutated to an electrically charged arginine followed by a hydrophobic glycine in the mutated gene. The substitution of the charged amino acid here clearly has an influence on the on-rate (Ka) of the antibody. However, the full impact of this change, albeit minor, could not be investigated without being able to put an exact value on the Ka. The fact that the change in on-rate appears to be very small, when visually examined, and that the mutant and wild type exhibit similar affinity would indicate that there has not been a significant impact on the characteristics of the antibody as a result of the amino acid changes.

The DNA sequence (figure 6.3.2.8.2) reveals the presence of 7 base substitutions, which translate to only two amino acid substitutions. The remaining base changes have an insignificant effect on protein folding. The actual pre-panned library carried extensive

and complete mutation of the targeted CDR's (figure 6.3.2.5.1) so the fact that the best clone post-panning revealed the presence of only 2 amino acid substitutions is strongly indicative that the wild-type Fab has already achieved its maximum sensitivity. It is possible that the mutations observed here are merely tolerated by the antibody fragment rather than enhancing the affinity.

In direct ELISA, the His-purified and concentrated (to 500µl final volume) antibody preparations provided a titre of 1/25,600 (figure 6.3.2.8.3). ELISA conditions for each antibody were optimised (data not shown). At an optimal antibody dilution of 1/6400, the Fab was shown to have a detection range of ~ 4 ng/ml (figure 6.3.2.8.4) very similar to that of the wild type Fab fragment (~ 3 ng/ml) (chapter 3).

An inhibition assay, based on similar conditions as set out in section 3.3.3.2, was set up on the Biacore. The linear range of detection of both wild type and mutant Fab fragments were very similar and comparable to the ELISA results (data not shown). Kinetic off rate analysis revealed very similar off rates for both Fab's with the wild-type showing a dissociation rate of 4.7×10^{-2} and the mutant Fab showing a dissociation rate of 2.9×10^{-2} (figure 6.3.2.8.5).

Light chain:

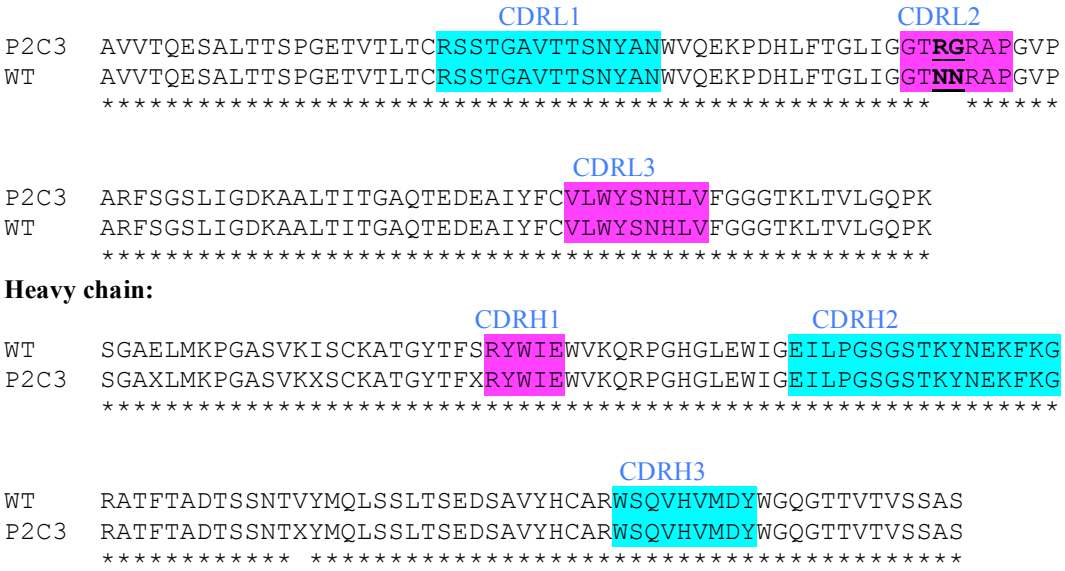

Heavy chain:

Figure 6.3.2.8.1 Protein equence analysis of clone P2C3, obtained through 4 rounds of panning. Mutated CDR's are highlighted in pink and unaltered CDR's are highlighted in blue. Changes in the mutated P2C3 are in bold and underlined in CDRL2. The wild type (wt) is included for comparison between the mutated sequences and the unaltered sequence.

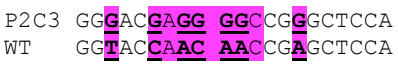

Figure 6.3.2.8.2 DNA sequence analysis of the CDRL2, with 7 base substitutions in total.

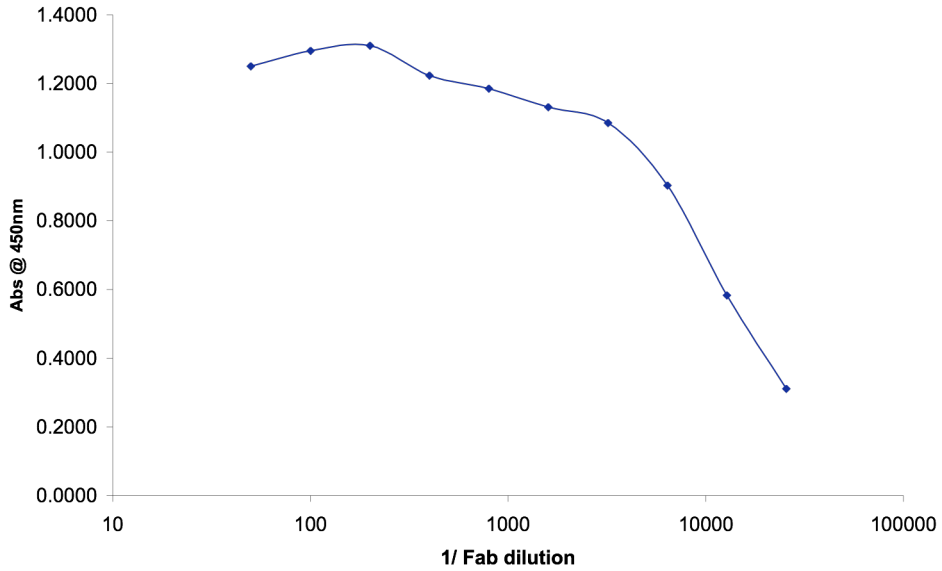

Figure 6.3.2.8.3 Direct ELISA performed on M3G-OVA coated wells performed to calculate the titre of the P2C3 Fab fragment. Data was expressed as absorbance.

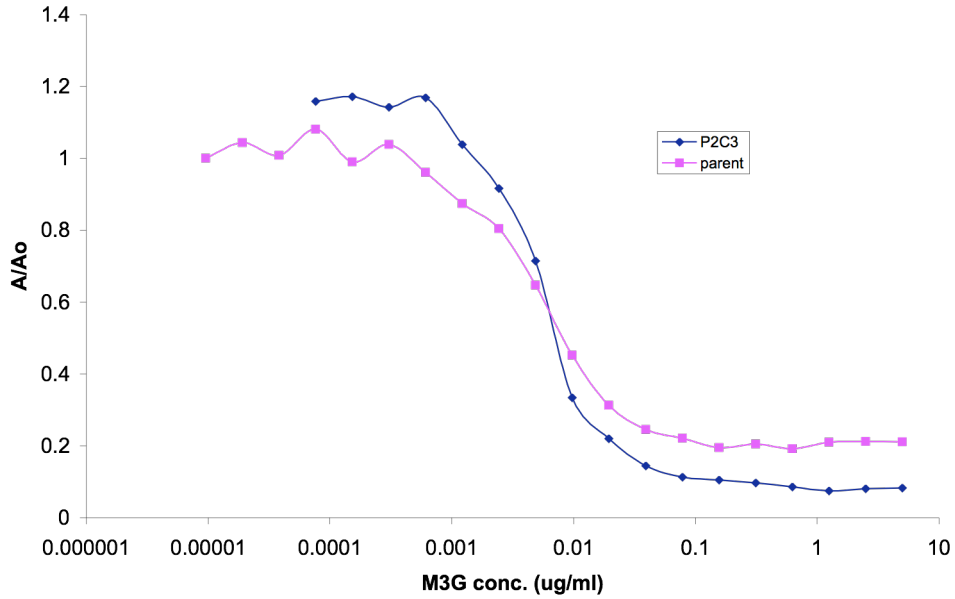

Figure 6.3.2.8.4 ELISA inhibition assay performed on M3G-OVA-coated wells comparing wild-type Fab (pink) and P2C3 Fab (blue) binding response versus competing free M3G concentration. Concentration range of 610 – 5,000,000 pg/ml) Data is expressed as A/Ao (i.e. the signal at different free analyte concentrations are expressed as a proportion of signal in the presence of no competing analyte).

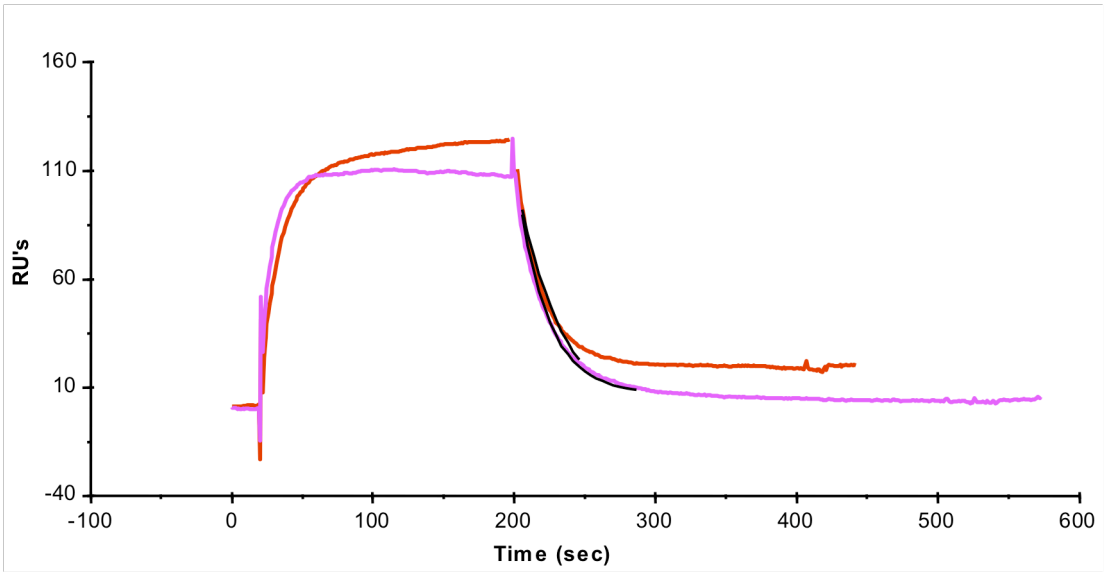

Figure 6.3.2.8.6 Representative sensogram demonstrating the slight difference between wt Fab (pink) and the mutated Fab (red) binding response under normal assay conditions described previously. On-line reference subtraction was performed against a flow-cell coated with OVA.

6.4 Conclusion

This chapter focused on the construction of two alternative mutagenesis libraries. The first attempt used a CDR walking approach based on methods outlined in Barbas *et al.* (2001). This strategy focused on the CDR3 of the heavy chain, a region of the antibody regarded as the primary point of contact with the antigen. The method resulted in total loss of antigen recognition. It is possible that the CDRH3 may have been heavily evolved and ultimately too critical to the function of the anti-M3G Fab to be targeted for mutagenesis, however, it is also acknowledged that panning stringency could also be a factor. A second strategy was designed based on a method outlined in Sidhu *et al.* (2000) which eliminated the use of PCR and focused on CDR2 and 3 of the light chain and CDR1 of the heavy chain of the anti – M3G Fab fragment. The CDR's targeted in this technique are generally thought to be involved in stabilising the antigen binding site (section 6.3.2) and possibly influencing the rigidity of the antibody structure, which may be more appropriate to anti-hapten antibody affinity maturations.

The resultant mutated library was successful in retaining target (M3G) recognition as a polyclonal population. Sequence analysis revealed that the antibody structure was tolerant to two amino-acid substitutions in the CDRL2 and that the other CDR's retained the wild type sequence. This result strongly suggested that the wild-type had the optimal sequence, and, given that it has already undergone functional mutation *in vivo* since it came from a monoclonal parent structure, this would hold true.

There is tremendous scope for future work here. The effects of the substitution of further charged amino acids into the peripheral CDR's would be very interesting with regard to examining 'off-rate' changes in the anti-M3G Fab fragment. Given that the small change in 'on-rate' seen in figure 6.3.2.8.6 has clearly had some impact on the dissociation rate, one could hypothesise that substitution of more charged amino acids may result in significantly slowing down the 'off-rate' and, therefore, improving the affinity of the Fab fragment.

We have clearly demonstrated the value of this anti-hapten engineering strategy. The anti-M3G antibody was already highly characterised and as such provided an ideal template for this work. While the strategy did not result in a significantly improved antibody binding site, it did result in a new antibody fragment that retains binding of the target molecule and more importantly demonstrates excellent expression and inhibition characteristics (section 6.3.2.8). Scope is provided for more focused mutagenesis involving specific residues with potential to achieve improved binding. In earlier chapters important discoveries were made regarding the choice of recombinant structure to use (scFv / Fab). In this chapter, important discoveries were made regarding the improvement of anti-hapten antibodies. These include, the significance of the CDRH3 in an antibody raised against a hapten which does not possess multiple binding sites and the significance of not forcing multiple mutations in parallel but instead creating bias for one CDR via the stop mutant strategy laid out in section 6.3.2.3, and further discussed in section 6.3.2.5.

The optimised mutagenesis strategies outlined throughout this chapter have significant potential for use for improvement of the lower affinity anti-amphetamine Fab fragment. In addition, the anti-THC scFv fragment, that was not cloned from a monoclonal but instead selected from a leporine immune library, could benefit enormously from such *in-vitro* maturation techniques.

Chapter 7
7.0 Overall Conclusions

7.1 Overall Conlcusions

The research in this thesis describes the succcessful production and characterisation of novel genetically-derived antibody fragments to morphine-3-glucuronide (M3G), amphetamine and tetrahydrocannibinol, their structural modification, *in-vitro* mutagenesis and application in a multi-analyte assay.

Chapter 3 focused on the production and characterisation of a genetically derived Fab fragment specific to amphetamine. A previously described anti-amphetamine antibody-secreting hybridoma was the source of the cDNA used to isolate the DNA encoding the antibodies variable heavy and variable light chains. The constant heavy and constant light chains were cloned from the pComb3xTT vector. The anti-amphetamine Fab fragment was successfully used in the development of a Biacore inhibition assay and the Fab fragment demonstrated superior sensitivity to that of the parent IgG molecule. Under optimised conditions the Fab demonstrated an IC50 of 200 ng/ml compared to an IC50 of ~ 600 ng/ml for the monoclonal antibody. The purified antibody provided excellent titres with working dilutions in the range of 1 in 2000 when purified from a 500ml culture volume, further increasing its superiority over the IgG, where lower concentrations of antibody were obtained following purification. The second part of this chapter described the potential of producing an anti-amphetamine scFv fragment by similar means. Several attempts were made but no specific scFv was isolated. It is probable that the antibody encoded in the parent IgG was heavily reliant on the stabilising nature of the whole IgG structure. The Fab fragment, with the presence of the human constant chains, was able to retain and in fact improve the affinity while the 'floppy' nature of the scFv molecule was not capable of retaining the critical cavity shaped binding epitope common to anti-hapten antibodies.

In chapter 4 the prodruction of an anti-M3G Fab fragment via the structural conversion of an anti-M3G scFv was described. The genes encoding the variable regions were amplified from the scFv fragment and the human constant regions for the Fab were

amplifed from the pComb3xTT vector, as in chapter 3. The successful generation of an M3G-specific Fab fragment directed the research towards the examination of the influence of scFv multimerisation, Fab constant region stability and SPR chip surface coating chemistry, on anti-hapten surface plasmon resonance (SPR) assay development. Under optimised conditions, the anti-M3G scFv was found to have an IC50 value of 30 ng/ml, while the Fab construct exhibited an IC50 value of 2.4 ng/ml. In an SPR-based competitive assay on an M3G-OVA-coated chip surface, the two constructs again differed in sensitivity, with IC50 values of 117 and 19 ng/ml for the scFv and Fab, respectively. However, when M3G was directly immobilized onto the SPR chip surface, both antibody constructs exhibited good linearity of response, with similar high sensitivity IC50 values (scFv 30 ng/ml; Fab 14 ng/ml). During SPR assay development it was noticed that scFv and Fab constructs gave differing off-rate profiles. Subsequent HPLC, ELISA and electrophoretic analyses confirmed that a portion of the scFv population multimerises. Bivalent scFv was found to profoundly affect the dissociation curve for scFv in stringent SPR kinetic analyses, leading to a 40-fold difference in calculated off-rate values. This finding has significant implications when ranking recombinant antibodies libraries via off-rate analysis.

Previous investigations (Brennan, 2004; unpublished data) into the production of novel recombinant antibody fragments against tetrahydrocannabinol were reported as unsuccessful. However, chapter 5, details the successful generation of an anti-THC scFv fragment. A rabbit immune library was constructed and panned yielding a soluble secreting anti-THC scFv clone. The affinity of this anti-THC scFv and that of the commercially available monoclonal antibody were compared on ELISA. While their affinities were comparable, the reproducibility achieved with the scFv in competitive assay was superior. The anti-THC scFv applied to a SPR inhibition assay on Biacore demonstrated an 1C50 of 625 ng/ml. Future work could entail the conversion of the scFv to a Fab fragment in order to investigate if any improvement would be observed (as in chapters 3 and 4). However, solubility issues with the free drug require further

investigation prior to any extensive work on increasing the affinity of the antibody fragment or on improving the SPR assay using different surface chemistries as described for the anti-M3G Biacore assay.

A low-density SPR-based assay array on a Biacore chip was designed and characterized. The success of this assay is illustrative of the potential of these novel recombinant antibodies for use in a multi-drug detection format and their potential for commercialization. These assays may eventually be used to combat a rapidly increasing, social, health and legal problems related to drug abuse. Future work envisaged would include a novel microfluidics-based bio-chip with a larger number of antibodies against a range of drugs of abuse.

Mutagenesis of the anti-M3G Fab fragment is discussed in chapter 6. Two alternative approaches were investigated. The first utilised CDR walking and focused on the primary region of antigen binding, the CDRH3. The second strategy used the PCR eliminating method described by Kunkle (1985), and targeted the more peripheral CDR's such as the CDRL2, CDRL3 and CDRH1. Several attempts were made to obtain a functional clone from the mutated CDRH3 library. However, it was concluded that the CDRH3 was simply too critical to the function of the anti-M3G Fab fragment and no mutation in this region was tolerated. The second strategy which investigated regions of the antibody fragment that are thought to be more involved in stabilisation and structural rigidity were found to be more tolerant of mutation. With functionality of the anti-M3G Fab retained, sequence analysis revealed mutations in the CDRL2 while all other regions retained wildtype sequence.

This research records important discoveries with regard to anti-hapten antibodies. These include the optimal recombinant antibody structure to use, the impact of this structural choice on library screening and assay development (chapters 3 and 4 and 5), and the significance of the CDRH3 in anti-hapten binding compared to that of an anti-protein

(i.e. large antigen) antibody where multiple binding sites are available on the target. Moreover, these discoveries have lighthighlighted the need for careful analysis of strategy when working with recombinant antibodies. Here, antibodies against all three targets were achieved through target-specific tailoring of all experimental strategies.

Future work could entail the application of methods outlined in chapter 6 to improve the lower affinity anti-amphetamine antibody fragment. Similar methods should also be applied to the improvement of the anti-THC scFv, where the potential is even more signifcant due to its lack of *in-vivo* functional mutation, as discussed in chapter 6. There is enormous scope for the further development of the multi-drug assay outlined in chapter 5, each of the antibodies described here have been fully characterised by ELISA and Biacore on a single analyte assay format and then further characterised in the multi-drug SPR assay format. Each antibody has proven robust and functionally stable to perform in this multi-analyte assay with no compromise in sensitivity. The next step would be their application to a low-density micro-array for on-site testing allowing for sensitive, specific, rapid and simultaneous detection of multiple drug classes.

Chapter 7
7.0 Overall Conclusions

7.1 Overall Conlcusions

The research in this thesis describes the succcessful production and characterisation of novel genetically-derived antibody fragments to morphine-3-glucuronide (M3G), amphetamine and tetrahydrocannibinol, their structural modification, *in-vitro* mutagenesis and application in a multi-analyte assay.

Chapter 3 focused on the production and characterisation of a genetically derived Fab fragment specific to amphetamine. A previously described anti-amphetamine antibody-secreting hybridoma was the source of the cDNA used to isolate the DNA encoding the antibodies variable heavy and variable light chains. The constant heavy and constant light chains were cloned from the pComb3xTT vector. The anti-amphetamine Fab fragment was successfully used in the development of a Biacore inhibition assay and the Fab fragment demonstrated superior sensitivity to that of the parent IgG molecule. Under optimised conditions the Fab demonstrated an IC50 of 200 ng/ml compared to an IC50 of ~ 600 ng/ml for the monoclonal antibody. The purified antibody provided excellent titres with working dilutions in the range of 1 in 2000 when purified from a 500ml culture volume, further increasing its superiority over the IgG, where lower concentrations of antibody were obtained following purification. The second part of this chapter described the potential of producing an anti-amphetamine scFv fragment by similar means. Several attempts were made but no specific scFv was isolated. It is probable that the antibody encoded in the parent IgG was heavily reliant on the stabilising nature of the whole IgG structure. The Fab fragment, with the presence of the human constant chains, was able to retain and in fact improve the affinity while the 'floppy' nature of the scFv molecule was not capable of retaining the critical cavity shaped binding epitope common to anti-hapten antibodies.

In chapter 4 the prodruction of an anti-M3G Fab fragment via the structural conversion of an anti-M3G scFv was described. The genes encoding the variable regions were amplified from the scFv fragment and the human constant regions for the Fab were

amplifed from the pComb3xTT vector, as in chapter 3. The successful generation of an M3G-specific Fab fragment directed the research towards the examination of the influence of scFv multimerisation, Fab constant region stability and SPR chip surface coating chemistry, on anti-hapten surface plasmon resonance (SPR) assay development. Under optimised conditions, the anti-M3G scFv was found to have an IC50 value of 30 ng/ml, while the Fab construct exhibited an IC50 value of 2.4 ng/ml. In an SPR-based competitive assay on an M3G-OVA-coated chip surface, the two constructs again differed in sensitivity, with IC50 values of 117 and 19 ng/ml for the scFv and Fab, respectively. However, when M3G was directly immobilized onto the SPR chip surface, both antibody constructs exhibited good linearity of response, with similar high sensitivity IC50 values (scFv 30 ng/ml; Fab 14 ng/ml). During SPR assay development it was noticed that scFv and Fab constructs gave differing off-rate profiles. Subsequent HPLC, ELISA and electrophoretic analyses confirmed that a portion of the scFv population multimerises. Bivalent scFv was found to profoundly affect the dissociation curve for scFv in stringent SPR kinetic analyses, leading to a 40-fold difference in calculated off-rate values. This finding has significant implications when ranking recombinant antibodies libraries via off-rate analysis.

Previous investigations (Brennan, 2004; unpublished data) into the production of novel recombinant antibody fragments against tetrahydrocannabinol were reported as unsuccessful. However, chapter 5, details the successful generation of an anti-THC scFv fragment. A rabbit immune library was constructed and panned yielding a soluble secreting anti-THC scFv clone. The affinity of this anti-THC scFv and that of the commercially available monoclonal antibody were compared on ELISA. While their affinities were comparable, the reproducibility achieved with the scFv in competitive assay was superior. The anti-THC scFv applied to a SPR inhibition assay on Biacore demonstrated an 1C50 of 625 ng/ml. Future work could entail the conversion of the scFv to a Fab fragment in order to investigate if any improvement would be observed (as in chapters 3 and 4). However, solubility issues with the free drug require further

investigation prior to any extensive work on increasing the affinity of the antibody fragment or on improving the SPR assay using different surface chemistries as described for the anti-M3G Biacore assay.

A low-density SPR-based assay array on a Biacore chip was designed and characterized. The success of this assay is illustrative of the potential of these novel recombinant antibodies for use in a multi-drug detection format and their potential for commercialization. These assays may eventually be used to combat a rapidly increasing, social, health and legal problems related to drug abuse. Future work envisaged would include a novel microfluidics-based bio-chip with a larger number of antibodies against a range of drugs of abuse.

Mutagenesis of the anti-M3G Fab fragment is discussed in chapter 6. Two alternative approaches were investigated. The first utilised CDR walking and focused on the primary region of antigen binding, the CDRH3. The second strategy used the PCR eliminating method described by Kunkle (1985), and targeted the more peripheral CDR's such as the CDRL2, CDRL3 and CDRH1. Several attempts were made to obtain a functional clone from the mutated CDRH3 library. However, it was concluded that the CDRH3 was simply too critical to the function of the anti-M3G Fab fragment and no mutation in this region was tolerated. The second strategy which investigated regions of the antibody fragment that are thought to be more involved in stabilisation and structural rigidity were found to be more tolerant of mutation. With functionality of the anti-M3G Fab retained, sequence analysis revealed mutations in the CDRL2 while all other regions retained wildtype sequence.

This research records important discoveries with regard to anti-hapten antibodies. These include the optimal recombinant antibody structure to use, the impact of this structural choice on library screening and assay development (chapters 3 and 4 and 5), and the significance of the CDRH3 in anti-hapten binding compared to that of an anti-protein

(i.e. large antigen) antibody where multiple binding sites are available on the target. Moreover, these discoveries have lighthighlighted the need for careful analysis of strategy when working with recombinant antibodies. Here, antibodies against all three targets were achieved through target-specific tailoring of all experimental strategies.

Future work could entail the application of methods outlined in chapter 6 to improve the lower affinity anti-amphetamine antibody fragment. Similar methods should also be applied to the improvement of the anti-THC scFv, where the potential is even more signifcant due to its lack of *in-vivo* functional mutation, as discussed in chapter 6. There is enormous scope for the further development of the multi-drug assay outlined in chapter 5, each of the antibodies described here have been fully characterised by ELISA and Biacore on a single analyte assay format and then further characterised in the multi-drug SPR assay format. Each antibody has proven robust and functionally stable to perform in this multi-analyte assay with no compromise in sensitivity. The next step would be their application to a low-density micro-array for on-site testing allowing for sensitive, specific, rapid and simultaneous detection of multiple drug classes.

Chapter 8
8.0 Bibliography

Alt, F. W., Blackwell, T. K. and Yancopoulos, G. D. (1987). Development of the primary antibody repertoire. *Science.* **238**, 1079-1087.

Barbas, C. F. (1993). Recent advances in phage display. *Current Opinion in Biotechnology.* **4,** 526-530

Benjamini, E., Coico, R. and Sunshine, G. (2000). *Immunology: A short course.* 4th. New York, USA: Wiley and sons.

Biermann, T., Schwarze, B., Zedler, B. and Betz, P. (2004). On-site testing of illicit drugs: the use of the drug-testing device "Toxiquick®". *Forensic Science International*. **143**, 21-25.

Braithwaite, R. A., Jarvie, D. R. and Minty, P. S. B, Simpson D, Widdop B. (1995). Screening for drugs of abuse. I: Opiates, amphetamines and cocaine. *Annals of Clinical Biochemistry*. **32**, 123-153.

Brennan, J., Dillon, P. and O'Kennedy, R. (2003). Production, purification and characterisation of genetically derived scFv and bifunctional antibody fragments capable of detecting illicit drug residues. *Journal of chromatography.B, Analytical Technologies in the Biomedical and Life Sciences*. **786**, 327-342.

Brichta, J., Hilova, M. and Viskovic, T. (2005). Generation of hapten-specific recombinant antibodies: antibody phage display technology: a review. *Veterinary Medicine-Czech*. 231-252.

Campbell, F. A., Tramer, M. R. and Carroll, D, Reynolds D. J. M., Moore R. A., McQuay H. J. (2001). Are cannabinoids an effective and safe treatment option in the

management of pain? A qualitative systematic review. *British Medical Journal (Clinical research ed.)*. **323**, 13-16.

Chames, P., Coulon, S. and Baty, D. (1998). Improving the affinity and the fine specificity of an anti-cortisol antibody by parsimonious mutagenesis and phage display. *Journal of Immunology*. **161**, 5421-5429.

Charlton, K., Harris, W. J. and Porter, A. J. (2001). The isolation of super-sensitive anti-hapten antibodies from combinatorial antibody libraries derived from sheep. *Biosensors and Bioelectronics*. **16**, 639-646.

Cirimele, V., Villain, M. and Mura, P., Bernard, M. and Kintz, P. (2006). Oral fluid testing for cannabis: On-site OraLine® IV s.a.t. device versus GC/MS. *Forensic Science International*. **161**, 180-184.

Clarke, J. and Wilson, J. F. (2005). Proficiency testing (external quality assessment) of drug detection in oral fluid. *Forensic Science International*. **150**, 161-164.

Click, E. M. and Webster, R. E. (1997). Filamentous phage infection: Required interactions with the Tol A protein. *Journal of Bacteriology*. **179,** 6464-6471.

Batra, S. K., Jain, M., Wittel, A. U., Chauhan, S. C. and Colcher, D. (1998) Pharmacokinetics and biodistribution of genetically engineered antibodies *Current Opinion in Biotechnology*, **13,** 603-608.

Cone, E. J., Darwin, W. D. and Wang, W. L. (1993). The occurrence of cocaine, heroin and metabolites in hair of drug abusers. *Forensic Science International*. **63**, 55-68.

Cone, E. J., Presley, L. and Lehrer, M. (2002). Oral fluid testing for drugs of abuse: positive prevalence rates by Intercept immunoassay screening and GC-MS-MS

confirmation and suggested cutoff concentrations. *Journal of Analytical Toxicology*. **26**, 541-546.

Connell, J. A., Parry, J. V., Mortimer, P. P. and Duncan, J. (1993). Novel assay for the detection of immunoglobulin G antihuman immunodeficiency virus in untreated saliva and urine. *Journal of Medical Virology*. **41**, 159-164.

Dillon, P., Manning, B. and Daly, S., Killard, T. and O'Kennedy, R. (2003). Production of a recombinant anti-morphine-3-glucuronide single-chain variable fragment (scFv) antibody for the development of a “real-time” biosensor-based immunoassay. *Journal of Immunological Methods.* **276**,151-161.

Dooley, H., Flajnik, M. F. and Porter, A. J. (2003). Selection and characterization of naturally occurring single-domain (IgNAR) antibody fragments from immunized sharks by phage display. *Molecular Immunology*. **40**, 25-33.

Eliasson, C., Macleod, N. A. and Matousek, P. (2008). Non-invasive detection of cocaine dissolved in beverages using displaced Raman spectroscopy. *Analytica Chimica Acta*. **607**, 50-53.

Elliott, C. T., Baxter, G. A. and Hewett, S. A. (1998). Use of biosensors for rapid drug residue analysis without sample deconjugation or clean-up: a possible way forward. *The Analyst*. **123**, 2469-2473.

Ewald, A. H., Fritschi, G. and Maurer, H. H. (2007). Metabolism and toxicological detection of the designer drug 4-iodo-2,5-dimethoxy-amphetamine (DOI) in rat urine using gas chromatography–mass spectrometry. *Journal of Chromatography B.* **857**, 170-174.

Endemann, H. and Model, P. (1995). Location of Filamentous Phage Minor Coat Proteins in Phage and in Infected Cells. *Journal of Molecular Biology.* **250,** 495-506.

Freund, C., Ross, A. and Guth, B., Pluckthun, A. and Holackt, A. (1993). Characterization of the linker peptide of the single-chain Fv fragment of an antibody by NMR spectroscopy. *FEBS letters*. **320**, 97-100.

Fucci, N., De Giovanni, N. and Chiarotti, M. (2003). Simultaneous detection of some drugs of abuse in saliva samples by SPME technique. *Forensic Science International*. **134**, 40-45.

Glockshuber, R., Malia, M., Pfitzinger, I. and Pluckthun, A. (1990). A comparison of strategies to stabilize immunoglobulin Fv-fragments. *Biochemistry*. **29**, 1362-1367.

Gross, J., Johnson, J., Sigler, L. and Stitzer, M. L. (1995). Dose effects of nicotine gum. *Addictive Behaviors*. **20**, 371-381.

Hofman, L. F. (2001). Human saliva as a diagnostic specimen. *The Journal of Nutrition*. **131**, 1621S-5S.

Holliger, P. and Hudson, P. J. (2005). Engineered antibody fragments and the rise of single domains. *Nature Biotechnology*. **23**, 1126-1136.

Hoogenboom, H. R., de Bruïne, A. P. and Hufton, S. E., Hoet, R. M., Arends, J.W. and Roovers, R. C. (1998). Antibody phage display technology and its applications. *Immunotechnology*. **4**, 1-20.

Huestis, M. A. and Cone, E. J. (2004). Relationship of Delta 9-tetrahydrocannabinol concentrations in oral fluid and plasma after controlled administration of smoked cannabis. *Journal of Analytical Toxicology*. **28**, 394-399.

Huse, W. D., Sastry, L., Iverson, S. A., Kang, A. S., Alting-Mees, M., Burton, D. R., Benkovic, S. J. and Lerner, R. A. (1989). Generation of large combinatorial libraries of the immunoglobulin repertoire in phage lambda. *Science.* **246,** 1275-1281.

Hust, M. and Dubel, S. (2004). Mating antibody phage display with proteomics. *Trends in Biotechnology*. **22**, 8-14.

Huston, J. S., Margolies, M. N. and Haber, E. (1996). Antibody Binding Sites. *Advances in Protein Chemistry*. **49**, 329-450.

Kacinko, S. L., Reid, C., Cooper, G. A., Huestis, M. A., Baldwin, D., Moolchan, E. T., Barnes, A. J., Hand, C. W., Wilson, L. and Kim, I. (2004). Performance characteristics of the Cozart® RapiScan Oral Fluid Drug Testing System for opiates in comparison to ELISA and GC/MS following controlled codeine administration. *Forensic Science International*. **141**, 41-48.

Kato, K., Hillsgrove, M. and Weinhold, L., Gorelick, D.A., Darwin, W.D. and Cone, E.J. (1993). Cocaine and metabolite excretion in saliva under stimulated and nonstimulated conditions. *Journal of Analytical Toxicology*. **17**, 338-341.

Kintz, P. and Samyn, N. (1999). Determination of "Ecstasy" components in alternative biological specimens. *Journal of Chromatography B: Biomedical Sciences and Applications*. **733**, 137-143.

Lazzaroni, J. C., Germon, P., Ray, M. C. and Vianney, A. (1999). The Tol proteins of Escherichia coli and their involvement in the uptake of biomolecules and outer membrane stability. *FEMS Microbiology Letters.* **177,** 191-197.

Lowman, H. B. and Wells, J. A. (1991). Monovalent phage display: A method for selecting variant proteins from random libraries. *Methods*. **3**, 205-216.

Li, Y., Cockburn, W., Kilpatrick, J. B. and Whitelam, G. C. (2000). High affinity ScFvs from a single rabbit immunized with multiple haptens. *Biochemical and Biophysical Research Communications*. **268**, 398-404.

Li, Z., Woo, C. J. and Iglesias-Ussel, M. D. (2004). The generation of antibody diversity through somatic hypermutation and class switch recombination. *Genes and Development*. **18**, 1-11.

Lu, D., Shen, J. and Vil, M. D. (2003). Tailoring in vitro selection for a picomolar affinity human antibody directed against vascular endothelial growth factor receptor 2 for enhanced neutralizing activity. *The Journal of Biological Chemistry*. **278**, 43496-43507.

Lu, H., Kreuzer, M., Takkinen, K. and Guilbault, G. (2007). A recombinant Fab fragment-based electrochemical immunosensor for the determination of testosterone in bovine urine. *Biosensors and Bioelectronics*. **22**, 1756-1763.

Lu, N. T. and Taylor, B. G. (2005). Drug screening and confirmation by GC–MS: Comparison of EMIT II and Online KIMS against 10 drugs between US and England laboratories. *Forensic Science International.* **157**, 106-116.

Lubkowski, J., Hennecke, F., Plückthun, A. and Wlodawer, A. (1999). Filamentous phage infection: crystal structure of g3p in complex with its coreceptor, the C-terminal domain of TolA. *Structure.* **7,** 711-722.

Lurie, I. S. (1998). Capillary electrophoresis of illicit drug seizures. *Forensic Science International*. **92**, 125-136.

Marks, J. D., Hoogenboom, H. R., Bonnert, T. P., Mc Cafferty, J., Griffiths, A. D. and Winter, G. (1991). By-passing immunization. Human antibodies from V-gene libraries displayed on phage. *Journal of Molecular Biology*. **222**, 581-597.

Moore, L., Wicks, J., Spiehler, V. and Holgate, R.(2001). Gas chromatography-mass spectrometry confirmation of Cozart RapiScan saliva methadone and opiates tests. *Journal of Analytical Toxicology*. **25**, 520-524.

Niedbala, R. S., Kardos, K. W., Fritch, D. F. (2001b). Detection of marijuana use by oral fluid and urine analysis following single-dose administration of smoked and oral marijuana. *Journal of Analytical Toxicology*. **25**, 289-303.

Ogert, R. A., Kusterbeck, A. W., Wemhoff, G. A., Burke, R. and Ligler, F. S. (1992). Detection of cocaine using flow immunosensors. *Analytical Letters*. **25**, 1999-2019.

Persson, H., Wallmark, H., Ljungars, A., Hallborn, J. and Ohlin, M. (2008). In vitro evolution of an antibody fragment population to find high-affinity hapten binders. *Protein Engineering, Design and Selection: PEDS*. **21**, 485-493.

Petersen-Mahrt, S. K., Harris, R. S. and Neuberger, M. S. (2002). AID mutates E. coli suggesting a DNA deamination mechanism for antibody diversification. *Nature*. **418**, 99-103.

Poltoratsky, V., Goodman, M. F. and Scharff, M. D. (2000). Error-prone candidates vie for somatic mutation. *The Journal of Experimental Medicine*. **192**, 27-30.

Puder, K. S., Kagan, D. V. and Morgan, J. P. (1988). Illicit methamphetamine: analysis, synthesis, and availability. *The American Journal of Drug and Alcohol Abuse*. **14**, 463-473.

Roth, D. B. and Craig, N. L. (1998). VDJ recombination: a transposase goes to work. *Cell*. **94**, 411-414.

Popkov, M., Mage, R. G., Alexander, C. B., Thundivalappil, S., Barbas, C. F. and Rader, C. (2003). Rabbit Immune Repertoires as Sources for Therapeutic Monoclonal Antibodies: The Impact of Kappa Allotype-correlated Variation in Cysteine Content on Antibody Libraries Selected by Phage Display. *Journal of Molecular Biology.* **325,** 325-335.

Raag, R. and Whitlow, M. (1995). Single-chain Fv's. FASEB,J. **1**, 73-80.

Roitt I. M. (1989). *Immunology.* Gower Medical Publishing, London.

Reynaud, C. A., Anquez, V., Grimal, H. and Weill, J. C. (1987). A hyperconversion mechanism generates the chicken light chain preimmune repertoire. *Cell.* **3,** 379-388.

Samyn, N. and van Haeren, C. (2000). On-site testing of saliva and sweat with Drugwipe and determination of concentrations of drugs of abuse in saliva, plasma and urine of suspected users. *International Journal of Legal Medicine*. **113**, 150-154.

Santala, V. and Saviranta, P. (2004). Affinity-independent elution of antibody-displaying phages using cleavable DNA linker containing streptavidin beads. *Journal of Immunological Methods.* **284**, 159-163.

Schmitz, U., Versmold, A., Kaufmann, P. and Frank, H. G. (2000). Phage display: a molecular tool for the generation of antibodies--a review. *Placenta*. **21,** 106-12.

Sheedy, C., Roger MacKenzie, C. and Hall, J. C. (2007). Isolation and affinity maturation of hapten-specific antibodies. *Biotechnology Advances.* **25**, 333-352.

Skerra, A. and Pluckthun, A. (1988). Assembly of a functional immunoglobulin Fv fragment in Escherichia coli. *Science.* **240**, 1038-1041.

Simons, G. F., Konings, R. N., and Schoenmakers, J. G. (1981). Genes VI, VII, and IX of phage M13 code for minor capsid proteins of the viron. *PNAS.* **78,** 4194-4198.

Townsend, S., Finlay, W. J. J., Hearty, S. and O'Kennedy, R. (2006). Optimizing recombinant antibody function in SPR immunosensing: The influence of antibody structural format and chip surface chemistry on assay sensitivity. *Biosensors and Bioelectronics*. **22**, 268-274.

Wan, S. H., Matin, S. B. and Azarnoff, D. L. (1978). Kinetics, salivary excretion of amphetamine isomers, and effect of urinary pH. *Clinical Pharmacology and Therapeutics*. **23**, 585-590.

Ward, E. S., Gussow, D. and Griffiths, A. D., Jones, P. T and Winter, G. (1989). Binding activities of a repertoire of single immunoglobulin variable domains secreted from Escherichia coli. *Nature*. **341**, 544-546.

Webster, R. L. (1996). Biology of the Filamentous Bacteriophage. *Phage Display of Peptides and Proteins*. 1-20

Wish, E. D., Hoffman, J. A. and Nemes, S. (1997). The validity of self-reports of drug use at treatment admission and at followup: comparisons with urinalysis and hair assays. *NIDA Research Monograph*. **167**, 200-226.

Wu, A. M., Chen, W., Raubitschek, A., Williams, L. E., Neumaier, M., Fischer,R., Hu, S. Z., Odom-Maryon, T., Wong, J. Y. and Shively, J. E. (1996). Tumor localization of anti-CEA single-chain Fvs: improved targeting by non-covalent dimmers. *Immunotechnology.* **1,** 21-36.

Xu, L., Basheer, C. and Lee, H. K. (2007). Developments in single-drop microextraction. *Journal of Chromatography A.* **1152**, 184-192.

Yacoubian, G. S. (2000). A typology of St. Louis arrestees surveyed through the arrestee drug abuse monitoring (ADAM) program. *Journal of Drug Education*. **30**, 247-264.

Yacoubian, G. S., Wish, E. D. and Choyka, J. D. (2002). A comparison of the OnTrak Testcup-5 to laboratory urinalysis among arrestees. *Journal of Psychoactive Drugs*. **34**, 325-329.

Yacoubian, G. S.,Jr, Wish, E. D. and Perez, D. M. (2001). A comparison of saliva testing to urinalysis in an arrestee population. *Journal of Psychoactive Drugs*. **33**, 289-294.

Yau, K. Y., Groves, M. A. and Li, S. (2003). Selection of hapten-specific single-domain antibodies from a non-immunized llama ribosome display library. *Journal of Immunological Methods*. **281**, 161-175.

Zhang, Z., Zhang, C. and Su, X. (2008). Carrier-mediated liquid phase microextraction coupled with high performance liquid chromatography for determination of illicit drugs in human urine. *Analytica Chimica Acta,*. **621**, 185-192.

Zheng, **M.,** McErlane, K. M. and Ong, M. C. (1998). High-performance liquid chromatography-mass spectrometry-mass spectrometry analysis of morphine and morphine metabolites and its application to a pharmacokinetic study in male Sprague–Dawley rats1. *Journal of Pharmaceutical and Biomedical Analyses.* **6,** 971-980.

Barbas, C. F., Kang, A. S., Lerner, R. A. and Benkovic, S. J. (1991). Assembly of combinatorial antibody libraries on phage surfaces: the gene III site. *PNAS.* **88**, 7978-7982.

Bradbury, A., Velappan, N. and Verzillo, V., Ovecka, M. and Chasteen, L. (2003). Antibodies in proteomics I: generating antibodies. *Trends in Biotechnology*. **21**, 275-281.

Glockshuber, R., Malia, M., Pfitzinger, I. and Pluckthun, A. (1990). A comparison of strategies to stabilize immunoglobulin Fv-fragments. *Biochemistry*. **29**, 1362-1367.

Hust, M. and Dübel, S. (2004). Mating antibody phage display with proteomics. *Trends in Biotechnology*.**22**, 8-14

Kirsch, M., Zaman, M. and Meier, D. (2005). Parameters affecting the display of antibodies on phage. *Journal of Immunological Methods*. **301**, 173-185.

Krebber, A., Bornhauser, S. and Burmester, J., Honegger, A., Willuda, J., Bosshard, H. R. and Pluckthun, A. (1997). Reliable cloning of functional antibody variable domains from hybridomas and spleen cell repertoires employing a reengineered phage display system. *Journal of Immunological Methods*. **201**, 35-55.

Persson, H., Lantto, J. and Ohlin, M. (2006). A focused antibody library for improved hapten recognition. *Journal of Molecular Biology*. **357**, 607-620.

Pluckthun, A. (1991). Antibody engineering: advances from the use of Escherichia coli expression systems. *Biotechnology*. **9**, 545-551.

Scott, J. K. and Smith, G. P. (1990). Searching for peptide ligands with an epitope library. *Science.* **249**, 386-390.

Smith, G. P. and Petrenko, V. A. (1997). Phage Display. *Chemical Reviews*. **97**, 391-410.

Yau, K. Y., Groves, M. A. and Li, S. (2003). Selection of hapten-specific single-domain antibodies from a non-immunized llama ribosome display library. *Journal of Immunological Methods*. **281**, 161-175.

Lipsinki, C. A., Lombardo, F., Dominy, B. W. and Feeney, P. (1997). Experimental and computational approaches to estimate solubility and permeability in drug discovery and development settings. *Advances in Drug Delivery*. **23**, 3-25.

Ahmad, A., Ramakrishnan, A., McLean, M. A. and Breau, A. P. (2003). Use of surface plasmon resonance biosensor technology as a possible alternative to detect differences in binding of enantiomeric drug compounds to immobilized albumins. *Biosensors and Bioelectronics*. **18**, 399-404.

Andris-Widhopf, J., Rader, C., Steinberger, P., Fuller, R. and Barbas, III. C. F. (2000). Methods for the generation of chicken monoclonal antibody fragments by phage display. *Journal of Immunological Methods*. **242**, 159-181.

Arndt, K. M., Muller, K. M. and Pluckthun, A. (1998). Factors influencing the dimer to monomer transition of an antibody single-chain Fv fragment. *Biochemistry*. **37**, 12918-12926.

Borrebaeck, C. A., Malmborg, A. C. and Furebring, C., Michaelsson, A., Ward, S., Danielsson, L. and Ohlin, M. (1992). Kinetic analysis of recombinant antibody-antigen interactions: relation between structural domains and antigen binding. *Biotechnology*. **10**, 697-698.

Byfield, M. P. and Abuknesha, R. A. (1994). Biochemical aspects of biosensors. *Biosensors and Bioelectronics.* **9**, 373-399.

Barbas, C. F., Burton, D., Scott, J. K. and Silverman, G. J. (2001). *Phage Display: A Laboratory Manual.* Cold Spring Harbour Laboratory Press

Daly, S. J., Keating, G. J. and Dillon, P. P., Manning, B. M., O'Kennedy, R., Lee, H. A. and Morgan, M. R. A. (2000). Development of surface plasmon resonance-based

immunoassay for aflatoxin B(1). *Journal of Agricultural and Food Chemistry*. **48**, 5097-5104.

Fredericks, Z. L., Forte, C. and Capuano, I. V. (2004). Identification of potent human anti-IL-1RI antagonist antibodies. *Protein Engineering, Design and Selection: PEDS*. **17**, 95-106.

Frostell-Karlsson, A., Remaeus, A., Roos, H., Anderson, K., Borg, P., Hamalainen, M. and Karlsson, R. (2000). Biosensor analysis of the interaction between immobilized human serum albumin and drug compounds for prediction of human serum albumin binding levels. *Journal of Medicinal Chemistry*. **43**, 1986-1992.

George, A. J. T., French, R. R. and Glennie, M. J. (1995). Measurement of kinetic binding constants of a panel of anti-saporin antibodies using a resonant mirror biosensor. *Journal of Immunological Methods*. **183**, 51-63.

Griffiths, A. D., Malmqvist, M. and Marks, J. D., Bye, J. M., Embleton, M. J., McCafferty, J., Baier, M., Holliger, K.P., Gorick, B.D. and Hughes-Jones, N.C. (1993). Human anti-self antibodies with high specificity from phage display libraries. *The EMBO journal*. **12**, 725-734.

Karp, N. A., Edwards, P. R. and Leatherbarrow, R. J. (2005). Analysis of calibration methodologies for solvent effects in drug discovery studies using evanescent wave biosensors. *Biosensors and Bioelectronics.* **21**, 128-134.

Kortt, A. A., Lah, M. and Oddie, G. W. Gruen, C. L., Burns, J. E., Pearce, L. A., Atwell, J. L., McCoy, A. J., Howlett, G. J., Metzger, D. W., Webster, R. G. and Hudson, P. J. (1997). Single-chain Fv fragments of anti-neuraminidase antibody NC10 containing five-

and ten-residue linkers form dimers and with zero-residue linker a trimer. *Protein Engineering*. **10**, 423-433.

Leonard, P., Säfsten, P. and Hearty, S., McDonnell, B., Finlay, B., O'Kennedy R. (2007). High throughput ranking of recombinant avian scFv antibody fragments from crude lysates using the Biacore A100. *Journal of Immunological Methods*. **323**, 172-179.

Li, Y., Cockburn, W., Kilpatrick, J. B. and Whitelam, G. C. (2000). High affinity ScFvs from a single rabbit immunized with multiple haptens. *Biochemical and Biophysical Research Communications*. **268**, 398-404.

MacKenzie, C. R., Hirama, T. and Deng, S. J., Bundle, D. R., Narang, S. A. and Young, N. M. (1996). Analysis by surface plasmon resonance of the influence of valence on the ligand binding affinity and kinetics of an anti-carbohydrate antibody. *The Journal of Biological Chemistry*. **271**, 1527-1533.

Marazuela, D. and Moreno-Bondi, M. C. (2002). Fiber-optic biosensors--an overview. *Analytical and Bioanalytical Chemistry*. **372**, 664-682.

Maynard, J. and Georgiou, G. (2000). Antibody engineering. *Annual Review of Biomedical Engineering*. **2**, 339-376.

McGregor, D. P., Molloy, P. E., Cunningham, C. and Harris, W. J. (1994). Spontaneous assembly of bivalent single chain antibody fragments in Escherichia coli. *Molecular Immunology*. **31**, 219-226.

O'Shannessy, D. J. and Winzor, D. J. (1996). Interpretation of deviations from pseudo-first-order kinetic behavior in the characterization of ligand binding by biosensor technology. *Analytical Biochemistry*. **236**, 275-283.

Quinn, J. G. and O'Kennedy, R. (2001). Biosensor-based estimation of kinetic and equilibrium constants. *Analytical Biochemistry*. **290**, 36-46.

Rader, C., Ritter, G. and Nathan, S., Elia, M., Gout, I., Jungbluth, A. A., Cohen, L. S., Welt, S., Old, L. J., Barbas, C. F. (2000). The rabbit antibody repertoire as a novel source for the generation of therapeutic human antibodies. *The Journal of Biological Chemistry*. **275**, 13668-13676.

Rau, D., Kramer, K. and Hock, B. (2002). Cloning, functional expression and kinetic characterization of pesticide-selective Fab fragment variants derived by molecular evolution of variable antibody genes. *Analytical and Bbioanalytical Chemistry*. **372**, 261-267.

Redshaw, N., Dickson, S. J., Ambrose, V. and Horswell, J. (2007). A preliminary investigation into the use of biosensors to screen stomach contents for selected poisons and drugs. *Forensic Science International,*. **172**, 106-111.

Rodriguez-Mozaz, S., Alda, M. J. L. d., Marco, M. and Barceló, D. (2005). Biosensors for environmental monitoring: A global perspective. *Talanta,*. **65**, 291-297.

Rogers, K. R. (2006). Recent advances in biosensor techniques for environmental monitoring. *Analytica Chimica Acta.* **568**, 222-231.

Rogers, K. R. (2000). Principles of affinity-based biosensors. *Molecular Biotechnology*. **14**, 109-129.

Stacy, J. E., Kausmally, L. and Simonsen, B., Nordgard, S. H. Alsoe, L., Michaelsen T. E. and Brekke O. H. (2003). Direct isolation of recombinant human antibodies against group B Neisseria meningitidis from scFv expression libraries. *Journal of Immunological Methods*. **283**, 247-259.

Tout, N. L., Yau, K. Y. and Trevors, J. T. (2001). Synthesis of ligand-specific phage-display ScFv against the herbicide picloram by direct cloning from hyperimmunized mouse. *Journal of Agricultural and Food Chemistry*. **49**, 3628-3637.

Crane, M. A., Kingzette, M. and Knight, K. L. (1996). Evidence for limited B-lymphopoiesis in adult rabbits. *The Journal of Experimental Medicine*. **183**, 2119-2121.

Popkov, M., Mage, R. G. and Alexander, C. B., Thundivalappil, S., Barbas, C. F. and Rader, C. (2003). Rabbit immune repertoires as sources for therapeutic monoclonal antibodies: the impact of kappa allotype-correlated variation in cysteine content on antibody libraries selected by phage display. *Journal of Molecular Biology*. **325**, 325-335.

Ratcliffe, M. J. (2006). Antibodies, immunoglobulin genes and the bursa of Fabricius in chicken B cell development. *Developmental and Comparative Immunology*. **30**, 101-118.

Boder, E. T., Midelfort, K. S. and Wittrup, K. D. (2000). Directed evolution of antibody fragments with monovalent femtomolar antigen-binding affinity. *PNAS*. **97**, 10701-10705.

Coia, G., Hudson, P. J. and Irving, R. A. (2001). Protein affinity maturation in vivo using E. coli mutator cells. *Journal of Immunological Methods*. **251**, 187-193.

Comtesse, N., Heckel, D. and Maldener, E., Glass, B. and Meese, E. (2000). Probing the human natural autoantibody repertoire using an immunoscreening approach. *Clinical and Experimental Immunology*. **121**, 430-436.

Cox, E. C. (1976). Bacterial mutator genes and the control of spontaneous mutation. *Annual Review of Genetics*. **10**, 135-156.

Daugherty, P. S., Chen, G., Iverson, B. L. and Georgiou, G. (2000). Quantitative analysis of the effect of the mutation frequency on the affinity maturation of single chain Fv antibodies. *PNAS*. **97**, 2029-2034.

Dong, L., Chen, S., Richter, M. and Schachner, M. (2002). Single-chain variable fragment antibodies against the neural adhesion molecule CHL1 (close homolog of L1) enhance neurite outgrowth. *Journal of Neuroscience Research*. **69**, 437-447.

Kunkel, T. A. (1985). Rapid and efficient site-specific mutagenesis without phenotypic selection. *PNAS*. **82**, 488-492.

Lee, P. C., Mijts, B. N. and Petri, R. (2004). Alteration of product specificity of Aeropyrum pernix farnesylgeranyl diphosphate synthase (Fgs) by directed evolution. *Protein Engineering, Design and Selection: PEDS*. **17**, 771-777.

Low, N. M., Holliger, P. H. and Winter, G. (1996). Mimicking somatic hypermutation: affinity maturation of antibodies displayed on bacteriophage using a bacterial mutator strain. *Journal of Molecular Biology*. **260**, 359-368.

Lu, D., Shen, J., Vil, M. D. (2003). Tailoring in vitro selection for a picomolar affinity human antibody directed against vascular endothelial growth factor receptor 2 for enhanced neutralizing activity. *The Journal of Biological Chemistry*. **278**, 43496-43507.

Notkins, A. L. (2004). Polyreactivity of antibody molecules. *Trends in Immunology*. **25**, 174-179.

Padlan, E. A. (1994). Anatomy of the antibody molecule. *Molecular Immunology*. **31**, 169-217.

Park, S. G., Lee, J. S. and Je, E. Y., Kim, I., Chung J. and Choi, I. (2000). Affinity maturation of natural antibody using a chain shuffling technique and the expression of recombinant antibodies in Escherichia coli. *Biochemical and Biophysical Research Communications*. **275**, 553-557.

Razai, A., Garcia-Rodriguez, C. and Lou, J., Geren, I. N., Forsyth, C. M., Robles, Y., Tsai, R., Smith, T. J., Smith L. A., Siegel, R. W., Feldhaus, M. and Marks, J.D (2005). Molecular evolution of antibody affinity for sensitive detection of botulinum neurotoxin type A. *Journal of Molecular Biology*. **351**, 158-169.

Schier, R., McCall, A. and Adams, G. P., Marshall K.W., Merritt H., Yim M., Crawford R.S., Weiner L.M., Marks C. and Marks J. D. (1996). Isolation of picomolar affinity anti-c-erbB-2 single-chain Fv by molecular evolution of the complementarity determining regions in the center of the antibody binding site. *Journal of Molecular Biology*. **263**, 551-567.

Sidhu, S. S., Lowman, H. B., Cunningham, B. C. and Wells, J. A. (2000). Phage display for selection of novel binding peptides. *Methods in Enzymology*. **328**, 333-363.

Valjakka, J., Hemminki, A. and Niemi, S. (2002). Crystal structure of an in vitro affinity- and specificity-matured anti-testosterone Fab in complex with testosterone. Improved affinity results from small structural changes within the variable domains. *The Journal of Biological Chemistry*. **277**, 44021-44027.

Wedemayer, G. J., Patten, P. A. and Wang, L. H., Schultz, P. G. and Stevens, R. C. (1997). Structural insights into the evolution of an antibody combining site. *Science.* **276**, 1665-1669.

Yang, W. P., Green, K. and Pinz-Sweeney, S., Briones, A. T., Burton D.R. and Barbas, C.F. (1995). CDR walking mutagenesis for the affinity maturation of a potent human anti-HIV-1 antibody into the picomolar range. *Journal of Molecular Biology*. **254**, 392-403.

Zahnd, C., Spinelli, S. and Luginbuhl, B., Amstutz, P., Cambillau, C. and Plückthun, A. (2004). Directed in vitro evolution and crystallographic analysis of a peptide-binding single chain antibody fragment (scFv) with low picomolar affinity. *The Journal of Biological Chemistry*. **279**, 18870-18877.

Zimmermann, J., Oakman, E. L. and Thorpe, I. F., Shi, X., Abbyad, P., Brooks, C.L. 3rd, Boxer, S.G. and Romesberg, F. E. (2006). Antibody evolution constrains conformational heterogeneity by tailoring protein dynamics. *PNAS*. **103**, 13722-13727.